Conventional and Intelligent Control of Nonlinear Systems

A thesis submitted
in fulfillment of the requirement for the award of degree
of
Doctor of Philosophy

Submitted by

VIKRAM

Registration No. 951104003

Supervisor

Dr. SUNIL K. SINGLA
(Thapar University Patiala)

&

Dr. LILLIE DEWAN
(N.I.T. Kurukshetra)

DEPARTMENT OF ELECTRICAL AND INSTRUMENTATION ENGINEERING

THAPAR UNIVERSITY, PATIALA

2015

DECLARATION

I hereby declare that the thesis entitled **"Conventional and Intelligent Control of Nonlinear Systems"** which is being submitted to Department of Electrical and Instrumentation Engineering, Thapar University, Patiala in the partial fulfilment of the requirement for the degree of **Doctor of Philosophy,** has previously not formed the basis for the award of degree, diploma, fellowship or any other similar title. It is certified that the thesis is entirely my own and that the idea and references cited herein have been duly acknowledged.

(Vikram)
Regn No. 951104003

CERTIFICATE

Certified that the thesis entitled "**Conventional and Intelligent Control of Nonlinear Systems**" being submitted by **Mr. Vikram** to the **Department of Electrical & Instrumentation Engineering**, **Thapar University**, **Patiala** in fulfillment of the requirements for the award of degree of "**Doctor of Philosophy**" is a record of bonafide research work carried out by him. He has worked under our guidance and supervision and fulfilled the requirements for the submission of this thesis, which has reached the requisite standard. The matter presented in this thesis has not been submitted in part or full for the award of any degree in any other University or Institute.

(Dr. Lillie Dewan)
Professor
Department of Electrical Engineering
N.I.T. Kurukshetra
Haryana, India

(Dr. Sunil K. Singla)
Assistant Professor
E.I.E.D.
Thapar University Patiala
Punjab, India

ACKNOWLEDGEMENT

The real spirit of achieving a goal is through the way of excellence and austerous discipline. I would not have made it to the end of this degree, and to the end of this thesis, without the help and support of a number of individuals. Here I hope to give some recognition for their efforts on my behalf.

First, I thank the ALMIGHTY for giving strength to complete this work. I could never have accomplished this without the faith I have in the Almighty.

I would like to express my sincere thanks and gratitude to my supervisors Dr. Sunil Kumar Singla and Dr. Lillie Dewan for their guidance and constant support. Without their valuable advice and encouragement, this thesis would never be completed. They greatly enriched my knowledge & constantly inspirited me in pursuit of this thesis, had to sacrifice many of their precious hours. From deep inside thank their family members for their opportune support and help. I am thankful to the Almighty for giving me mentors like them.

I express my deepest gratitude to Dr. Prakash Gopalan (Director, Thapar University, Patiala), Dr. R.S. Kaler (Deputy Director I), Dr Susheel Mittal (Deputy Director II), Dr. O.P. Pandey (Dean RSP) and Mr. Chiranjiv Singh (O.S.D., Thapar University, Patiala) for their encouragement and support, especially on the administrative grounds during the completion of this research work.

I am grateful to Dr Ravinder Agarwal (Head, E.I.E.D.) for his guidance and support during the completion of this research work.

I am thankful to my doctoral committee members Dr. R.K. Sharma and Dr. Sanjay Jain for their help, valuable suggestions and constant encouragement throughout the period of research.

I am also thankful to Mr. Gurbinder Singh (Registrar, Thapar University, Patiala) and Mr. E. Samule (Former Registrar, Thapar University Patiala) for helping with smooth proceeding of the administrative needs associated with the work.

Special thanks to, Mr. Nirbhojap Singh, Dr. Jitender Kumar, Mr. Shakti Singh, Dr. Saurabh Bhardwaj, Mr. Inderpreet Singh, Dr.Nitin Narang, , Mr. Vijay, Dr. Vikas Sharma, Mr. Rajeev, Mr. Amit Choudhary, Mr. Davinder and Dr. Ajay for constantly encouraging me to complete the thesis on time.

Lastly, for any successful accomplishment, the support, faith and blessings of near and dear one is a must. I am totally indebted to my mother Smt. Amrit Rani for showering her blessings all the time. Words fail me to give expression to my immense gratitude to my

father Sh. Ramesh Chopra for his love and support, my loving wife Sheenu who always stood beside me in my difficult times. Special love package for my little angel Diksha for hugging me in all the tough times during my Ph.D work. Thanks are also due to my sisters, Hemlata and Chanchal my dear Dhruv, Kush, Liesha and Hanna for their love, patience, understanding and endurance during the whole tenure of the work.

Finally, I would like to thanks Mr. Sunny Thapar and my inlaws for helping me in successfully completion of this work.

Vikram

ABSTRACT

In the real world, most of the systems are nonlinear by nature. Nonlinearities can be inherent or intentionally introduced into the system. The control of a nonlinear system can be achieved using linear and nonlinear models. In this work, two nonlinear systems are considered for control, one an inverted pendulum system, while the other a continuous stirred tank reactor (CSTR). The inverted pendulum system uses the nonlinear state equation model while the CSTR uses the linear transfer function model.

An inverted pendulum is a renowned benchmark problem in control literature because the control of many real time systems such as segways, rocket launchers, crane lifting containers and self-balancing robots, resembles the inverted pendulum system. It is a highly nonlinear, under-actuated and non minimum phase system. In this, the control objective is to keep the inverted pendulum in the upright position while following a desired reference trajectory by the base thus resulting into one (x), two (x - y and x - z) and three (x - y - z) dimensional inverted pendulum problem. For this system (one, two and three-dimensional inverted pendulum) conventional fixed gain proportional integral derivative (PID) controller may not produce satisfactory performance under all operating regions. Therefore, adaptive controller is preferred over a conventional controller.

For the tuning of PID controller, an adaptation mechanism using gain scheduling as a function of time and error has been proposed in this work. The gain scheduling depends upon the transient and the steady state part of the response. The proposed time as well as error adaptive gain scheduling PID controllers have been implemented in the MATLAB environment for the stabilization and tracking control of x, x - y and x - z inverted pendulums. The stability analysis of these different types of inverted pendulums with the proposed controllers has been performed using the Lyapunov stability criterion. The performance of the proposed controllers has been compared with the conventional PID scheme in terms of various performance specifications such as rise time, maximum overshoot, settling time and steady-state error etc. Simulation results reveal that the proposed adaptive gain scheduling PID controllers provide better stabilization for all the three types of inverted pendulums while keeping the tracking at the same level as of conventional PID controllers.

The mathematical model of a new three-dimensional x - y - z inverted pendulum in the form of state equations has been developed. The necessary and sufficient condition for

stability of the proposed three-dimensional x-y-z inverted pendulum has been derived using the Lyapunov stability criterion. The stabilization and tracking control of the proposed x-y-z inverted pendulum has been obtained using conventional and proposed adaptive gain scheduling PID controllers. The simulation results show that the proposed adaptive gain scheduling PID controllers provide better performance than the conventional PID controllers in terms of different performance specifications.

The effect of uncertainties (which are fast acting external disturbances, noise and frictional forces) on the performance of x, x-y, x-z and x-y-z inverted pendulums have been analysed using conventional and proposed adaptive gain scheduling PID controllers. The simulation results show an improvement in performance parameters with adaptive gain scheduling PID controllers in the presence of disturbance and noise in the controllers. Moreover, in case of friction, the conventional PID controllers perform poorly as compared to the proposed adaptive gain scheduling PID controllers, which perform quite satisfactorily in the presence of friction.

CSTR has widespread applications in the process industry, for example, in wastewater treatment units (i.e. activated sludge reactors). A chemical reactor is a vessel where reactions are carried out to produce products from the reactants by means of one or more chemical reactions. The control objectives in a CSTR are the concentration and the temperature control of the product, which can be accomplished by controlling the inlet/outlet of the reactor/product or the coolant/heater flow rate.

For the concentration control of a CSTR different hybrid control schemes based on fuzzy logic, artificial neural network, adaptive neuro fuzzy inference system and genetic algorithms have been used for PID controller tuning. Simulation results show that the best performance in terms of settling time and overshoot has been given by adaptive neuro fuzzy inference system tuned PID controller. Moreover, the magnitude of the inverse response behaviour in case of adaptive neuro fuzzy inference system tuned PID controller is less than the conventional Ziegler Nichols and fuzzy PID methods. Furthermore, to improve reference tracking and disturbance rejection H_∞ based preview control scheme has been implemented for concentration control of a CSTR.

The findings of this research work can be utilized to improve the existing control of nonlinear systems using gain scheduling or hybrid control methods.

TABLE OF CONTENTS

Decleration ii

Certificate iii

Acknowledgement iv

Abstract vi

Table of Contents viii

List of Figures xii

List of Tables xix

Symbols xxi

Abbreviations xxiv

1. Introduction 1

1.1 Control Schemes for Nonlinear Systems 2

1.1.1 Proportional Integral Derivative Control 2

1.1.2 Adaptive Control 2

1.1.3 Sliding Mode Control 2

1.1.4 Model Predictive Control 3

1.1.5 Preview Control 3

1.1.6 Fuzzy logic Control 3

1.1.7 Artificial Neural Networks 3

1.1.8 Adaptive Neuro Fuzzy Inference System 3

1.1.9 Genetic Algorithms 4

1.2 Literature Survey 4

1.2.1 Inverted Pendulum 4

1.2.2 Continuous Stirred Tank Reactor (CSTR) 7

1.3 Observations from Literature Survey 10

1.4 Objectives of the Thesis 10

1.5 Contribution in Thesis 11

1.6 Organization of the Thesis 12

2. Stabilization and Tracking Control of One Dimensional Inverted Pendulum 14

2.1 Introduction 14

2.2 State Space Modeling of x Inverted Pendulum 14

2.2.1 Modeling without Uncertainties 15
2.2.2 Modeling with Uncertainties 16
2.3 Control Structure of x Inverted Pendulum 17
2.3.1 Time Adaptive Gain Scheduling (AGS) PID Controllers 17
2.3.2 Error Adaptive Gain Scheduling (AGS) PID Controllers 18
2.4 Stability Analysis of x Inverted Pendulum 20
2.5 Simulation Results 21
2.5.1 Stabilization with Time AGS PID Controllers 21
2.5.1.1 Stabilization without Uncertainties 21
2.5.1.2 Stabilization with Uncertainties 22
2.5.2 Tracking Control with Time AGS PID Controllers 26
2.5.3 Stabilization with Error AGS PID Controllers 28
2.5.3.1 Stabilization without Uncertainties 28
2.5.3.2 Stabilization with Uncertainties 28
2.5.4 Tracking Control with Error AGSPID Controllers 31
2.6 Conclusion 32
3. Stabilization and Tracking Control of Two Dimensional Inverted Pendulum 34
3.1 Introduction 34
3.2 State Space Modeling of x - y Inverted Pendulum 34
3.2.1 Modeling without Uncertainties 35
3.2.2 Modeling with Uncertainties 37
3.3 Control Structure of x - y Inverted Pendulum 38
3.4 Stability Analysis of x - y Inverted Pendulum 39
3.5 Simulation Results 41
3.5.1 Stabilization with Time AGS PID Controllers 41
3.5.1.1 Stabilization without Uncertainties 41
3.5.1.2 Stabilization with Uncertainties 42
3.5.2 Tracking Control with Time AGS PID Controllers 45
3.5.3 Stabilization with Error AGS PID Controllers 48
3.5.3.1 Stabilization without Uncertainties 48
3.5.3.2 Stabilization with Uncertainties 50
3.5.4 Tracking Control with Error AGS PID Controllers 53

3.6 State Space Modeling of x - z Inverted Pendulum 56
3.6.1 Modeling without Uncertainties 57
3.6.2 Modeling with Uncertainties 58
3.7 Control Structure of x - z Inverted Pendulum 59
3.8 Stability Analysis of x - z Inverted Pendulum 59
3.9 Simulation Results 61
3.9.1 Stabilization with Time AGS PID Controllers 61
3.9.1.1 Stabilization without Uncertainties 61
3.9.1.2 Stabilization with Uncertainties 62
3.9.2 Tracking Control with Time AGS PID Controllers 65
3.9.3 Stabilization with Error AGS PID Controllers 67
3.9.3.1 Stabilization without Uncertainties 68
3.9.3.2 Stabilization with Uncertainties 69
3.9.4 Tracking control with Error AGS PID Controllers 72
3.10 Conclusion 75
4. Modelling and Control of a Three Dimensional Inverted Pendulum 77
4.1 Introduction 77
4.2 State Space Modeling of x - y - z Inverted Pendulum 77
4.2.1 Modeling without Uncertainties 78
4.2.2 Modeling with Uncertainties 81
4.3 Control Structure of x - y - z Inverted Pendulum 82
4.4 Stability Analysis of x - y - z Inverted Pendulum 84
4.5 Simulation Results 85
4.5.1 Stabilization with Time AGS PID Controllers 85
4.5.1.1 Stabilization without Uncertainties 85
4.5.1.2 Stabilization with Uncertainties 87
4.5.2 Tracking Control with Time AGS PID Controllers 92
4.5.3 Stabilization with Error AGS PID Controllers 96
4.5.3.1 Stabilization without Uncertainties 97
4.5.3.2 Stabilization with Uncertainties 98
4.5.4 Tracking Control with Error AGS PID Controllers 103

4.6 Conclusion 108

5. Hybrid Control of a Continuous Stirred Tank Reactor 109

5.1 Introduction 109

5.2 Model of a Continuous Stirred Tank Reactor 109

5.3 Conventional Control of a CSTR 111

5.3.1 Conventional PID Controller 111

5.4 Hybrid Control of a CSTR 112

5.4.1 Fuzzy Logic Based PID Controller 112

5.4.2 Artificial Neural Networks based PID Controller 119

5.4.3 Adaptive Neuro Fuzzy Inference System (ANFIS) based PID Controller 120

5.4.4 Genetic Algorithms based PID Controller 123

5.5 H_∞ based Preview Control 125

5.6 Conclusion 126

6. Conclusion and Future Scope 128

6.1 Conclusions 128

6.2 Scope for Future Work 130

References 131

Appendix 140

List of Research Papers Published and Communicated 142

List of Figures

Figure 2.1 x Inverted Pendulum System

Figure 2.2 Control Structure of x Inverted Pendulum

Figure 2.3 Stability Analysis of x Inverted Pendulum with AGS PID Controllers

Figure 2.4 Stabilization of x Inverted Pendulum using Time AGS PID Controllers without Uncertainties

Figure 2.5 Stabilization of x Inverted Pendulum using Time AGS PID Controllers with Disturbance

Figure 2.6 Simulink Block-Set for x Inverted Pendulum Control with Noise in Controllers

Figure 2.7 Stabilization of x Inverted Pendulum using Time AGS PID Controllers with Noise in the Controllers

Figure 2.8 Simulink Model of x Inverted Pendulum with Simple Friction Model

Figure 2.9 Stabilization of x Inverted Pendulum using Time AGS PID Controllers with Simple Friction Model

Figure 2.10 Simulink Block-Set of x Inverted Pendulum with Exponential Friction Model

Figure 2.11 Stabilization of x Inverted Pendulum using Time AGS PID Controllers with Exponential Friction Model

Figure 2.12 Tracking Control of x Inverted Pendulum using Time AGS PID Controllers without Uncertainties

Figure 2.13 Tracking Control of x Inverted Pendulum using Time AGS PID Controllers with Disturbance

Figure 2.14 Tracking Control of x Inverted Pendulum using Time AGS PID Controllers with Noise in Controllers

Figure 2.15 Tracking Control of x Inverted Pendulum using Time AGS PID Controllers with Simple Friction Model

Figure 2.16 Tracking Control of x Inverted Pendulum using Time AGS PID Controllers With Exponential Friction Model

Figure 2.17 Stabilization of x Inverted Pendulum using Error AGS PID Controllers without Uncertainties

Figure 2.18 Stabilization of x Inverted Pendulum Error AGS PID Controllers with Disturbance

Figure 2.19 Stabilization of x Inverted Pendulum Error AGS PID Controllers with Noise in Controllers

Figure 2.20 Stabilization of x Inverted Pendulum Error AGS PID Controllers with Simple Friction Model

Figure 2.21 Stabilization of x Inverted Pendulum Error AGS PID Controllers with Exponential Friction Model

Figure 2.22 Tracking Control of x Inverted Pendulum Error AGS PID Controllers without Uncertainties

Figure 2.23 Tracking Control of x Inverted Pendulum Error AGS PID Controllers with Disturbance

Figure 2.24 Tracking Control of x Inverted Pendulum Error AGS PID Controllers with Noise in Controllers

Figure 2.25 Tracking Control of x Inverted Pendulum Error AGS PID Controllers with Simple Friction Model

Figure 2.26 Tracking Control of x Inverted Pendulum Error AGS PID Controllers with Exponential Friction Model

Figure 3.1 x - y Inverted Pendulum System

Figure 3.2 Control Structure of x - y Inverted Pendulum

Figure 3.3 $\dot{V}$ Vs Time for x - y Inverted Pendulum

Figure 3.4 Stabilization of x - y Inverted Pendulum using Time AGS PID Controllers without Uncertainties

Figure 3.5 Stabilization of x - y Inverted Pendulum using Time AGS PID Controllers with Disturbance

Figure 3.6 Stabilization of x - y Inverted Pendulum using Time AGS PID Controllers with Noise in the Controllers

Figure 3.7 Stabilization of x - y Inverted Pendulum using Time AGS PID Controllers with Simple Friction Model

Figure 3.8 Stabilization of x - y Inverted Pendulum using Time AGS PID Controllers with Exponential Friction Model

Figure 3.9 Tracking Control of x - y Inverted Pendulum using Time AGS PID Controllers without Uncertainties
Figure 3.10 Tracking Control of x - y Inverted Pendulum using Time AGS PID Controllers with Disturbance
Figure 3.11 Tracking Control of x - y Inverted Pendulum using Time AGS PID Controllers with Noise in the Controllers
Figure 3.12 Tracking Control of x - y Inverted Pendulum using Time AGS PID Controllers with Simple Friction Model
Figure 3.13 Tracking Control of x - y Inverted Pendulum using Time AGS PID Controllers with Exponential Friction Model
Figure 3.14 Stabilization of x - y Inverted Pendulum using Error AGS PID Controllers without Uncertainties
Figure 3.15 Stabilization of x - y Inverted Pendulum using Error AGS PID Controllers with Disturbance
Figure 3.16 Stabilization of x - y Inverted Pendulum using Error AGS PID Controllers with Noise in the Controllers
Figure 3.17 Stabilization of x - y Inverted Pendulum using Error AGS PID Controllers with Simple Friction Model
Figure 3.18 Stabilization of x - y Inverted Pendulum using Error AGS PID Controllers with Exponential Friction Model
Figure 3.19 Tracking Control of x - y Inverted Pendulum using Error AGS PID Controllers without Uncertainties
Figure 3.20 Tracking Control of x - y Inverted Pendulum using Error AGS PID Controllers with Disturbance
Figure 3.21 Tracking Control of x - y Inverted Pendulum using Error AGS PID Controllers with Noise in the Controllers
Figure 3.22 Tracking Control of x - y Inverted Pendulum using Error AGS PID Controllers with Simple Friction Model
Figure 3.23 Tracking Control of x - y Inverted Pendulum using Error AGS PID Controllers with Exponential Friction Model
Figure 3.24 x - z Inverted Pendulum System

Figure 3.25 Control Structure of $x-z$ Inverted Pendulum

Figure 3.26 $\dot{V}$ Vs Time for $x-z$ Inverted Pendulum

Figure 3.27 Stabilization of $x-z$ Inverted Pendulum using Time AGS PID Controllers without Uncertainties

Figure 3.28 Stabilization of $x-z$ Inverted Pendulum using Time AGS PID Controllers with Disturbance

Figure 3.29 Stabilization of $x-z$ Inverted Pendulum using Time AGS PID Controllers with Noise in the Controllers

Figure 3.30 Stabilization of $x-z$ Inverted pendulum using Time AGS PID Controllers with Simple Friction Model

Figure 3.31 Stabilization of $x-z$ Inverted Pendulum using Time AGS PID Controllers with Exponential Friction Model

Figure 3.32 Tracking Control of $x-z$ Inverted Pendulum using Time AGS PID Controllers without Uncertainties

Figure 3.33 Tracking Control of $x-z$ Inverted Pendulum using Time AGS PID Controllers with Disturbance

Figure 3.34 Tracking Control of $x-z$ Inverted Pendulum using Time AGS PID Controllers with Noise in the Controllers

Figure 3.35 Tracking Control of $x-z$ Inverted Pendulum using Time AGS PID Controllers with Simple Friction Model

Figure 3.36 Tracking Control of $x-z$ Inverted Pendulum using Time AGS PID Controllers with Exponential Friction Model

Figure 3.37 Stabilization of $x-z$ Inverted Pendulum using Error AGS PID Controllers without Uncertainties

Figure 3.38 Stabilization of $x-z$ inverted pendulum using Error AGS PID Controllers with Disturbance

Figure 3.39 Stabilization of $x-z$ Inverted Pendulum using Error AGS PID Controllers with Noise in the Controllers

Figure 3.40 Stabilization of $x-z$ Inverted Pendulum using Error AGS PID Controllers with Simple Friction Model

Figure 3.41 Stabilization of $x-z$ Inverted pendulum using Error AGS PID Controllers with Exponential Friction Model

Figure 3.42 Tracking Control of x-z Inverted Pendulum using Error AGS PID Controllers without Uncertainties

Figure 3.43 Tracking Control of x-z Inverted Pendulum using Error AGS PID Controllers with Disturbance

Figure 3.44 Tracking Control of x-z Inverted Pendulum using Error AGS PID Controllers with Noise in the Controllers

Figure 3.45 Tracking Control of x-z Inverted Pendulum using Error AGS PID Controllers with Simple Friction

Figure 3.46 Tracking Control of x-z Inverted Pendulum using Error AGS PID Controllers with Exponential Friction

Figure 4.1 x-y-z Inverted Pendulum System

Figure 4.2 Control structure of x-y-z Inverted Pendulum

Figure 4.3 $\dot{V}$ Vs Time for x-y-z Inverted Pendulum

Figure 4.4 Stabilization of x-y-z Inverted Pendulum using Time AGS PID Controllers without Uncertainties

Figure 4.5 Stabilization of x-y-z Inverted Pendulum using Time AGS PID Controllers with Disturbance

Figure 4.6 Stabilization of x-y-z Inverted Pendulum using Time AGS PID Controllers with Noise in the Controllers

Figure 4.7 Stabilization of x-y-z Inverted Pendulum using Time AGS PID Controllers with Simple Friction Model

Figure 4.8 Stabilization of x-y-z Inverted pendulum using Time AGS PID Controllers with Exponential Friction Model

Figure 4.9 Tracking control of x-y-z Inverted Pendulum using Time AGS PID Controllers without Uncertainties

Figure 4.10 Tracking control of x-y-z Inverted Pendulum using Time AGS PID Controllers with Disturbance

Figure 4.11 Tracking control of x-y-z Inverted Pendulum using Time AGS PID Controllers with noise in the Controllers

Figure 4.12 Tracking control of x-y-z Inverted Pendulum using Time AGS PID Controllers with Simple Friction Model

Figure 4.13 Tracking control of x - y - z Inverted Pendulum using Time AGS PID Controllers with Exponential Friction Model
Figure 4.14 Stabilization of x - y - z Inverted pendulum using Error AGS PID Controllers without Uncertainties
Figure 4.15 Stabilization of x - y - z Inverted Pendulum using Error AGS PID Controllers with Disturbance
Figure 4.16 Stabilization of x - y - z Inverted Pendulum using Error AGS PID Controllers with Noise in the Controllers
Figure 4.17 Stabilization of x - y - z Inverted Pendulum using Error AGS PID Controllers with Simple Friction Model
Figure 4.18 Stabilization of x - y - z Inverted Pendulum using Error AGS PID Controllers with Exponential Friction Model
Figure 4.19 Tracking control of x - y - z Inverted Pendulum using Error AGS PID Controllers without Uncertainties
Figure 4.20 Tracking control of x - y - z Inverted pendulum using Error AGS PID Controllers with Disturbance
Figure 4.21 Tracking control of x - y - z Inverted Pendulum using Error AGS PID Controllers with Noise in the Controllers
Figure 4.22 Tracking control of x - y - z Inverted Pendulum using Error AGS PID Controllers with Simple Friction Model
Figure 4.23 Tracking Control of x - y - z Inverted Pendulum using Error AGS PID Controllers with Exponential Friction Model
Figure 5.1 CSTR with a Cooling Jacket
Figure 5.2 Closed loop Response with ZN based PID Controller
Figure 5.3 Closed-Loop System with Fuzzy-PID Controller
Figure 5.4 Fuzzy Membership functions for e
Figure 5.5 Fuzzy Membership functions for de/dt
Figure 5.6 Fuzzy Membership functions for k_{p1}
Figure 5.7 Fuzzy Membership functions for k_{i1}
Figure 5.8 Fuzzy Membership functions for k_{d1}
Figure 5.9 Fuzzy PID Controller Implementation in MATLAB Simulink

Figure 5.10 Closed Loop Response using Fuzzy PID Controller
Figure 5.11 Closed Loop System with Single Neuron ANN Structure
Figure 5.12 Closed Loop Response using ANN Based PID Controller
Figure 5.13 ANFIS Structure
Figure 5.14 Adaptive Neuro Fuzzy Controller Implementation using MATLAB Simulink
Figure 5.15 Closed loop Response using ANFIS based PID Controller
Figure 5.16 Closed Loop System with GA Based PID Controller
Figure 5.17 Closed Loop Response using GA Based PID Controller
Figure 5.18 Closed Loop Preview Control Scheme
Figure 5.19 Closed Loop H_2 and H_∞ Preview Control of a CSTR

List of Tables

Table 2.1 Inverted Pendulum Parameters

Table 2.2 Parameters of Adaptive Gain Scheduling PID Controllers for Controlling x Inverted Pendulum

Table 2.3 Quantitative Analysis of x Inverted Pendulum Control using Time AGS PID Controllers without Uncertainties

Table 2.4 Quantitative Analysis of x Inverted Pendulum Control using Time AGS PID Controllers with Disturbance

Table 2.5 Quantitative Analysis of x Inverted Pendulum Control using Error AGS PID Controllers without Uncertainties

Table 2.6 Quantitative Analysis of x Inverted Pendulum Control using Error AGS PID Controllers with Disturbance

Table 3.1 Parameters of AGS PID Controllers for Controlling x - y Inverted Pendulum

Table 3.2 Quantitative Analysis of x - y Inverted Pendulum Control using Time AGS PID Controllers without Uncertainties

Table 3.3 Quantitative Analysis of x - y Inverted Pendulum Control using Time AGS PID Controllers with Disturbance

Table 3.4 Quantitative Analysis of x - y Inverted Pendulum Control using Error AGS PID Controllers without Uncertainties

Table 3.5 Quantitative Analysis of x - y Inverted Pendulum Control using Error AGS PID Controllers with Disturbance

Table 3.6 Parameters of AGS PID Controllers for x - z Inverted Pendulum Control

Table 3.7 Quantitative Analysis of x - z Inverted Pendulum Control using Time AGS PID Controllers without Uncertainties

Table 3.8 Quantitative Analysis of x - z Inverted Pendulum Control using Time AGS PID Controllers with Disturbance

Table 3.9 Quantitative Analysis of x - z Inverted Pendulum Control using Error AGS PID Controllers without Uncertainties

Table 3.10 Quantitative Analysis of x - z Inverted Pendulum Control using Error AGS PID Controllers with Disturbance

Table 4.1 Parameters of Adaptive Gain Scheduling PID Controllers for x - y - z Inverted Pendulum Control

Table 4.2 Quantitative analysis of x - y - z Inverted Pendulum Control using Time AGS PID Controllers without Uncertainties

Table 4.3 Quantitative analysis with of x - y - z Inverted Pendulum Control using Time AGS PID Controllers with Disturbance

Table 4.4 Quantitative analysis of x - y - z Inverted Pendulum Control using Error AGS PID Controllers without Uncertainties

Table 4.5 Quantitative analysis without disturbance of x - y - z Inverted Pendulum Control using Error AGS PID Controllers with Disturbance

Table 5.1 Ziegler Nichols Method for PID Controller Tuning

Table 5.2 Universe of Discourse for Input and Output Fuzzy Sets

Table 5.3 Fuzzy Variable Ranges and Membership Functions for e

Table 5.4 Fuzzy Variable Ranges and Membership Functions for de/dt

Table 5.5 Fuzzy Variable Ranges and Membership Functions for k_{p1}

Table 5.6 Fuzzy Variable Ranges and Membership Functions for k_{i1}

Table 5.7 Fuzzy Variable Ranges and Membership Functions for k_{d1}

Table 5.8 Quantitative Analysis Among Different PID Tuning Methods

List of Symbols

k_p	Proportional gain
k_i	Integral gain
k_d	Derivative gain
T_i	Integral time
T_d	Derivative time
$e(t)$	Error signal
$u(t)$	Control signal
F_x	Applied force in x direction
θ	Angle made by the inverted pendulum with the vertical axis when the base moves in x direction
ϕ	Angle made by the inverted pendulum with vertical axis when the base moves in y direction
M	Mass of the base
m	Mass of the pendulum
l	Length from the pivot to the mass center of the pendulum
g	Acceleration due to gravity
L	Lagrange
$K.E$	Kinetic Energy
$P.E$	Potential Energy
F_{xfric}	Frictional force in x direction
d	Disturbance
$k_{p\min}$	Minimum value of proportional gain
$k_{P\max}$	Maximum value of proportional gain
$k_{i\min}$	Minimum value of integral gain
$k_{i\max}$	Maximum value of integral gain
$k_{d\min}$	Minimum value of derivative gain
$k_{d\max}$	Maximum value of derivative gain

k	Constant for deciding the rate at which the PID gains vary from minima to maxima
x_t	Tracking signal in x direction
y_t	Tracking signal in y direction
z_t	Tracking signal in z direction
M_P	Maximum overshoot
t_r	Rise time
t_s	Settling time
e_{ss}	Steady state error
V	Lyapunov Function
$\dot{V}$	Derivative of Lyapunov function
F_y	Force applied in y direction
F_{yfric}	Frictional force in y direction
F_z	Force applied in z direction
F_{zfric}	Frictional force in z direction
$x_1(k)$	Proportional error
$x_2(k)$	Integral error
$x_3(k)$	Derivative error
$w_1(k)$	Proportional weight
$w_2(k)$	Integral weight
$w_3(k)$	Derivative weight
$u(k)$	Control signal
η	Neuron proportional coefficient
η_P	Proportional learning speed
η_I	Integral learning speed
η_D	Derivative learning speed
J	Performance Index
$z(t)$	Controlled output
$k_{di}\ (t+i)$	Previewed signal

$w(t)$	Command signal
e	Error
Δe	Change in error

ABBREVIATIONS

AC	Adaptive Control
AGS PID	Adaptive Gain Scheduling Proportional Integral Derivative
ANFIS	Adaptive Neuro Fuzzy Inference System
ANN	Artificial Neural Network
CSTR	Continuous Stirred Tank Reactor
DOF	Degree Of Freedom
FF	Feed Forward
FL	Fuzzy Logic
FLC	Fuzzy Logic Control
GA	Genetic Algorithm
GS	Gain Scheduling
IMC	Internal Model Control
IMC-FC	Internal Model Control-Feedback Compensation
IT2-FLC	Internal Type 2-Fuzzy Logic Control
ISE	Integral System Error
LQR	Linear Quadratic Regulator
MIMO	Multi Input Multi Output
MPC	Model Predictive Control
MRAC	Model Reference Adaptive Control
NB	Negative Big
NS	Negative Small
PB	Positive Big
PI	Proportional Integral
PID	Proportional Integral Derivative

PS	Positive Small
RHP	Right Half Plane
SESIP	Self Erecting Single Inverted Pendulum
SMC	Sliding Mode Control
STC	Self Tuning Controller
TS	Takagi Sugeno
Z	Zero
ZN	Ziegler Nichols

CHAPTER 1

Introduction

In the real world, most of the systems are nonlinear by nature. Nonlinearities can be inherent or intentionally introduced into the system. Intentional nonlinearities such as On-Off/relay may be introduced intentionally to provide better performance either technically or economically. Inherent nonlinearities are those which naturally come with the system's hardware and motion. Coulomb friction amongst contacting surfaces and centripetal forces in rotatory motion are typical examples of inherent nonlinearities. These types of nonlinearities have inadmissible effects upon the control system performance. Therefore, these nonlinearities should be taken into consideration while designing a controller.

The control of a nonlinear system can be achieved using linear and nonlinear models. Various conventional methods for designing linear controllers for nonlinear systems exist within the literature (Pendharkar and Pillai, 2011; Woo, 1992). In these approaches, the nonlinear system is linearized about an operating point, and a suitable controller is designed. The linear model will perform satisfactorily if the operating range of the system is small, and the nonlinearities present within the system are smooth, otherwise, nonlinear control for the system is required (Khalil, 1996).

In this work, two nonlinear systems are considered for control purpose, one an inverted pendulum system, while the other a continuous stirred tank reactor (CSTR). The inverted pendulum system uses the nonlinear state space model while the CSTR uses the linear transfer function model for designing controllers.

An inverted pendulum is a renowned benchmark problem in control literature because the control of many real time systems such as segways, rocket launchers, crane lifting containers and self-balancing robots, resembles the inverted pendulum system. It is a highly nonlinear, under-actuated and non minimum phase system (Astrom and Furuta, 1999). The control objective is to keep the inverted pendulum in the upright position while following a desired reference trajectory by the base/cart.

CSTR has widespread applications in the process industry, for example, in wastewater treatment units (i.e. activated sludge reactors). A chemical reactor is a vessel where reactions are carried out to produce products from the reactants by means of one or more chemical reactions (Bequette, 2003). The control objectives in a CSTR are the concentration and the

temperature control of the product which can be accomplished by controlling the inlet/outlet or the coolant/heater flow rate.

1.1 Control Schemes for Nonlinear Systems

Different type of control schemes exists within the literature for controlling nonlinear systems. These are classified into conventional, advanced and intelligent control techniques. The different control schemes are briefly given as follows:

1.1.1 Proportional Integral Derivative Control

Due to its simplicity and unexceptional capability of solving a number of practical control problems, a proportional integral derivative (PID) controller is the most widely used controller in many non-linear applications, from process control to servo control.

The PID algorithm is described by (Astrom and Hagglund, 1995):

$$u(t) = k_p\left(e(t) + \frac{1}{T_i}\int e(t)dt + T_d \frac{de(t)}{dt} \right) \tag{1.1}$$

Where $u(t)$ is the control signal, $e(t)$ the error signal defined as the difference between the set-point and the output, k_p the proportional gain, T_i the integral time and T_d the derivative time. The parameters of the PID controller are tuned using various conventional techniques such as Ziegler Nichols, Cohen Coon (Kuo and Golnaraghi, 2009; Bequette, 2003), pole placement (Goodwin *et al*., 2001; Zhu and Guo, 2002) and intelligent techniques such as fuzzy logic and artificial neural networks (Zhu and Warwick, 2000) etc.

1.1.2 Adaptive Control

The variations in the dynamics of a process due to disturbances lead to the development of adaptive controllers, which adjusts the controller parameters according to the situation to accommodate these changes (Astrom and Wittenmark, 2009). The most commonly used adaptive controller is a gain scheduling controller in which the controller parameters change as a function of operating conditions in a preprogrammed way. Gain scheduling is a way of mapping the process parameters to the controller parameters.

1.1.3 Sliding Mode Control

In sliding mode control (SMC) the system states are forced to slide along a particular surface known as sliding surface by applying a discontinuous control signal. Once the states reach the sliding surface, SMC keeps the system states in the close vicinity of the sliding surface (Utkin, 2003). One of the major advantages of SMC is its capability of handling plant uncertainties and external disturbances (Ginoya *et al*., 2014).

1.1.4 Model Predictive Control

Model predictive control (MPC) is one of the advanced control techniques used to predict future control signal and its trajectory by knowing the present input output variables and future control signals with the help of a process model (Kumar and Ahmad, 2012). The biggest advantage of MPC is its simplicity in handling the constraints.

1.1.5 Preview Control

The preview of reference signal or exogenous signals plays a vital role in enhancing the performance of a control system in terms of tracking control and disturbance rejection. The use of future information (reference and/or disturbance) in the design of control systems is termed as preview control (Takaba, 2003). The optimal preview controller utilizes the future information about reference and disturbances to obtain better tracking and disturbance rejection with minimum control effort (Kojima, 2015).

1.1.6 Fuzzy Logic Control

Fuzzy logic control is a model free controller design technique as the controller implements a set of logical rules depending on the input-output behaviour of the plant for obtaining the control signal (Lee, 1990). Three types of fuzzy models, i.e. Mamdani, Sugeno and Sukamoto are used depending upon the application. Different defuzzification methods such as centroid of area, mean of maximum, etc. have been used to obtain a crisp value from the fuzzified output (Jang, *et al.*, 2009).

1.1.7 Artificial Neural Networks

Artificial neural networks (ANNs) are information processing nonlinear computational models built up from interconnected elementary processing devices called neurons (Sivanandam *et al.*, 2007). ANNs are used for nonlinear mapping between the input and output, making them a cost effective tool to synthesize accurate forward and inverse models of nonlinear dynamical systems. Furthermore, ANN can be employed in auto-tuning of PID controllers.

1.1.8 Adaptive Neuro Fuzzy Inference System

Adaptive Neuro Fuzzy Inference System (ANFIS) is a kind of neural network based on Takagi–Sugeno fuzzy inference system (Jang, *et al.*, 2009). It combines the features of artificial neural networks (i.e. their learning capability) and fuzzy logic (i.e. their expert knowledge) to get the benefits of both in a single structure (Woo, 2002). ANFIS develops an input-output mapping based on both the human knowledge and the input-output data pairs.

1.1.9 Genetic Algorithms

Genetic algorithms are derivative free stochastic optimization methods. They are based upon the principle of natural selection and evolutionary processes (Jang *et al*., 2009). They can be implemented on parallel processing machines due to their parallel search procedures, to speed up their operation. Genetic algorithms are used in control systems for tuning the parameters of a PID controller in an optimized way (Saini *et al.*, 2005).

1.2 Literature Survey

An extensive literature survey has been carried out for the control schemes of an inverted pendulum and a continuous stirred tank reactor (CSTR) which is given below:

1.2.1 Inverted Pendulum

Inverted pendulums discussed within the literature are x inverted pendulum (Kumar and Jerome, 2013), $x-y$ inverted pendulum or spherical inverted pendulum (Liu *et al*., 2008) and $x-z$ inverted pendulum (Maravall, 2004). The x inverted pendulum can move in x horizontal direction, while the $x-y$ inverted pendulum can move in xy horizontal plane, and an $x-z$ inverted pendulum can move in xz horizontal and vertical plane. Due to the gravity effect, controlling an inverted pendulum is a challenging task. The control of an inverted pendulum has been divided into three parts, i.e. the swing up control (Muskinja and Tovornik, 2006, Mason *et al*., 2008) the stabilization control (Bloch *et al.*, 2000) and the tracking control (Chang and Lee, 2007).

The stabilization and tracking control of x, $x-y$ and $x-z$ inverted pendulums using PID controllers have been discussed by Wang (2011). The author proposed a simple method for implementing PID controllers for three different types of inverted pendulums. The proposed scheme provides robustness to outer large and fast disturbances. The author also presented a sliding mode control strategy for the stabilization and tracking control of $x-z$ inverted pendulum (Wang, 2012). A two-loop PID controller has been designed by Nasir (2007) for the stabilization and tracking control of an inverted cart–pendulum system. The proposed scheme uses two PID controllers, one PID controller for position control of the cart whereas the other for angle control of the pendulum. PID controllers designed via pole placement technique have been used by Ghosh *et al*. (2012) for stabilization of the inverted pendulum system. A two-loop robust PID controller has been designed via pole placement technique in which the position of the closed-loop poles have been attained from a linear quadratic regulator (LQR) design. The proposed scheme provides good robustness as

compared with the LQR design method. Prasad *et al.* (2011) proposed conventional and intelligent control schemes for stabilizing an inverted pendulum system. Apart from proposing a two loop PID controller for the stabilization of an inverted pendulum system the authors presented a PID plus linear quadratic regulator (LQR) control scheme. The authors also proposed a fuzzy logic based controller and also carried out the comparative analysis of the three control schemes. Kumar and Jerome (2013) proposed a robust LQR technique for the stabilization and tracking control of Self Erecting Single Inverted Pendulum (SESIP). The proposed scheme stabilizes the pendulum in upright position keeping the cart system to track the given reference signal even in the presence of disturbance. The proposed scheme consists of two controllers, i.e. the swing up controller for swinging up the pendulum in the vertical position and the stabilizing controller for maintaining the pendulum to stand vertically upright. Postelnik (2011) proposed an approximate output regulation control for the stabilization of a spherical inverted pendulum. Ping and Huang (2012) proposed the approximate output regulation of spherical inverted pendulum by neural network control. Lee *et al.* (2014) used an output feedback controller for the stabilization of inverted cart pendulum system in the presence of uncertainties. Liu *et al.* (2008) proposed a nonlinear control law for stabilizing a spherical inverted pendulum.

Apart from the above control strategies, Lyapunov approach (Ibanez *et al.*, 2006) and continuous state feedback approach (Angeli, 2001) have also been implemented for controlling an inverted pendulum. Energy based approach for the stabilization of the inverted pendulum has been presented by Spong and Praly (1996). A partial feedback linearization method was used for linearizing the cart dynamics followed by shifting of energy from cart to pendulum. Joglekar (2001) used the energy based method for swing up and stabilization of an inverted pendulum system. An energy based method for the swing up and stabilization of an inverted pendulum system with restricted cart length has been presented by Chatterjee *et al.* (2002). Henmi *et al.* (2010) presented a state feedback controller for stabilizing an inverted pendulum with linearization of the inverted pendulum around an equilibrium point. Lozano *et al.* (2000) stabilized the inverted pendulum about its homoclinic orbit prior to stabilization. A Lagrangian approach to find out the desired closed-loop response for stabilizing an inverted pendulum system has been implemented by Bloch *et al.* (2001)

Stabilization of an inverted cart pendulum system in the presence of disturbances using two sliding surfaces, one for the inverted pendulum and the other for cart has been presented by Park and Chwa (2009). Adhikary and Mahanta (2013) used backstepping along with

SMC to stabilize the inverted pendulum. An integral SMC for dealing with model uncertainties in controlling a two-wheeled mobile inverted pendulum system has been presented by Xu *et al.* (2013) ; Cau and Xu, (2004). The nonlinear control of a two wheeled mobile robot based on SMC has been presented by Sinha *et al.* (2015).

A new pole placement fractional PI-state feedback design for the stabilization of an inverted cart pendulum system has been presented by Bettayeb *et al.* (2014). Ray *et al.* (2007) proposed the stabilization of an inverted pendulum via fuzzy control. A survey on various control techniques such as bang bang control, PID control, fuzzy logic control, neural network control, etc. implemented on an inverted pendulum system has been presented by Boubaker (2012).

Kar and Behera (2009) proposed a Takagi Sugeno fuzzy model for balancing a cart-pole system. Lu *et al.* (2011) proposed an adaptive fuzzy neural network controller for tracking control of an inverted pendulum system. A comparative analysis of different control techniques applied for stabilizing an inverted pendulum has been reported in the literature by Yadav *et al.* (2010). The authors used conventional PID controller and fuzzy logic controllers for controlling the inverted pendulum. Nagar et al. (2014) proposed the interval type-2 fuzzy logic controller (IT2-FLC) for controlling the inverted pendulum mounted on a cart. Also Bardini *et al.* (2014) proposed interval type-2 fuzzy PID controller for uncertain nonlinear inverted pendulum system. The proposed IT2F-PID controller is able to handle the effect of structure uncertainties due to the structure of the interval type-2 fuzzy logic system (IT2-FLS). Anderson (1989) proposed neural network based control of an inverted pendulum system. The ANN based control of an inverted pendulum has also been presented by Jaleel and Francis (2013). In the proposed scheme the weights and bias of the ANN controller were optimized using simulated annealing optimization technique (Ingber, 2012). Lin and Sheu (1992) proposed a hybrid control scheme using fuzzy logic control and a linear state-feedback control approach for controlling an inverted pendulum system. The hybrid control for global stabilization of the cart-pendulum system has been presented by Zhao and Spoong (2001). The control of an inverted pendulum system based on Kalman filter has been presented by Wanli and Guoxin (2014). However, none of the authors have discussed the modelling and control of a three dimensional x-y-z inverted pendulum which can move in xy horizontal plane by two horizontal forces and z vertical direction by a vertical force. Also, a little or no efforts have been made in designing PID controllers based on gain

scheduling method for the stabilization and tracking control of the inverted pendulum system in the presence of uncertainties such as friction or noise.

1.2.2 Continuous Stirred Tank Reactor (CSTR)

The control objective in a CSTR is the concentration and temperature control of the product. Viel *et al.* (1997) proposed a set of state feedback controllers that guarantee the temperature stabilization of CSTR in spite of strong uncertainties. However, the upper bound on input has not been considered in the proposed approach which may affect the global stabilization property. An output feedback controller to regulate the concentration in a CSTR having Van de Vusse reaction has been presented by Kuntanaprida and Marusak (2012). The authors proposed a nonlinear observer and an extended nonlinear state feedback controller to control the concentration. Longchamp (1980) developed a feedback control law for a class of bilinear plants. The proposed approach has been applied to a CSTR. But if the unique positive definite solution of the Lyapunov matrix equation is discontinuous Lyapunov direct method cannot be used. Burghart and Lefkowitz (1969) presented an optimal control system design technique to determine the optimal static operating conditions of the process by using measured disturbances. The given approach is used to control the operation of a stirred tank heater. However, for more complex systems the dimension of the parameter space increases, which degrades the system performance. Ramirez *et al.* (1999) proposed a robust PI controller for stabilizing a CSTR. Gallegos (1988) developed a nonlinear control algorithm for regulation of concentration, temperature and jacket temperature of a non isothermal CSTR. The developed algorithm uses a linear system transformation which leads to a robust and stable nonlinear regulator. The advantage of the proposed algorithm is stabilization of the original nonlinear system. The major problem when using a linear system transformation is that it is not possible to transform all the nonlinear systems of linear equivalent systems. Hoang *et al.* (2011) proposed a pseudo Hamiltonian approach for the modelling and control of a CSTR. Lyapunov based approach for controlling a CSTR has been presented in the literature by Haong *et al*. (2012).

Dasgupta *et al.* (2010) proposed an internal model control (IMC) based controller design for MIMO systems with time delay. The proposed controller has been applied to a stirred water tank. The advantage of the proposed scheme is its good reference tracking, disturbance rejection and robustness. Hu and Rangaiah (2010) presented an IMC with feedback compensation (IMC-FC) for uncertain nonlinear systems. The proposed approach has been applied to control a CSTR and results in better performance of the IMC control system due to attenuation of the modeling errors. The authors assumed the functions in the

system model to be smooth for developing IMC and IM-FC. An adaptive IMC and an augmented IMC with anti-wind up have been proposed by Hu and Rangaiah (2000) for nonlinear systems having input constraints. The proposed approach is applied to control the temperature of a CSTR. But for higher-order systems the IMC based method becomes mathematically complex. Aoyama *et al.* (1995) presented an IMC scheme using fuzzy neural network for modeling nonlinear processes. The authors developed a novel fuzzy neural network structure using hyper ellipsoids to avoid the increase in the number of hidden nodes. The proposed approach has been applied to model and control a CSTR and a pH neutralization process.

A self-learning PID control scheme for multivariable nonlinear systems with unknown dynamics has been presented by Yu *et al.* (2007). The proposed scheme uses an online adaptive neural network model to learn system dynamics, while the PID control parameters are updated by the Lyapunov method to minimize squared tracking error. The proposed approach has been applied to a CSTR but requires more computational time. A Stable adaptive neuro-control of nonlinear discrete-time systems has been presented by Zhu and Guo (2007). Yu *et al.* (2005) developed a fault-tolerant control scheme for a CSTR using an auto tuning PID controller. The proposed algorithm computes an optimal control variable based on an adaptive neural network model to minimize the sum squared error (tracking error) function of the predicted system. Since the adaptive neural network model is online trained, modeling errors may occur due to sensor faults, which may lead to process tracking error. Perez and Albertos (2004) analyzed the time response of a PI controlled, CSTR with an exothermic first-order irreversible reaction. The authors observed that self-oscillations and chaotic dynamics can appear by analyzing the parameters of the PI controller and saturation of cooling water temperature. The advantage of the given analysis is that it helps in developing more sophisticated mathematical models and control systems. A non linear PID control scheme and a nonlinear MPC scheme using local linear models has been presented by Prakash and Srinivasan (2009). The proposed approach has been applied to a CSTR. The advantages of the proposed scheme are good set-point tracking, robustness, disturbance rejection and lesser computational time. Zheng *et al.* (2004) designed a robust adaptive stabilizing controller for nonlinear systems. The proposed approach is applied in Takagi-Sugeno fuzzy model with both parameter uncertainties and external disturbances and is used to control a CSTR. The given scheme does not guarantee the robust stability of the original plant. Huebsh *et al.* (2009) presented an adaptive robust controller with varying tuning gains for controlling a CSTR. The given controller proves to be robust in the presence

of model uncertainty and disturbances. Zhang *et al.* (2009) designed a dynamic output compensator with anti-windup to deal with the robust H_∞ output feedback control problem of nonlinear processes with amplitude and rate actuator saturations. A piecewise fuzzy anti-windup dynamic output feedback controller is designed using fuzzy modelling of nonlinear systems based on piecewise quadratic Lyapunov functions. The resulting system is guaranteed to be stable with robust H_∞ control performance. But the effect of time delay on the performance of the designed compensator has not been tested by the authors. Balan and Umapathy (2002) presented a variable structure/sliding mode control for CSTR process. Sliding mode control schemes for controlling a nonlinear plant have also been discussed within the literature by Daly and Wang (2009), Roopaei *et al.* (2009), Shahraz and Boozarjomehry (2009), Chen and Peng (2005).

Ozkan (2004) presented predictive based control of a jacketed CSTR. Thornhill *et al.* (2007) presented the Simulink model of a CSTR which uses PI controller for controlling the CSTR.

An adaptive fuzzy control design scheme has been proposed by Chen and Liu (2005) to control a CSTR. The proposed approach uses the back stepping technique to control a CSTR. The proposed controller guarantees internal stability of the closed-loop adaptive systems and has a bounded approximate gain from disturbance input to system's output. Lin *et al.* (2005) studied the stability problem for uncertain Takagi-Sugeno fuzzy time delay systems in the presence of parameter perturbations and external disturbances. The proposed approach has been applied to a CSTR. Galluzo and Cosenza (2011) designed type-2 fuzzy logic controllers (FLC) and a mixed feedback–feedforward control configuration for temperature control of a CSTR having bifurcations, parameter variations and uncertainty in variable measurements. The authors proposed a feed-forward control loop to maintain effective control in the presence of disturbances. Sing and Postlethwaite (1997) proposed the application of fuzzy relational models for nonlinear control of a pH Process. A model predictive controller incorporating a fuzzy model is used to control the pH in a CSTR.

ANN based control of a CSTR has been given in the literature by Yang and Linkens (1994), Lightbody and Irwin (1995). Hussain (1998) presented a review paper which discusses the role of ANN in controlling a CSTR. Li (2014) proposed an adaptive neural network based control for a CSTR having a dead zone with unknown functions. The system is transformed into three subsystems with unknown interconnection terms. Thereafter, the neural networks are used to approximate the unknown functions and finally the adaptive compensatory terms are given to compensate for the unknown parameters of the dead-zone.

But the design procedure seems to be very complex, which needs to be simplified. A neural predictive controller and a feedback controller have been designed by Wu *et al.* (2011). The predictive controller regulates the flow of limestone slurry to control the PH value while the feedback controller controls the loop slurry flow to control the outlet concentration. The given scheme provides good dynamic performance and robustness without any need of multivariable predictive controllers. Different model order reduction techniques have been discussed within the literature (Prasad, 1997) for designing controllers for different type of systems. Irrespective of the different control schemes other issues such as sensor selection for nonlinear systems in large sensor networks has been discussed within the literature (Shen *et al*., 2014).

1.3 Observations from Literature Survey

From the above literature survey, following observations have been obtained:

i. Modelling of x, $x-y$ and $x-z$ inverted pendulums have been discussed, but the modelling of a three dimensional $x-y-z$ inverted pendulum (which can move in xy horizontal plane and z vertical direction) has not been considered so far.
ii. The effect of uncertainties such as friction and the presence of noise/disturbance on the performance of x, $x-y$, $x-z$ and $x-y-z$ inverted pendulums has not been explored.
iii. Although many control schemes have been proposed, but the simplest and economically possible gain scheduling method for the adaptive control of an inverted pendulum has not been implemented.
iv. Implementation of advance control schemes such as preview control in process control applications is yet to be done. Furthermore, very few researchers have explored the use of hybrid control schemes in process control applications.

1.4 Objectives of the Thesis

Based on the literature survey the objectives of the Ph.D thesis entitled ***"Conventional and Intelligent Control of Nonlinear Systems"*** are:

i. Study of different conventional and intelligent control schemes as applicable to the nonlinear system.
ii. Implementation of a conventional controller for nonlinear system.
iii. Implementation of an intelligent controller for nonlinear system.
iv. Design of a hybrid controller for nonlinear system.

v. Implementation of advance control schemes to the nonlinear system.

1.5 Contribution in Thesis

Keeping in mind, the objectives of the thesis entitled “Conventional and Intelligent Control of Nonlinear Systems," the following work has been performed:

For an inverted pendulum

i. The gains of the conventional PID controller are fixed and can be obtained using different tuning methods such as Ziegler Nichols and relay auto tuning. However, for a nonlinear system a fixed gain PID controller may not produce satisfactory performance under all operating regions. Hence adaptive controller is preferred over a conventional controller in case of nonlinear systems. An adaptation mechanism using gain scheduling as a function of time and error has been proposed for the tuning of PID controller gains. The proposed schemes have been implemented for the stabilization and tracking control of one and two dimensional inverted pendulums i.e. x, $x-y$ and $x-z$. The stability analysis of these different types of inverted pendulums with the proposed controllers has been performed using Lyapunov stability criterion. The performance of the proposed schemes has been compared with the conventional PID scheme in terms of various performance specifications such as rise time, maximum overshoot, steady-state error, etc. Simulation results reveal that the proposed adaptive gain scheduling PID controllers provide better stabilization for all the three types of inverted pendulums while keeping the tracking at the same level as of conventional PID.

ii. The mathematical model of a new three dimensional $x-y-z$ inverted pendulum has been developed. The modelling equations obtained in the state space form are used to develop the simulink model of $x-y-z$ inverted pendulum. The stabilization and tracking control of $x-y-z$ inverted pendulum has been obtained using conventional and proposed adaptive gain scheduling PID controllers. The simulation results show that the adaptive gain scheduling PID controllers provide better performance than the conventional PID controllers in terms of maximum overshoot, rise time and settling time for x, y, θ and ϕ control. Moreover, the proposed controllers improve inverse response behaviour of the system.

iii. The effect of uncertainties (i.e. fast acting external disturbances, frictional forces in the inverted pendulum and noise in the controllers) on the performance of x, $x-y$, $x-z$

and $x-y-z$ inverted pendulums has been analysed using conventional and proposed controllers. The simulation results reveal an improvement in various time domain performance parameters with proposed controllers in the presence of disturbances and noise. Moreover when the simple friction model is considered the conventional PID controllers give an unstable response while the proposed PID controllers give a stable response. Similarly for the exponential friction model the conventional PID controllers results in oscillatory response while the proposed controllers give a stable response with zero steady state error

For CSTR

iv. A comparative analysis of tuning a PID controller using Ziegler Nichols (ZN), fuzzy logic, artificial neural network, genetic algorithm and adaptive neuro fuzzy inference system (ANFIS) has been carried out for the concentration control of a CSTR. The simulation results show an improvement in various time domain performance specifications using the intelligent methods except the rise time which is less in case of ZN method. The best performance has been given by ANFIS. Moreover the inverse response magnitude of the system in case of ANFIS method is less than the ZN and fuzzy PID methods. The steady state error remains zero with all the tuning methods.

iiv. The optimal preview controller makes use of future information about reference and disturbances to obtain better tracking and disturbance rejection in order to minimize the control effort. A closed-loop H_∞ preview control scheme has been implemented for concentration control of a continuous stirred tank reactor. The implemented scheme provides improvement in reference tracking and disturbance rejection with lesser control effort.

1.6 Organization of the Thesis

After the brief introduction and literature survey given in chapter 1 rest of the thesis is organized as follows:

Chapter 2 proposes adaptive gain scheduling (AGS) PID controllers for the stabilization and tracking control of one dimensional inverted pendulum.

Chapter 3 introduces the stabilization and tracking control of two dimensional inverted pendulums using the proposed AGS PID controllers.

Chapter 4 proposes the mathematical modelling of a three dimensional inverted pendulum. The stabilization and tracking control of three dimensional inverted pendulum has been achieved using the proposed AGS PID controllers.

Chapter 5 presents different type of hybrid methods based upon fuzzy logic (FL), neural networks (NN), adaptive neuro fuzzy inference system (ANFIS), genetic algorithms (GA) and H_∞ preview control for concentration control of a CSTR.

Chapter 6 includes the specific observations and recommendations along with the future scope of research in this area.

This is followed in succession by References and Appendix.

CHAPTER 2

Stabilization and Tracking Control of One Dimensional Inverted Pendulum

2.1 Introduction

An inverted pendulum is an under-actuated, nonlinear and non minimum phase system with lesser control inputs than the degree of freedom (DOF) (Astrom and Furuta, 1999). It consists of an inverted cylindrical rod pivoted to a base which is free to move in a particular direction. If the movement of the base is only in $x/y/z$ direction then it is called as one dimensional inverted pendulum. In this work for one dimensional case the movement of the base is taken only in x horizontal direction. Since the y horizontal direction movement of the base will have the same results as that of x direction while for the vertical z direction movement, the angle of the inverted pendulum will not change.

The control of an inverted pendulum has been divided into three parts i.e. the swing up control, the stabilization control and the tracking control. The swing up control is related to the movement of the cylindrical rod from horizontal rest position to vertically upright position. The stabilization control is related to keeping the inverted pendulum in the upright position, while in tracking control a desired reference trajectory is being followed by the base keeping the inverted pendulum in the upright position. In this chapter the stabilization and tracking control of x inverted pendulum has been discussed using the proposed adaptive gain scheduling (AGS) PID controllers. The controller gains are tuned by adaptive gain scheduling, which are functions of time and error. The condition for the stability of the system has been analyzed using Lyapunov stability criterion. The effect of uncertainties such as fast acting external disturbances, noise in the controllers and friction on the performance of an x inverted pendulum has been analyzed using the proposed AGS PID controllers. The simulation results have been compared with the conventional PID scheme given in the literature.

2.2 State Space Modeling of x Inverted Pendulum

An inverted pendulum pivoted to a base is shown in Figure 2.1. The movement of the base is taken only one dimensional i.e. x direction, therefore, the inverted pendulum is

called as an x inverted pendulum. In Figure 2.1, M represents the mass of the base, m represents mass of the pendulum and $2l$ represent the total length of the pendulum.

θ = Angle made by the inverted pendulum with the vertical axis

(x, z) and $(\dot{x}, \dot{z})$ = Position and velocity of the base in the xoz coordinate respectively

(x_P, z_P) and $(\dot{x}_P, \dot{z}_P)$ = Position and velocity of the base in $x'o'z'$ coordinate respectively

$$x_P = x + l\sin\theta \tag{2.1a}$$

$$z_p = z + l\cos\theta \tag{2.1b}$$

$$\dot{x}_p = \dot{x} + l\cos\theta\dot{\theta} \tag{2.1c}$$

$$\dot{z}_p = \dot{z} - l\sin\theta\dot{\theta} \tag{2.1d}$$

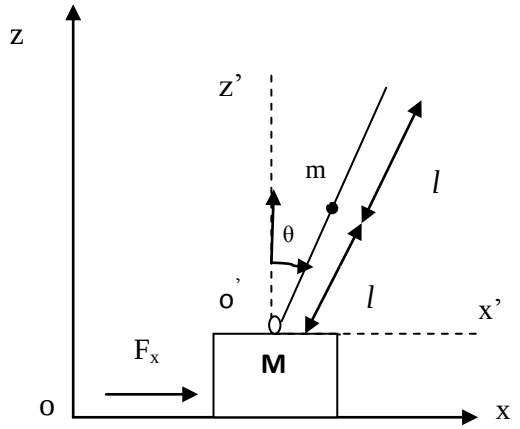

Figure 2.1 x Inverted Pendulum System (Wang, 2011)

Stabilization and tracking control of the inverted pendulum depends upon the horizontal displacement of the base in x direction which in term depends upon the applied force (F_x).

2.2.1 Modeling without Uncertainties

The Lagrange equations of the x inverted pendulum are given as (Wang, 2011):

$$\frac{d}{dt}\left(\frac{\partial L}{\partial \dot{x}}\right) - \frac{\partial L}{\partial x} = F_x \tag{2.2a}$$

$$\frac{d}{dt}\left(\frac{\partial L}{\partial \dot{\theta}}\right) - \frac{\partial L}{\partial \theta} = 0 \tag{2.2b}$$

Where Lagrangian L is defined as:

$$L = K.E. - P.E. \tag{2.3}$$

Here, $K.E.$ is the kinetic energy and $P.E.$ the potential energy of the system.

$$K.E. = \frac{1}{2}[M\,\dot{x}^2 + m(\dot{x}_P^2 + \dot{z}_P^2)] \tag{2.4a}$$

$$P.E. = mgz_p \tag{2.4b}$$

Here g represents the acceleration due to gravity.

$$K.E. = \frac{1}{2}\left[M\dot{x}^2 + m[(\dot{x} + l\cos\theta\dot{\theta})^2 + (\dot{z} - l\sin\theta\dot{\theta})^2]\right] \tag{2.5a}$$

$$P.E. = mg(z + l\cos\theta) \tag{2.5b}$$

Put Eq. (2.5 a) and Eq. (2.5 b) in Eq. (2.3)

$$L = \frac{1}{2}\left[M\dot{x}^2 + m[(\dot{x} + l\cos\theta\dot{\theta})^2 + (\dot{z} - l\sin\theta\dot{\theta})^2]\right] - mg(z + l\cos\theta) \tag{2.6}$$

Solving Eq. (2.2 a) and Eq. (2.2 b) using Eq. (2.6)

$$(M + m)\ddot{x} + ml\cos\theta\ddot{\theta} - ml\sin\theta\dot{\theta}^2 = F_x \tag{2.7a}$$

$$\cos\theta\,\ddot{x} + l\ddot{\theta} - g\sin\theta = 0 \tag{2.7b}$$

Defining $x_1 = x, x_2 = \dot{x}$ and $x_3 = \theta, x_4 = \dot{\theta}$ the state equations of the x inverted pendulum obtained from Eq. (2.7a) and Eq. (2.7b) are:

$$\dot{x}_1 = x_2 \tag{2.8}$$

$$\dot{x}_2 = \frac{-mg\cos x_3 \sin x_3 + ml\sin x_3 {x_4}^2 + F_x}{M + m\sin^2 x_3} \tag{2.9}$$

$$\dot{x}_3 = x_4 \tag{2.10}$$

$$\dot{x}_4 = \frac{-ml\cos x_3 \sin x_3 x_4^2 - \cos x_3 F_x + (M + m)g\sin x_3}{Ml + ml\sin^2 x_3} \tag{2.11}$$

From the above state equations it can be observed the x inverted pendulum is a single input (F_x) and multi output (x and θ) system.

2.2.2 Modeling with Uncertainties

The state equations of the x inverted pendulum after considering the effect of external disturbance d and friction (F_{xfric}) can be written as:

$$\dot{x}_1 = x_2 \tag{2.12}$$

$$\dot{x}_2 = \frac{-mg\cos x_3 \sin x_3 + ml\sin x_3 {x_4}^2 + F_x + F_{xfric}}{M + m\sin^2 x_3} + d \tag{2.13}$$

$$\dot{x}_3 = x_4 \tag{2.14}$$

$$\dot{x}_4 = \frac{-ml\cos x_3 \sin x_3 x_4^2 - \cos x_3 (F_x + F_{xfric}) + (M + m)g\sin x_3}{Ml + ml\sin^2 x_3} + d \tag{2.15}$$

Here, the external disturbance d is defined as:

$$d = 20\sin(20\pi t) \tag{2.16}$$

F_{xfric} is defined using simple and exponential friction models given in Appendix A.

2.3 Control Structure of x Inverted Pendulum

The control structure of x inverted pendulum is shown in Figure 2.2 (Ghosh *et al*., 2012).

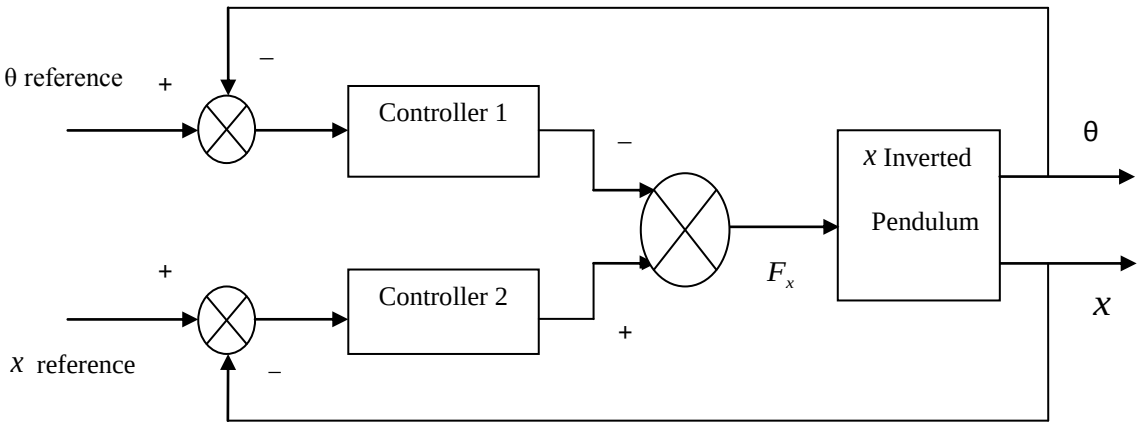

Figure 2.2 Control Structure of x Inverted Pendulum

Since an x inverted pendulum is a single input multi output system, therefore, two control loop scheme is used, one for controlling angle θ and the other position x. The reference signal for position control is a step signal while for angle control the reference angle is 0^0. For an inverted pendulum (a nonlinear system) a fixed gain PID controller may not produce satisfactory performance under all operating regions. Further, the performance of conventional PID controller may degrade in the presence of uncertainties. Therefore under such circumstances, adaptive controller (AC) is preferred over conventional controller. Different adaptive control schemes such as model reference adaptive control (MRAC), self tuning control (STC) and gain scheduling (GS) are possible (Astrom and Wittenmark, 2009). In this work conventional PID controller has been made adaptive by using Gain scheduling scheme which is based on time and error.

2.3.1 Time Adaptive Gain Scheduling (AGS) PID Controllers

In case of time adaptive gain scheduling, the PID controller gains are designed to be a function of time which varies within the specified range. The gains of k_p, k_i and k_d are scheduled to fulfill the requirements of the system and make the system more efficient. The value of k_p, k_i and k_d has been chosen based upon the following factors:

(i) ***Proportional gain*** (k_p): The value of k_P should be higher during the initial part of the system response to reduce the rise time of the system and low during the later stages to overcome overshoot and the settling time. Therefore the proportional gain scheduler is defined as:

$$k_p(t) = k_{p\min} + (k_{p\max} - k_{p\min})e^{-kt} \tag{2.17}$$

Where k is a constant for deciding the rate at which k_p varies between minimum and maximum values. For the initial phase (i.e. $t = 0$) e^{-kt} is approximately one therefore, $k_p = k_{p\max}$. As time $t \to \infty$, $e^{-kt} \to 0$, $k_p = k_{p\min}$.

(ii) ***Integral gain*** (k_i): The main function of the integral term is to remove the offset which comes in the steady state part of the response. Hence a large value of k_i is required as $t \to \infty$ and minimum value is required during the initial stage. Therefore, the integral gain can be scheduled according to:

$$k_i(t) = k_{i\max} - (k_{i\max} - k_{i\min})e^{-kt} \tag{2.18}$$

Initially i.e at $t = 0$, e^{-kt} is approximately one therefore, $k_i = k_{i\min}$. As time $t \to \infty$, $e^{-kt} \to 0$, $k_i = k_{i\max}$.

(iii) ***Derivative gain*** (k_d): The derivative term can be scheduled in accordance with:

$$k_d(t) = k_{d\min} + (k_{d\max} - k_{d\min})e^{-kt} \tag{2.19}$$

As the derivative term is used to reduce oscillations which are present during the initial stage of the response, therefore, a high value for the derivative gain is required during the initial part of the response, while during the steady state part of the response a small value is sufficient. For the initial phase (i.e. $t = 0$) e^{-kt} is approximately one therefore, $k_d = k_{d\max}$. As time $t \to \infty$, $e^{-kt} \to 0$, $k_d = k_{d\min}$.

2.3.2 Error Adaptive Gain Scheduling (AGS) PID Controllers

In error AGS PID controllers, the gains of the PID controller are scheduled as a function of error which varies within specified ranges. . The value of k_p, k_i and k_d has been chosen based upon the following factors:

(i) ***Proportional gain*** (k_p): Since the magnitude of error is high during the transient part of the system response therefore a large value of k_p is required to reduce the error of the

system. The value of k_p should be small during the steady state part of the system response, as the error will be small. Therefore the proportional gain is defined as:

$$k_p(t) = k_{p\max} - (k_{p\max} - k_{p\min})e^{-ke(t)} \tag{2.20}$$

(ii) ***Integral gain*** (k_i): A large value of k_i is required as $e(t) \to 0$ and minimum value is required during the initial stage of the response. Therefore, the integral gain can be specified as:

$$k_i(t) = k_{i\min} - (k_{i\min} - k_{i\max})e^{-ke(t)} \tag{2.21}$$

(iii) ***Derivative gain*** (k_d): The derivative term is formalized as:

$$k_d(t) = k_{d\max} - (k_{d\max} - k_{d\min})e^{-ke(t)} \tag{2.22}$$

A high value for the derivative gain is required when the error is high, while during the steady state part of the response where the value of error is low, a small value is sufficient.

These time and error AGS PID controllers have been implemented for controlling the x inverted pendulum whose parameters are given in Table 2.1. The range of gains for AGS PID 1 (Controller 1) and AGS PID 2 (Controller 2) are given in Table 2.2.

Table 2.1 Inverted Pendulum Parameters

M (kg)	m (kg)	l (m)	g (m/s^2)
1	0.1	0.3	9.8

Table 2.2 Parameters of AGS PID Controllers for x Inverted Pendulum

Parameter	$k_{p\min}$	$k_{p\max}$	$k_{i\min}$	$k_{i\max}$	$k_{d\min}$	$k_{d\max}$
PID1	24	36	1.5	3.6	3	5
PID2	-3	-2.4	-1.2	-1	-4.8	-2

The minimum and the maximum values of gains have been obtained using the trial and error method. The value of k is taken as 0.1, 0.1 and 0.05 for proportional, integral and derivative terms respectively for AGS PID 1, while for AGS PID 2 the value of k is taken as 0.1, 0.1 and 0.25 for proportional, integral and derivative terms respectively. The minimum and the maximum values of gains have been obtained using the trial and error method.

2.4 Stability Analysis of x Inverted Pendulum

The stability analysis of the x inverted pendulum system has been done using Lyapunov stability criterion (Slotine and Lee, 1999).

Theorem 2.1: The x inverted pendulum system will be stable if and only if $F_x\dot{x} \leq 0$

Proof: Defining the Lyapunov function V (a positive definite function) as the sum of kinetic energy and potential energy of the system.

$$V = \frac{1}{2}M(\dot{x}^2) + \frac{1}{2}m(\dot{x}_p^2 + \dot{z}_p^2) + mgz_p \tag{2.23}$$

Using Eq. (2.1c) and Eq. (2.1d)

$$V = \frac{1}{2}M(\dot{x}^2) + \frac{1}{2}m[(\dot{x} + l\cos\theta\dot{\theta})^2 + (\dot{z} - l\sin\theta\dot{\theta})^2] + mg(z + l\cos\theta) \tag{2.24}$$

According to Lyapunov stability criterion, for a system to be stable the derivative of the Lyapunov function should be less than or equal to zero.

i.e. $\dot{V} \leq 0$ (2.25)

$$\dot{V} = M(\dot{x}\ddot{x}) + m[(\dot{x} + l\cos\theta\dot{\theta})(\ddot{x} - l\sin\theta\dot{\theta}^2 + l\cos\theta\ddot{\theta}) + (\dot{z} - l\sin\theta\dot{\theta})(\ddot{z} - l\cos\theta\dot{\theta}^2 - l\sin\theta\ddot{\theta})] + mg(\dot{z} - l\sin\theta\dot{\theta}) \tag{2.26}$$

$$\dot{V} = M(\dot{x}\ddot{x}) + m[\dot{x}\ddot{x} - \dot{x}l\sin\theta\dot{\theta}^2 + \dot{x}l\cos\theta\ddot{\theta} + l\cos\theta\dot{\theta}\ddot{x} - l^2\sin\theta\cos\theta\dot{\theta}\dot{\theta}^2 + l^2\cos^2\theta\dot{\theta}\ddot{\theta} + \dot{z}\ddot{z} - \dot{z}l\cos\theta\dot{\theta}^2 - \dot{z}l\sin\theta\ddot{\theta} - \ddot{z}l\sin\theta\dot{\theta} + l^2\sin\theta\cos\theta\dot{\theta}\dot{\theta}^2 + l^2\sin^2\theta\dot{\theta}\ddot{\theta}] + mg\dot{z} - mgl\sin\theta\dot{\theta}] \tag{2.27}$$

Since the movement of the base is only in x direction therefore $\dot{z} = 0$

Hence Eq. (2.27) reduces to:

$$\dot{V} = M(\dot{x}\ddot{x}) + m[\dot{x}\ddot{x} - \dot{x}l\sin\theta\dot{\theta}^2 + \dot{x}l\cos\theta\ddot{\theta} + l\cos\theta\dot{\theta}\ddot{x} - l^2\sin\theta\cos\theta\dot{\theta}\dot{\theta}^2 + l^2\cos^2\theta\dot{\theta}\ddot{\theta} + l^2\sin\theta\cos\theta\dot{\theta}\dot{\theta}^2 + l^2\sin^2\theta\dot{\theta}\ddot{\theta}] - mgl\sin\theta\dot{\theta} \tag{2.28}$$

$$\dot{V} = M(\dot{x}\ddot{x}) + m[\dot{x}\ddot{x} - \dot{x}l\sin\theta\dot{\theta}^2 + \dot{x}l\cos\theta\ddot{\theta} + l\cos\theta\dot{\theta}\ddot{x} + l^2\dot{\theta}\ddot{\theta}] - mgl\sin\theta\dot{\theta} \tag{2.29}$$

$$\dot{V} = [(M + m)\ddot{x} + ml\cos\theta\ddot{\theta} - ml\sin\theta\dot{\theta}^2]\dot{x} + [\cos\theta\ddot{x} + l\ddot{\theta} - g\sin\theta]ml\dot{\theta} \tag{2.30}$$

Using Eq. (2.7a) and Eq. (2.7b) in Eq. (2.30)

$$\dot{V} = F_x\dot{x} \tag{2.31}$$

Therefore for the x inverted pendulum system to be stable:

$$F_x\dot{x} \leq 0 \tag{2.32}$$

To check the stability of x inverted pendulum with the proposed controllers the derivative of the Lyapunov function is plotted w.r.t. time.

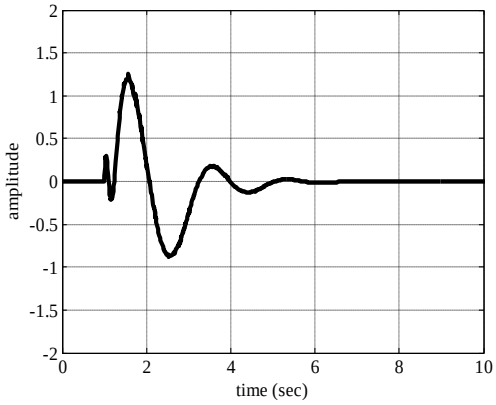

(a) $\dot{V}$ Vs. Time with Time AGS PID

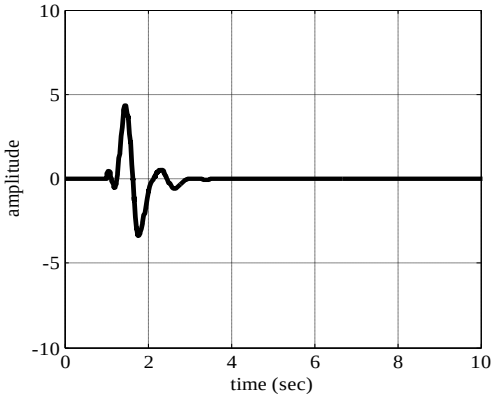

(b) $\dot{V}$ Vs. Time with Error AGS PID

Figure 2.3 Stability Analysis of x Inverted Pendulum with AGS PID Controllers

As shown in Figure 2.3 the derivative of the Lyapunov function for the given system with the proposed AGS PID controllers tends towards zero which means that the system is stable.

2.5 Simulation Results

The simulation results for the stabilization and tracking control of x inverted pendulum are given below:

2.5.1 Stabilization with Time AGS PID Controllers

Stabilization of the x inverted pendulum in vertically upward position depends upon the horizontal displacement of the base in x direction which in term depends upon the applied force (F_x).

2.5.1.1 Stabilization without Uncertainties

The simulation results without uncertainties are given in Figure 2.4.

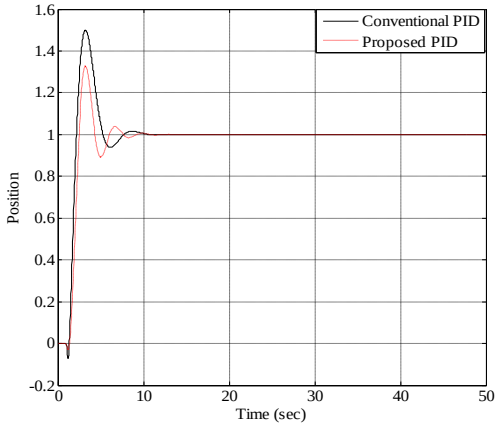

(a) Position Vs Time

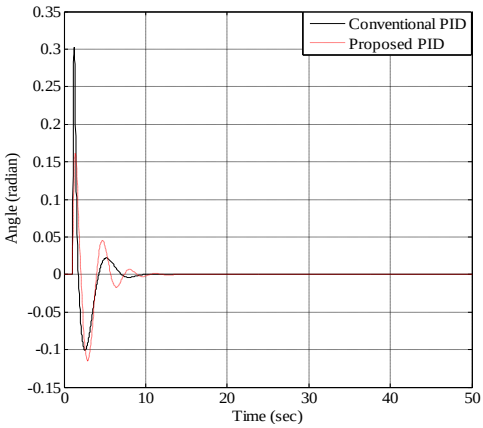

(b) Angle Control

Figure 2.4 Stabilization of x Inverted Pendulum using Time AGS PID Controllers without Uncertainties

The results are quantified in Table 2.3.

Table 2.3 Quantitative Analysis of x Inverted Pendulum Control using Time AGS PID Controllers without Uncertainties

Parameters	Without disturbance				% Improvement	
	Conventional		Proposed			
	x	θ	x	θ	x	θ
M_P	0.5	0.3	0.33	0.16	51.5	87.5
t_r	2.07	—	2.36	—	-12.2	—
t_s	7.26	5.58	7.25	5.37	0.14	3.9
e_{ss}	0	0	0	0	0	0

The Percentage (%) improvement has been calculated by using the following formula:

$$Percentage\ improvement = \frac{conventional - proposed}{proposed} \times 100$$

From the results shown above it has been observed that although the rise time (t_r) has increased slightly but there is a considerable improvement in maximum overshoot (M_p) with time AGS PID controllers due to which wear and tear on the system will be less. Moreover a slight improvement in settling time (t_s) has been obtained while the steady state error (e_{ss}) remains same at zero.

2.5.1.2 Stabilization with Uncertainties

The uncertainties considered are the fast acting external disturbances, noise in the controllers and frictional forces. Figure 2.5 gives the simulation results with fast acting external disturbances acting upon the system.

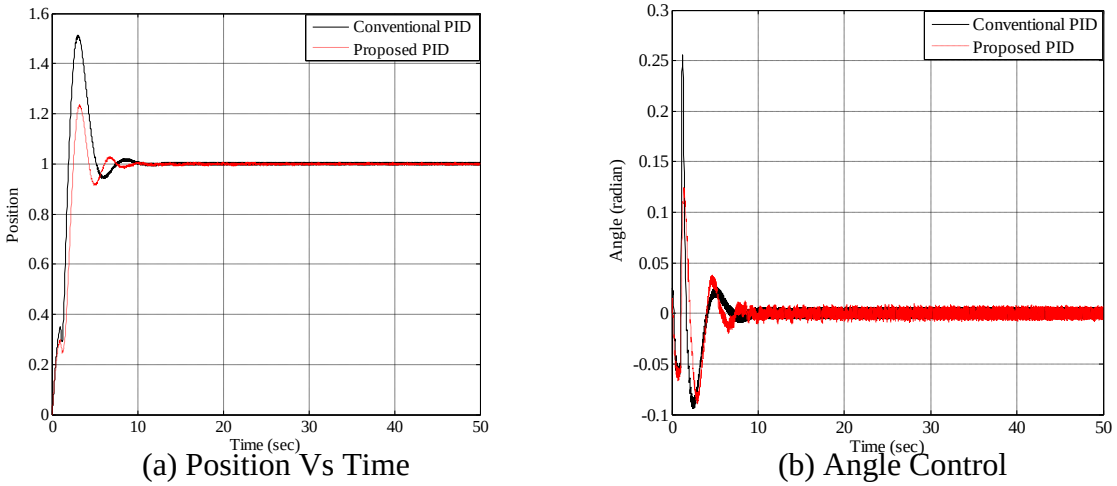

(a) Position Vs Time (b) Angle Control

Figure 2.5 Stabilization of x Inverted Pendulum using Time AGS PID Controllers with Disturbance

Table 2.4 gives the quantitative analysis in terms of various performance specifications

Table 2.4 Quantitative Analysis of x Inverted Pendulum Control using Time AGS PID Controllers with Disturbance

Parameters	With disturbance				% Improvement	
	Conventional		Proposed			
	x	θ	x	θ	x	θ
M_P	0.51	0.26	0.23	0.12	121.7	116.6
t_r	1.85	—	2.37	—	-21.9	—
t_s	8.88	5.79	7.19	5.29	23.5	9.45
e_{ss}	0	0	0	0	0	0

The quantitative analysis reveals a large amount of improvement in M_p and a considerable amount of improvement in t_s with a small deterioration in t_r using the time AGS PID controllers.

A band limited white noise has been introduced into the controllers as shown in Figure 2.6 along with disturbance in the pendulum. The simulation results are shown in Figure 2.7.

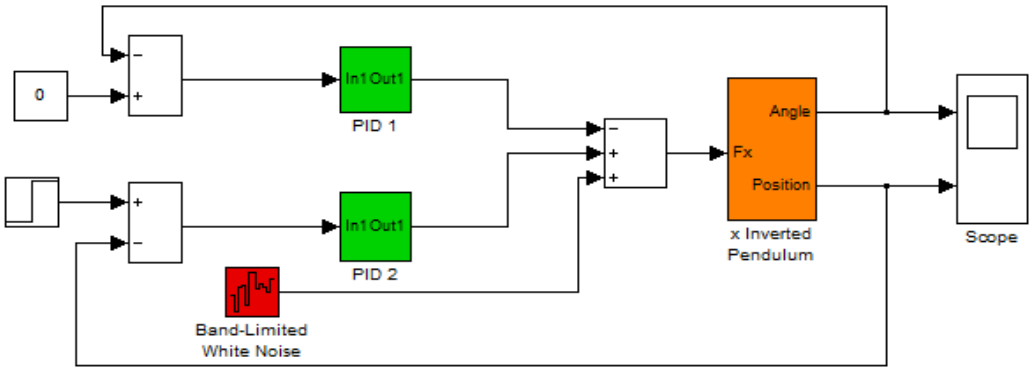

Figure 2.6 Simulink Block-Set for x Inverted Pendulum Control with Noise in Controllers

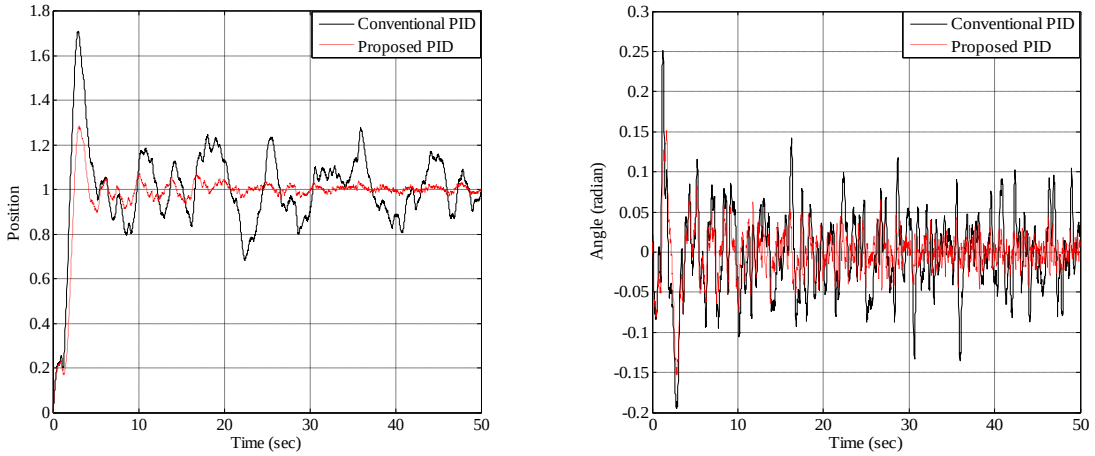

(a) Position Vs Time (b) Angle Vs Time

Figure 2.7 Stabilization of x Inverted Pendulum using Time AGS PID Controllers with Noise in the Controllers

The simulation results show that while using time AGS PID controllers less chattering has been observed in the output response of the system as compared to the conventional PID scheme.

The effect of friction into the x inverted pendulum system has been incorporated in terms of simple friction and the exponential friction models (Appendix A). The simulink representation of the x inverted pendulum when the simple friction model has been considered is shown in Figure 2.8.

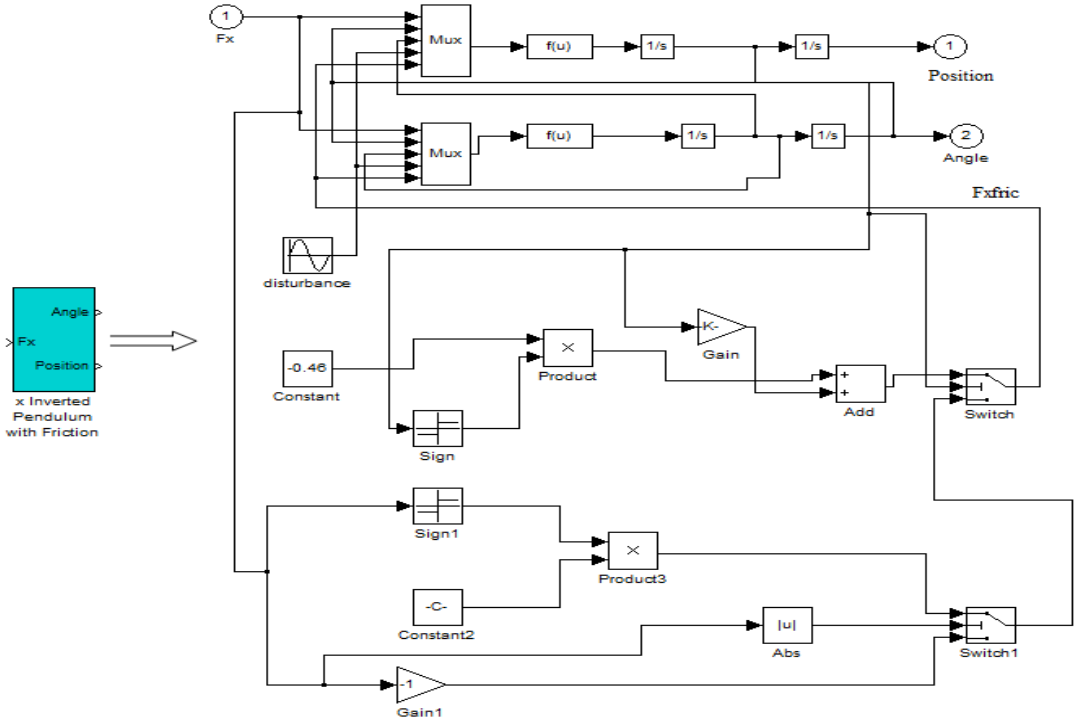

Figure 2.8 Simulink Model of x Inverted Pendulum with Simple Friction Model

The simulation results are given in Figure 2.9 for position and angle control.

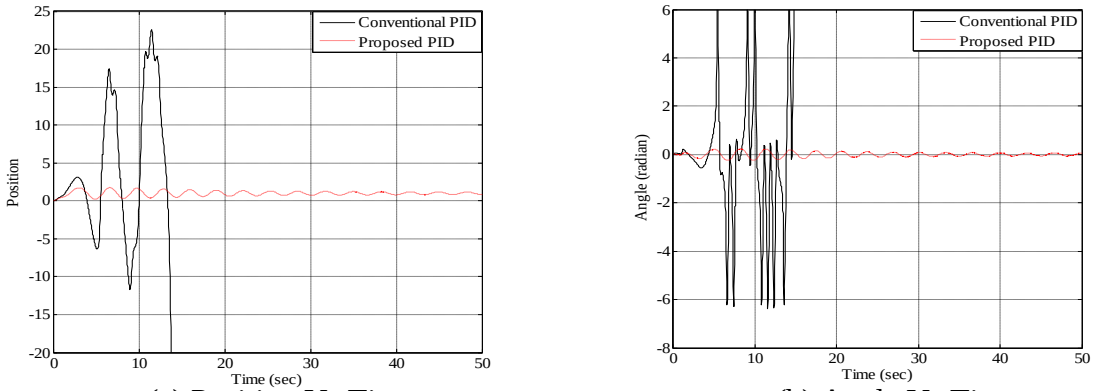

(a) Position Vs Time (b) Angle Vs Time

Figure 2.9 Stabilization of x Inverted Pendulum using Time AGS PID Controllers with Simple Friction Model

The above simulation results show that the conventional PID controllers give an unstable response while the proposed time AGS PID controllers give a stable output response.

The exponential friction model has been incorporated into the inverted pendulum system as shown in Figure 2.10 and the simulation results are given in Figure 2.11.

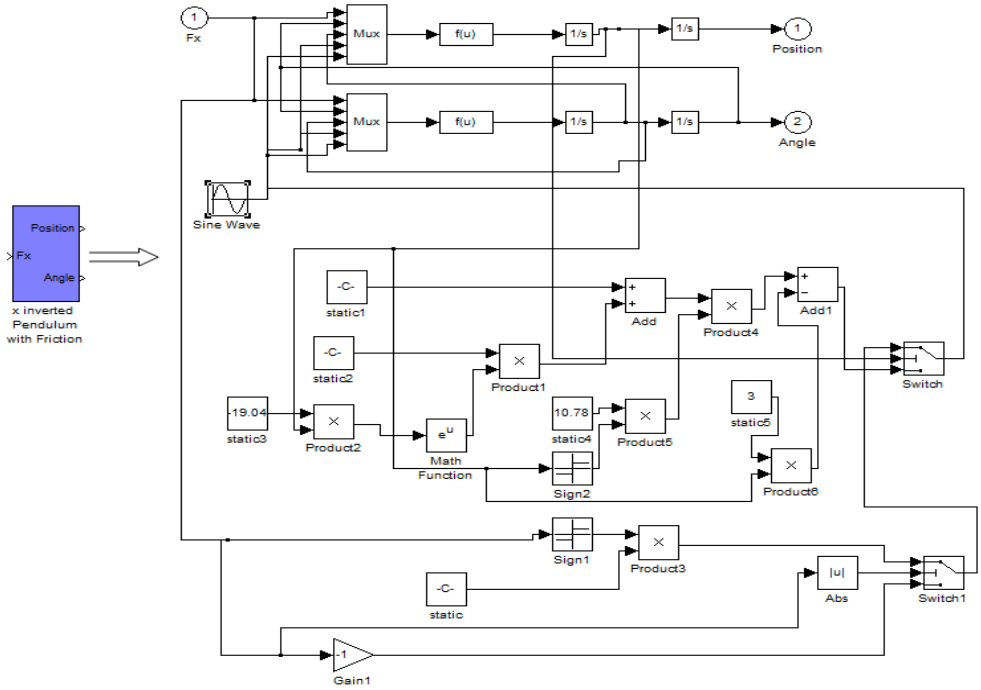

Figure 2.10 Simulink Block-Set of *x* Inverted Pendulum with Exponential Friction Model

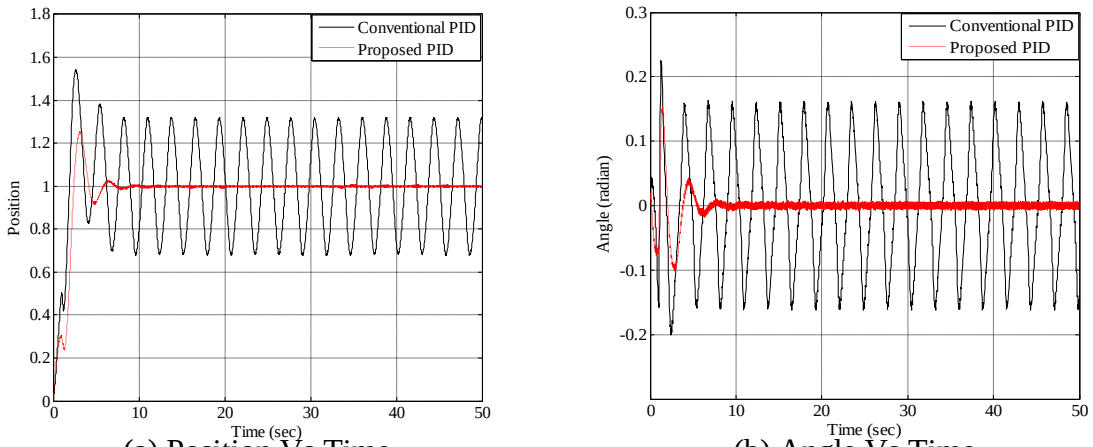

(a) Position Vs Time (b) Angle Vs Time

Figure 2.11 Stabilization of *x* Inverted Pendulum using Time AGS PID Controllers with Exponential Friction Model

The simulation results show the effectiveness of the proposed Time AGS PID controllers which give a stable response with zero steady state error as compared to the conventional PID controllers whose response is oscillatory.

2.5.2 Tracking Control with Time AGS PID Controllers

To check whether the proposed controllers provide good reference tracking, tracking signal $x_t = 0.3\sin(0.05\pi t)$ has been applied as the reference input in place of a step signal. The simulation results under different conditions are given from Figure 2.12 to Figure 2.16.

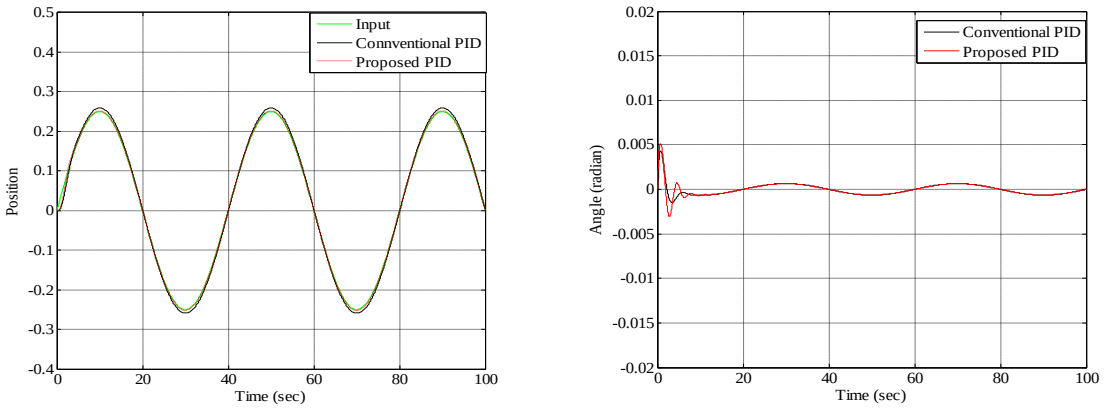

(a) Position Vs Time (b) Angle Vs Time

Figure 2.12 Tracking Control of x Inverted Pendulum using Time AGS PID Controllers without Uncertainties

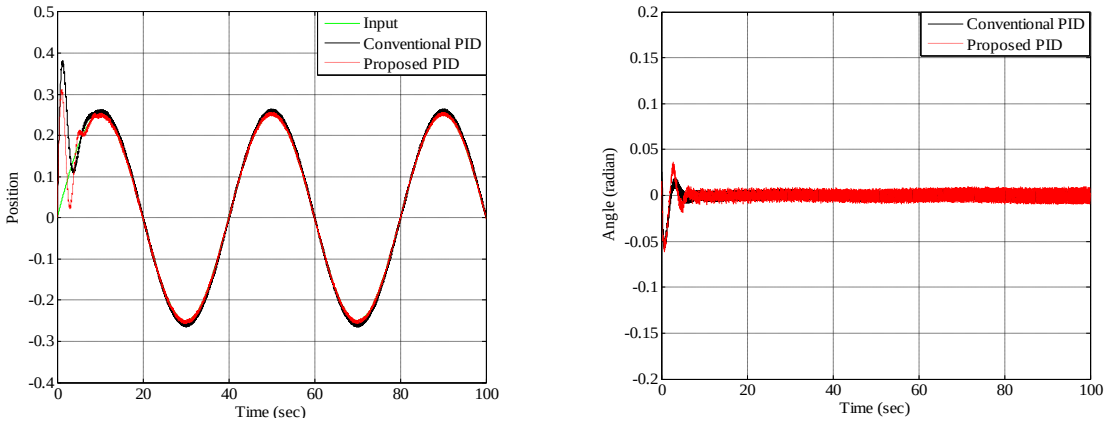

(a) Position Vs Time (b) Angle Vs Time

Figure 2.13 Tracking Control of x Inverted Pendulum using Time AGS PID Controllers with Disturbance

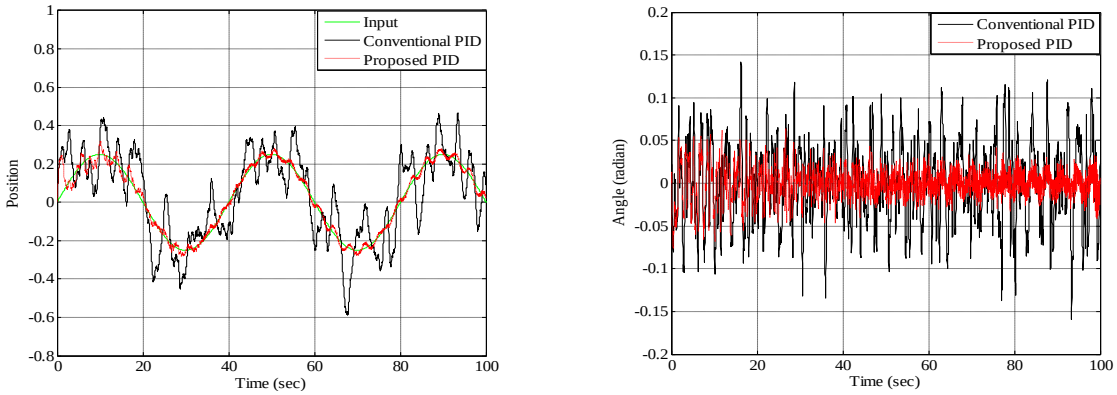

(a) Position Vs Time (b) Angle Vs Time

Figure 2.14 Tracking Control of x Inverted Pendulum using Time AGS PID Controllers with Noise in Controllers

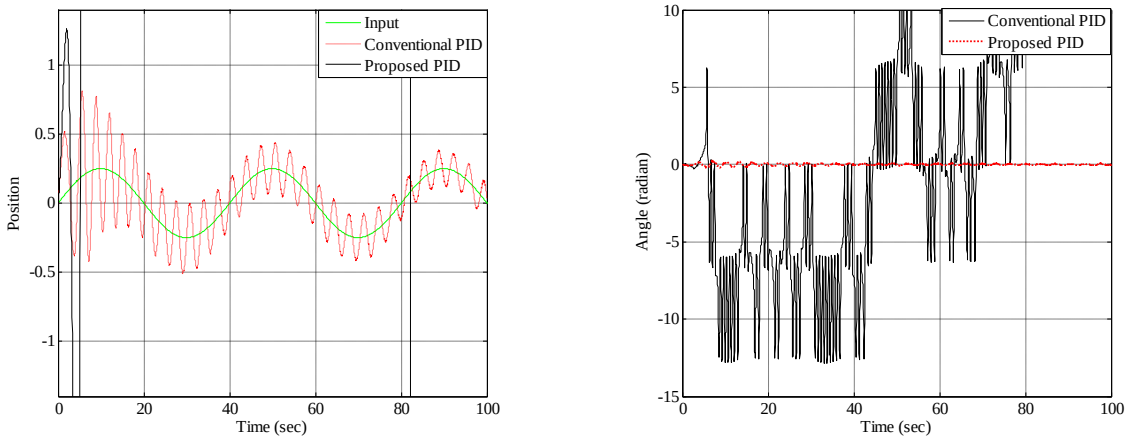

(a) Position Vs Time (b) Angle Vs Time

Figure 2.15 Tracking Control of x Inverted Pendulum using Time AGS PID with Simple Friction Model

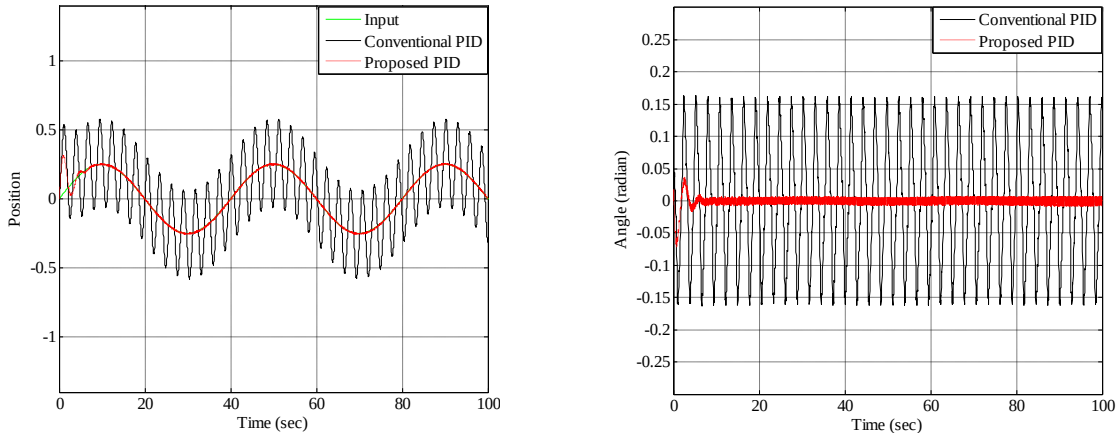

(a) Position Vs Time (b) Angle Vs Time

Figure 2.16 Tracking Control of x Inverted Pendulum using Time AGS PID Controllers with Exponential Friction Model

The simulation results in Figure 2.12 and Figure 2.13 show that both conventional as well as time AGS PID controllers provide good reference tracking. The simulation results in Figure 2.14 show that when the effect of noise is considered more chattering is observed in the system response when the conventional PID controllers are used as compared to time AGS PID controllers. The simulation results in Figure 2.15 show that when the effect of friction is considered in terms of simple friction model the conventional PID controllers fail to respond while the time AGS PID controllers provide a descent performance. Similarly, in case of exponential friction model as shown in Figure 2.16 the tracking control provided by the time AGS PID controllers is almost perfect which is not in case of conventional PID controllers.

2.5.3 Stabilization with Error AGS PID Controllers

The time AGSPID controllers are replaced by error AGSPID controllers. The simulation results under different conditions are shown below:

2.5.3.1 Stabilization without Uncertainties

The simulation results for the stabilization of x inverted pendulum without the considering the effect of uncertainties are shown in Figure 2.17 while its quantitative analysis in terms of various performance specifications is given in Table 2.5.

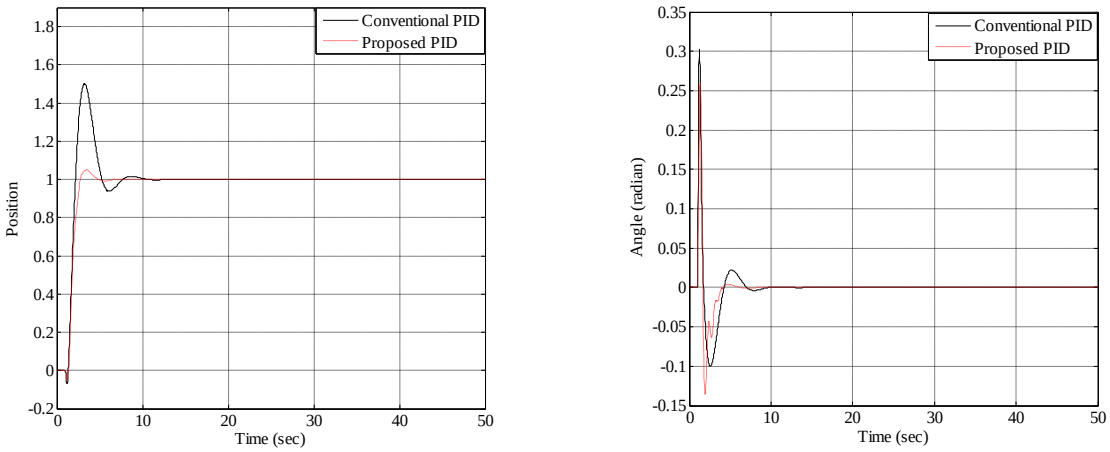

(a) Position Vs Time (b) Angle Vs Time

Figure 2.17 Stabilization of x Inverted Pendulum using Error AGS PID Controllers without Uncertainties

Table 2.5 Quantitative Analysis of x Inverted Pendulum Control using Error AGS PID Controllers without Uncertainties

Parameters	Without disturbance				% Improvement	
	Conventional		Proposed			
	x	θ	x	θ	x	θ
M_P	0.5	0.3	0.05	0.27	900	11.1
t_r	2.07	—	2.43	—	-14.8	—
t_s	7.26	5.58	4.33	3.12	67.6	78.8
e_{ss}	0	0	0	0	0	0

From the quantitative analysis it can be analyzed that while using error AGS PID controllers a large reduction in M_p takes place for both position and angle control with a significant improvement in t_s while keeping e_{ss} zero.

2.5.3.2 Stabilization with Uncertainties

The simulation results in the presence of external disturbance d are shown in Figure 2.18 while its quantitative analysis is given in Table 2.6.

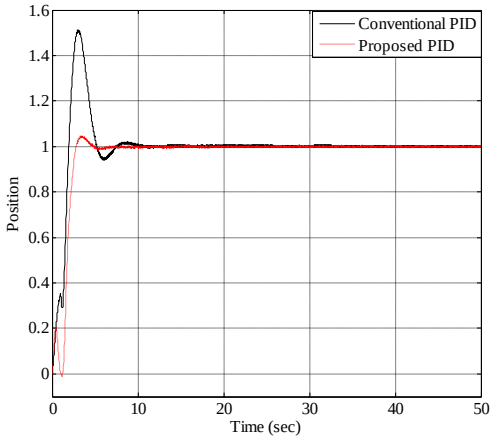

(a) Position Vs Time

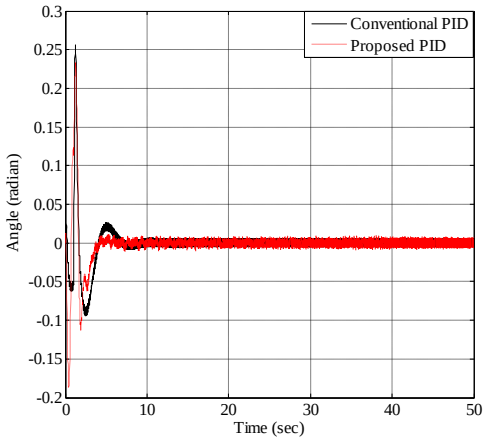

(b) Angle Vs Time

Figure 2.18 Stabilization of x Inverted Pendulum using Error AGS PID Controllers with Disturbance

Table 2.6 Quantitative Analysis of x Inverted Pendulum Control using Error AGS PID Controllers with Disturbance

Parameters	With disturbance				% Improvement	
	Conventional		Proposed			
	x	θ	x	θ	x	θ
M_P	0.51	0.26	0.05	0.24	920	8.33
t_r	1.85	—	2.44	—	-24.1	—
t_s	8.88	5.79	4.19	3.43	111.9	68.8
e_{ss}	0	0	0	0	0	0

The quantitative analysis shows that a huge amount of improvement in M_p and t_s takes place when error AGS PID controllers are used for stabilization purpose. The simulation results with noise in the controllers are shown in Figure 2.19.

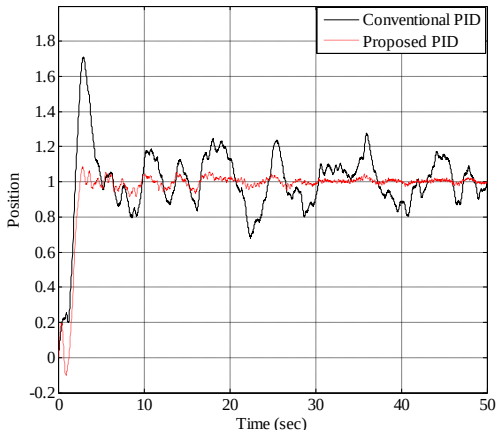

(a) Position Vs Time

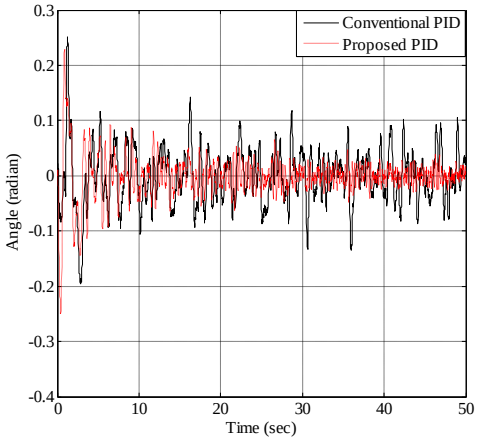

(b) Angle Vs Time

Figure 2.19 Stabilization of x Inverted Pendulum using Error AGS PID Controllers with Noise in Controllers

The results show a less chattered response in case of error AGS PID controllers as compared to the conventional PID scheme.

The simulation results when considering the effect of friction on the inverted pendulum system are given in Figure 2.20 and Figure 2.21 for simple and exponential friction models respectively.

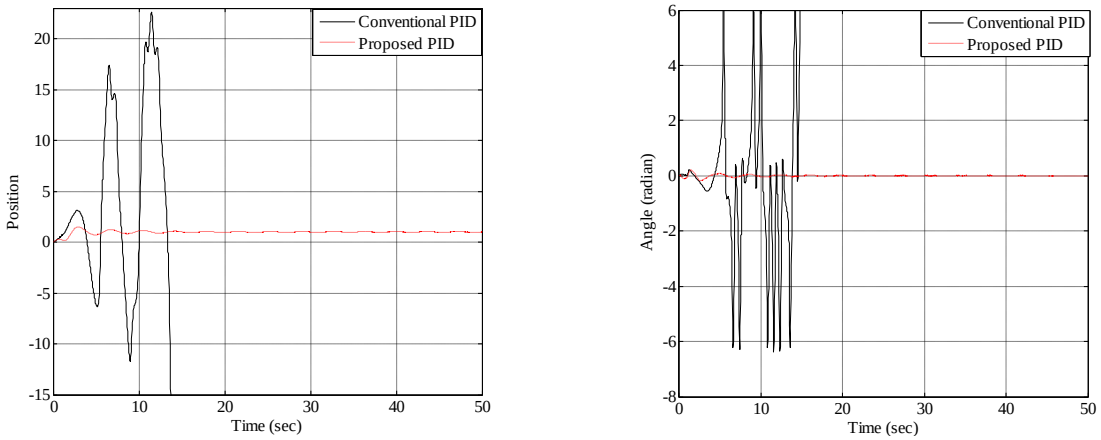

(a) Position Vs Time (b) Angle Vs Time

Figure 2.20 Stabilization of x Inverted Pendulum using Error AGS PID Controllers with Simple Friction Model

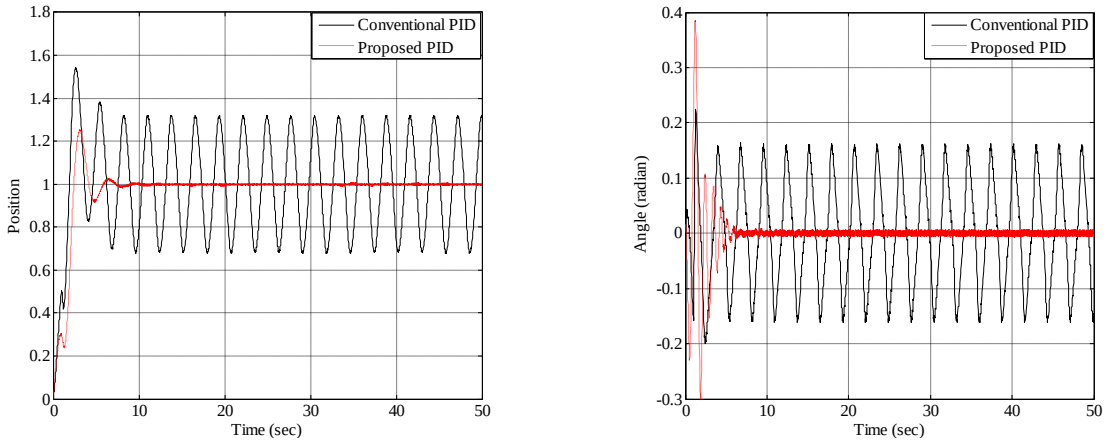

(a) Position Vs Time (b) Angle Vs Time

Figure 2.21 Stabilization of x Inverted Pendulum using Error AGS PID Controllers with Exponential Friction Model

Figure 2.20 shows that the system response becomes unbounded when the effect of friction is incorporated in terms of simple friction model for conventional PID controllers. On the other hand the error AGS PID controllers give satisfactory results.

Similarly when the exponential friction model is considered the error AGS PID controllers provide almost perfect control with zero e_{ss} as shown in Figure 2.21, while the conventional PID controllers give oscillatory response.

2.5.4 Tracking Control with Error AGS PID Controllers

The simulation results for tracking control are given from Figure 2.22 to Figure 2.26.

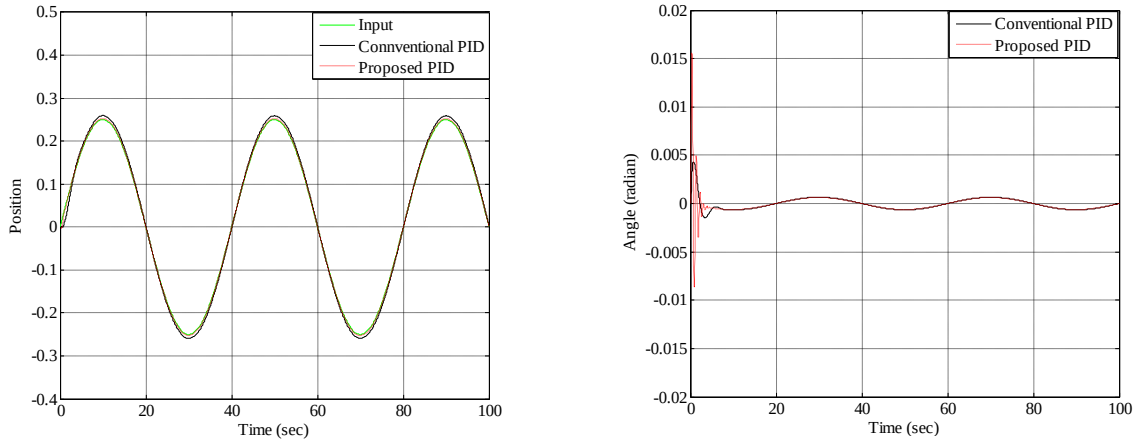

Figure 2.22 Tracking Control of x Inverted Pendulum using Error AGS PID Controllers without Uncertainties

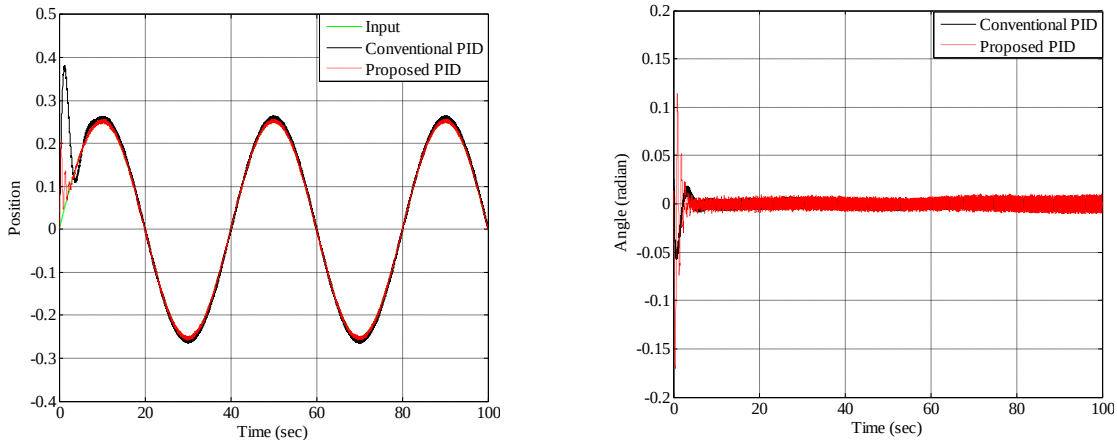

(a) Position Vs Time (b) Angle Vs Time

Figure 2.23 Tracking Control of x Inverted Pendulum using Error AGS PID Controllers with Disturbance

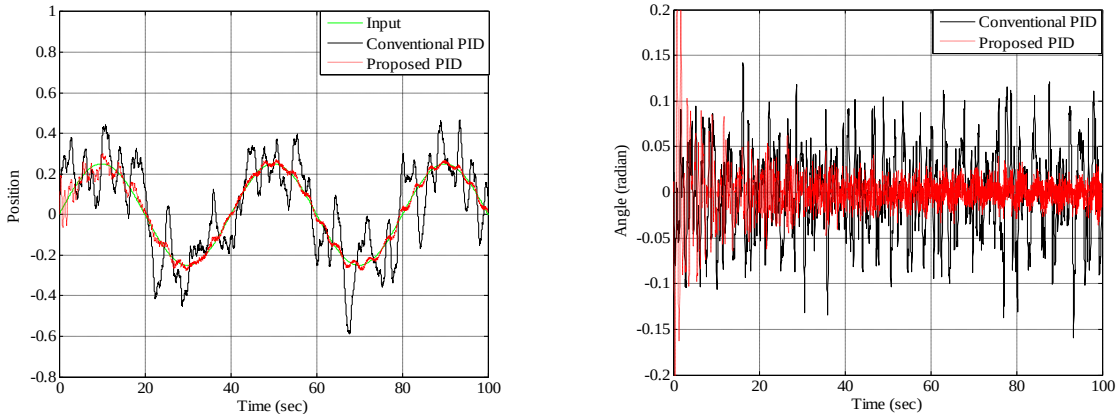

(a) Position Vs Time (b) Angle Vs Time

Figure 2.24 Tracking Control of x Inverted Pendulum using Error AGS PID Controllers with Noise in Controllers

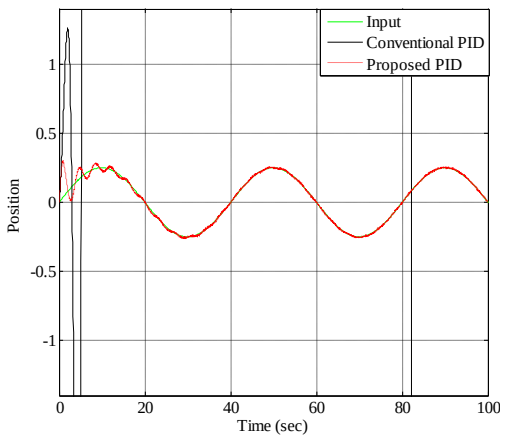

(a) Position Vs Time

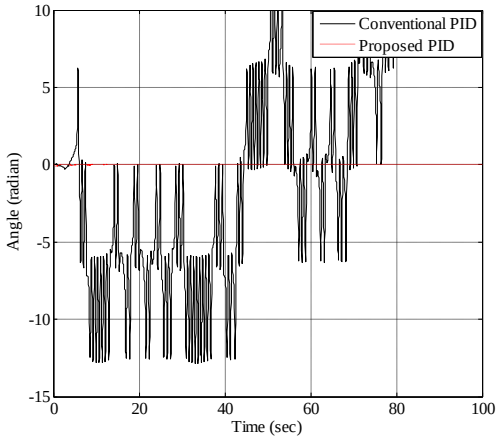

(b) Angle Vs Time

Figure 2.25 Tracking Control of x Inverted Pendulum using Error AGS PID Controllers with Simple Friction Model

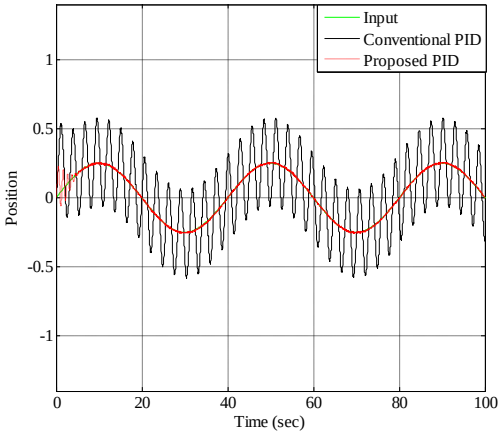

(a) Position Vs Time

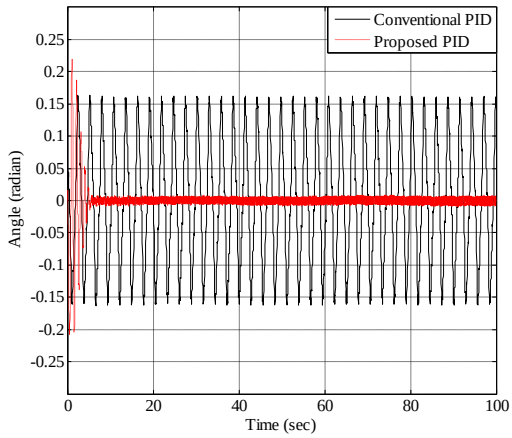

(b) Angle Vs Time

Figure 2.26 Tracking Control of x Inverted Pendulum using Error AGS PID Controllers with Exponential Friction Model

The above simulation results show that the error AGS PID controllers are more efficient than the conventional PID controllers for tracking control especially in the presence of uncertainties.

2.6 Conclusion

In this chapter, adaptive gain scheduling (AGS) PID controllers are designed for the stabilization and tracking control of one dimensional (x) inverted pendulum system using a two control loop structure. The PID controller gains are scheduled as a function of time and error that are varied within a specified range depending upon the transient and the steady-state part of the response. The performance of the proposed time AGS PID controllers and error AGS PID controllers have been compared with the conventional PID controllers given

in the literature. The simulation results show a large reduction in maximum overshoot of 51.5% in case of position control and 87.5% in case of angle control when the time AGS PID controllers are used for stabilization. Similarly, when error AGS PID controllers are used a huge amount of improvement in maximum overshoot i.e. 900% for position control and 11.1% for angle control and a significant amount of improvement in settling time of 67.6% for position control and 78.8% for angle control has been observed in the system response. A comparative study between time AGS PID controllers and error AGS PID controllers reveal that for position control maximum overshoot and settling time are less by 560% and 67.43% in case of error AGS PID controllers while the rise time improves by 2.96% with time AGS PID controllers. Similarly for angle control maximum overshoot in case of time AGS is less by 68.75% while the settling time for error AGS PID controllers is less by 72.11%. Moreover, the proposed controllers are stable and provide good reference tracking even in the presence of uncertainties such as, disturbance in the inverted pendulum, noise in the controller and friction.

The motion of the base is possible not only in one dimension but also in two dimensions. Hence the performance of the proposed controllers has also been carried out for a two-dimensional inverted pendulum.

CHAPTER 3

Stabilization and Tracking Control of Two Dimensional Inverted Pendulums

3.1 Introduction

A two dimensional inverted pendulum is one in which the movement of the base is two dimensional (either xy or xz) to stabilize the pendulum vertically upwards. If the movement of the base is in xy plane the inverted pendulum is called as an x-y inverted pendulum or a spherical inverted pendulum, while, if the base moves in xz plane the inverted pendulum is called as an x-z inverted pendulum. In this chapter the stability conditions of x-y and x-z inverted pendulums have been analyzed using Lyapunov stability criterion. The stabilization and tracking control of both x-y and x-z inverted pendulums have been achieved using the proposed time as well as error adaptive gain scheduling (AGS) PID controllers. The effect of uncertainties such as fast acting external disturbances, noise in the controllers and friction on the performance of x-y and x-z inverted pendulums has been analyzed using the proposed AGS PID controllers. The simulation results have been compared with the conventional PID scheme given in the literature.

3.2 State Space Modeling of x-y Inverted Pendulum

An x-y inverted pendulum pivoted to a base is shown in Figure 3.1. Here M represents the mass of the base, m represents mass of the pendulum and $2l$ represent the total length of the inverted pendulum.

θ = Angle made by the inverted pendulum with the vertical axis

ϕ = Angle made by the inverted pendulum with the vertical axis when the base moves in y direction.

(x, y) and $(\dot{x}, \dot{y})$ = Position and velocity of the base in the xoy coordinate respectively

(x_P, y_P) and $(\dot{x}_P, \dot{y}_P)$ = Position and velocity of the base in $x'o'y'$ coordinate respectively

$$x_p = x + l\sin\theta \tag{3.1a}$$

$$y_p = y + l\cos\theta\sin\phi \tag{3.1b}$$

$$z_p = z + l\cos\theta\cos\phi \tag{3.1c}$$

$$\dot{x}_p = \dot{x} + l\cos\theta\dot{\theta} \tag{3.1d}$$

$$\dot{y}_p = \dot{y} + l\cos\theta\cos\phi\dot{\phi} - l\sin\theta\sin\phi\dot{\theta} \tag{3.1e}$$

$$\dot{z}_p = \dot{z} - l\sin\theta\cos\phi\dot{\theta} - l\cos\theta\sin\phi\dot{\phi} \tag{3.1f}$$

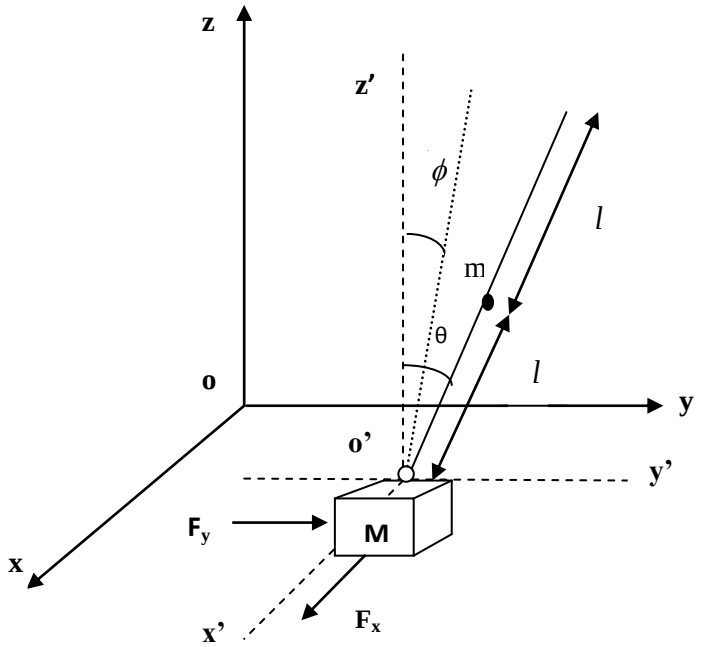

Figure 3.1 x - y Inverted Pendulum System

Stabilization and tracking control of the inverted pendulum depends upon the horizontal displacement of the base which in turn depends upon the applied forces F_x and F_y.

3.2.1 Modeling without Uncertainties

The state space modeling of the x - y inverted pendulum has been obtained using Euler Lagrange equations. The Lagrange equations of the x - y inverted pendulum without considering the effect of uncertainties are given as (Wang, 2011):

$$\frac{d}{dt}\left(\frac{\partial L}{\partial \dot{x}}\right) - \frac{\partial L}{\partial x} = F_x \tag{3.2a}$$

$$\frac{d}{dt}\left(\frac{\partial L}{\partial \dot{y}}\right) - \frac{\partial L}{\partial y} = F_y \tag{3.2b}$$

$$\frac{d}{dt}\left(\frac{\partial L}{\partial \dot{\theta}}\right) - \frac{\partial L}{\partial \theta} = 0 \tag{3.2c}$$

$$\frac{d}{dt}\left(\frac{\partial L}{\partial \dot{\phi}}\right) - \frac{\partial L}{\partial \phi} = 0 \tag{3.2d}$$

Where Lagrangian L is defined as:

$$L = K.E. - P.E. \tag{3.3}$$

The kinetic energy $K.E.$ and the potential energy $P.E.$ of the system are given as:

$$K.E. = \frac{1}{2}[M(\dot{x}^2 + \dot{y}^2) + m(\dot{x}_P^2 + \dot{y}_p^2 + \dot{z}_P^2)] \tag{3.4a}$$

$$P.E. = mgz_p \tag{3.4b}$$

Here g represents the acceleration due to gravity.

$$K.E. = \frac{1}{2}\Big[M(\dot{x}^2 + \dot{y}^2) + m[(\dot{x} + l\cos\theta\dot{\theta})^2 + (\dot{y} + l\cos\theta\cos\phi\dot{\phi} - l\sin\theta\sin\phi\dot{\theta})^2 + (\dot{z} - l\sin\theta\cos\phi\dot{\theta} - l\cos\theta\sin\phi\dot{\phi})^2]\Big] \tag{3.5a}$$

$$P.E. = mg(z + l\cos\theta\cos\phi) \tag{3.5b}$$

Put (3.5 a) and (3.5 b) in Eq. (3.3)

$$L = \frac{1}{2}\Big[M(\dot{x}^2 + \dot{y}^2) + m[(\dot{x} + l\cos\theta\dot{\theta})^2 + (\dot{y} + l\cos\theta\cos\phi\dot{\phi} - l\sin\theta\sin\phi\dot{\theta})^2 + (\dot{z} - l\sin\theta\cos\phi\dot{\theta} - l\cos\theta\sin\phi\dot{\phi})^2]\Big] - mg(z + l\cos\theta\cos\phi) \tag{3.6}$$

Solving Eq. (3.2a) to Eq. (3.2d) using Eq. (3.6)

$$(M + m)\ddot{x} + ml\cos\theta\ddot{\theta} - ml\sin\theta\dot{\theta}^2 = F_x \tag{3.7}$$

$$(M + m)\ddot{y} + ml\cos\theta\cos\phi\ddot{\phi} - ml\sin\theta\sin\phi\ddot{\theta} - 2ml\sin\theta\cos\phi\dot{\theta}\dot{\phi} - ml\cos\theta\sin\phi(\dot{\theta}^2 + \dot{\phi}^2) = F_y \tag{3.8}$$

$$l\ddot{\theta} + \cos\theta\ddot{x} - \sin\theta\sin\phi\ddot{y} + l\cos\theta\cos\phi\dot{\phi}^2 - g\sin\theta\cos\phi = 0 \tag{3.9}$$

$$l\cos\theta\ddot{\phi} + l\cos\phi\ddot{y} - g\sin\phi = 0 \tag{3.10}$$

Defining the states as $x_1 = x, x_2 = \dot{x}, x_3 = y, x_4 = \dot{y}, x_5 = \theta, x_6 = \dot{\theta}, x_7 = \phi$ and $x_8 = \dot{\phi}$ the state equations of the x - y inverted pendulum obtained from Eq. (3.7) to Eq. (3.10) are:

$$\dot{x}_1 = x_2 \tag{3.11}$$

$$\dot{x}_2 = \frac{Mml\sin x_5 x_6^2 + Mml\cos^2 x_5 \sin x_5 x_8^2 - Mmg\cos^2 x_5 \sin x_5 \cos^2 x_7 + m\cos^2 x_5 \sin^2 x_7 F_x + MF_x - m\cos^2 x_5 \sin x_5 \sin x_7 F_y}{M^2 + Mm\sin^2 x_5 \cos^2 x_7 + Mm\sin^2 x_7} \tag{3.12}$$

$$\dot{x}_3 = x_4 \tag{3.13}$$

$$\dot{x}_4 = \frac{(M + m)F_y - m\cos^2 x_5 F_y + m\sin x_5 \cos x_5 \sin x_7 F_x - Mmg\cos^2 x_5 \sin x_7 \cos x_7 + Mml\cos^3 x_5 \sin x_7 x_8^2 - Mml\cos x_5 \sin x_7 x_6^2}{M^2 + Mm\sin^2 x_5 \cos^2 x_7 + Mm\sin^2 x_7} \tag{3.14}$$

$$\dot{x}_5 = x_6 \tag{3.15}$$

$$\dot{x}_6 = \frac{\begin{array}{l} m\cos x_5 \cos^2 x_7 F_x - (M+m)\cos x_5 F_x + (M+m)\sin x_5 \sin x_7 F_y + M(m+M)g \sin x_5 \cos x_7 \\ - Mml \sin x_5 \cos x_5 \cos^2 x_7 x_6^2 - M(m+M)l \cos x_5 \sin x_7 x_8^2 \end{array}}{(M^2 + Mm\sin^2 x_5 \cos^2 x_7 + Mm\sin^2 x_7)l} \quad (3.16)$$

$$\dot{x}_7 = x_8 \quad (3.17)$$

$$\dot{x}_8 = \frac{\begin{array}{l} -m\sin^2 x_5 \cos x_7 F_y - M\cos x_7 F_y + m\sin x_5 \cos x_5 \sin x_7 \cos x_7 F_x + \\ 2Mml \sin x_5 x_6 x_8 + M(m+M)g \sin x_7 + 2M^2 l \sin x_5 x_6 x_8 - 2Mml \sin x_5 \cos^2 x_5 \cos^2 x_7 x_6 x_8 - \\ Mml \cos^3 x_5 \sin x_7 \cos x_7 x_8^2 - Mml \cos x_5 \sin x_7 \cos x_7 x_6^2 \end{array}}{M^2 + Mm\sin^2 x_5 \cos^2 x_7 + Mm\sin^2 x_7} \quad (3.18)$$

From Eq. (3.11) to Eq. (3.18) it can be concluded that the x-y inverted pendulum is a multi input multi output (MIMO) system with two inputs and four outputs. The two inputs are the applied forces F_x and F_y while the outputs are the positions x, y of the base and the angles θ, ϕ made by the inverted pendulum with the vertical axis.

3.2.2 Modeling with Uncertainties

The uncertainties that may exist in an x-y inverted pendulum system are the fast acting external disturbances and frictional forces. The state equations of the x-y inverted pendulum after considering the effect of external disturbance (d) and frictional forces (F_{xfric} and F_{yfric}) can be written as:

$$\dot{x}_1 = x_2 \quad (3.19)$$

$$\dot{x}_2 = \frac{\begin{array}{l} Mml \sin x_5 x_6^2 + Mml \cos^2 x_5 \sin x_5 x_8^2 - Mmg \cos^2 x_5 \sin x_5 \cos^2 x_7 + \\ m\cos^2 x_5 \sin^2 x_7 (F_x + F_{xfric}) + M(F_x + F_{xfric}) - m\cos^2 x_5 \sin x_5 \sin x_7 (F_y + F_{yfric}) \end{array}}{M^2 + Mm\sin^2 x_5 \cos^2 x_7 + Mm\sin^2 x_7} + d \quad (3.20)$$

$$\dot{x}_3 = x_4 \quad (3.21)$$

$$\dot{x}_4 = \frac{\begin{array}{l} (M+m)(F_y + F_{yfric}) - m\cos^2 x_5 (F_y + F_{yfric}) + m\sin x_5 \cos x_5 \sin x_7 (F_x + F_{xfric}) - \\ Mmg \cos^2 x_5 \sin x_7 \cos x_7 + Mml \cos^3 x_5 \sin x_7 x_8^2 - Mml \cos x_5 \sin x_7 x_6^2 \end{array}}{M^2 + Mm\sin^2 x_5 \cos^2 x_7 + Mm\sin^2 x_7} + d \quad (3.22)$$

$$\dot{x}_5 = x_6 \quad (3.23)$$

$$\dot{x}_6 = \frac{\begin{array}{l} m\cos x_5 \cos^2 x_7 (F_x + F_{xfric}) - (M+m)\cos x_5 (F_x + F_{xfric}) + (M+m)\sin x_5 \sin x_7 (F_y + F_{yfric}) + \\ M(m+M)g \sin x_5 \cos x_7 - Mml \sin x_5 \cos x_5 \cos^2 x_7 x_6^2 - M(m+M)l \cos x_5 \sin x_7 x_8^2 \end{array}}{(M^2 + Mm\sin^2 x_5 \cos^2 x_7 + Mm\sin^2 x_7)l} + d \quad (3.24)$$

$$\dot{x}_7 = x_8 \quad (3.25)$$

$$
\begin{aligned}
&-m\sin^2 x_5\cos x_7(F_y+F_{yfric})-M\cos x_7(F_y+F_{yfric})+m\sin x_5\cos x_5\sin x_7\cos x_7(F_x+F_{xfric})\\
&+2Mml\sin x_5x_6x_8+M(m+M)g\sin x_7+2M^2l\sin x_5x_6x_8-\\
\dot{x}_8=&\frac{2Mml\sin x_5\cos^2 x_5\cos^2 x_7x_6x_8-Mml\cos^3 x_5\sin x_7\cos x_7x_8^2-Mml\cos x_5\sin x_7\cos x_7x_6^2}{M^2+Mm\sin^2 x_5\cos^2 x_7+Mm\sin^2 x_7}+d
\end{aligned}
\tag{3.26}
$$

The disturbance is defined as:

$$d = 20\sin(20\pi t) \tag{3.27}$$

The frictional forces (F_{xfric} and F_{yfric}) have been defined in Appendix A.

3.3 Control Structure of x - y Inverted Pendulum

The control structure of x - y inverted pendulum is shown in Figure 3.2.

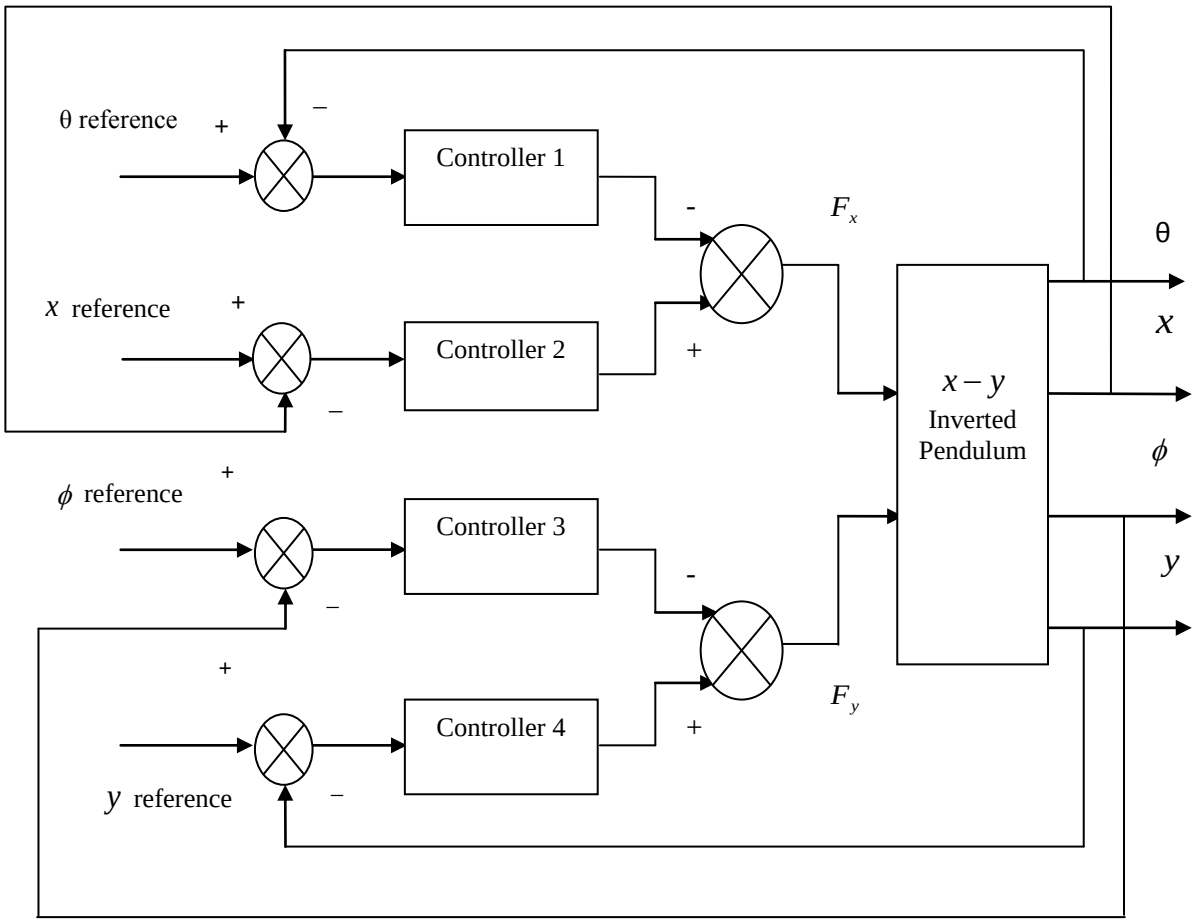

Figure 3.2 Control Structure of x - y Inverted Pendulum

Since an x - y inverted pendulum is a multi input multi output (MIMO) system, therefore it requires a set of four controllers to control the four outputs (Wang, 2011). As shown in Figure 3.2 a four loop control scheme with two loops for position control of the base while the remaining two for angle control of the pendulum have been implemented for controlling

the inverted pendulum. Here controller 1 is used for controlling angle θ while controller 2 for x position control of the base. Similarly controller 3 has been used for controlling angle ϕ while controller 4 for y position control of the base.

As the dynamics of the x-y inverted pendulum remains same in both x or y direction. Therefore the controller 1 and controller 2 (designed for controlling x and θ of an x inverted pendulum) can directly be used as controller 3 and controller 4 respectively when the control of x-y inverted pendulum is considered. The proposed AGS PID controllers have been implemented for the stabilization and tracking control of x-y inverted pendulum.The minimum and the maximum value of gains for AGS PID controllers are given in Table 3.1.

Table 3.1 Parameters of AGS PID Controllers for x-y Inverted Pendulum Control

Parameter	$k_{p\min}$	$k_{p\max}$	$k_{i\min}$	$k_{i\max}$	$k_{d\min}$	$k_{d\max}$
PID1	24	36	1.5	3.6	3	5
PID2	-3	-2.4	-1.2	-1	-4.8	-2
PID3	24	36	1.5	3.6	3	5
PID4	-3	-2.4	-1.2	-1	-4.8	-2

From the above table it can be observed that the minimum and maximum values of gains are same for PID1 and PID 3. Similarly PID2 and PID 4 have the same values of gains.

3.4 Stability Analysis of x-y Inverted Pendulum

The stability analysis of the given system has been done using Lyapunov stability criterion.

Theorem 3.1: The x-y inverted pendulum system will be stable if and only if

$$F_x\dot{x} + F_y\dot{y} \le 0 \tag{3.28}$$

Proof: Defining the Lyapunov function V as the sum of kinetic energy and potential energy of the system.

$$V = \frac{1}{2}M(\dot{x}^2 + \dot{y}^2) + \frac{1}{2}m(\dot{x}_p^2 + \dot{y}_p^2 + \dot{z}_p^2) + mgz_p \tag{3.29}$$

Using Eq. (3.1a) to Eq. (3.1f)

$$V = \frac{1}{2}M(\dot{x}^2 + \dot{y}^2) + \frac{1}{2}m[(\dot{x} + l\cos\theta\dot{\theta})^2 + (\dot{y} + l\cos\theta\cos\phi\dot{\phi} - l\sin\theta\sin\phi\dot{\theta}^2)$$
$$+ (\dot{z} - l\sin\theta\cos\phi\dot{\theta} - l\cos\theta\sin\phi\dot{\phi})^2] + mg(z + l\cos\theta\cos\phi) \tag{3.30}$$

According to Lyapunov stability criterion for a system to be stable $\dot{V} \le 0$

$$\begin{aligned}\dot{V} = M(\dot{x}\ddot{x} + \dot{y}\ddot{y}) + m[(\dot{x} + l\cos\theta\dot{\theta})(\ddot{x} - l\sin\theta\dot{\theta}^2 + l\cos\theta\ddot{\theta}) + \\ (\dot{y} + l\cos\theta\cos\phi\dot{\phi} - l\sin\theta\dot{\theta}\sin\phi)(\ddot{y} + l\cos\theta\cos\phi\ddot{\phi} - l\sin\theta\dot{\theta}\cos\phi\dot{\phi} - l\sin\phi\dot{\phi}^2\cos\theta - \\ l\sin\theta\sin\phi\ddot{\theta} - l\cos\theta\dot{\theta}^2\sin\phi - l\sin\theta\dot{\theta}\cos\phi\dot{\phi}) + (\dot{z} - l\sin\theta\cos\phi\dot{\theta} - \\ l\cos\theta\sin\phi\dot{\phi})(\ddot{z} - l\sin\theta\cos\phi\ddot{\theta} - l\cos\theta\cos\phi\dot{\theta}^2 + l\sin\theta\sin\phi\dot{\theta}\dot{\phi} - l\cos\theta\sin\phi\ddot{\phi} + \\ l\sin\theta\sin\phi\dot{\theta}\dot{\phi} - l\cos\theta\cos\phi\dot{\phi}^2)] + mg(\dot{z} - l\cos\theta\sin\phi\dot{\phi} - l\sin\theta\cos\phi\dot{\theta})\end{aligned} \quad (3.31)$$

Since the movement of base is in x and y direction, therefore $\dot{z} = 0$.

Hence Eq.(3.31) reduces to:

$$\begin{aligned}\dot{V} = M(\dot{x}\ddot{x} + \dot{y}\ddot{y}) + m[(\dot{x} + l\cos\theta\dot{\theta})(\ddot{x} - l\sin\theta\dot{\theta}^2 + l\cos\theta\ddot{\theta}) + \\ (\dot{y} + l\cos\theta\cos\phi\dot{\phi} - l\sin\theta\dot{\theta}\sin\phi)(\ddot{y} + l\cos\theta\cos\phi\ddot{\phi} - l\sin\theta\dot{\theta}\cos\phi\dot{\phi} - l\sin\phi\dot{\phi}^2\cos\theta - \\ l\sin\theta\sin\phi\ddot{\theta} - l\cos\theta\dot{\theta}^2\sin\phi - l\sin\theta\dot{\theta}\cos\phi\dot{\phi}) + (-l\sin\theta\cos\phi\dot{\theta} - \\ l\cos\theta\sin\phi\dot{\phi})(-l\sin\theta\cos\phi\ddot{\theta} - l\cos\theta\cos\phi\dot{\theta}^2 + l\sin\theta\sin\phi\dot{\theta}\dot{\phi} - l\cos\theta\sin\phi\ddot{\phi} + \\ l\sin\theta\sin\phi\dot{\theta}\dot{\phi} - l\cos\theta\cos\phi\dot{\phi}^2)] + mg(-l\cos\theta\sin\phi\dot{\phi} - l\sin\theta\cos\phi\dot{\theta})\end{aligned} \quad (3.32)$$

Putting Eq. (3.7) to Eq. (3.10) in eq. (3.32) the derivative of the energy function ($\dot{V}$) reduces to:

$$\dot{V} = F_x\dot{x} + F_y\dot{y} \quad (3.33)$$

Therefore for the system to be stable $F_x\dot{x} + F_y\dot{y} \le 0$

To check the stability of x-y inverted pendulum with the proposed controllers the derivative of the Lyapunov function is plotted w.r.t. time.

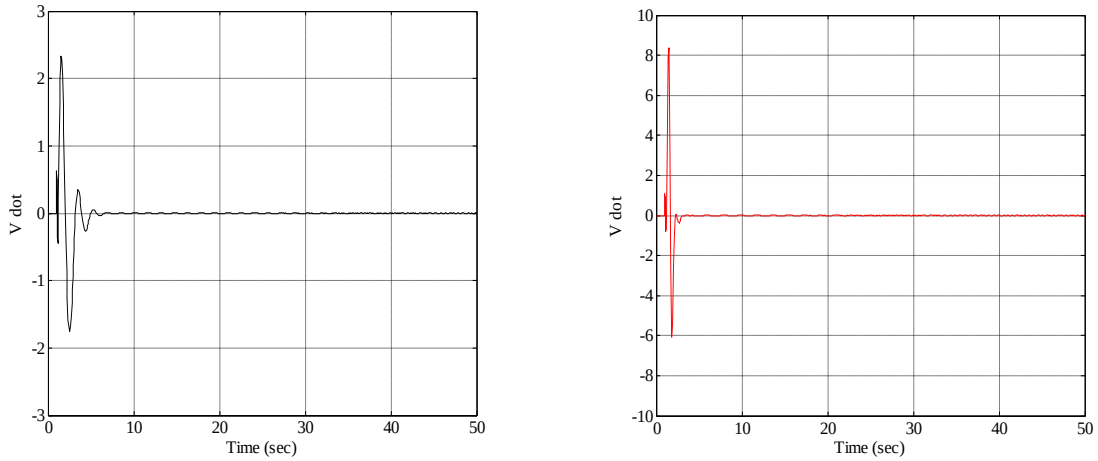

(a) Time AGS PID controller (b) Error AGS PID controller

Figure 3.3 $\dot{V}$ Vs Time for x-y Inverted Pendulum

As shown in Figure 3.3 the derivative of the Lyapunov function for the given system with the proposed AGS PID controllers tends towards zero which means that the system is stable.

3.5 Simulation Results

The simulation results for the stabilization and tracking control of x-y inverted pendulum are given below:

3.5.1 Stabilization with Time AGS PID Controllers

The stabilization of an x-y inverted pendulum can be achieved by applying forces F_x and F_y to the base so that the pendulum should remain in the vertical upward position.

3.5.1.1 Stabilization without Uncertainties

The simulation results without Uncertainties in the x-y inverted pendulum are given in Figure 3.4.

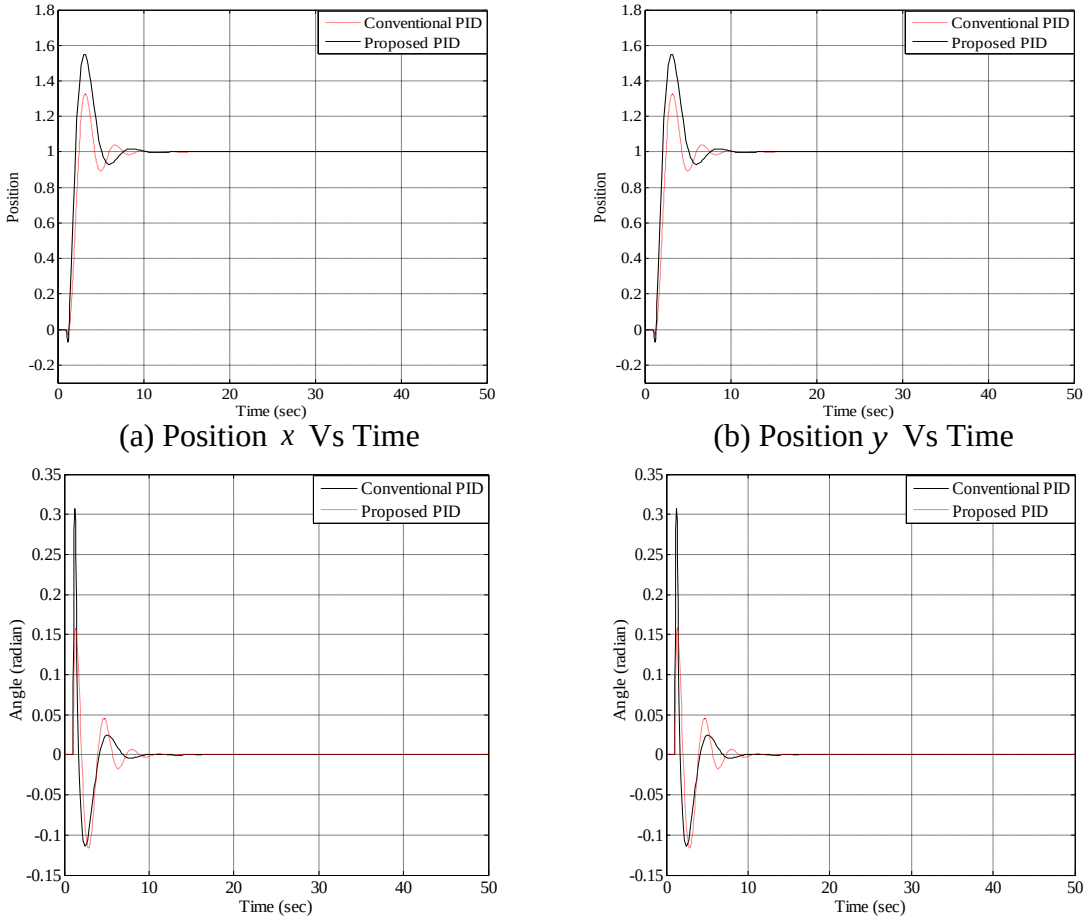

(a) Position x Vs Time (b) Position y Vs Time

(c) Angle θ Vs Time (d) Angle ϕ Vs Time

Figure 3.4 Stabilization of x-y Inverted Pendulum using Time AGS PID Controllers without Uncertainties

From the above results it is observed that although the rise time (t_r) has been increased slightly but there is a considerable improvement in overshoot (M_p) in all the outputs due to which wear and tear on the system will be less. The results are quantified in Table 3.2.

Table 3.2 Quantitative Analysis of x - y inverted pendulum using Time AGS PID Controllers without Uncertainties

Parameters	Without disturbance								% Improvement			
	Conventional				Proposed							
	x	θ	y	ϕ	x	θ	y	ϕ	x	ϕ	y	ϕ
M_P	0.55	0.31	0.55	0.31	0.33	0.16	0.33	0.16	66.66	93.75	66.66	93.75
t_r	2.0	—	2.0	—	2.35	—	2.35	—	-14.89	—	-14.89	—
t_s	7.19	5.64	7.19	5.64	7.22	5.35	7.22	5.35	-0.41	5.42	-0.41	5.42
e_{ss}	0	0	0	0	0	0	0	0	0	0	0	0

3.5.1.2 Stabilization with Uncertainties

The uncertainties considered are the external disturbances, noise and frictional forces. Figure 3.5 gives the simulation results with fast acting external disturbances.

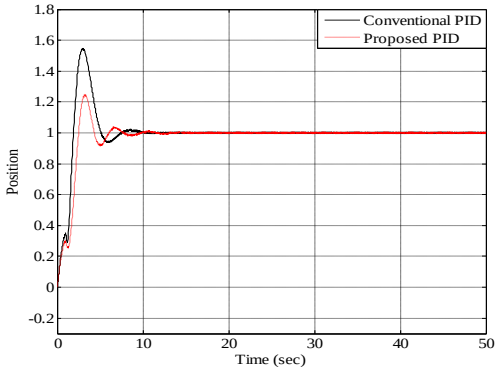

(a) Position x Vs Time

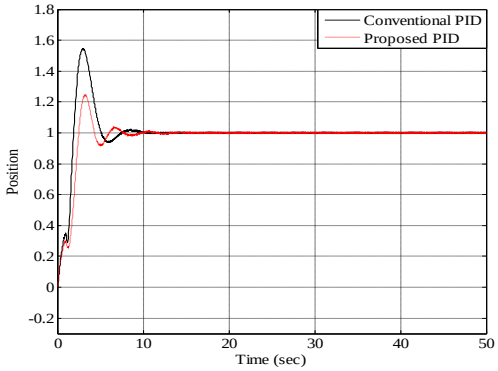

(b) Position y Vs Time

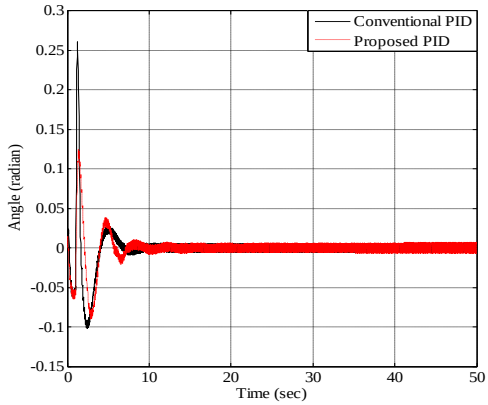

(c) Angle θ Vs Time

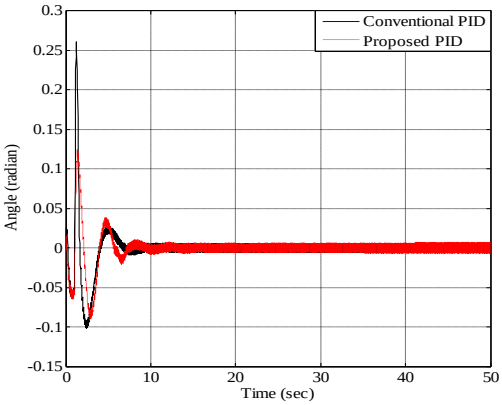

(d) Angle ϕ Vs Time

Figure 3.5 Stabilization of x - y Inverted Pendulum using Time AGS PID Controllers with Disturbance

The results are quantified in Table 3.3.

Table 3.3 Quantitative Analysis of x - y Inverted Pendulum using Time AGS PID Controllers with Disturbance

Parameters	With disturbance								% Improvement			
	Conventional				Proposed							
	x	θ	y	ϕ	x	ϕ	y	ϕ	x	ϕ	y	ϕ
M_P	0.55	0.26	0.55	0.26	0.25	0.12	0.25	0.12	120	116	120	116
t_r	1.81	__	1.81	__	2.36	__	2.36	__	-23.30	__	-23.3	__
t_s	7.14	5.79	7.14	5.79	7.21	5.38	7.21	5.38	-0.97	7.62	-0.97	7.62
e_{ss}	0	0	0	0	0	0	0	0	0	0	0	0

Table 3.3 shows that a large amount of improvement has been observed in M_p with a small deterioration in t_r while keeping e_{ss} to zero.

The simulation results with noise in the controllers are shown in Figure 3.6.

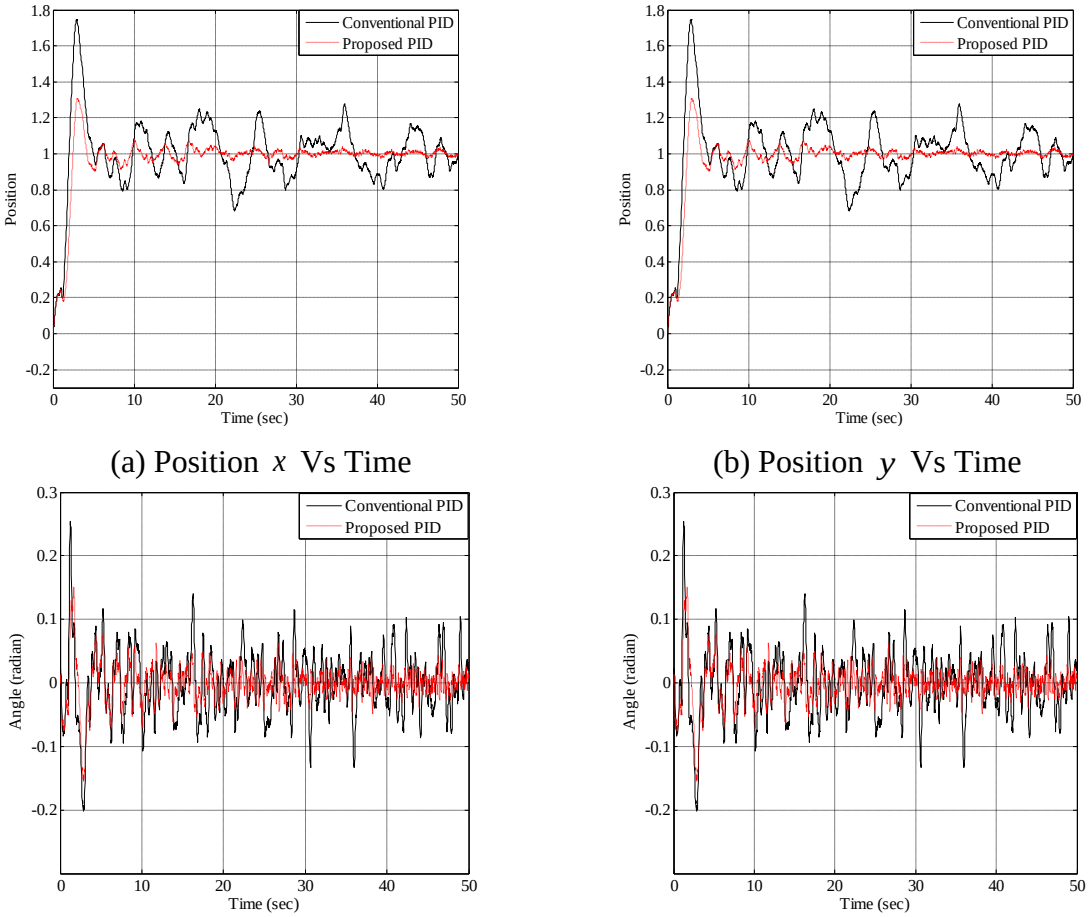

(a) Position x Vs Time

(b) Position y Vs Time

(c) Angle θ Vs Time

(d) Angle ϕ Vs Time

Figure 3.6 Stabilization of x - y Inverted Pendulum using Time AGS PID Controllers with Noise in the Controllers

The above simulation results show lesser chattering in the system response with time AGS PID controllers. The simulation results with friction effect on the inverted pendulum system

are given in Figure 3.7 and Figure 3.8 for simple and exponential friction models.

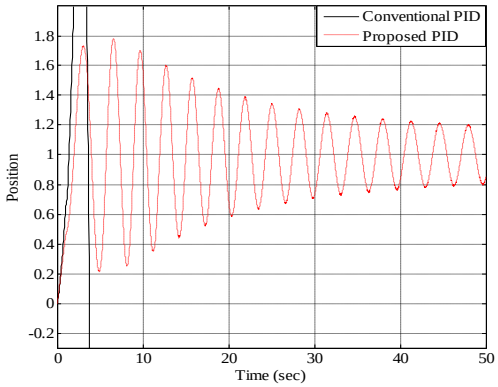

(a) Position x Vs Time

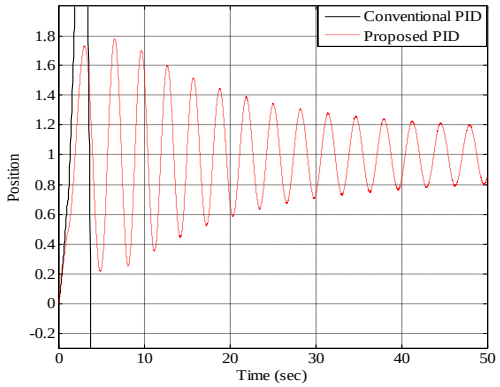

(b) Position y Vs Time

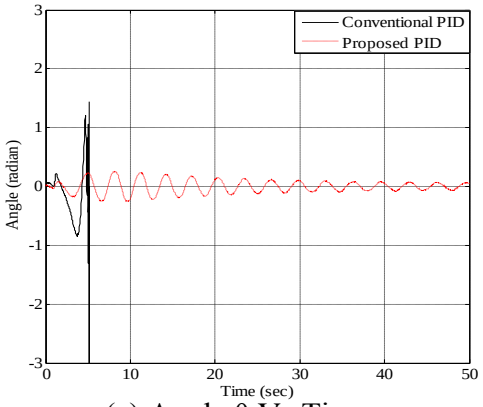

(c) Angle θ Vs Time

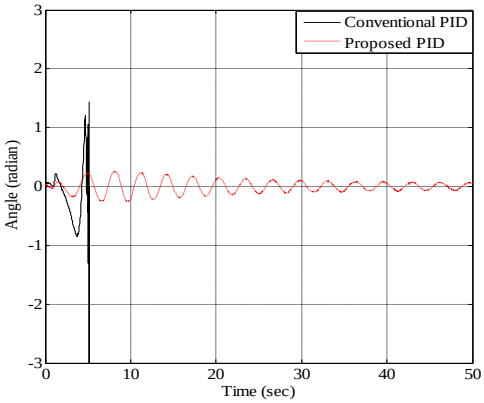

(d) Angle ϕ Vs Time

Figure 3.7 Stabilization of x - y Inverted Pendulum using Time AGS PID Controllers with Simple Friction Model

Figure 3.7 shows that using the proposed time AGS PID controllers the system response is stable as compared to the conventional PID controllers, whose response becomes unbounded in the presence of friction.

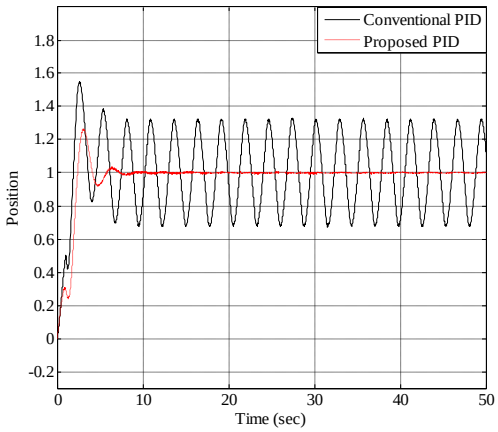

(a) Position x Vs Time

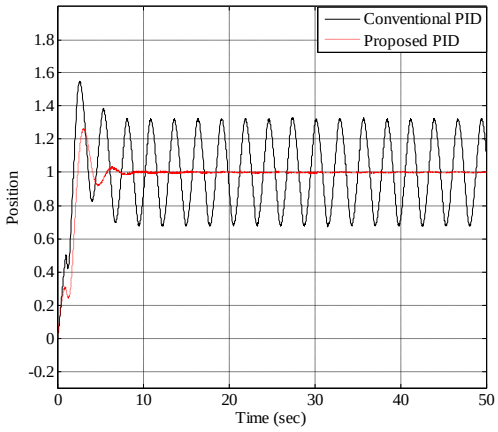

(b) Position y Vs Time

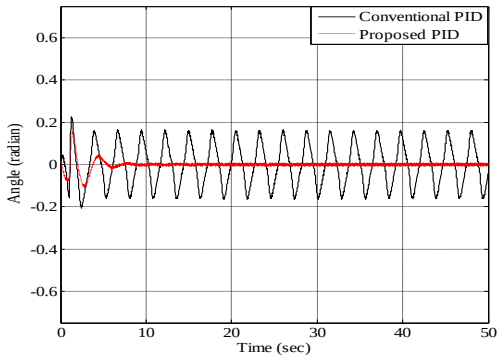

(c) Angle θ Vs Time

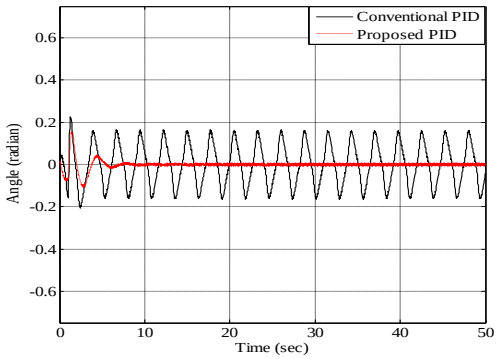

(d) Angle ϕ Vs Time

Figure 3.8 Stabilization of x - y Inverted Pendulum using Time AGS PID Controllers with Exponential Friction Model

The simulation results in Figure 3.8 show the effectiveness of the proposed Time AGS PID controllers which give a stable response with zero steady state error as compared to the conventional PID controllers whose response is oscillatory.

3.5.2 Tracking Control with Time AGS PID Controllers

Tracking signals $x_t = 0.3\sin(0.05\pi t)$ and $y_t = 0.3\sin(0.05\pi t)$ have been applied as the reference inputs. The simulation results are given in Figure 3.9 to Figure 3.13.

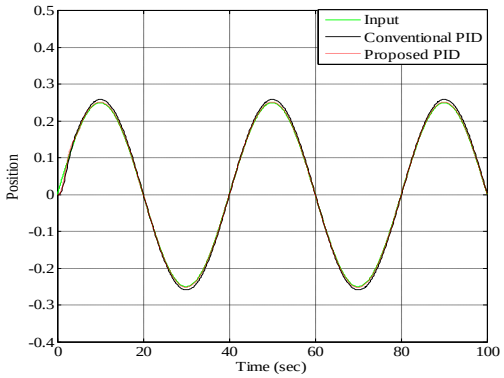

(a) Position x Vs Time

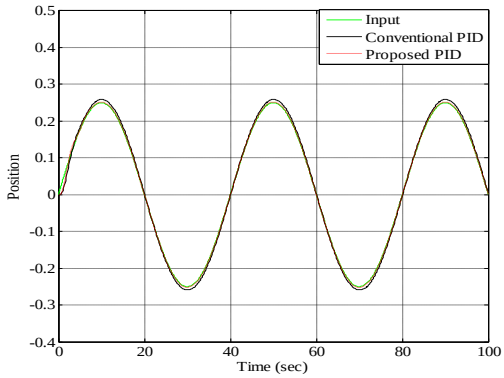

(b) Position y Vs Time

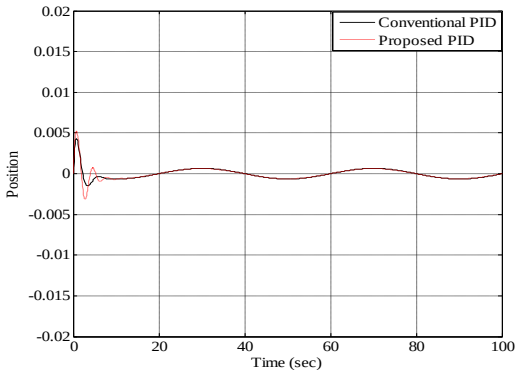

(c) Angle θ Vs Time

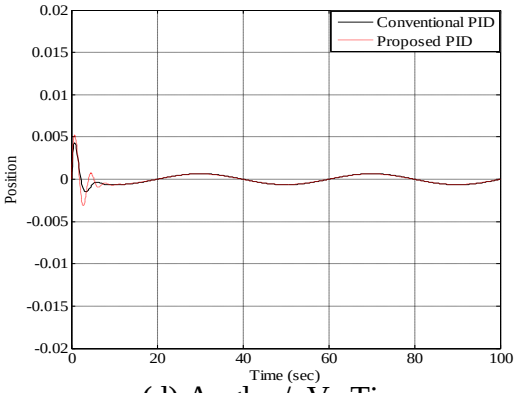

(d) Angle ϕ Vs Time

Figure 3.9 Tracking Control of x - y Inverted Pendulum using Time AGS PID Controllers without Uncertainties

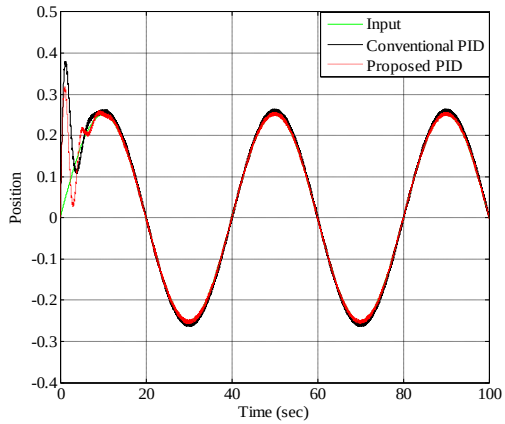

(a) Position x Vs Time

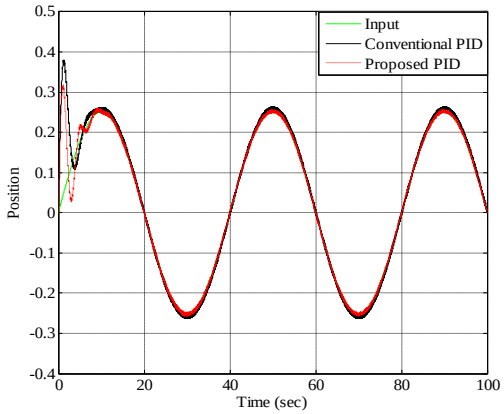

(b) Position y Vs Time

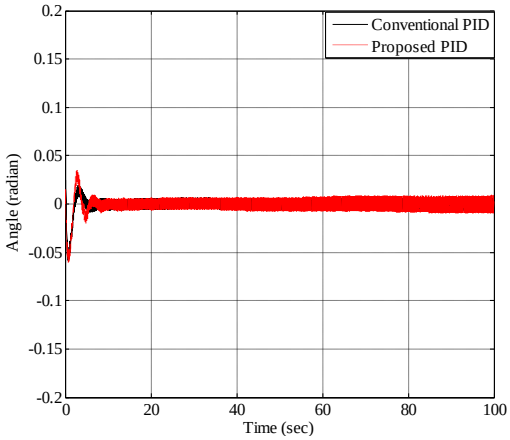

(c) Angle θ Vs Time

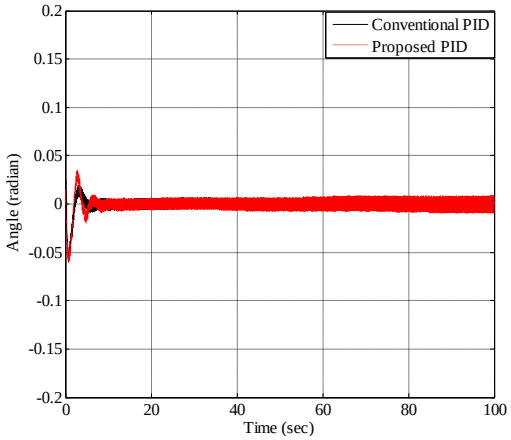

(d) Angle ϕ Vs Time

Figure 3.10 Tracking Control of x - y Inverted Pendulum using Time AGS PID Controllers with Disturbance

The simulation results in Figure 3.9 and Figure 3.10 show that both the conventional and time AGS PID controllers give almost same responses for position as well as angle control of the inverted pendulum.

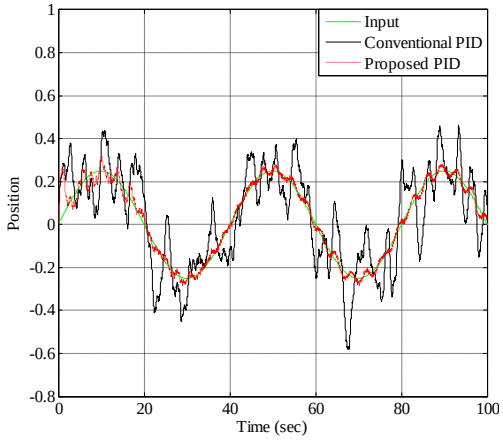

(a) Position x Vs Time

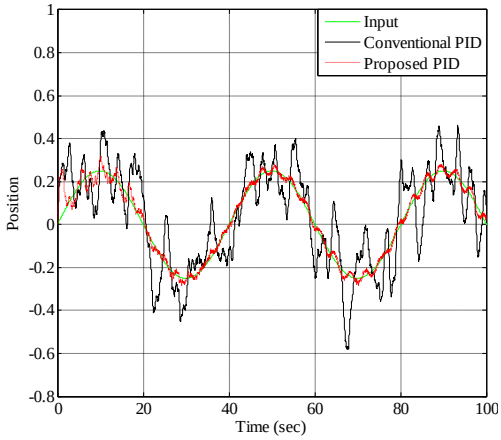

(b) Position y Vs Tim

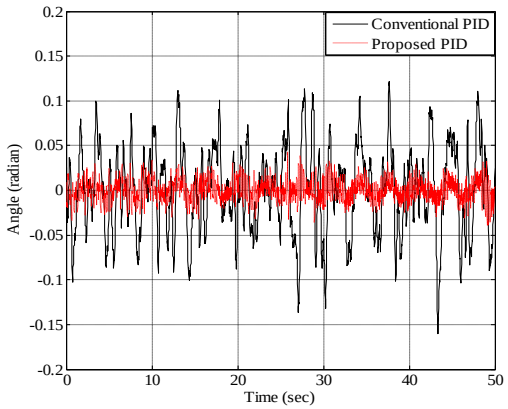

(c) Angle θ Vs Time

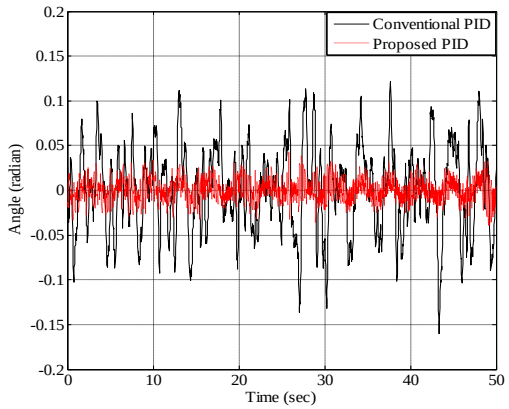

(d) Angle ϕ Vs Time

Figure 3.11 Tracking Control of x - y Inverted Pendulum using Time AGS PID Controllers with Noise in the Controllers

When the effect of noise is considered into the controllers time AGS PID controllers outperforms conventional PID controllers as shown in Figure 3.11 by minimizing the chattering in the system response.

The simulation results under the effect of frictional forces (in terms of simple and exponential friction model) are shown below.

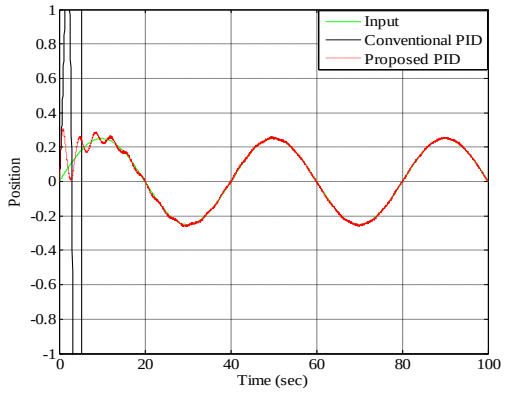

(a) Position x Vs Time

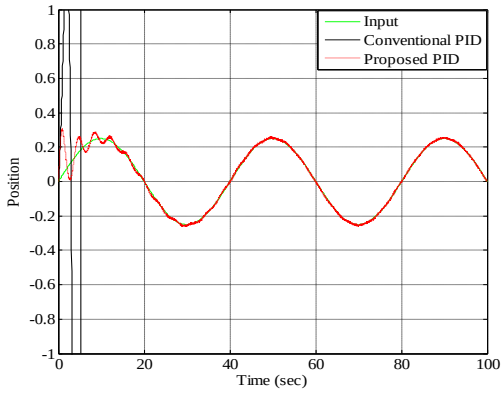

(b) Position y Vs Time

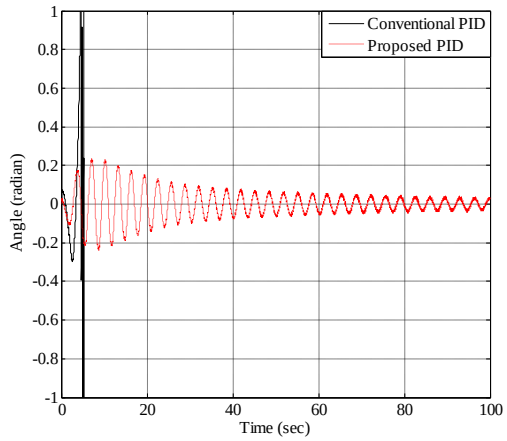

(c) Angle θ Vs Time

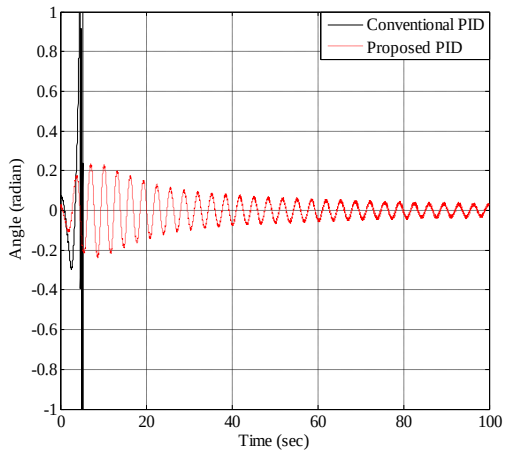

(d) Angle ϕ Vs Time

Figure 3.12 Tracking Control of x - y Inverted Pendulum using Time AGS PID Controllers with Simple Friction Model

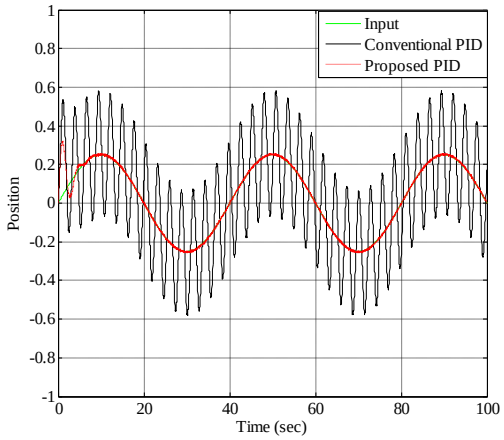

(a) Position x Vs Time

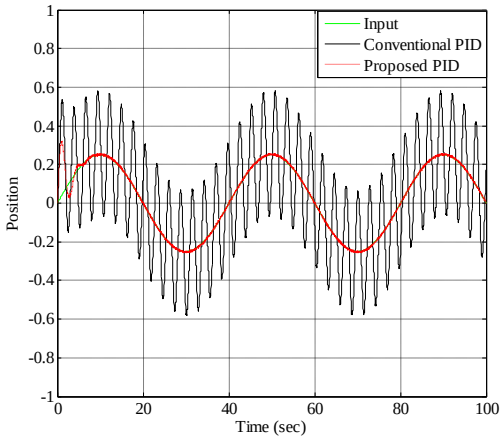

(b) Position y Vs Time

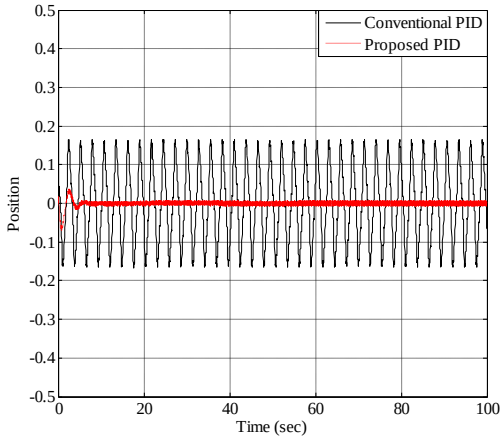

(c) Angle θ Vs Time

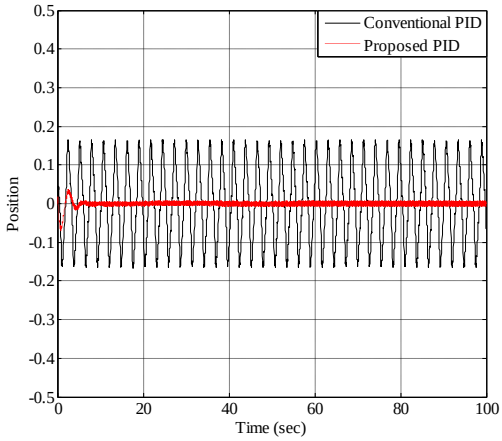

(d) Angle ϕ Vs Time

Figure 3.13 Tracking Control of x - y Inverted Pendulum using Time AGS PID Controllers with Exponential Friction Model

The simulation results in Figure 3.12 shows that when the effect of friction is considered in terms of simple friction model the system response becomes unbounded while using conventional PID controllers. On the other hand the time AGS PID controllers give a satisfactory performance. Similarly in case of exponential friction model a perfect tracking control is provided by the time AGS PID controllers as shown in Figure 3.13 which is not in case of conventional PID controllers.

3.5.3 Stabilization with Error AGS PID Controllers

The time AGS PID controllers are replaced by error AGS PID controllers. The simulation results under different conditions are shown below:

3.5.3.1 Stabilization without Uncertainties

The simulation results for the stabilization of x - y inverted pendulum without the effect of uncertainties are shown in Figure 3.14.

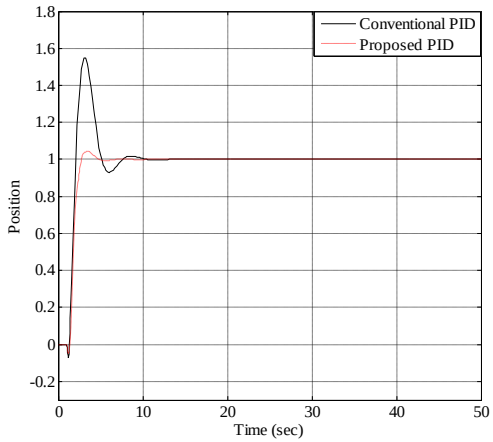

(a) Position x Vs Time

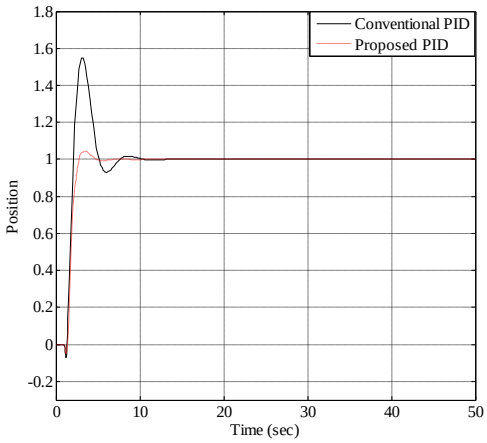

(b) Position y Vs Time

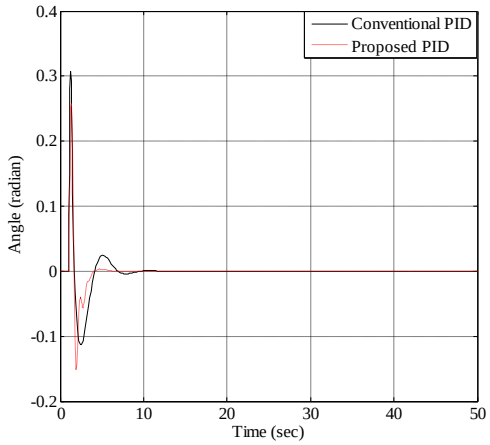

(c) Angle θ Vs Time

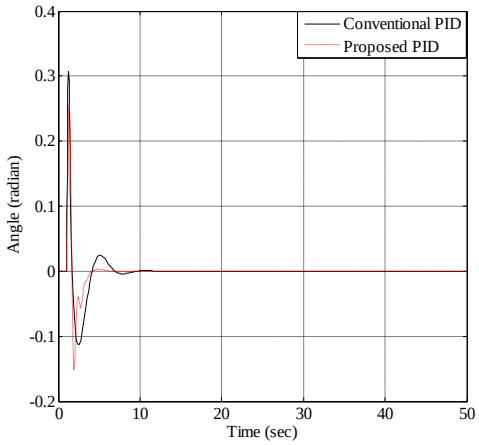

(d) Angle ϕ Vs Time

Figure 3.14 Stabilization of x - y Inverted Pendulum using Error AGS PID Controllers without Uncertainties

The quantitative analysis in terms of various performance specifications is given in Table 3.4.

Table 3.4 Quantitative Analysis of x - y Inverted Pendulum using Error AGS PID Controllers without Uncertainties

Parameters	Without disturbance								% Improvement			
	Conventional				Proposed							
	x	θ	y	ϕ	x	θ	y	ϕ	x	ϕ	y	ϕ
M_P	0.55	0.31	0.55	0.31	0.04	0.26	0.04	0.26	1275	19.2	1275	19.2
t_r	2.0	—	2.0	—	2.41	—	2.41	—	-17.01	—	-17.01	—
t_s	7.19	5.64	7.19	5.64	4.22	3.14	4.22	3.14	70.37	79.6	70.37	79.6
e_{ss}	0	0	0	0	0	0	0	0	0	0	0	0

The quantitative analysis shows a large reduction in M_p with error AGS PID controllers. Furthermore a significant amount of improvement in t_s has been analyzed for both position and angle control with the proposed controllers.

3.5.3.2 Stabilization with Uncertainties

Figure 3.15 gives the simulation results under the effect of fast acting external disturbances acting on the system. The quantitative analysis is given in Table 3.5.

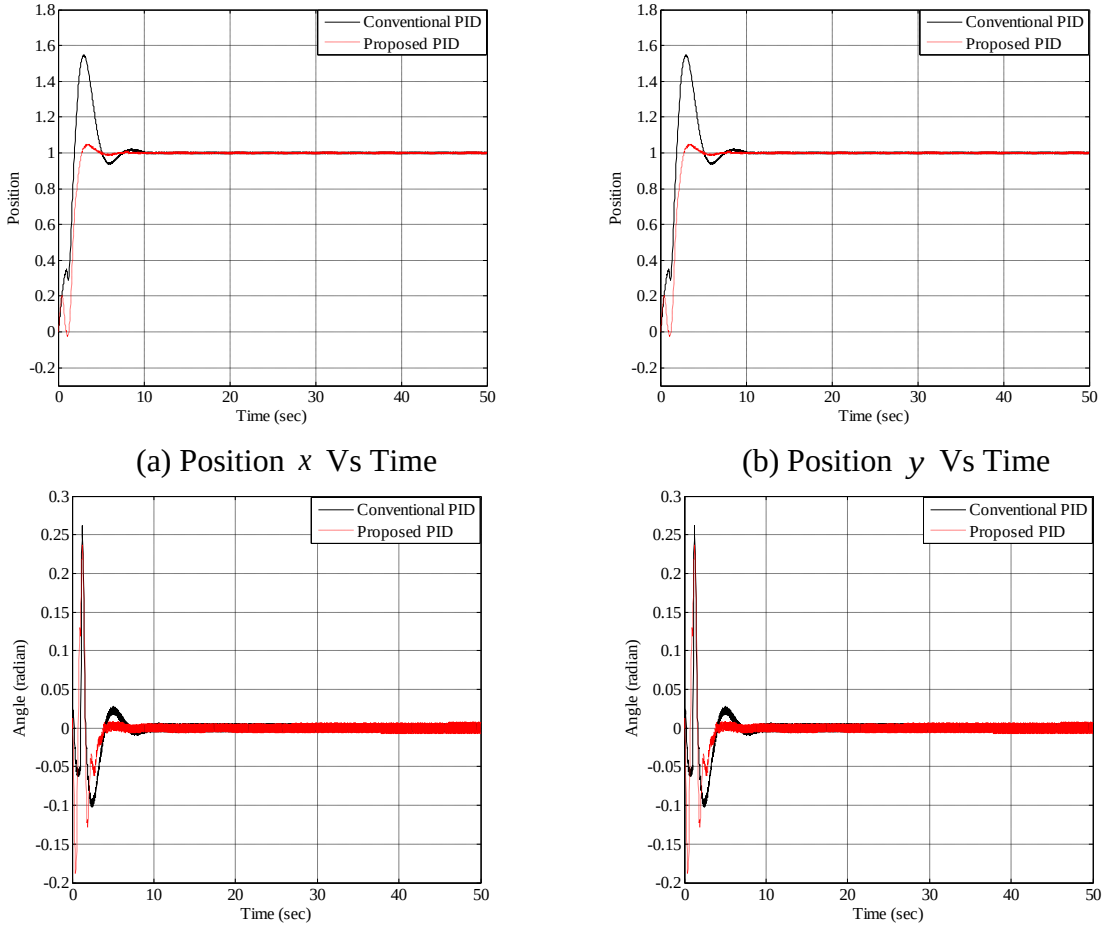

(a) Position x Vs Time

(b) Position y Vs Time

(c) Angle θ Vs Time

(d) Angle ϕ Vs Time

Figure 3.15 Stabilization of x - y Inverted Pendulum using Error AGS PID Controllers with Disturbance

Table 3.5 Quantitative Analysis of x - y Inverted Pendulum using Error AGS PID Controllers with Disturbance

Parameters	With disturbance								% Improvement			
	Conventional				Proposed							
	x	θ	y	ϕ	x	θ	y	ϕ	x	θ	y	ϕ
M_P	0.55	0.26	0.55	0.26	0.05	0.24	0.05	0.24	1000	8.33	1000	8.33
t_r	1.81	—	1.81	—	2.44	—	2.44	—	-25.81	—	-25.81	—
t_s	7.14	5.79	7.14	5.79	4.39	3.53	4.39	3.53	62.64	64.02	62.64	64.02
e_{ss}	0	0	0	0	0	0	0	0	0	0	0	0

Table 3.5 shows that using error AGS PID controllers a huge improvement in M_p and a considerable amount of improvement in t_s has been observed in the system response.

The simulation results under the effect of band limited white noise in the controllers are shown in Figure 3.16**.**

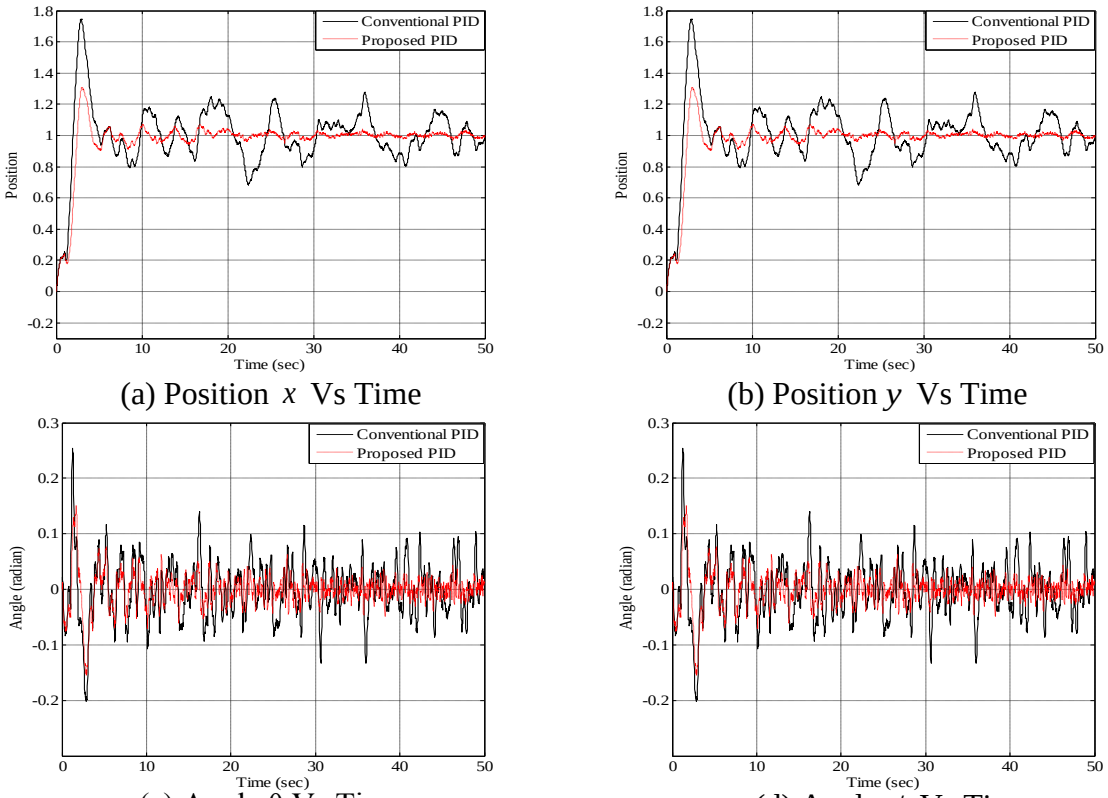

(a) Position x Vs Time (b) Position y Vs Time

(c) Angle θ Vs Time (d) Angle ϕ Vs Time

Figure 3.16 Stabilization of x - y Inverted Pendulum using Error AGS PID Controllers with Noise in the Controllers

The simulation results show a less chattered response as compared to the conventional PID scheme. The simulation results when considering the effect of friction on the inverted pendulum system are given in Figure 3.17 and Figure 3.18.

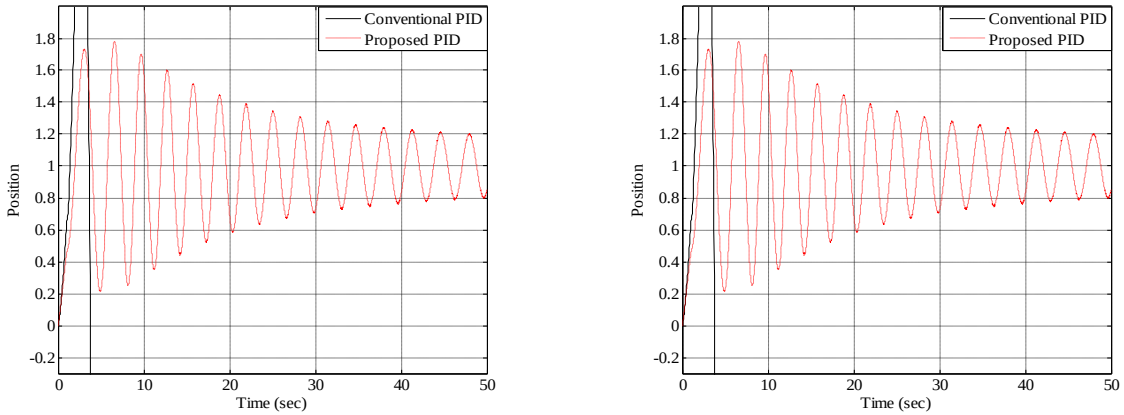

(a) Position x Vs Time (b) Position y Vs Time

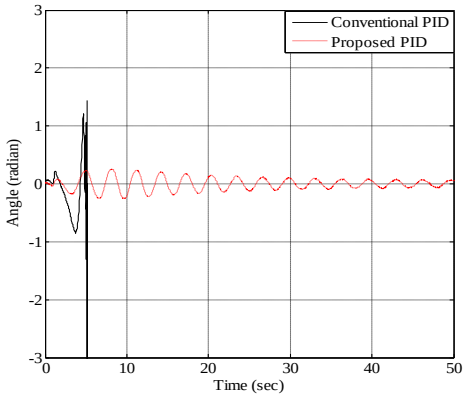

(c) Angle θ Vs Time

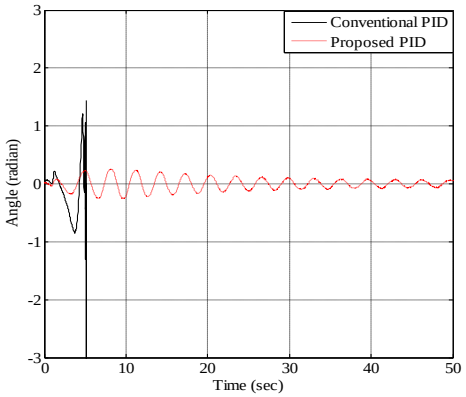

(d) Angle ϕ Vs Time

Figure 3.17 Stabilization of x - y Inverted Pendulum using Error AGS PID Controllers with Simple Friction Model

The above results show that the system response has become unbounded when the effect of friction is considered in terms of simple friction model while using conventional PID controllers. On the other hand the error AGS PID controllers give satisfactory results.

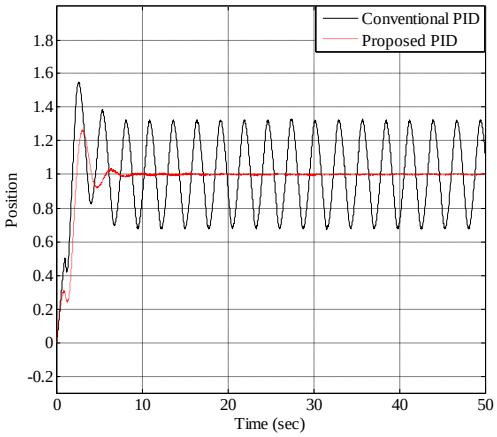

(a) Position x Vs Time

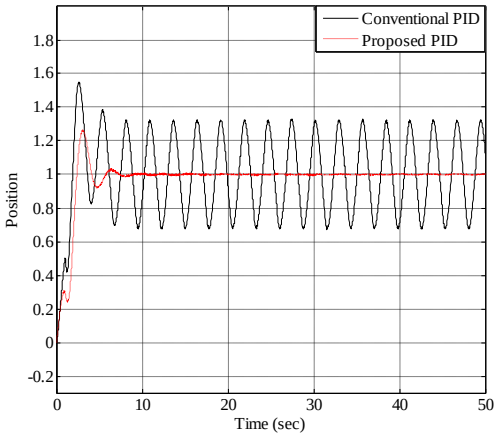

(b) Position y Vs Time

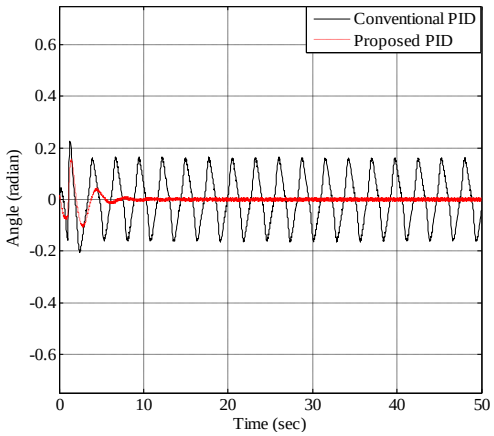

(c) Angle θ Vs Time

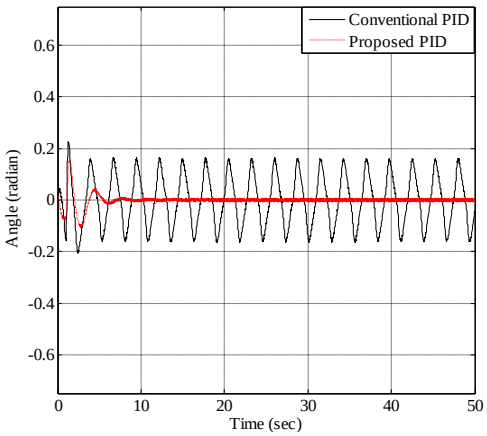

(d) Angle ϕ Vs Time

Figure 3.18 Stabilization of x - y Inverted Pendulum using Error AGS PID Controllers with Exponential Friction Model

When the exponential friction model is considered the error AGS PID controllers provide almost perfect control with zero e_{ss} as shown in Figure 3.18, while the conventional PID controllers give oscillatory response.

3.5.4 Tracking Control with Error AGS PID Controllers

Tracking signals $x_t = 0.3\sin(0.05\pi t)$ and $y_t = 0.3\sin(0.05\pi t)$ have been applied as the reference inputs. The simulation results for tracking control without Uncertainties are given in Figure 3.19.

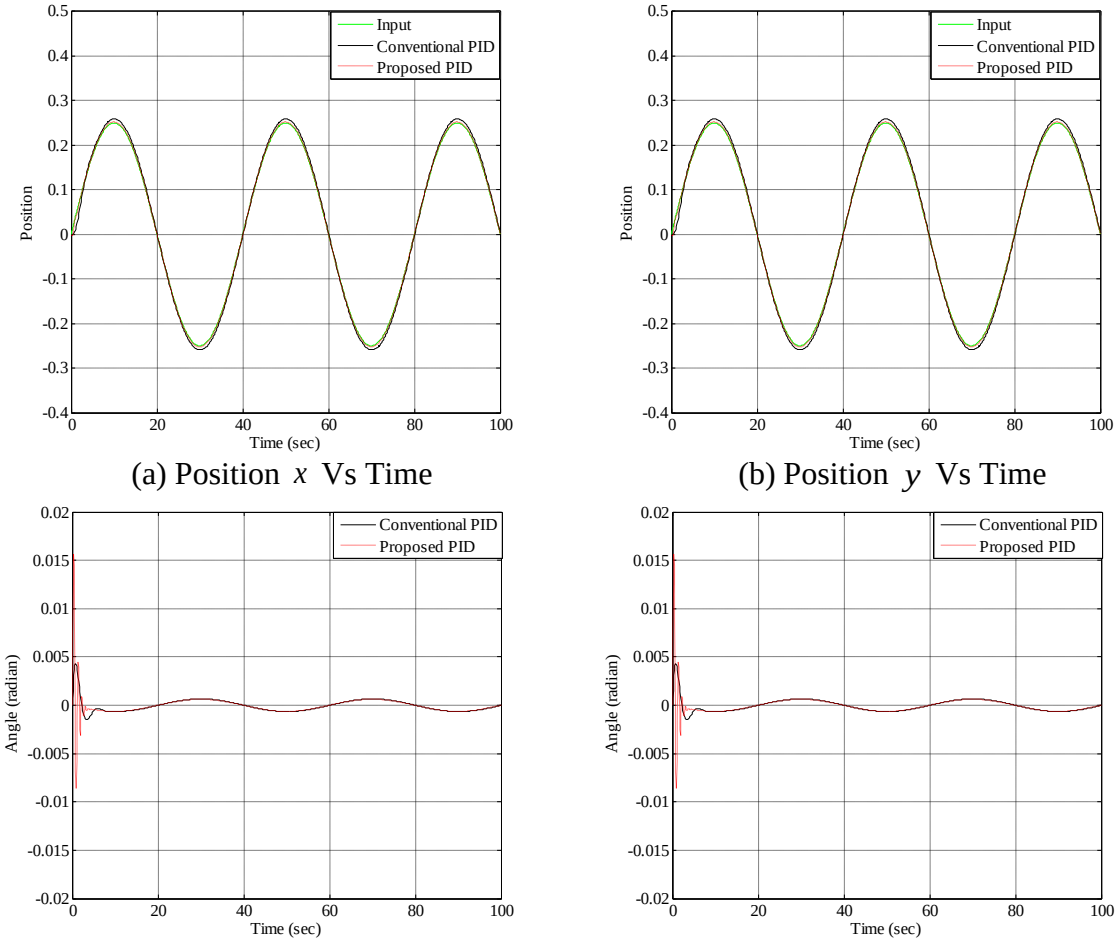

(a) Position x Vs Time

(b) Position y Vs Time

(c) Angle θ Vs Time

(d) Angle ϕ Vs Time

Figure 3.19 Tracking Control of x - y Inverted Pendulum using Error AGS PID Controllers without Uncertainties

The above simulation results show that both the conventional and AGS PID controllers give almost same tracking performance when no disturbances are acting on the x - y inverted pendulum. Figure 3.20 gives simulation results in the presence of disturbances.

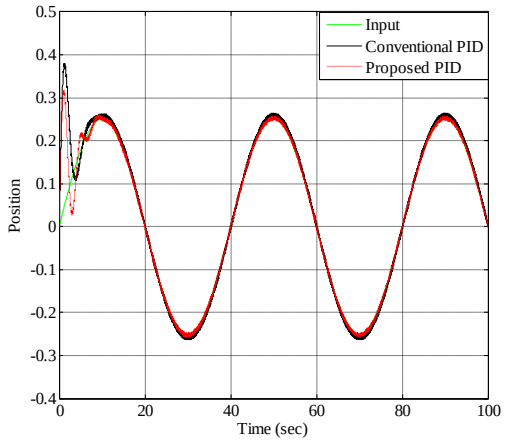

(a) Position x Vs Time

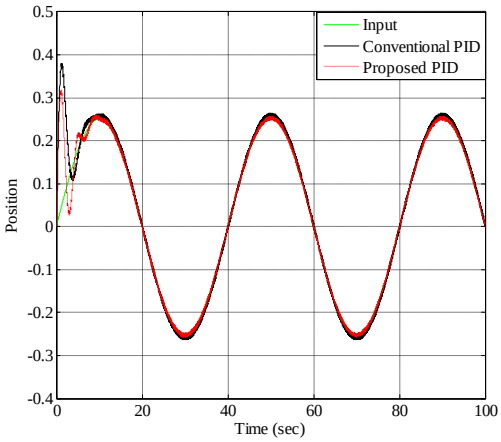

(b) Position y Vs Time

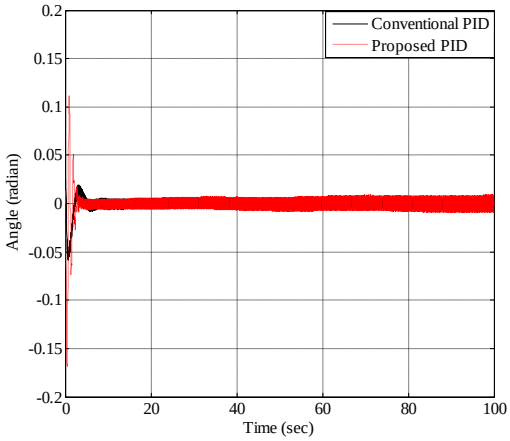

(c) Angle θ Vs Time

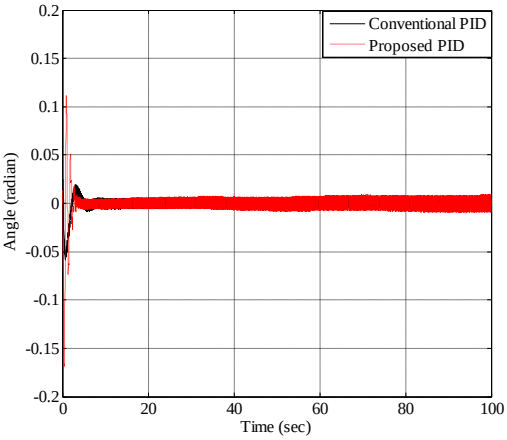

(d) Angle ϕ Vs Time

Figure 3.20 Tracking Control of x - y Inverted Pendulum using Error AGS PID Controllers with Disturbance

From Figure 3.20 it can be revealed that both the controllers perform well in the presence of external disturbances. Figure 3.21 gives the tracking results in the presence of noise in the controllers.

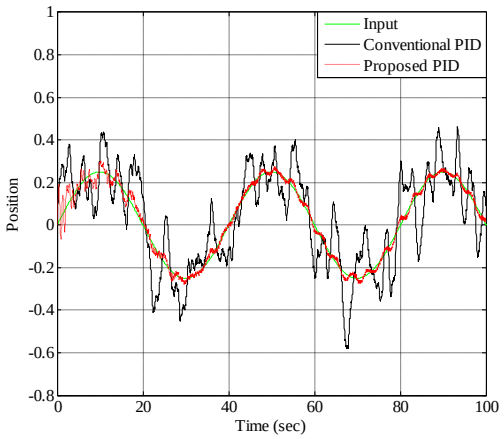

(a) Position x Vs Time

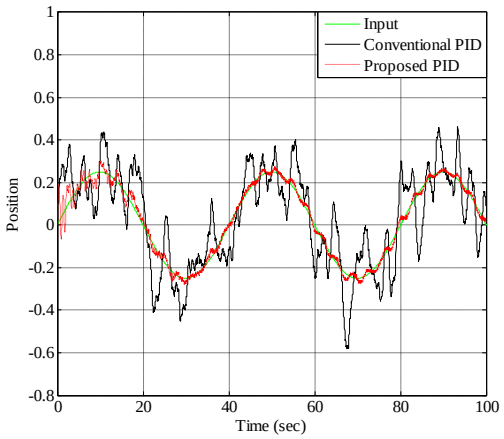

(b) Position y Vs Time

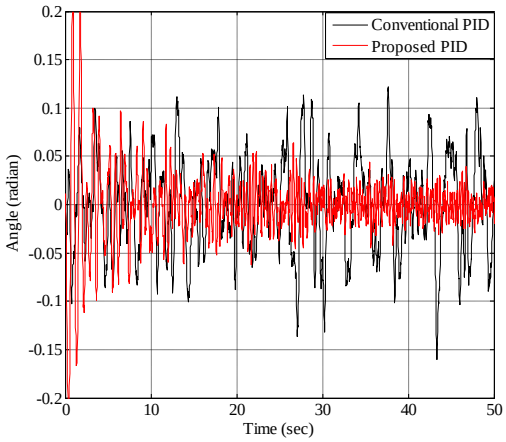

(c) Angle θ Vs Time

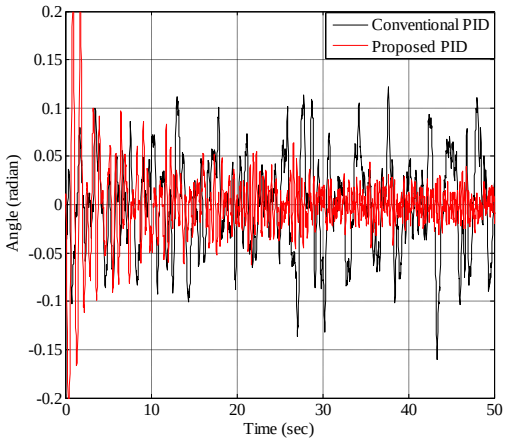

(d) Angle ϕ Vs Time

Figure 3.21 Tracking Control of x - y Inverted Pendulum using Error AGS PID Controllers with Noise in the Controllers

The above results show that when the error AGS PID controllers are used less chattering has been observed in the system response. The tracking results in the presence of frictional forces are given in Figure 3.22 and Figure 3.23.

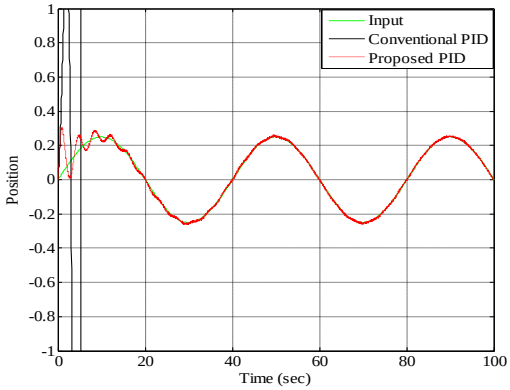

(a) Position x Vs Time

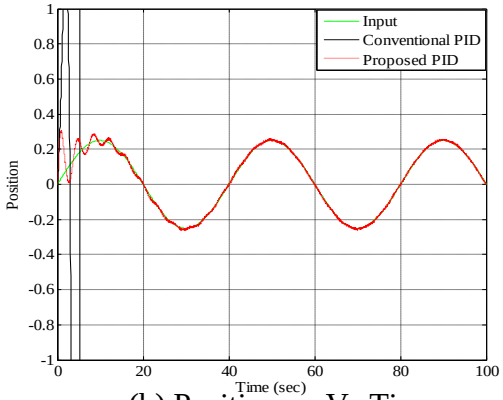

(b) Position y Vs Time

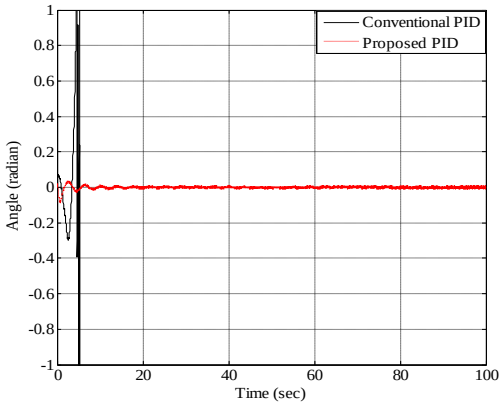

(c) Angle θ Vs Time

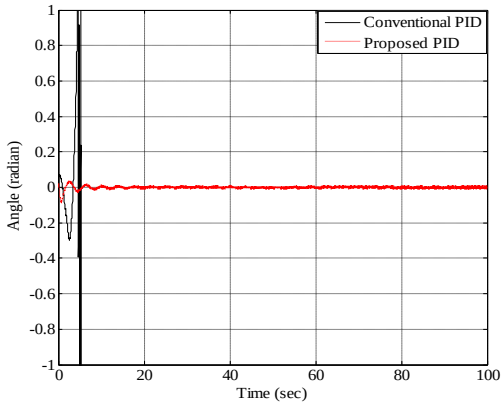

(d) Angle ϕ Vs Time

Figure 3.22 Tracking Control of x - y Inverted Pendulum using Error AGS PID Controllers with Simple Friction Model

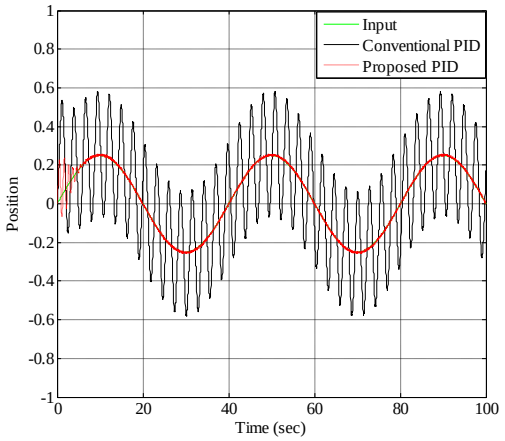

(a) Position x Vs Time

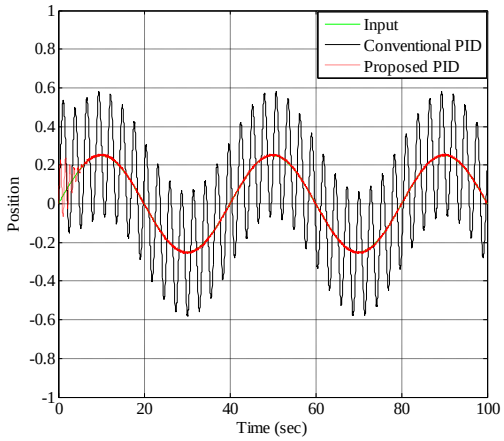

(b) Position y Vs Time

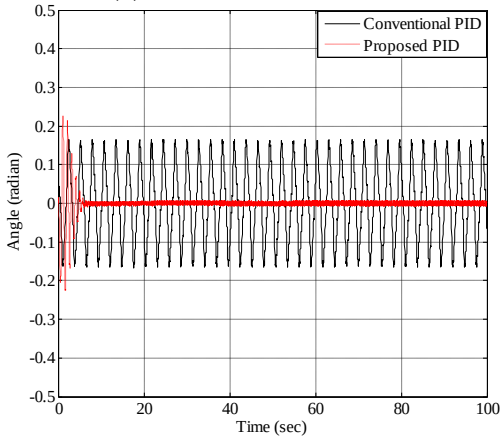

(c) Angle θ Vs Time

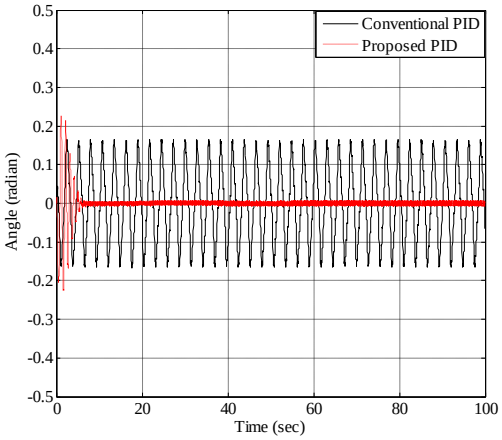

(d) Angle ϕ Vs Time

Figure 3.23 Tracking Control of x - y Inverted Pendulum using Error AGS PID Controllers with Exponential Friction Model

From the above simulation results it can be revealed that the error AGS PID controllers provide better reference tracking than the conventional PID controllers in the presence of frictional forces.

The movement of the base is possible not only in xy horizontal plane but also in xz horizontal and vertical plane. Hence the performance of the proposed controllers has also been tested for an x - z inverted pendulum.

3.6 State Space Modeling of x - z Inverted Pendulum

An x - z inverted pendulum mounted on a base has been shown in Figure 3.24. The movement of the base is in x - z horizontal and vertical plane with the help of applied forces F_x and F_z.

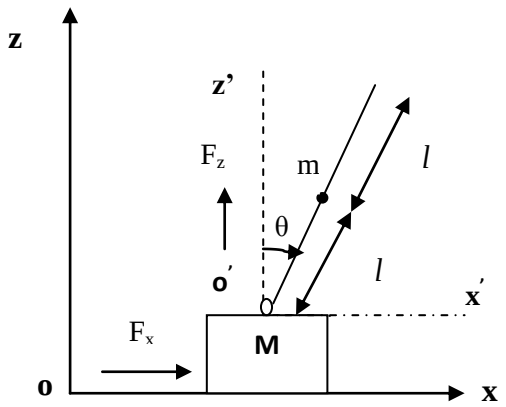

Figure 3.24 x - z Inverted Pendulum System

The state space modeling of the x - z inverted pendulum has been obtained using Euler Lagrange's equations.

3.6.1 Modeling without Uncertainties

The Lagrange's equations of the x - z inverted pendulum without uncertainties are given as (Wang, 2011):

$$\frac{d}{dt}\left(\frac{\partial L}{\partial \dot{x}}\right)-\frac{\partial L}{\partial x}=F_x \tag{3.34a}$$

$$\frac{d}{dt}\left(\frac{\partial L}{\partial \dot{z}}\right)-\frac{\partial L}{\partial z}=F_z \tag{3.34b}$$

$$\frac{d}{dt}\left(\frac{\partial L}{\partial \dot{\theta}}\right)-\frac{\partial L}{\partial \theta}=0 \tag{3.34c}$$

Where Lagrangian L is defined as:

$$L=K.E.-P.E. \tag{3.35}$$

Here $K.E.$ is the kinetic energy and $P.E.$ the potential energy of the system.

$$K.E.=\frac{1}{2}[M(\dot{x}^2+\dot{z}^2)+m(\dot{x}_P^2+\dot{z}_P^2)] \tag{3.36a}$$

$$P.E.=Mgz+mgz_p \tag{3.36b}$$

$$K.E.=\frac{1}{2}\left[M(\dot{x}^2+\dot{z}^2)+m[(\dot{x}+l\cos\theta\dot{\theta})^2+(\dot{z}-l\sin\theta\dot{\theta})^2]\right] \tag{3.37a}$$

$$P.E.=Mgz+mg(z+l\cos\theta) \tag{3.37b}$$

Putting (3.37 a) and (3.37 b) in Eq. (3.33)

$$L=\frac{1}{2}[M(\dot{x}^2+\dot{z}^2)+m(\dot{x}+l\cos\theta\dot{\theta})^2+(\dot{z}-l\sin\theta\dot{\theta})^2]-[Mgz+mg(z+l\cos\theta)] \tag{3.38}$$

Solving Eq. (3.34a) to Eq. (3.34c) using Eq. (3.38)

$$(M+m)\ddot{x} + ml\cos\theta\ddot{\theta} - ml\sin\theta\dot{\theta}^2 = F_x \tag{3.39}$$

$$(M+m)\ddot{z} - ml\sin\theta\ddot{\theta} - ml\cos\theta\dot{\theta}^2 + (M+m)g = F_z \tag{3.40}$$

$$l\ddot{\theta} + \cos\theta\ddot{x} - \sin\theta\ddot{z} - g\sin\theta = 0 \tag{3.41}$$

Defining $x_1 = x$, $x_2 = \dot{x}$, $x_3 = z$, $x_4 = \dot{z}$, $x_5 = \theta$ and $x_6 = \dot{\theta}$ the state space equations of the x-z inverted pendulum system are given by:

$$\dot{x}_1 = x_2 \tag{3.42}$$

$$\dot{x}_2 = \frac{-m\sin\theta\cos\theta F_z + F_x(M+m-m\sin^2\theta) + Mml\sin\theta\dot{\theta}^2}{M(M+m)} \tag{3.43}$$

$$\dot{x}_3 = x_4 \tag{3.44}$$

$$\dot{x}_4 = \frac{mF_z(1-\cos^2\theta) - m\sin\theta\cos\theta F_x + M(F_z - Mg) + Mml\cos\theta\dot{\theta}^2}{M(M+m)} \tag{3.45}$$

$$\dot{x}_5 = x_6 \tag{3.46}$$

$$\dot{x}_6 = \frac{-\cos\theta F_x + \sin\theta F_z}{Ml} \tag{3.47}$$

From Eq. (3.42) to Eq. (3.47) it can be concluded that the x-z inverted pendulum is a two input three output system. The two inputs are the applied forces F_x and F_z while the outputs are the positions x, z and the angle θ.

3.6.2 Modeling with Uncertainties

The state equations of the x-z inverted pendulum after considering the effect of external disturbance (d) and friction (F_{xfric} and F_{zfric}) can be written as:

$$\dot{x}_1 = x_2 \tag{3.48}$$

$$\dot{x}_2 = \frac{-m\sin\theta\cos\theta(F_z + F_{zfric}) + (F_x + F_{xfric})(M+m-m\sin^2\theta) + Mml\sin\theta\dot{\theta}^2}{M(M+m)} + d \tag{3.49}$$

$$\dot{x}_3 = x_4 \tag{3.50}$$

$$\dot{x}_4 = \frac{m(F_z + F_{zfric})(1-\cos^2\theta) - m\sin\theta\cos\theta(F_x + F_{xfric}) + M(F_z + F_{zfric} - Mg) + Mml\cos\theta\dot{\theta}^2}{M(M+m)} + d$$

(3.51)

$$\dot{x}_5 = x_6 \tag{3.52}$$

$$\dot{x}_6 = \frac{-\cos\theta(F_x + F_{xfric}) + \sin\theta(F_z + F_{zfric})}{Ml} + d \tag{3.53}$$

Here $d = 20\sin(20\pi t)$

The frictional forces (F_{xfric} and F_{zfric}) have been defined in Appendix A.

3.7 Control Structure of x-z Inverted Pendulum

The control structure of x-z inverted pendulum is shown in Figure 3.25 (Wang, 2011).

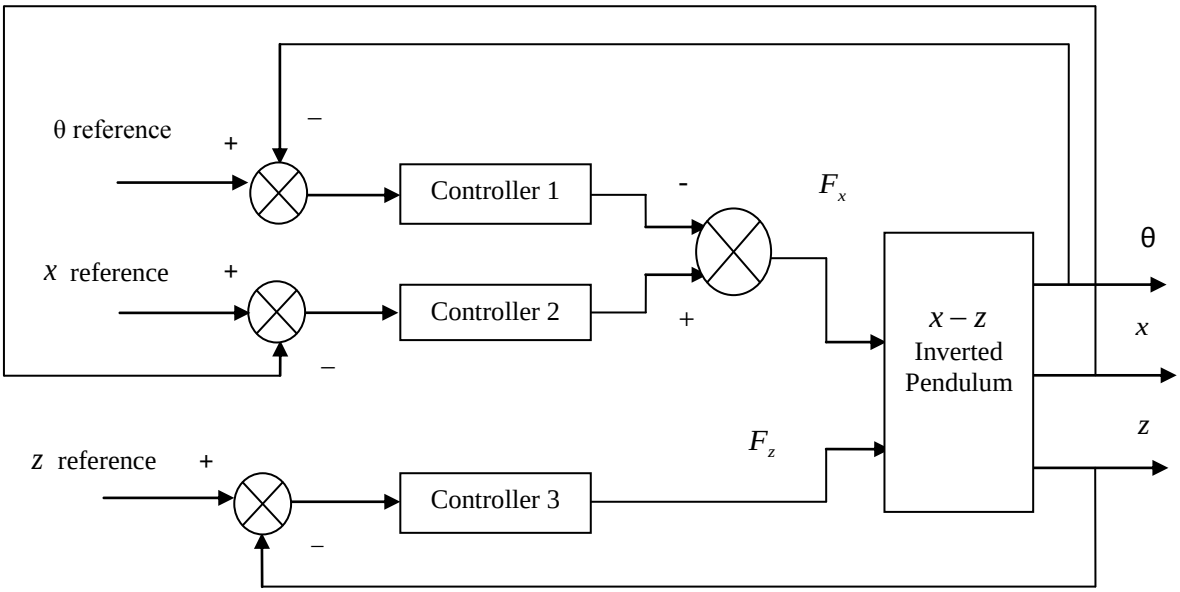

Figure 3.25 Control Structure of x-z Inverted Pendulum

From Figure 3.25 it can be revealed that an x-z inverted pendulum is a two input three output system, therefore a three loop control scheme with two loops for position control of the base while the remaining one for angle control of the pendulum has been implemented. Here controller 1 controls angle θ while controller 2 and controller 3 provides x and z position control.

PID controllers used for controlling the x-z inverted pendulum are tuned using time as well as error adaptive gain scheduling method. The minimum and the maximum value of gains for are given in Table 3.6.

Table 3.6 Parameters of AGS PID Controllers for x-z Inverted Pendulum Control

Parameter	$k_{p\min}$	$k_{p\max}$	$k_{i\min}$	$k_{i\max}$	$k_{d\min}$	$k_{d\max}$
PID1	24	36	1.5	3.6	3	5
PID2	-3	-2.4	-1.2	-1	-4.8	-2
PID3	25	15	15	10	15	10

3.8 Stability Analysis of x-z Inverted Pendulum

Theorem 3.2: The x-z inverted pendulum system will be stable if and only if

$$F_x\dot{x} + F_z\dot{z} \leq 0 \tag{3.54}$$

Proof: The Lyapunov function for an x-z inverted pendulum is defined as:

$$V = \frac{1}{2}M(\dot{x}^2 + \dot{z}^2) + \frac{1}{2}m(\dot{x}_p^2 + \dot{z}_p^2) + Mgz + mgz_p \tag{3.55}$$

Which is the sum of kinetic energy and the potential energy of the system.

$$V = \frac{1}{2}M(\dot{x}^2 + \dot{z}^2) + \frac{1}{2}m[(\dot{x} + l\cos\theta\dot{\theta})^2 + (\dot{z} - l\sin\theta\dot{\theta})^2] + Mgz + mg(z + l\cos\theta) \tag{3.56}$$

For the system to be stable the derivative of the Lyapunov function i.e. $\dot{V} \leq 0$

$$\begin{aligned}\dot{V} &= M(\dot{x}\ddot{x} + \dot{z}\ddot{z}) + m[(\dot{x} + l\cos\theta\dot{\theta})(\ddot{x} - l\sin\theta\dot{\theta}^2 + l\cos\theta\ddot{\theta}) + \\ &(\dot{z} - l\sin\theta\dot{\theta})(\ddot{z} - l\cos\theta\dot{\theta}^2 - l\sin\theta\ddot{\theta})] \\ &+ Mg\dot{z} + mg(\dot{z} - l\sin\theta\dot{\theta})\end{aligned} \tag{3.57}$$

$$\begin{aligned}\dot{V} &= M\dot{x}\ddot{x} + M\dot{z}\ddot{z} + m[\dot{x}\ddot{x} - \dot{x}l\sin\theta\dot{\theta}^2 + \dot{x}l\cos\theta\ddot{\theta} + l\cos\theta\dot{\theta}\dot{x} - l^2\sin\theta\cos\theta\dot{\theta}\dot{\theta}^2 + \\ &l^2\cos^2\theta\dot{\theta}\ddot{\theta} + (\dot{z}\ddot{z} - \dot{z}l\cos\theta\dot{\theta}^2 - \dot{z}l\sin\theta\ddot{\theta} - l\sin\theta\dot{\theta}\dot{z} + l^2\sin\theta\cos\theta\dot{\theta}\dot{\theta}^2 + l^2\sin^2\theta\dot{\theta}\ddot{\theta}] + \\ &+ Mg\dot{z} + mg\dot{z} - mgl\sin\theta\dot{\theta}\end{aligned}$$

(3.58)

Using Eq. (3.37) to Eq. (3.39) in Eq. (3.56)

$$\dot{V} = F_x\dot{x} + F_z\dot{z} \tag{3.59}$$

Therefore for the system to be stable:

$$F_x\dot{x} + F_z\dot{z} \leq 0 \tag{3.60}$$

To check the stability of x-z inverted pendulum with the proposed controllers the derivative of the Lyapunov function is plotted w.r.t. time.

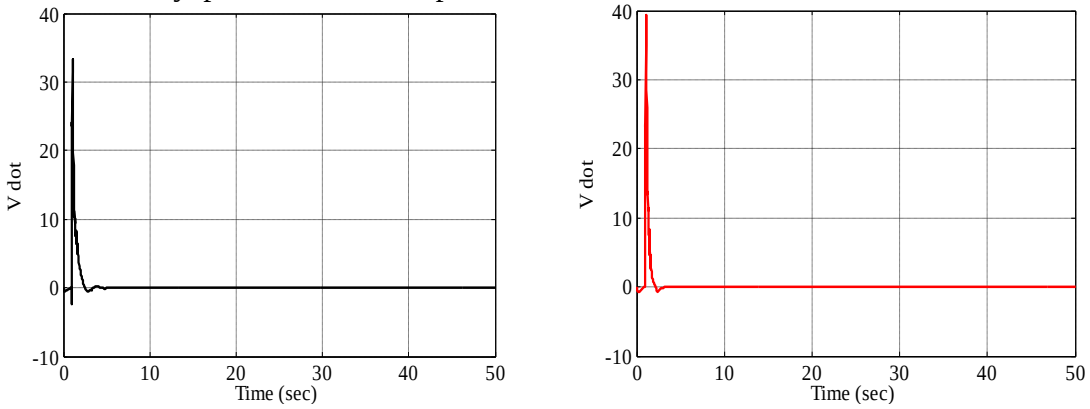

(a) Time AGS PID controller (b) Error AGS PID controller

Figure 3.26 $\dot{V}$ Vs Time for x-z Inverted Pendulum

The simulation results show that the derivative of the Lypunov function for the given system

with the proposed controllers tends towards zero which means that the system is stable with the proposed controllers.

3.9 Simulation Results

The simulation results for the stabilization and tracking control of $x-z$ inverted pendulum are given below:

3.9.1 Stabilization with Time AGS PID Controllers

The stabilization of $x-z$ inverted pendulum can be achieved by applying forces F_x and F_z to the base so that the pendulum should remain in the vertical upward position.

3.9.1.1 Stabilization without Uncertainties

The simulation results for stabilization without uncertainties are shown in Figure 3.27. The quantitative analysis is given in Table 3.7.

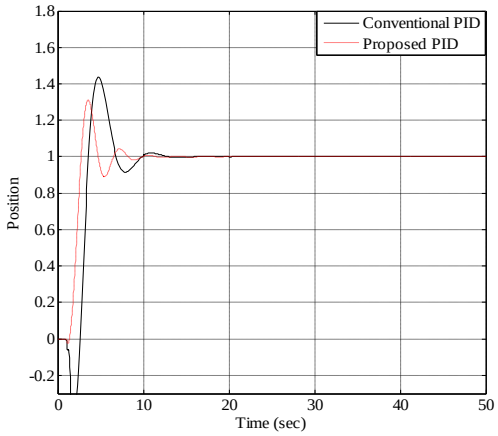

(a) Position x Vs Time

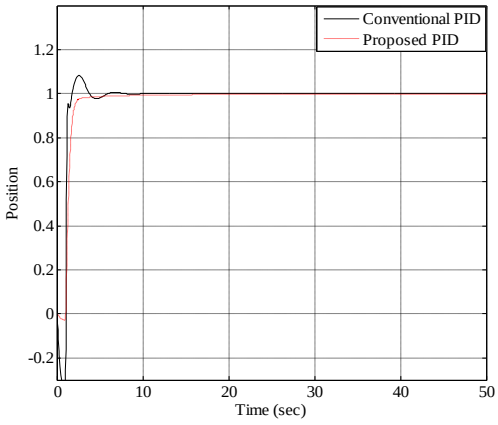

(b) Position z Vs Time

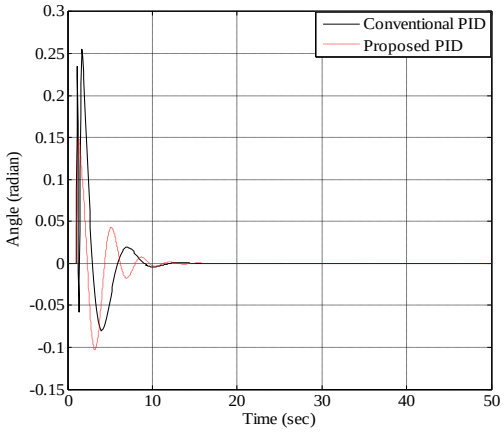

(c) Angle θ Vs Time

Figure 3.27 Stabilization of $x-z$ Inverted Pendulum using Time AGS PID Controllers without Uncertainties

Table 3.7 Quantitative Analysis of x - z Inverted Pendulum Control using Time AGS PID Controllers without Uncertainties

Parameters	Without disturbance						% improvement		
	Conventional			Proposed					
	x	z	θ	x	z	θ	x	z	θ
M_P	0.44	0.08	0.25	0.31	0	0.14	41.93	—	78.57
t_r	3.49	1.23	—	2.6	1.87	—	34.23	-34.22	—
t_s	11.13	4.98	5.4	7.84	2.95	5.82	41.96	68.81	-7.21
e_{ss}	0	0	0	0	0	0	0	0	0

The quantitative analysis shows that while using time AGS PID controllers there is an improvement in M_p, t_r and t_s for x position control while for z position control there is a increase in t_r. Furthermore in case of θ control there is a large reduction in overshoot when the proposed scheme is used.

3.9.1.2 Stabilization with Uncertainties

The simulation results in the presence of external disturbance are shown in Figure 3.28.

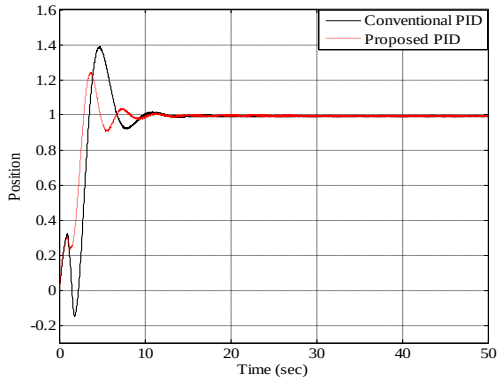

(a) Position x Vs Time

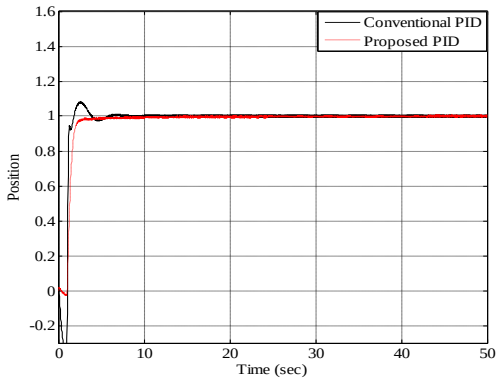

(b) Position z Vs Time

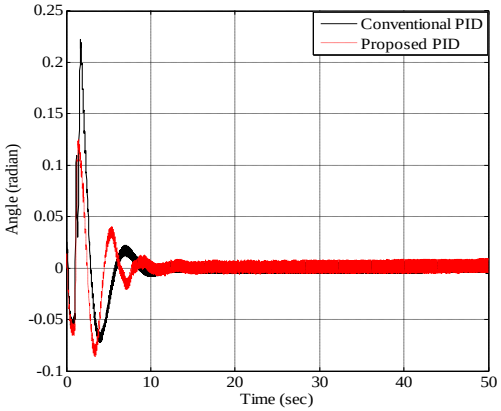

(c) Angle θ Vs Time

Figure 3.28 Stabilization of x - z Inverted Pendulum using Time AGS PID Controllers with Disturbance

Table 3.8 Quantitative Analysis of x - z Inverted Pendulum Control using Time AGS PID Controllers with Disturbance

Parameters	With disturbance						% improvement		
	Conventional			Proposed					
	x	z	θ	x	z	θ	x	z	θ
M_P	0.39	0.08	0.22	0.24	0	0.12	62.50	—	83.33
t_r	3.38	1.24	—	2.73	1.85	—	23.80	-32.97	—
t_s	9.44	5.23	7.37	9.74	3.74	5.72	-3.08	39.83	28.84
e_{ss}	0	0	0	0	0	0	0	0	0

Table 3.8 shows a large amount of improvement in M_p in case of both x and θ control. The simulation results with noise are shown are shown in Figure 3.29.

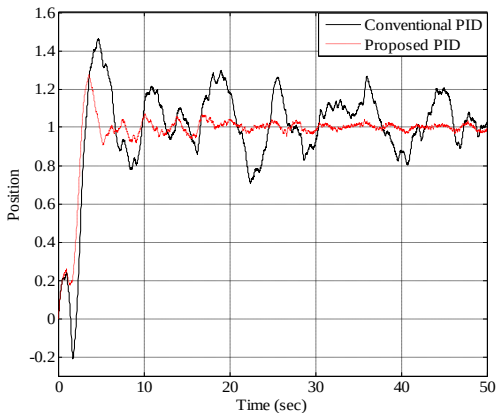

(a) Position x Vs Time

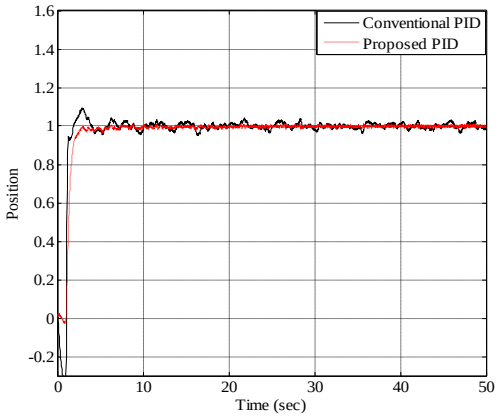

(b) Position z Vs Time

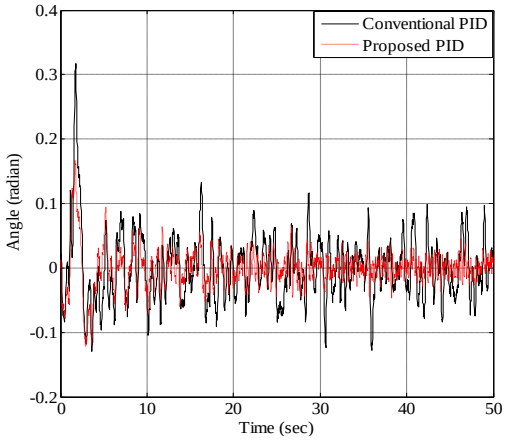

(c) Angle θ Vs Time

Figure 3.29 Stabilization of x - z Inverted Pendulum using Time AGS PID Controllers with Noise in the Controllers

The simulation results show that using time AGS PID controllers less chattering has been observed in the output response. The simulation results when considering the effect of friction are given in Figure 3.30 and Figure 3.31.

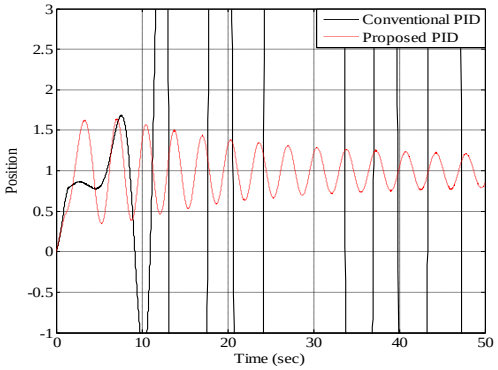

(a) Position x Vs Time

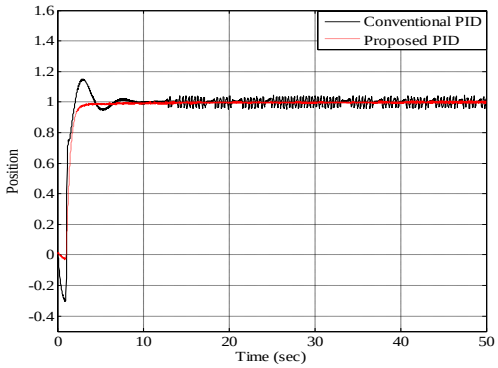

(b) Position z Vs Time

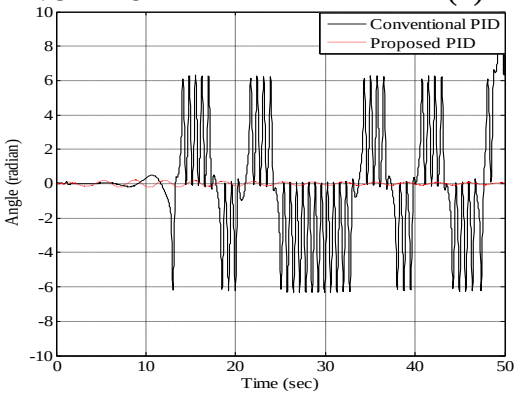

(c) Angle θ Vs Time

Figure 3.30 Stabilization of x - z Inverted pendulum using Time AGS PID Controllers with Simple Friction Model

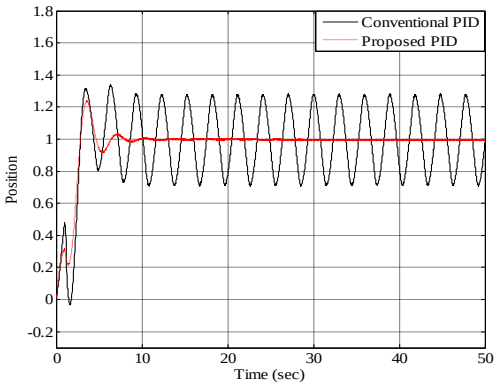

(a) Position x Vs Time

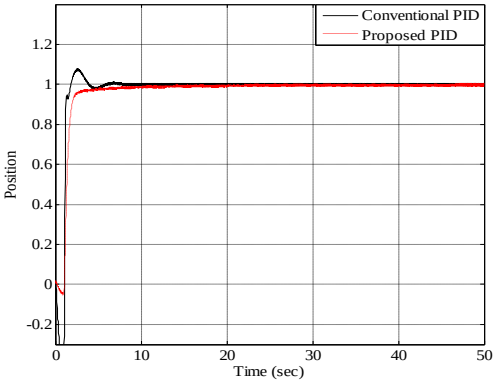

(b) Position z Vs Time

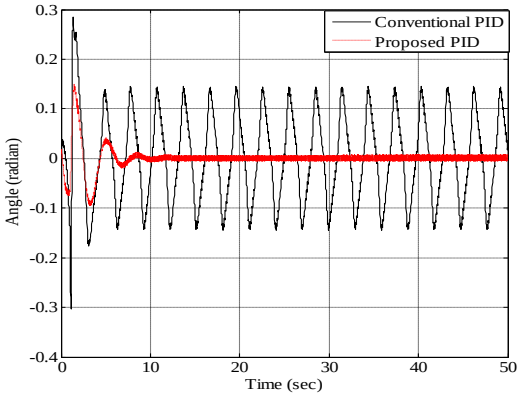

(c) Angle θ Vs Time

Figure 3.31 Stabilization of x - z Inverted Pendulum using Time AGS PID Controllers with Exponential Friction Model

The simulation results show the effectiveness of time AGS PID controllers as compared to the conventional PID controllers which perform poorly in the presence of friction.

3.9.2 Tracking Control with Time AGSPID Controllers

Tracking signals $x_t = 0.3\sin(0.05\pi t)$ and $x_z = 0.15\sin(0.05\pi t)$ have been applied as the reference input. The simulation results under different conditions are shown from Figure 3.32 to Figure 3.36.

.

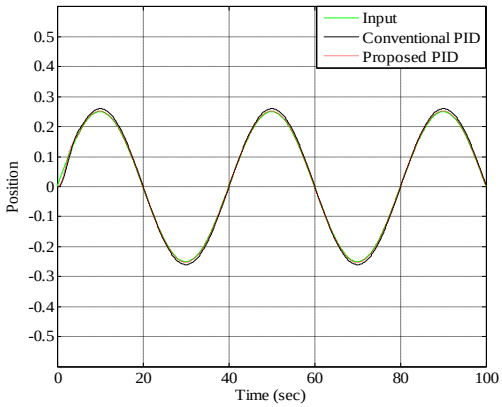

(a) Position x Vs Time

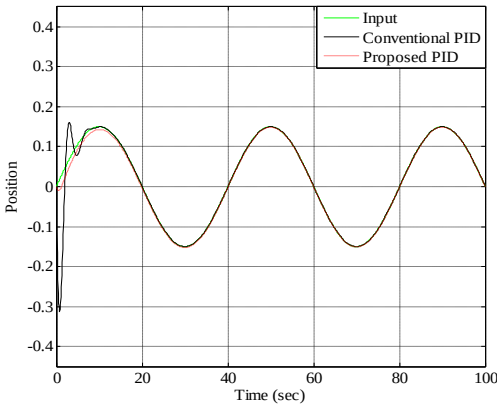

(b) Position z Vs Time

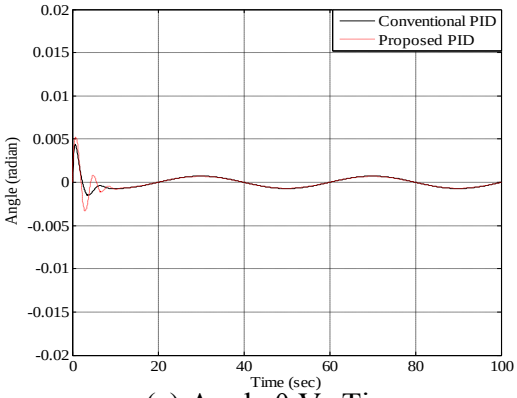

(c) Angle θ Vs Time

Figure 3.32 Tracking Control of x - z Inverted Pendulum using Time AGS PID Controllers without Uncertainties

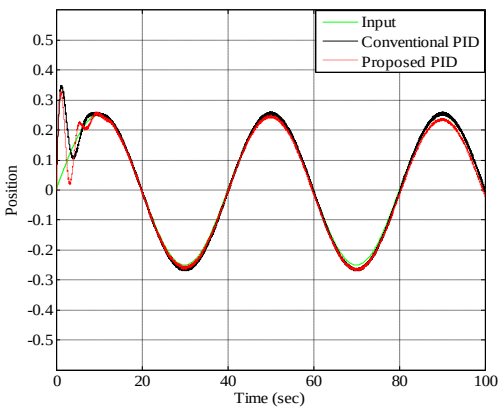

(a) Position x Vs Time

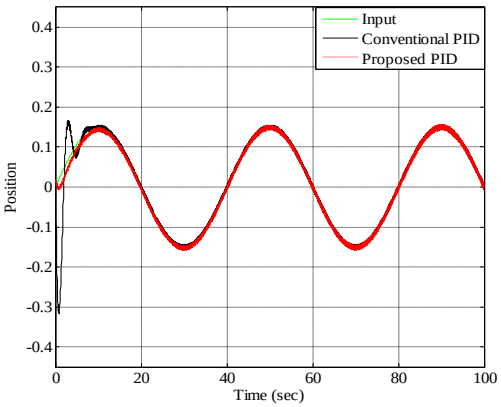

(b) Position z Vs Time

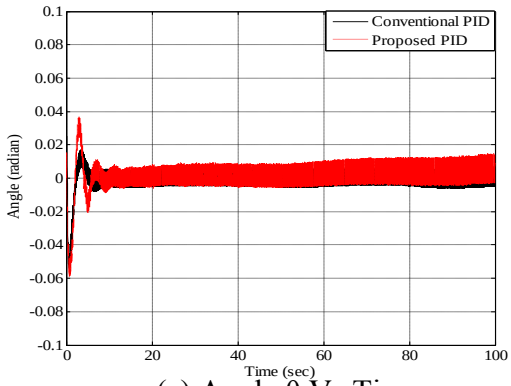

(c) Angle θ Vs Time

Figure 3.33 Tracking Control of x - z Inverted Pendulum using Time AGS PID Controllers with Disturbance

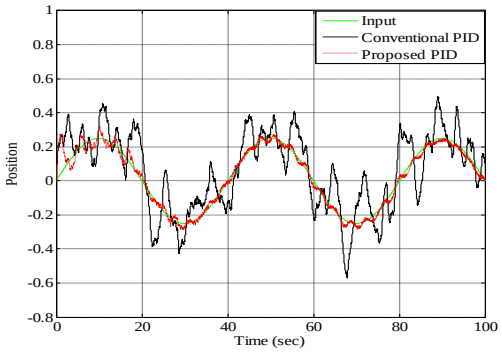

(a) Position x Vs Time

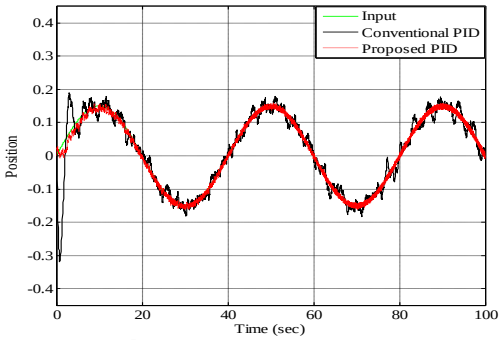

(b) Position z Vs Time

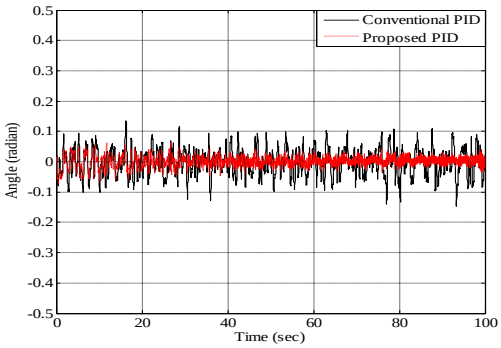

(c) Angle θ Vs Time

Figure 3.34 Tracking Control of x - z Inverted Pendulum using Time AGS PID Controllers with Noise in the Controllers

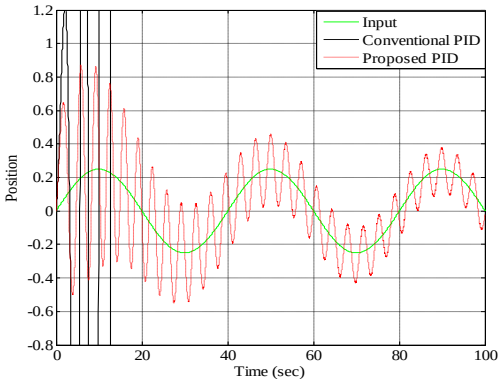

(a) Position x Vs Time

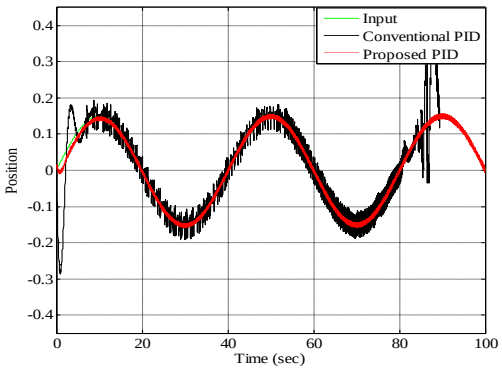

(b) Position z Vs Time

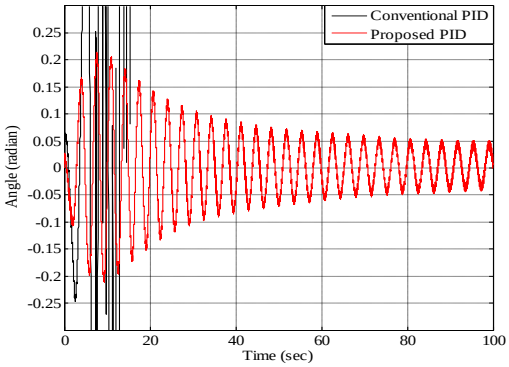

(c) Angle θ Vs Time

Figure 3.35 Tracking Control of x - z Inverted Pendulum using Time AGS PID Controllers with Simple Friction Model

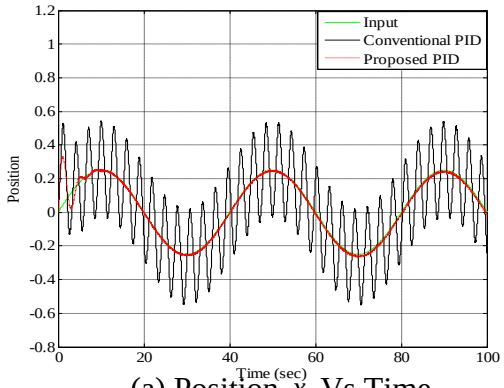

(a) Position x Vs Time

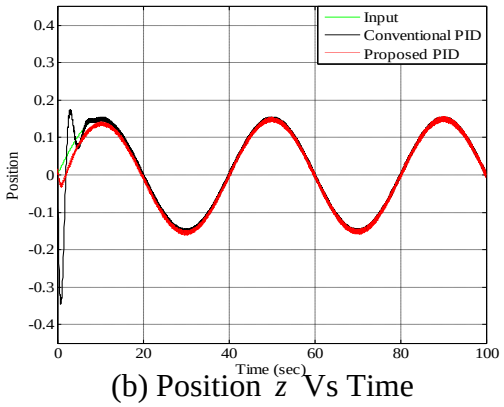

(b) Position z Vs Time

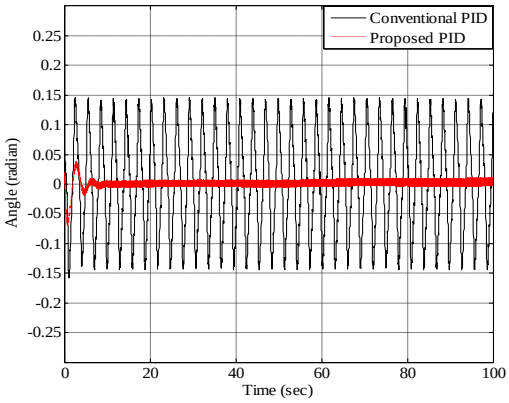

(c) Angle θ Vs Time

Figure 3.36 Tracking Control of x - z Inverted Pendulum using Time AGS PID Controllers with Exponential Friction Model

The above simulation results show the robust nature of time AGS PID controllers which performs quite satisfactory as compared to the conventional PID controllers even in the presence of noise and frictional forces.

3.9.3 Stabilization with Error AGSPID Controllers

The time AGSPID controllers are replaced by error AGSPID controllers. The simulation results under different conditions are shown below:

3.9.3.1 Stabilization without Uncertainties

The simulation results for the stabilization without the effect of external disturbance are shown in Figure 3.37. The quantitative analysis is given in Table 3.9.

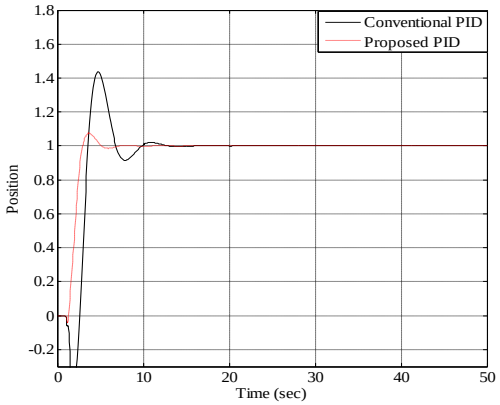

(a) Position x Vs Time

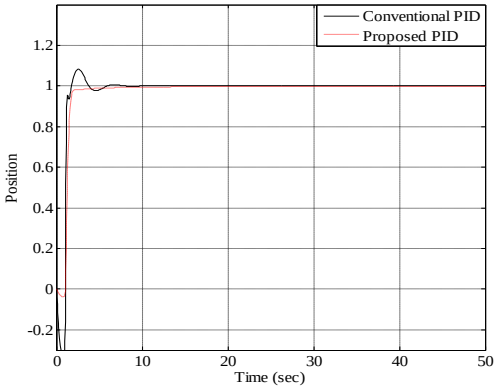

(b) Position z Vs Time

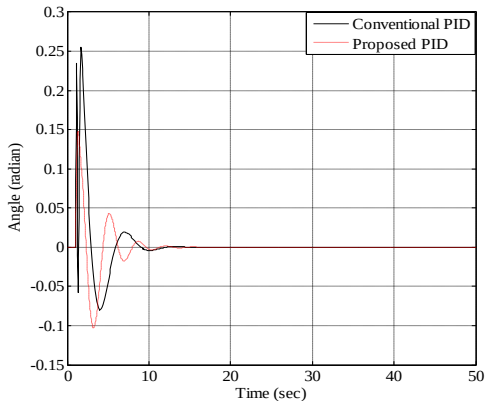

(c) Angle θ Vs Time

Figure 3.37 Stabilization of x - z Inverted Pendulum using Error AGS PID Controllers without Uncertainties

Table 3.9 Quantitative Analysis of x - z Inverted Pendulum Control using Error AGS PID Controllers without Uncertainties

Parameters	Without disturbance						% improvement		
	Conventional			Proposed					
	x	z	θ	x	z	θ	x	z	θ
M_P	0.44	0.08	0.25	0.07	0	0.25	528.57	__	0
t_r	3.49	1.23	__	2.66	1.62	__	31.203	-24.07	__
t_s	11.13	4.98	5.4	4.75	2.07	3.76	134.31	140.57	43.61
e_{ss}	0	0	0	0	0	0	0	0	0

The quantitative analysis shows a large reduction in M_p with a significant improvement in t_r and t_s for x position control.

3.9.3.2 Stabilization with Uncertainties

The simulation results in the presence of external disturbances are shown in Figure 3.38 while its quantitative analysis is given in Table 3.10.

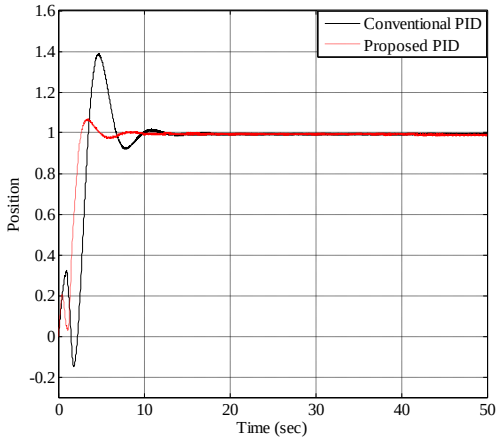

(a) Position x Vs Time

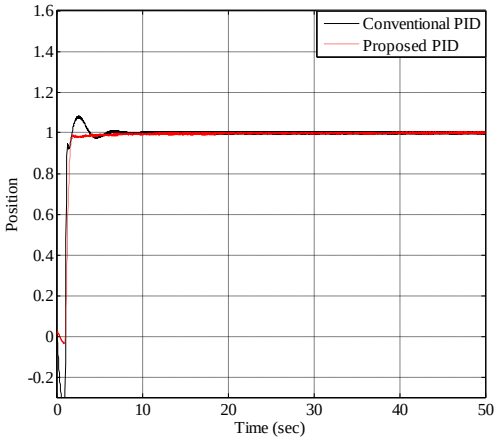

(b) Position z Vs Time

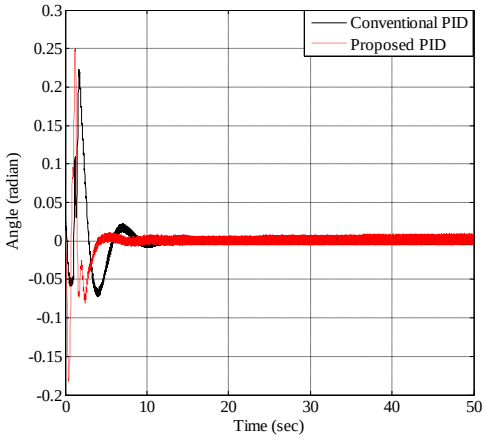

(c) Angle θ Vs Time

Figure 3.38 Stabilization of x - z Inverted Pendulum using Error AGS PID Controllers with Disturbance

Table 3.10 Quantitative Analysis of x - z Inverted Pendulum Control using Error AGS PID Controllers with Disturbance

Parameters	With disturbance						% improvement		
	Conventional			Proposed					
	x	z	θ	x	z	θ	x	z	θ
M_P	0.39	0.08	0.22	0.07	0	0.25	457.14	—	-12.00
t_r	3.38	1.24	—	2.36	1.6	—	43.22	-47.45	—
t_s	9.44	5.23	7.37	4.4	3.4	3.52	114.54	53.82	109.37
e_{ss}	0	0	0	0	0	0	0	0	0

The quantitative analysis shows a large reduction in M_p with a significant improvement in t_r and t_s for x position control. Similarly for z position control the M_p has been reduced to

zero with an improvement in t_s and a degradation in t_r. Finally for θ control the settling time has been reduced by a good amount with a minor increase in M_p.

The simulation results with noise in the controllers are shown in Figure 3.39.

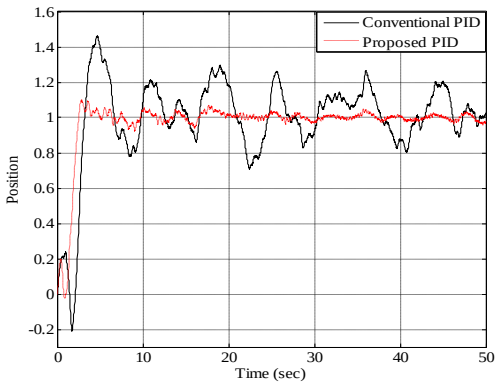

(a) Position x Vs Time

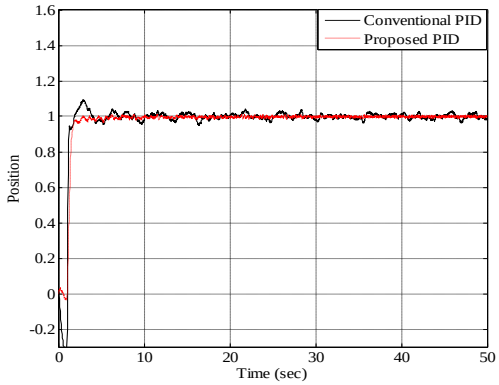

(a) Position z Vs Time

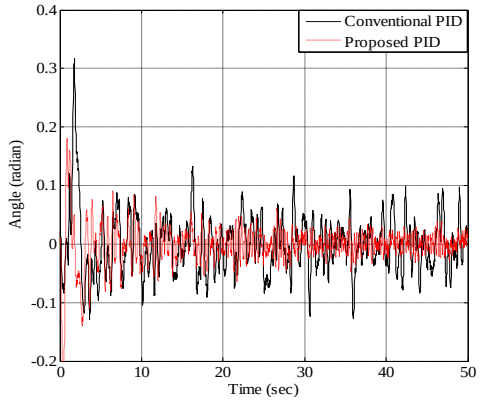

(c) Angle θ Vs Time

Figure 3.39 Stabilization of x - z Inverted Pendulum using Error AGS PID Controllers with Noise in the Controllers

The simulation results show a less chattered response in case of error AGS PID controllers as compared to the conventional PID scheme. The simulation results when considering the effect of friction on the inverted pendulum system are given in Figure 3.40 and Figure 3.41.

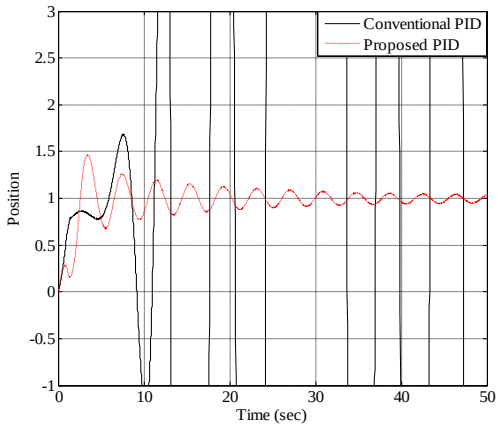

(a) Position x Vs Time

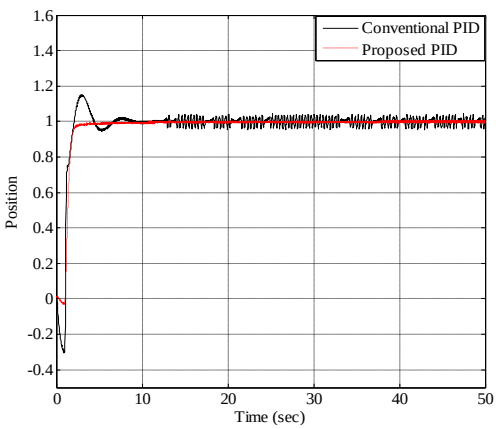

(b) Position z Vs Time

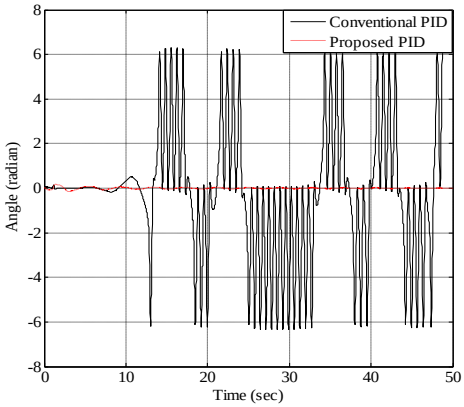

(c) Angle θ Vs Time

Figure 3.40 Stabilization of x - z Inverted Pendulum using Error AGS PID Controllers with Simple Friction Model

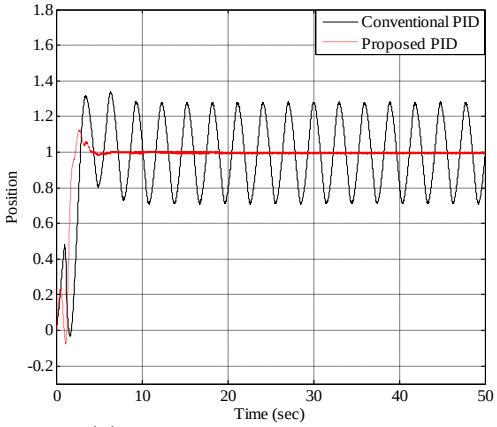

(a) Position x Vs Time

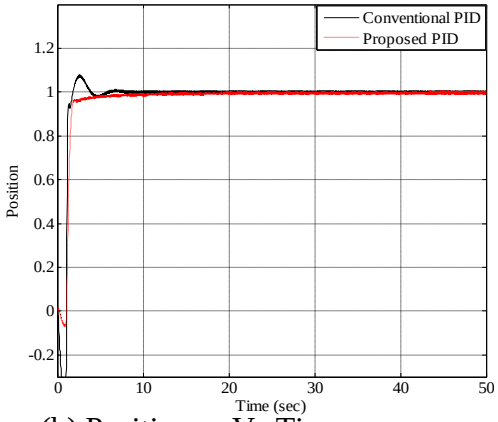

(b) Position z Vs Time

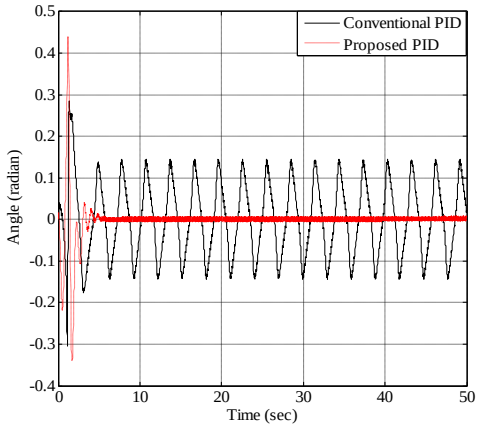

(c) Angle θ Vs Time

Figure 3.41 Stabilization of x - z Inverted pendulum using Error AGS PID Controllers with Exponential Friction Model

The simulation results in Figure 3.40 and Figure 3.41 show the adaptive nature of the proposed controllers which performs quite well as compared to the conventional scheme in the presence of friction.

3.9.4 Tracking control with Error AGS PID Controllers

The simulation results for tracking control under different conditions are given from Figure 3.42 to Figure 3.46.

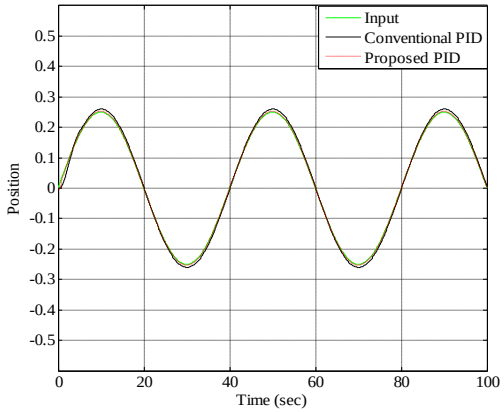

(a) Position x Vs Time

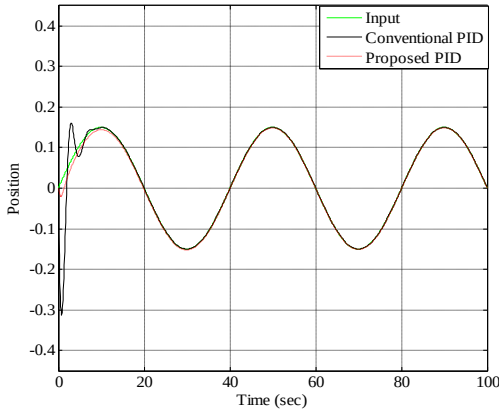

(b) Position z Vs Time

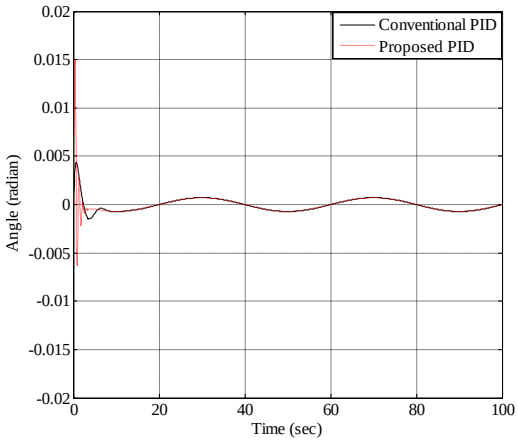

(c) Angle θ Vs Time

Figure 3.42 Tracking Control of x - z Inverted Pendulum using Error AGS PID Controllers without Uncertainties

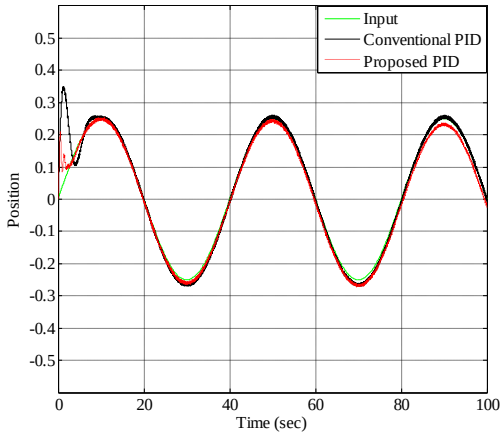

(a) Position x Vs Time

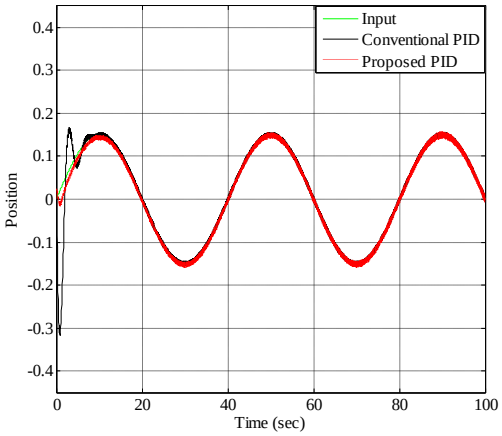

(b) Position z Vs Time

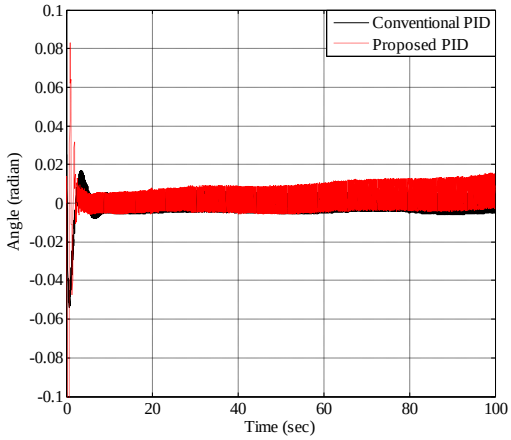

(c) Angle θ Vs Time

Figure 3.43 Tracking Control of x - z Inverted Pendulum using Error AGS PID Controllers with Disturbance

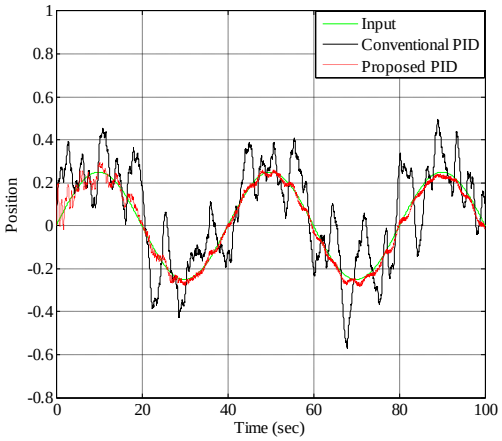

(a) Position x Vs Time

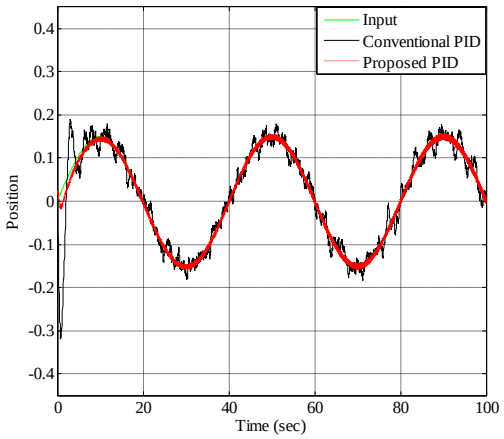

(b) Position z Vs Time

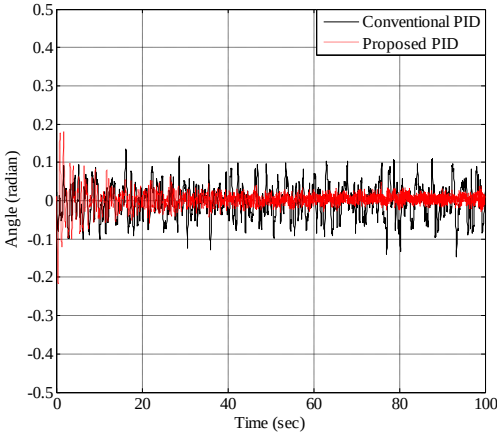

(c) Angle θ Vs Time

Figure 3.44 Tracking Control of x - z Inverted Pendulum using Error AGS PID Controllers with Noise in the Controllers

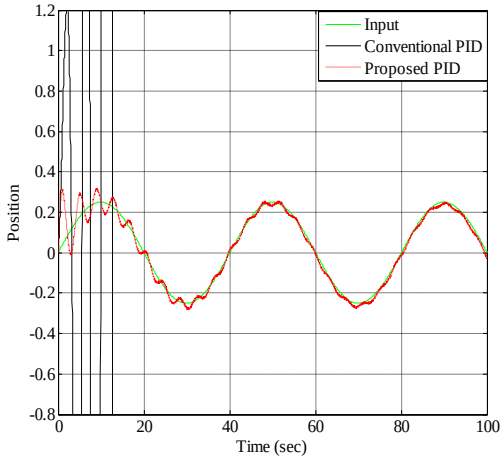

(a) Position x Vs Time

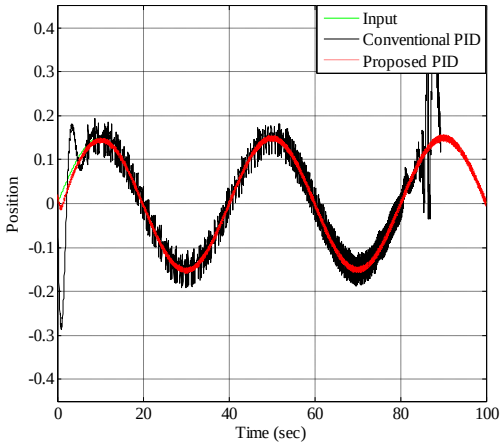

(b) Position z Vs Time

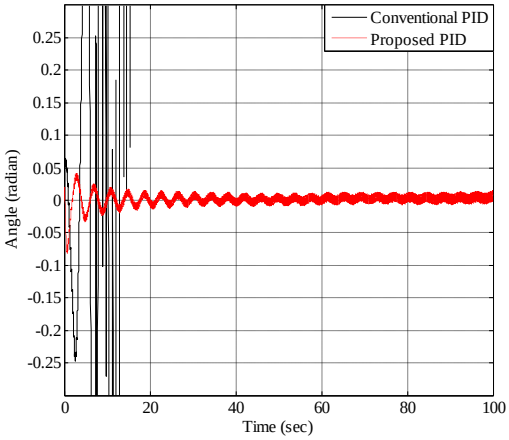

(c) Angle θ Vs Time

Figure 3.45 Tracking Control of x - z Inverted Pendulum using Error AGS PID Controllers with Simple Friction

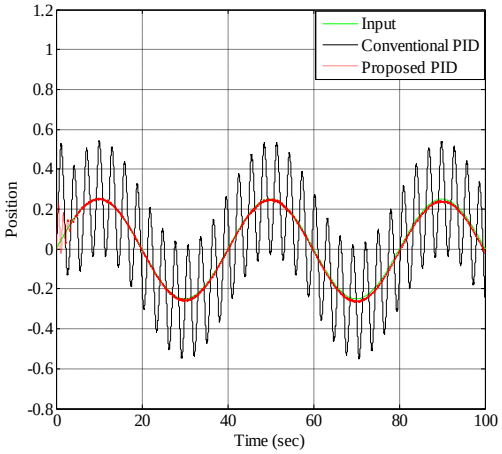

(a) Position x Vs Time

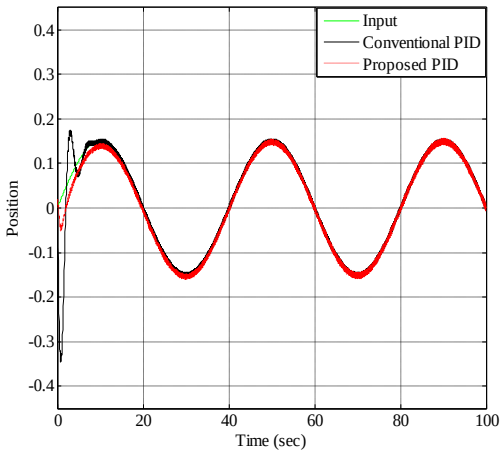

(b) Position z Vs Time

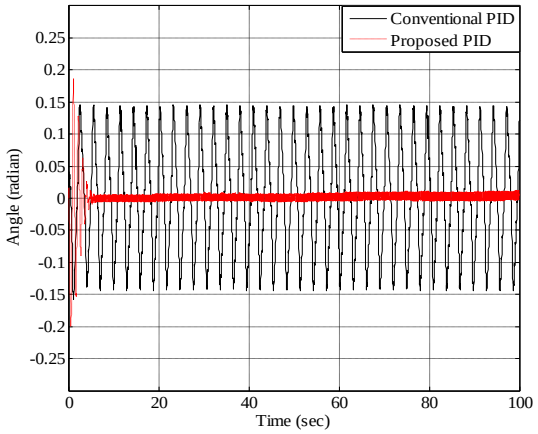

(c) Angle θ Vs Time

Figure 3.46 Tracking Control of x - z Inverted Pendulum using Error AGS PID Controllers with Exponential Friction

From the above simulation results it can be observed that the error AGS PID controllers provide better reference tracking as compared to the conventional PID controllers especially in the presence of uncertainties.

3.10 Conclusion

In this chapter, the proposed AGS PID controllers have been implemented for the stabilization and tracking control of x - y and x - z inverted pendulums. The performance of the proposed time AGS PID controllers and error AGS PID controllers have been compared with the conventional PID controllers given in the literature. For x - y inverted pendulum the simulation results show a large reduction in maximum overshoot (M_p) of 66.6% in case of position control and 93.75% in case of angle control when the time AGS PID controllers are used for stabilization. Similarly when error AGS PID controllers are used a huge amount of improvement in M_p i.e. 1275% for position control and 19.2% for angle control and a significant amount of improvement in settling time (t_s) of 70.37% for position control and 79.6% for angle control has been observed in the system response. A comparative study between time AGS PID controllers and error AGS PID controllers reveal that for position control M_p and t_s are less by 725% and 71.09% in case of error AGS PID controllers while the rise time (t_r) improves by 2.55% with time AGS PID controllers. Similarly for angle control M_p in case of time AGS is less by 62.5% while the t_s for error AGS PID controllers is less by 70.38%.

For an x - z inverted pendulum with time AGS PID controllers the simulation results show a reduction in M_p of 41.93%, t_r of 34.23% and t_s of 41.96% in case of x position control. Also for angle control M_p reduces by 78.57%. When error AGS PID controllers are used M_p reduces by 528.57% with a good mount of improvement in t_r and t_s of 31.2% and 134.3% respectively for x position control. For z position control t_s reduces by 140.57%. Similarly for angle the settling time improves to 43.61%. A comparative study between time AGS PID controllers and error AGS PID controllers reveal that for x position control the M_p and t_s improves by 342.85% and 52.42% in case of error AGS PID controllers with a small deterioration in t_r of 2.3%. For z position control t_r and t_s improves by 15.43% and 42.5% with error AGS PID controllers. In case angle control the time AGS PID controllers outperforms error AGS PID controllers with 78.57% improvement in M_p.

Moreover, the proposed controllers are stable and provide good reference tracking even in the presence of uncertainties such as, disturbance in the inverted pendulum, noise in the controller and friction.

The motion of the base is possible not only in one and two dimension but also three dimensional motion of the base is possible. Hence the performance of the proposed controllers has also been carried out for a proposed three dimensional inverted pendulum.

CHAPTER 4

Modelling and Control of a Three Dimensional Inverted Pendulum

4.1 Introduction

A three dimensional inverted pendulum is an inverted pendulum in which the movement of the base is three dimensional to stabilize the pendulum vertically upwards. The inverted pendulum can move in the xy horizontal and z vertical plane with the help of horizontal and vertical forces. Because of this movement of the base in all the three directions the inverted pendulum is called as an $x-y-z$ inverted pendulum. In this chapter the mathematical modelling of an $x-y-z$ inverted pendulum in the form of state space equations has been done using Euler Lagrange's method. The stability condition of the inverted pendulum has been analyzed using Lyapunov stability criterion. The stabilization and tracking control of the $x-y-z$ inverted pendulum has been achieved using the proposed adaptive gain scheduling (AGS) PID controllers. The effect of uncertainties on the performance of the inverted pendulums has been analyzed. The simulation results have been compared with the conventional PID scheme given in the literature.

4.2 State Space Modeling of $x-y-z$ Inverted Pendulum

An $x-y-z$ Inverted pendulum pivoted to a base has been shown in Figure 4.1.

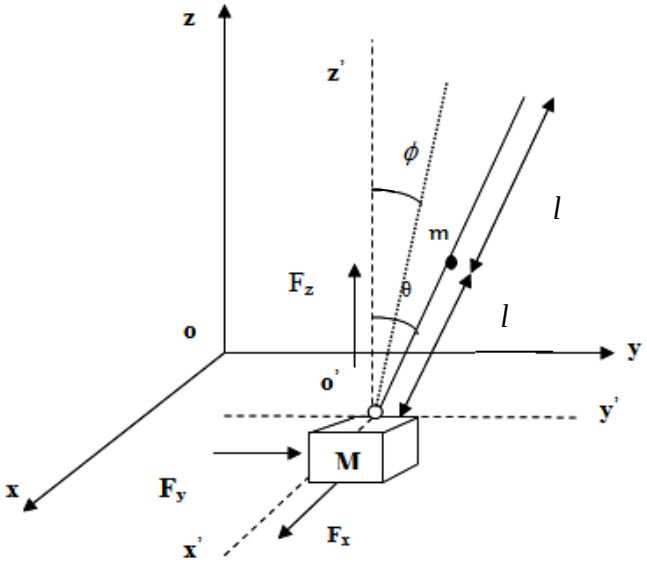

Figure 4.1 $x-y-z$ Inverted Pendulum System

Stabilization of the inverted pendulum in upright position depends upon the horizontal and vertical displacement of the base which in turn depends upon the applied forces, F_x, F_y and F_z.

Here (x, y, z) and $(\dot{x}, \dot{y}, \dot{z})$ = Position and velocity of the base in the xyz coordinate

(x_P, y_P, z_P) and $(\dot{x}_P, \dot{y}_P, \dot{z}_P)$ = Position and velocity of the base in $x'y'z'$ coordinate

$$x_p = x + l\sin\theta \tag{4.1a}$$

$$y_p = y + l\cos\theta\sin\phi \tag{4.1b}$$

$$z_p = z + l\cos\theta\cos\phi \tag{4.1c}$$

$$\dot{x}_p = \dot{x} + l\cos\theta\dot{\theta} \tag{4.1d}$$

$$\dot{y}_p = \dot{y} + l\cos\theta\cos\phi\dot{\phi} - l\sin\theta\sin\phi\dot{\theta} \tag{4.1e}$$

$$\dot{z}_p = \dot{z} - l\sin\theta\cos\phi\dot{\theta} - l\cos\theta\sin\phi\dot{\phi} \tag{4.1f}$$

The state space modeling of the x - y - z inverted pendulum can be obtained using Euler Lagrange equations.

4.2.1 Modeling without Uncertainties

The Lagrange equations of the x - y - z inverted pendulum are given as:

$$\frac{d}{dt}\left(\frac{\partial L}{\partial \dot{x}}\right) - \frac{\partial L}{\partial x} = F_x \tag{4.2a}$$

$$\frac{d}{dt}\left(\frac{\partial L}{\partial \dot{y}}\right) - \frac{\partial L}{\partial y} = F_y \tag{4.2b}$$

$$\frac{d}{dt}\left(\frac{\partial L}{\partial \dot{z}}\right) - \frac{\partial L}{\partial z} = F_z \tag{4.2c}$$

$$\frac{d}{dt}\left(\frac{\partial L}{\partial \dot{\theta}}\right) - \frac{\partial L}{\partial \theta} = 0 \tag{4.2d}$$

$$\frac{d}{dt}\left(\frac{\partial L}{\partial \dot{\phi}}\right) - \frac{\partial L}{\partial \phi} = 0 \tag{4.2e}$$

Where Lagrangian L is defined as:

$$L = K.E. - P.E. \tag{4.3}$$

The kinetic energy K and the potential energy P of the system are given as:

$$K.E. = \frac{1}{2}M(\dot{x}^2 + \dot{y}^2 + \dot{z}^2) + \frac{1}{2}m(\dot{x}_P^2 + \dot{y}_P^2 + \dot{z}_P^2) \tag{4.4a}$$

$$P.E. = Mgz + mgz_P \tag{4.4b}$$

$$K.E. = \frac{1}{2}\Big[M(\dot{x}^2 + \dot{y}^2 + \dot{z}^2) + m[(\dot{x} + l\cos\theta\dot{\theta})^2 + (\dot{y} + l\cos\theta\cos\phi\dot{\phi} - l\sin\theta\sin\phi\dot{\theta})^2 + (\dot{z} - l\sin\theta\cos\phi\dot{\theta} - l\cos\theta\sin\phi\dot{\phi})^2]] \tag{4.5a}$$

$$P.E. = Mgz + mg(z + l\cos\theta\cos\phi) \tag{4.5b}$$

Put Eq. (4.5 a) and Eq. (4.5 b) in Eq. (4.3)

$$L = \frac{1}{2}\Big[M(\dot{x}^2 + \dot{y}^2 + \dot{z}^2) + m[(\dot{x} + l\cos\theta\dot{\theta})^2 + (\dot{y} + l\cos\theta\cos\phi\dot{\phi} - l\sin\theta\sin\phi\dot{\theta})^2 + (\dot{z} - l\sin\theta\cos\phi\dot{\theta} - l\cos\theta\sin\phi\dot{\phi})^2]] - [Mgz + mgz + mg(z + l\cos\theta\cos\phi)] \tag{4.6}$$

Now calculating

$$\left(\frac{\partial L}{\partial \dot{x}}\right) = M\dot{x} + m(\dot{x} + l\cos\theta\dot{\theta}) \tag{4.7a}$$

$$\frac{d}{dt}\left(\frac{\partial L}{\partial \dot{x}}\right) = (M + m)\ddot{x} + ml\cos\theta\ddot{\theta} - ml\sin\theta\dot{\theta}^2 \tag{4.7b}$$

$$\frac{\partial L}{\partial x} = 0 \tag{4.7c}$$

Putting Eq. (4.7a) to Eq. (4.7c) in Eq. (4.2a)

$$(M + m)\ddot{x} + ml\cos\theta\ddot{\theta} - ml\sin\theta\dot{\theta}^2 = F_x \tag{4.8}$$

Similarly,

$$(M + m)\ddot{y} + ml\cos\theta\cos\phi\ddot{\phi} - ml\sin\theta\sin\phi\ddot{\theta} - 2ml\sin\theta\cos\phi\dot{\theta}\dot{\phi} - ml\cos\theta\sin\phi(\dot{\theta}^2 + \dot{\phi}^2) = F_y \tag{4.9}$$

$$(M + m)\ddot{z} - ml\sin\theta\cos\phi\ddot{\theta} + 2ml\sin\theta\sin\phi\dot{\theta}\dot{\phi} - ml\cos\theta\cos\phi(\dot{\theta}^2 + \dot{\phi}^2) - ml\cos\theta\sin\phi\ddot{\phi} + (M + m)g = F_z \tag{4.10}$$

$$l\ddot{\theta} + \cos\theta\ddot{x} - \sin\theta\sin\phi\ddot{y} - g\sin\theta\cos\phi - \sin\theta\cos\phi\ddot{z} + l\cos\theta\sin\theta\dot{\phi}^2 = 0 \tag{4.11}$$

$$\cos\theta\cos\phi\ddot{y} - \cos\theta\sin\phi\ddot{z} + l\cos^2\theta\ddot{\phi} - 2l\cos\theta\sin\theta\dot{\theta}\dot{\phi} - g\sin\phi\cos\theta = 0 \tag{4.12}$$

Solving Eq. (4.8) to Eq. (4.12) for $\ddot{x}$, $\ddot{y}$, $\ddot{z}$, $\ddot{\theta}$ and $\ddot{\phi}$

$$\ddot{x} = \frac{(M + m)F_x + ml\sin\theta\dot{\theta}^2(M + m\cos^2\theta) + (M + m)ml\cos^2\theta\sin\theta\dot{\phi}^2 - m^2l\cos^2\theta\sin\theta(\dot{\theta}^2 + \dot{\phi}^2) - mF_y\sin\phi\cos\theta\sin\theta - mF_Z\cos\theta\sin\theta - mF_x\sin^2\theta}{M(M + m)} \tag{4.13}$$

$$\ddot{y} = \frac{Mml\cos\theta\sin\phi(\dot{\theta}^2 + \dot{\phi}^2)[m\sin^2\theta + M] - MmF_z\cos^2\theta\cos\phi\sin\phi - mF_x\sin\theta\cos\theta\sin\phi(M + 2m\cos^2\phi) - m^2l\sin^2\theta\sin\phi\cos\theta\dot{\theta}^2(2m\cos^2\phi + M) - (M + m)ml\cos\theta\sin^2\theta\sin\phi\dot{\phi}^2[M + 2m\cos^2\phi] - MF_y[-M - m + m\sin^2\phi\cos^2\phi]}{M^2(M + m)} \tag{4.14}$$

$$\ddot{z} = \frac{\begin{array}{l} Mml\cos\theta\cos\phi(\dot{\theta}^2+\dot{\phi}^2)[m\sin^2\theta+M]+2m^3l\sin^2\theta\cos\theta\sin^2\phi\cos\phi\dot{\theta}^2+ \\ m^2Ml\sin^2\theta\cos\theta\cos\phi\dot{\theta}^2 --MmF_Z\cos^2\theta\cos^2\phi+M^2F_Z+MmF_Z- \\ MmF_x\sin\theta\cos\theta\cos\phi-2m^2F_x\sin\theta\cos\theta\cos^3\phi+2mMF_x\sin\theta\cos\theta\cos\phi+ \\ 2m^2F_x\sin\theta\cos\theta\cos\phi-M(M+m)ml\cos\theta\sin^2\theta\cos\phi\dot{\phi}^2- \\ 2m(m+M)ml\cos\theta\sin^2\theta\cos^3\phi\dot{\phi}^2+2ml(M+m)^2\cos\theta\sin^2\theta\cos\phi\dot{\phi}^2- \\ MmF_y\cos^2\theta\cos\phi\sin\phi-M^3g-M^2mg \end{array}}{M^2(M+m)} \tag{4.15}$$

$$\ddot{\theta} = \frac{\begin{array}{l} -mF_x\cos^2\theta-m^2l\sin\theta\cos^2\theta\dot{\theta}^2-(M+m)ml\cos^2\theta\sin\theta\dot{\phi}^2+ \\ m^2l\cos^2\theta\sin\theta(\dot{\theta}^2+\dot{\phi}^2)+mF_y\sin\phi\cos\theta\sin\theta+mF_Z\cos\theta\sin\theta\cos\phi \end{array}}{Mml\cos\theta} \tag{4.16}$$

$$\ddot{\phi} = \frac{\begin{array}{l} MF_Z\sin\phi-MF_y\cos\phi+2M^2l\sin\theta\dot{\theta}\dot{\phi}+2mF_x\sin\theta\sin\phi\cos\phi\cos\theta+ \\ 2m^2l\sin^2\theta\cos\theta\sin\phi\cos\phi\dot{\theta}^2+2ml(M+m)\cos\theta\sin^2\theta\sin\phi\cos\phi\dot{\phi}^2 \end{array}}{M^2l\cos\theta} \tag{4.17}$$

Defining $x_1 = x$, $x_2 = \dot{x}$, $x_3 = y$, $x_4 = \dot{y}$, $x_5 = z$, $x_6 = \dot{z}$, $x_7 = \theta$, $x_8 = \dot{\theta}$, $x_9 = \phi$ and $x_{10} = \dot{\phi}$

The state equations of the $x-y-z$ inverted pendulum can be written as:

$$\dot{x}_1 = x_2 \tag{4.18}$$

$$\dot{x}_2 = \frac{\begin{array}{l} (M+m)F_x+ml\sin x_7{x_8}^2(M+m\cos^2 x_7)+(M+m)ml\cos^2 x_7\sin x_7{x_{10}}^2- \\ m^2l\cos^2 x_7\sin x_7({x_8}^2+{x_{10}}^2)-mF_y\sin x_9\cos x_7\sin x_7-mF_Z\cos x_7\sin x_7-mF_x\sin^2 x_7 \end{array}}{M(M+m)} \tag{4.19}$$

$$\dot{x}_3 = x_4 \tag{4.20}$$

$$\dot{x}_4 = \frac{\begin{array}{l} Mml\cos x_7\sin x_9({x_8}^2+{x_{10}}^2)[m\sin^2\theta+M]-MmF_z\cos^2 x_7\cos x_9\sin x_9- \\ mF_x\sin x_7\cos x_7\sin x_9[M+2m\cos^2 x_9]-m^2l\sin^2 x_7\sin x_9\cos x_7{x_8}^2(2m\cos^2 x_9+M) \\ -(M+m)ml\cos x_7\sin^2 x_7\sin x_9{x_{10}}^2[M+2m\cos^2 x_9]-MF_y[-M-m+m\sin^2 x_9\cos^2 x_9] \end{array}}{M^2(M+m)} \tag{4.21}$$

$$\dot{x}_5 = x_6 \tag{4.22}$$

$$\dot{x}_6 = \frac{\begin{array}{l} Mml\cos x_7\cos x_9({x_8}^2+{x_{10}}^2)[m\sin^2 x_7+M]+2m^3l\sin^2 x_7\cos x_7\sin^2 x_9\cos x_9{x_8}^2+ \\ m^2Ml\sin^2 x_7\cos x_7\cos x_9{x_8}^2 --MmF_Z\cos^2 x_7\cos^2 x_9+M^2F_Z+MmF_Z- \\ MmF_x\sin x_7\cos x_7\cos x_9-2m^2F_x\sin x_7\cos x_7\cos^3 x_9+2mMF_x\sin x_7\cos x_7\cos x_9+ \\ 2m^2F_x\sin x_7\cos x_7\cos x_9-M(M+m)ml\cos x_7\sin^2 x_7\cos x_9{x_{10}}^2- \\ 2m(m+M)ml\cos x_7\sin^2 x_7\cos^3 x_9{x_{10}}^2+2ml(M+m)^2\cos x_7\sin^2 x_7\cos x_9{x_{10}}^2- \\ MmF_y\cos^2 x_7\cos x_9\sin x_9-M^3g-M^2mg \end{array}}{M^2(M+m)} \tag{4.23}$$

$$\dot{x}_7 = x_8 \tag{4.24}$$

$$\dot{x}_8 = \frac{\begin{array}{l} -mF_x \cos^2 x_7 - m^2 l \sin x_7 \cos^2 x_7 x_8{}^2 - (M+m)ml\cos^2 x_7 \sin x_7 x_9{}^2 + \\ m^2 l \cos^2 x_7 \sin x_7 (x_8{}^2 + x_{10}{}^2) + mF_y \sin x_9 \cos x_7 \sin x_7 + mF_Z \cos x_7 \sin x_7 \cos x_9 \end{array}}{Mml\cos x_7} \tag{4.25}$$

$$\dot{x}_9 = x_{10} \tag{4.26}$$

$$\dot{x}_{10} = \frac{\begin{array}{l} MF_Z \sin x_9 - MF_y \cos x_9 + 2M^2 l \sin x_7 x_8 x_{10} + 2mF_x \sin x_7 \sin x_9 \cos x_9 \cos x_7 + \\ 2m^2 l \sin^2 x_7 \cos x_7 \sin x_9 \cos x_9 x_8{}^2 + 2ml(M+m)\cos x_7 \sin^2 x_7 \sin x_9 \cos x_9 x_{10}{}^2 \end{array}}{M^2 l \cos x_7} \tag{4.27}$$

From Eq. (4.18) to Eq. (4.27) it can be concluded that the x-y-z inverted pendulum is a three input five output system. The three inputs are the applied forces F_x, F_y and F_z while the outputs are the positions x, y, z and the angles θ, ϕ.

4.2.2 Modeling with Uncertainties

The uncertainties that may exist in an inverted pendulum system are the fast acting external disturbances and frictional forces. The state equations of the x-y-z inverted pendulum after considering the effect of external disturbances and friction can be written as:

$$\dot{x}_1 = x_2 \tag{4.28}$$

$$\dot{x}_2 = \frac{\begin{array}{l} (M+m)(F_x + F_{xfric}) + ml\sin x_7 x_8{}^2 (M + m\cos^2 x_7) + (M+m)ml\cos^2 x_7 \sin x_7 x_{10}{}^2 - \\ m^2 l \cos^2 x_7 \sin x_7 (x_8{}^2 + x_{10}{}^2) - m(F_y + F_{yfric})\sin x_9 \cos x_7 \sin x_7 - \\ m(F_z + F_{zfric})\cos x_7 \sin x_7 - m(F_x + F_{xfric})\sin^2 x_7 \end{array}}{M(M+m)} + d \tag{4.29}$$

$$\dot{x}_3 = x_4 \tag{4.30}$$

$$\dot{x}_4 = \frac{\begin{array}{l} Mml\cos x_7 \sin x_9 (x_8{}^2 + x_{10}{}^2)[m\sin^2\theta + M] - Mm(F_z + F_{zfric})\cos^2 x_7 \cos x_9 \sin x_9 - \\ m(F_x + F_{xfric})\sin x_7 \cos x_7 \sin x_9 [M + 2m\cos^2 x_9] - \\ m^2 l \sin^2 x_7 \sin x_9 \cos x_7 x_8{}^2 (2m\cos^2 x_9 + M) \\ -(M+m)ml\cos x_7 \sin^2 x_7 \sin x_9 x_{10}{}^2 [M + 2m\cos^2 x_9] - \\ M(F_y + F_{yfric})[-M - m + m\sin^2 x_9 \cos^2 x_9] \end{array}}{M^2 (M+m)} + d \tag{4.31}$$

$$\dot{x}_5 = x_6 \tag{4.32}$$

$$\dot{x}_6 = \frac{\begin{array}{l} Mml\cos x_7 \cos x_9 (x_8{}^2 + x_{10}{}^2)[m\sin^2 x_7 + M] + 2m^3 l \sin^2 x_7 \cos x_7 \sin^2 x_9 \cos x_9 x_8{}^2 + \\ m^2 Ml \sin^2 x_7 \cos x_7 \cos x_9 x_8{}^2 - -Mm(F_z + F_{zfric})\cos^2 x_7 \cos^2 x_9 + M^2 (F_z + F_{zfric}) + \\ Mm(F_z + F_{zfric}) - Mm(F_x + F_{xfric})\sin x_7 \cos x_7 \cos x_9 - \\ 2m^2 (F_x + F_{xfric})\sin x_7 \cos x_7 \cos^3 x_9 + 2mM(F_x + F_{xfric})\sin x_7 \cos x_7 \cos x_9 + \\ 2m^2 (F_x + F_{xfric})\sin x_7 \cos x_7 \cos x_9 - M(M+m)ml\cos x_7 \sin^2 x_7 \cos x_9 x_{10}{}^2 - \\ 2m(m+M)ml\cos x_7 \sin^2 x_7 \cos^3 x_9 x_{10}{}^2 + 2ml(M+m)^2 \cos x_7 \sin^2 x_7 \cos x_9 x_{10}{}^2 - \\ Mm(F_y + F_{yfric})\cos^2 x_7 \cos x_9 \sin x_9 - M^3 g - M^2 mg \end{array}}{M^2 (M+m)} + d \quad (4.33)$$

$$\dot{x}_7 = x_8 \quad (4.34)$$

$$\dot{x}_8 = \frac{\begin{array}{l} -m(F_x + F_{xfric})\cos^2 x_7 - m^2 l \sin x_7 \cos^2 x_7 x_8{}^2 - (M+m)ml\cos^2 x_7 \sin x_7 x_9{}^2 + \\ m^2 l \cos^2 x_7 \sin x_7 (x_8{}^2 + x_{10}{}^2) + m(F_y + F_{yfric})\sin x_9 \cos x_7 \sin x_7 + \\ m(F_z + F_{zfric})\cos x_7 \sin x_7 \cos x_9 \end{array}}{Mml\cos x_7} + d \quad (4.35)$$

$$\dot{x}_9 = x_{10} \quad (4.36)$$

$$\dot{x}_{10} = \frac{\begin{array}{l} M(F_Z + F_{Zfric})\sin x_9 - M(F_y + F_{yfric})\cos x_9 + 2M^2 l \sin x_7 x_8 x_{10} + \\ 2m(F_x + F_{xfric})\sin x_7 \sin x_9 \cos x_9 \cos x_7 + 2m^2 l \sin^2 x_7 \cos x_7 \sin x_9 \cos x_9 x_8{}^2 + \\ 2ml(M+m)\cos x_7 \sin^2 x_7 \sin x_9 \cos x_9 x_{10}{}^2 \end{array}}{M^2 l \cos x_7} + d \quad (4.37)$$

The disturbance is defined as:

$$d = 20\sin(20\pi t) \quad (4.38)$$

While F_{xfric}, F_{yfric} and F_{zfric} have been defined in Appendix A.

4.3 Control Structure of x - y - z Inverted Pendulum

The control structure of x - y - z inverted pendulum is shown in Figure 4.2. It is a five loop control scheme with three loops for position control of the base while the remaining two for angle control of the pendulum. Here controller 1 has been used for controlling angle θ of the inverted pendulum while controller 2 for x position control of the base. Similarly controller 3 has been used for controlling angle ϕ while controller 4 for y position control of the base and finally controller 5 has been used for z position control of the base. The reference signal for position control is a step signal while for angle control the reference angle is 0^0.

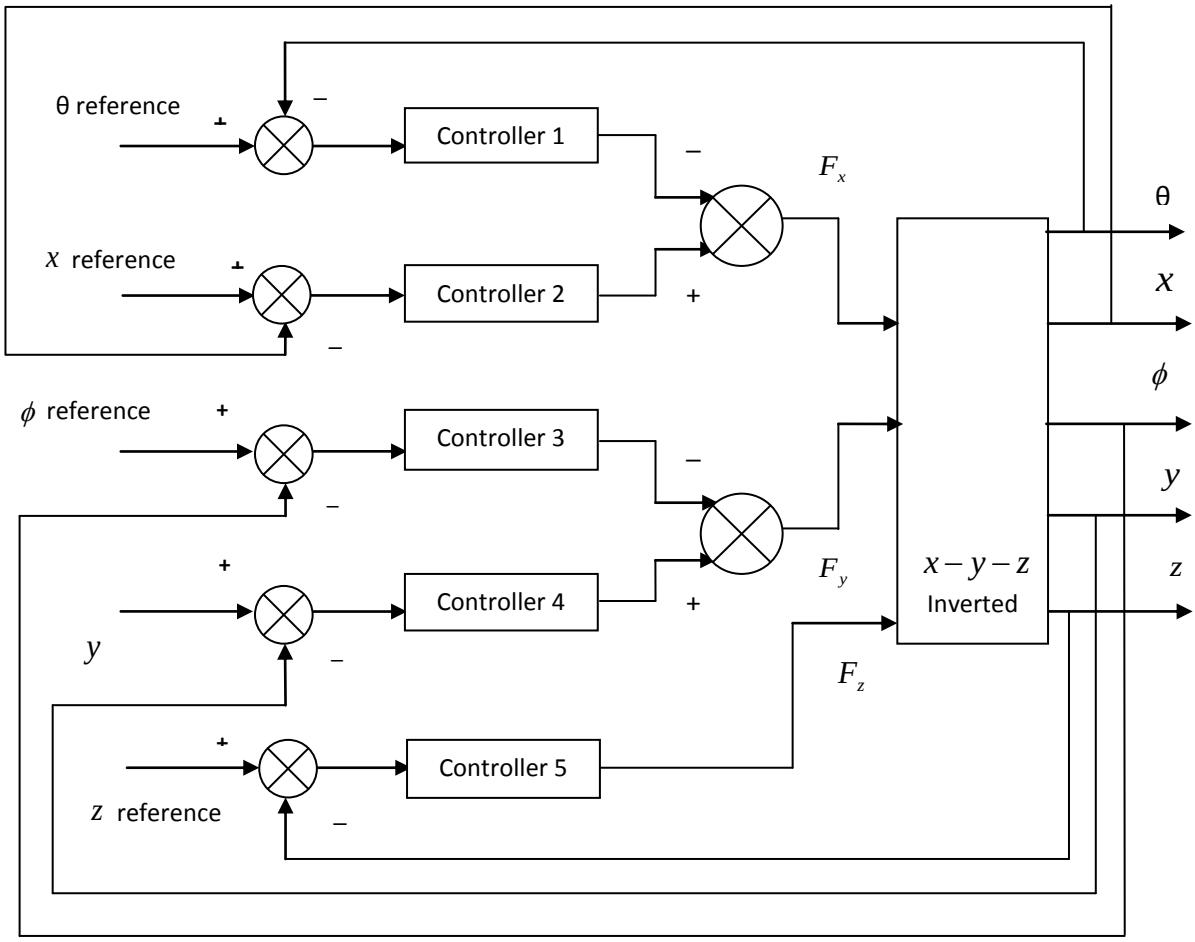

Figure 4.2 Control Structure of x - y - z Inverted Pendulum

At first, the conventional PID controllers have been implemented for controlling the inverted pendulum. PID1 and PID2 designed for x inverted pendulum can directly be used as PID 3 and PID 4 for y and ϕ control while PID5 has been tuned using trial and error method for z position control

The minimum and the maximum value of gains for AGS PID controllers are given in Table 4.1.

Table 4.1 Parameters of AGS PID Controllers for x - y - z Inverted Pendulum Control

Parameter	$k_{p\min}$	$k_{p\max}$	$k_{i\min}$	$k_{i\max}$	$k_{d\min}$	$k_{d\max}$
PID1	24	36	1.5	3.6	3	5
PID2	-3	-2.4	-1.2	-1	-4.8	-2
PID3	24	36	1.5	3.6	3	5
PID4	-3	-2.4	-1.2	-1	-4.8	-2
PID5	25	15	15	10	15	10

4.4 Stability Analysis of x - y - z Inverted Pendulum

The stability condition of the x - y - z inverted pendulum has been obtained using Lyapunov's stability criterion.

Theorem 4.1: The x - y - z inverted pendulum system will be stable if and only if:

$$F_x\dot{x} + F_y\dot{y} + F_z\dot{z} \le 0 \tag{4.39}$$

Proof: For an x - y - z inverted pendulum the Lyapunov function is defined as the sum of kinetic energy and potential energy of the system and is given as:

$$V = \frac{1}{2}M(\dot{x}^2 + \dot{y}^2 + \dot{z}^2) + \frac{1}{2}m(\dot{x}_p^2 + \dot{y}_p^2 + \dot{z}_p^2) + Mgz + mgz_p \tag{4.40}$$

$$V = \frac{1}{2}M(\dot{x}^2 + \dot{y}^2 + \dot{z}^2) + \frac{1}{2}m[(\dot{x} + l\cos\theta\dot{\theta})^2 + (\dot{y} + l\cos\theta\cos\phi\dot{\phi} - l\sin\theta\sin\phi\dot{\theta})^2 + (\dot{z} - l\sin\theta\cos\phi\dot{\theta} - l\cos\theta\sin\phi\dot{\phi})^2] + Mgz + mgz + mgl\cos\theta\cos\phi \tag{4.41}$$

For the system to be stable $\dot{V} \le 0$

$$\begin{aligned}\dot{V} = {} & M(\dot{x}\ddot{x} + \dot{y}\ddot{y} + \dot{z}\ddot{z}) + m[(\dot{x} + l\cos\theta\dot{\theta})(\ddot{x} + l\cos\theta\ddot{\theta} - l\sin\theta\dot{\theta}^2) + \\ & (\dot{y} + l\cos\theta\cos\phi\dot{\phi} - l\sin\theta\sin\phi\dot{\theta})(\ddot{y} + l\cos\theta\cos\phi\ddot{\phi} - l\cos\theta\sin\phi\dot{\phi}^2 - \\ & l\sin\theta\cos\phi\dot{\theta}\dot{\phi} - l\sin\theta\sin\phi\ddot{\theta} - l\sin\theta\cos\phi\dot{\theta}\dot{\phi} - l\cos\theta\sin\phi\dot{\theta}^2) + \\ & (\dot{z} - l\sin\theta\cos\phi\dot{\theta} - l\cos\theta\sin\phi\dot{\phi})(\ddot{z} - l\sin\theta\cos\phi\ddot{\theta} + l\sin\theta\sin\phi\dot{\theta}\dot{\phi} - \\ & l\cos\theta\cos\phi\dot{\theta}^2 - l\cos\theta\sin\phi\ddot{\phi} - l\cos\theta\cos\phi\dot{\phi}^2 + l\sin\theta\sin\phi\dot{\theta}\dot{\phi})] + Mg\dot{z} + \\ & mg\dot{z} - mgl\cos\theta\sin\phi\dot{\phi} - mgl\sin\theta\cos\phi\dot{\theta}\end{aligned} \tag{4.42}$$

$$\begin{aligned}\dot{V} = {} & M(\dot{x}\ddot{x} + \dot{y}\ddot{y} + \dot{z}\ddot{z}) + m(\dot{x}\ddot{x} + \dot{x}l\cos\theta\ddot{\theta} - \dot{x}l\sin\theta\dot{\theta}^2 + \ddot{x}l\cos\theta\dot{\theta} + l^2\cos^2\theta\dot{\theta}\ddot{\theta} - \\ & l^2\sin\theta\cos\theta\dot{\theta}^3 + \dot{y}\ddot{y} + \dot{y}l\cos\theta\cos\phi\ddot{\phi} - \dot{y}l\cos\theta\sin\phi\dot{\phi}^2 - \dot{y}l\sin\theta\cos\phi\dot{\theta}\dot{\phi} - \\ & \dot{y}l\sin\theta\sin\phi\ddot{\theta} - \dot{y}l\sin\theta\cos\phi\dot{\theta}\dot{\phi} - \dot{y}l\cos\theta\sin\phi\dot{\theta}^2 + l\cos\theta\cos\phi\ddot{\phi}\ddot{y} + \\ & l^2\cos^2\theta\cos^2\phi\dot{\phi}\ddot{\phi} - l^2\cos^2\theta\cos\phi\sin\phi\dot{\phi}^3 - l^2\cos\theta\sin\theta\cos^2\phi\dot{\theta}\dot{\phi}^2 - \\ & l^2\sin\theta\cos\theta\cos\phi\sin\phi\dot{\phi}\ddot{\theta} - l^2\sin\theta\cos\theta\cos^2\phi\dot{\theta}\dot{\phi}^2 - l^2\cos^2\theta\cos\phi\sin\phi\dot{\phi}\dot{\theta}^2 - \\ & l\sin\theta\sin\phi\dot{\theta}\ddot{y} - l^2\sin\theta\cos\theta\sin\phi\cos\phi\dot{\theta}\ddot{\phi} + l^2\cos\theta\sin\theta\sin^2\phi\dot{\theta}\dot{\phi}^2 + \\ & l^2\sin^2\theta\sin\phi\cos\phi\dot{\phi}\dot{\theta}^2 + l^2\sin^2\theta\sin^2\phi\dot{\theta}\ddot{\theta} + l^2\sin^2\theta\sin\phi\cos\phi\dot{\phi}\dot{\theta}^2 + \\ & l^2\sin\theta\cos\theta\sin^2\phi\dot{\theta}^3 + \dot{z}\ddot{z} - \dot{z}l\sin\theta\cos\phi\ddot{\theta} + \dot{z}l\sin\theta\sin\phi\dot{\theta}\dot{\phi} - \\ & \dot{z}l\cos\theta\cos\phi\dot{\theta}^2 - \dot{z}l\cos\theta\sin\phi\ddot{\phi} - \dot{z}l\cos\theta\cos\phi\dot{\phi}^2 + \dot{z}l\sin\theta\sin\phi\dot{\theta}\dot{\phi} - \\ & l\sin\theta\cos\phi\dot{\theta}\ddot{z} + l^2\sin^2\theta\cos^2\phi\dot{\theta}\ddot{\theta} - l^2\sin^2\theta\sin\phi\cos\phi\dot{\phi}\dot{\theta}^2 + l^2\sin\theta\cos\theta\cos^2\phi\dot{\theta}^3 + \\ & l^2\sin\theta\cos\theta\sin\phi\cos\phi\dot{\theta}\dot{\phi} + l^2\sin\theta\cos\theta\cos^2\phi\dot{\theta}\dot{\phi}^2 - l^2\sin^2\theta\sin\phi\cos\phi\dot{\phi}\dot{\theta}^2 - \\ & l\cos\theta\sin\phi\dot{\phi}\ddot{z} + l^2\cos\theta\sin\theta\sin\phi\cos\phi\dot{\phi}\ddot{\theta} - l^2\sin\theta\cos\theta\sin^2\phi\dot{\theta}\dot{\phi}^2 + \\ & l^2\cos^2\theta\cos\phi\sin\phi\dot{\phi}\dot{\theta}^2 + l^2\cos^2\theta\sin^2\phi\dot{\phi}\ddot{\phi} + l^2\cos^2\theta\cos\phi\sin\phi\dot{\phi}^3 - \\ & l^2\cos\theta\sin\theta\sin^2\phi\dot{\theta}\dot{\phi}^2) + Mg\dot{z} + mg\dot{z} - mgl\cos\theta\sin\phi\dot{\phi} - mgl\sin\theta\cos\phi\dot{\theta}\end{aligned} \tag{4.43}$$

Using the Lagrange's equations of the x - y - z inverted pendulum from Eq. (4.8) to Eq. (4.12) Eq. (4.43) has been reduced to:

$$\dot{V} = F_x \dot{x} + F_y \dot{y} + F_z \dot{z} \tag{4.44}$$

Therefore for the system to be stable $\dot{V} \leq 0$ or $F_x \dot{x} + F_y \dot{y} + F_z \dot{z} \leq 0$

Figure 4.24 shows the simulation results for $\dot{V}$ as a function of time

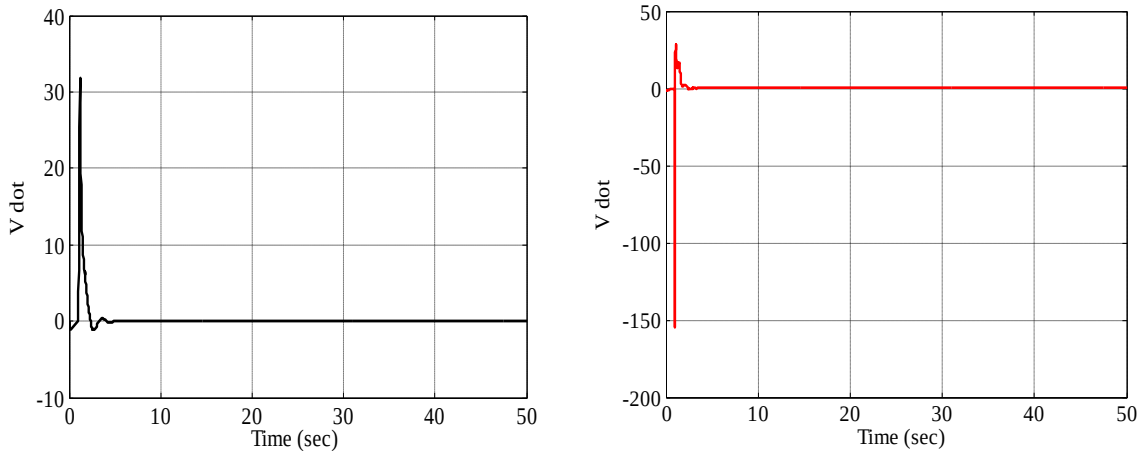

(a) Time AGS PID controller (b) Error AGS PID controller

Figure 4.3 $\dot{V}$ Vs Time for an x - y - z Inverted Pendulum

The simulation results show that the derivative of the Lyapunov's function for the given system while using the proposed controllers tends towards zero which means that the system is stable with the proposed controllers.

4.5 Simulation Results

Time adaptive gain scheduling and error adaptive gain scheduling PID controllers have been implemented for the stabilization and tracking control of x - y - z inverted pendulum. The simulation results are given below:

4.5.1 Stabilization with Time AGS PID Controllers

The stabilization of x - y - z inverted pendulum can be achieved by applying forces F_x, F_y and F_z to the base, so that the pendulum should remain in the vertical upward position. The simulation results under different conditions are given below:

4.5.1.1 Stabilization without Uncertainties

The simulation results for stabilization without the effect of uncertainties are shown in Figure 4.4. The quantitative analysis is given in Table 4.2.

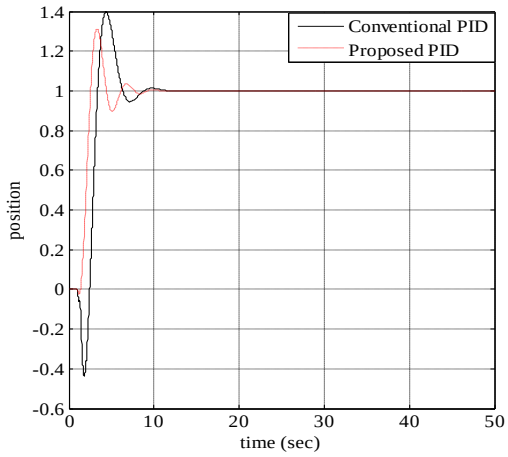

(a) Position x Vs Time

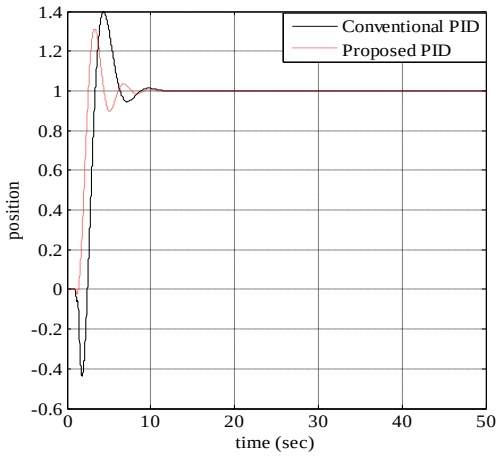

(b) Position y Vs Time

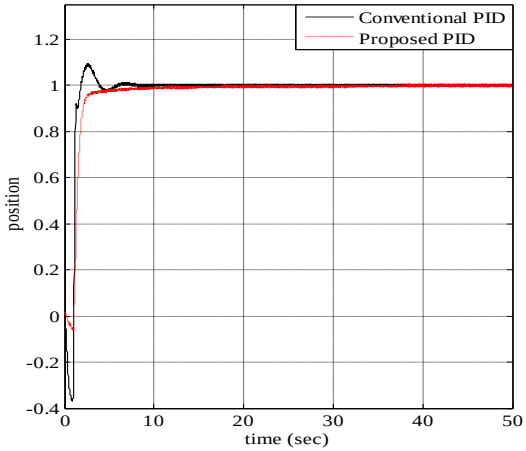

(c) Position z Vs Time

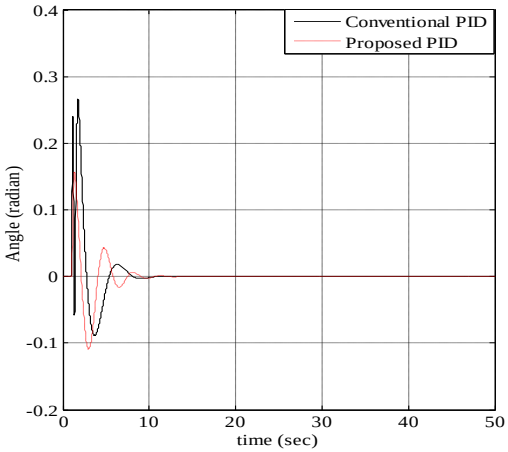

(d) Angle θ Vs Time

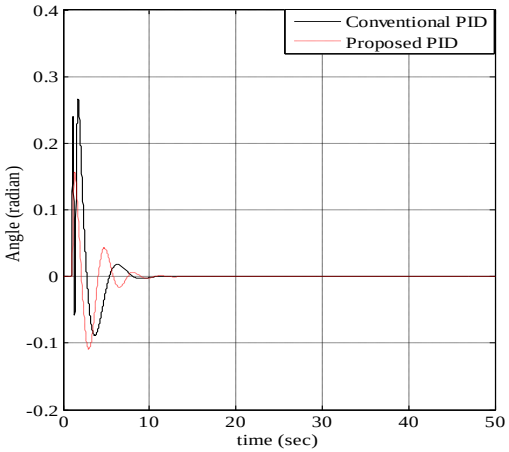

(e) Angle ϕ Vs Time

Figure 4.4 Stabilization of x - y - z Inverted Pendulum using Time AGS PID Controllers without Uncertainties

The results are quantified in Table 4.2.

Table 4.2 Quantitative analysis of x - y - z Inverted Pendulum Control using Time AGS PID Controllers without Uncertainties

Parameters	Conventional PID					Adaptive Gain Scheduling PID					% Improvement				
	x	y	z	θ	ϕ	x	y	z	θ	ϕ	x	y	z	θ	ϕ
M_p	0.40	0.40	0.09	0.27	0.27	0.29	0.29	0	0.16	0.16	37.93	37.93	__	68.75	68.75
t_r	3.25	3.25	1.25	__	__	2.45	2.45	2.01	__	__	32.65	32.65	-37.8	__	__
t_s	8.33	8.33	5.1	4.99	4.99	7.3	7.3	6.93	5.42	5.42	13.97	13.97	-26.4	-7.93	-7.93
e_{ss}	0	0	0	0	0	0	0	0	0	0	0	0	0	0	0

The simulation results show a large improvement in M_P, t_r and t_s in case of x and y position control while using time AGS PID controllers. For z position control the system response has become slightly sluggish with zero overshoot. Also the inverse response behavior of the system has been improved to a good amount. Similarly in case of angle control the overshoot has been improved to a large extent with a small increase in rise time using the proposed controllers.

4.5.1.2 Stabilization with Uncertainties

The Simulation results for stabilization after considering the effect of external disturbances are given in Figure 4.5 while the results are quantified in Table 4.3.

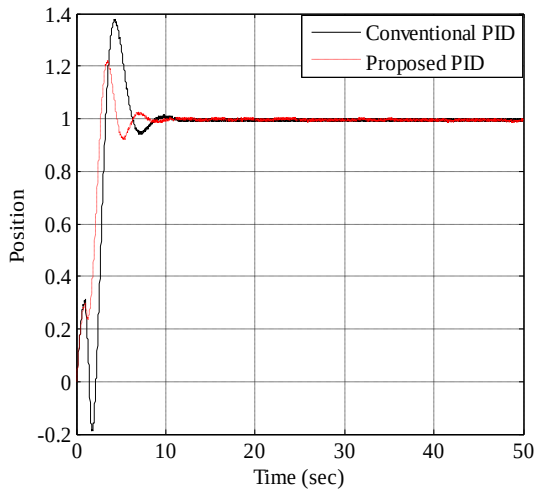

(a) Position x Vs Time

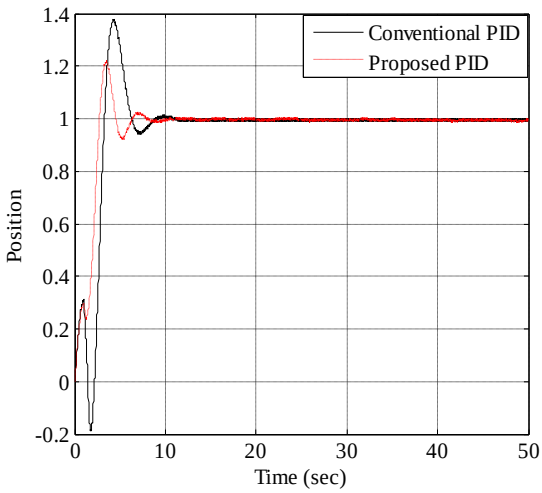

(b) Position y Vs Time

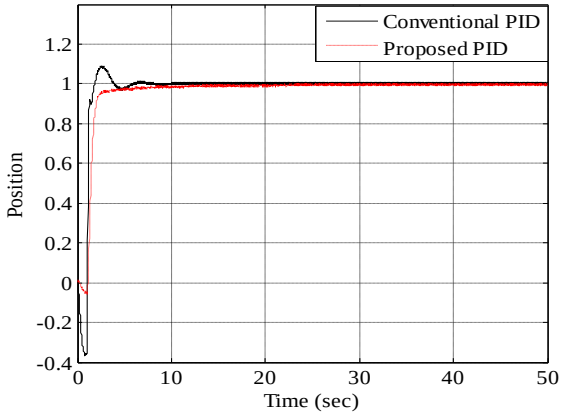

(c) Position z Vs Time

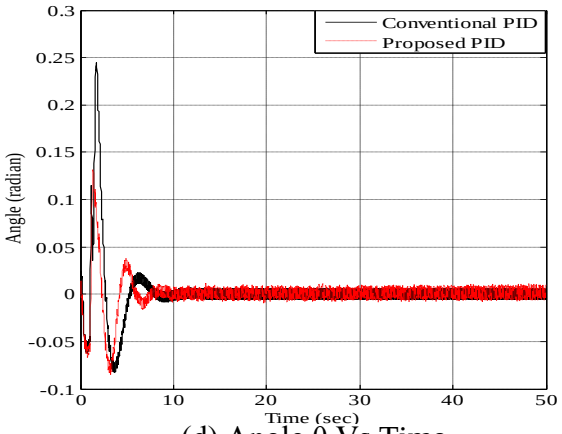

(d) Angle θ Vs Time

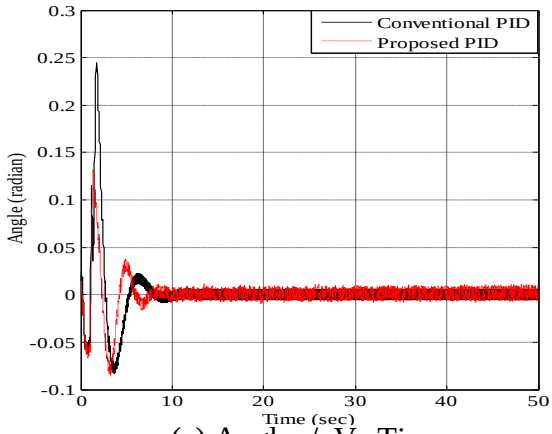

(e) Angle ϕ Vs Time

Figure 4.5 Stabilization of x - y - z Inverted Pendulum using Time AGS PID Controllers with Disturbance

Table 4.3 Quantitative analysis with of x - y - z Inverted Pendulum Control using Time AGS PID Controllers with Disturbance

Parameters	Conventional PID					Adaptive Gain Scheduling PID					% Improvement				
	x	y	z	θ	ϕ	x	y	z	θ	ϕ	x	y	z	θ	ϕ
M_p	0.38	0.38	0.09	0.24	0.24	0.22	0.22	0	0.13	0.13	72.72	72.72	__	84.6	84.6
t_r	3.15	3.15	1.26	__	__	2.57	2.57	1.99	__	__	22.56	22.56	-36.7	__	__
t_s	8.43	8.43	5.33	6.78	6.78	7.39	7.39	9.93	5.57	5.57	14.07	14.07	46.32	21.72	21.72
e_{ss}	0	0	0	0	0	0	0	0	0	0	0	0	0	0	0

Table 4.3 shows that using time AGS PID controllers there is a large improvement in M_P, t_r and t_s in case of x and y position control while for z position control overshoot has

been reduced to zero. Similarly in case of angle control M_P and t_r has been improved using the proposed controllers.

A band limited white noise has been introduced into the controllers. The simulation results are shown in Figure 4.6

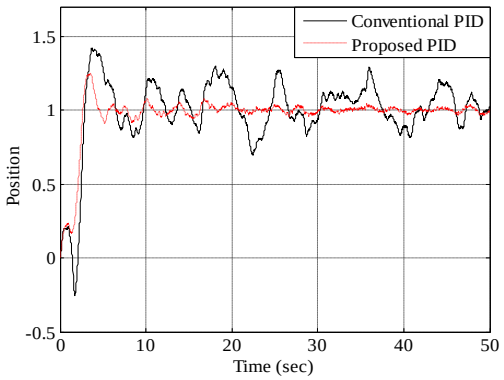

(a) Position x Vs Time

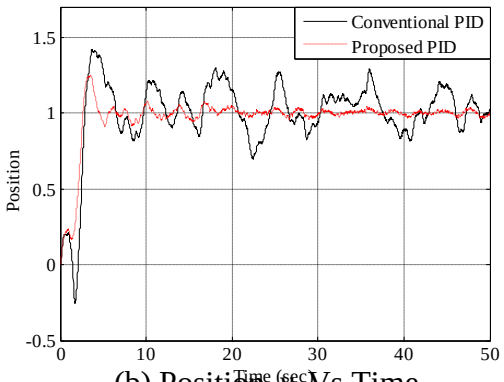

(b) Position y Vs Time

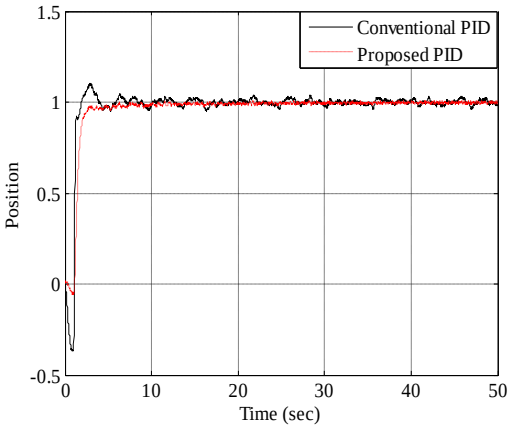

(c) Position z Vs Time

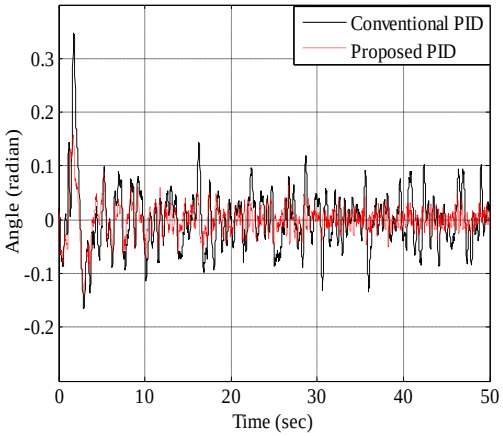

(d) Angle θ Vs Time

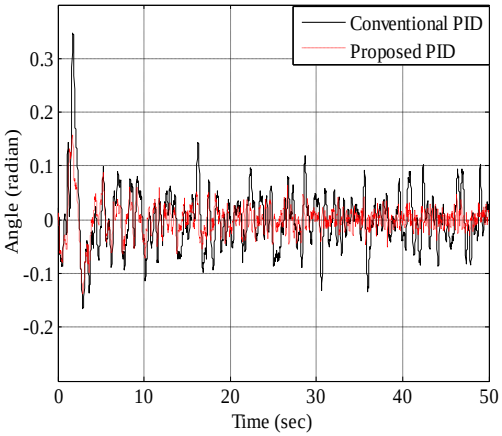

(e) Angle ϕ Vs Time

Figure 4.6 Stabilization of x - y - z Inverted Pendulum using Time AGS PID Controllers with Noise in the Controllers

The simulation results show that while using time AGS PID controllers less chattering has been observed in the system response as compared to the conventional PID Controllers.

The simulation results when considering the effect of friction on the inverted pendulum system are given in Figure 4.7 and Figure 4.8 for simple and exponential friction models respectively.

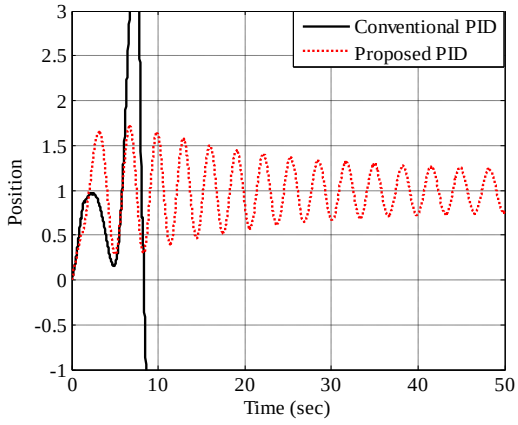

(a) Position x Vs Time

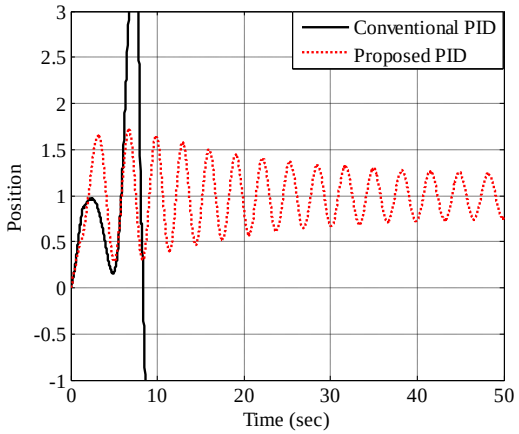

(b) Position y Vs Time

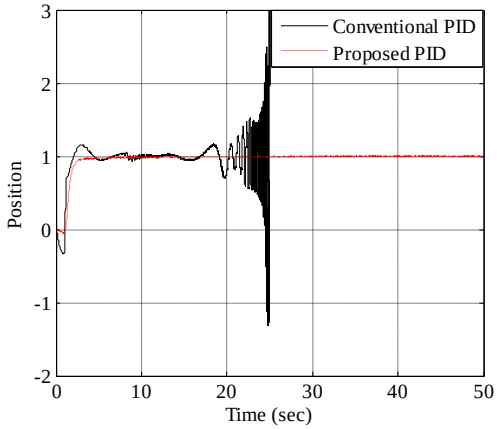

(c) Position z Vs Time

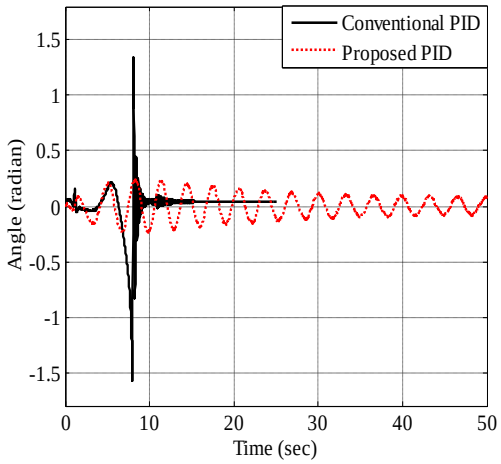

(d) Angle θ Vs Time

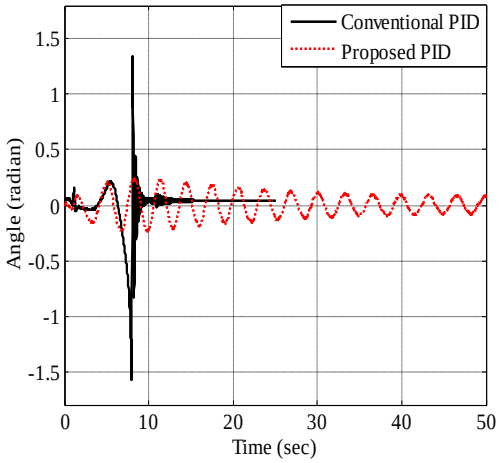

(e) Angle ϕ Vs Time

Figure 4.7 Stabilization of x - y - z Inverted Pendulum using Time AGS PID Controllers with Simple Friction Model

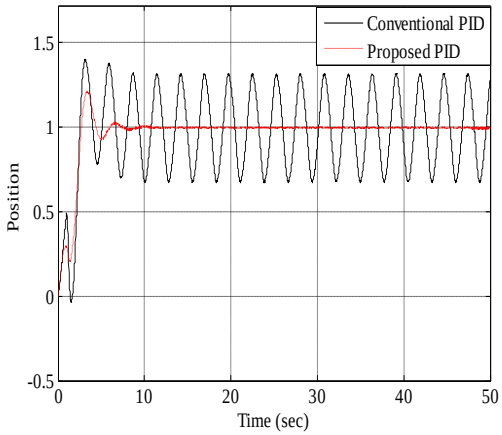

(a) Position x Vs Time

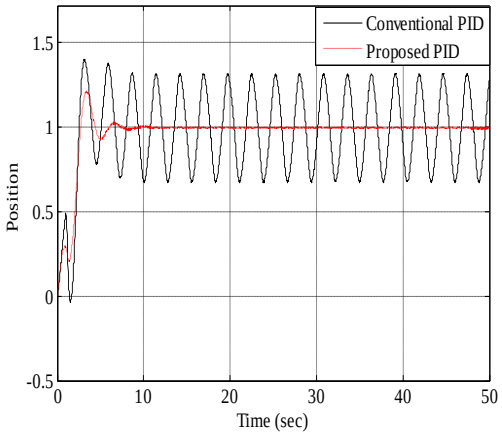

(b) Position y Vs Time

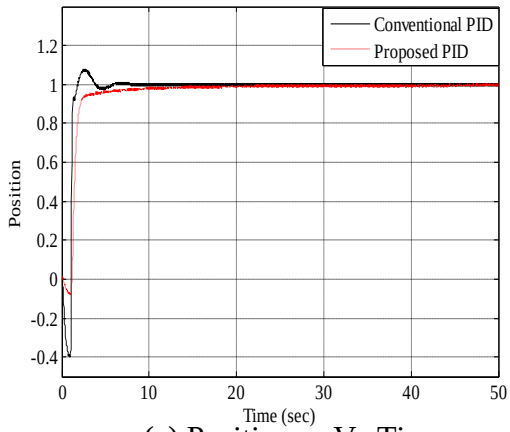

(c) Position z Vs Time

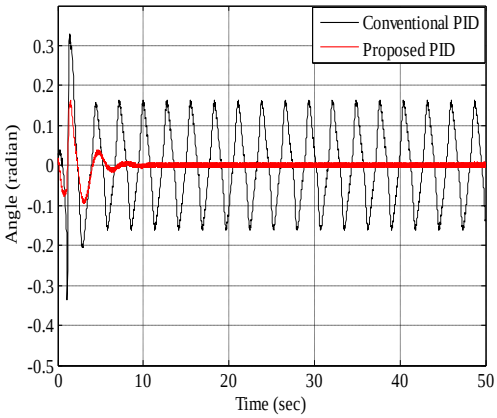

(d) Angle θ Vs Time

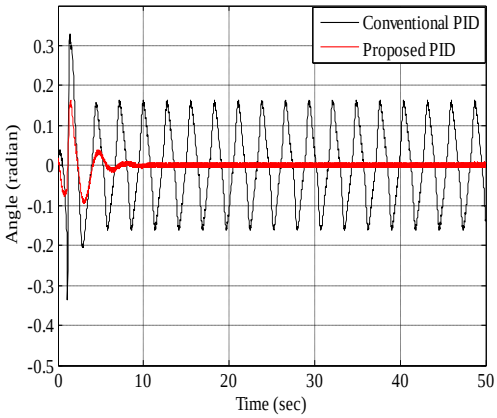

(e) Angle ϕ Vs Time

Figure 4.8 Stabilization of x - y - z Inverted pendulum using Time AGS PID Controllers with Exponential Friction Model

The simulation results reveal that the system response becomes unbounded (except for z position control) in case of simple friction model while using conventional PID controllers. On the other hand the time AGS PID controllers give stable results. Similarly when the exponential friction model is considered the time AGS PID controllers provide almost

perfect control with zero e_{ss} while the conventional PID controllers give an oscillatory response.

4.5.2 Tracking Control with Time AGS PID Controllers

To check whether the proposed controllers provide good reference control, signals $x_t = 0.25\sin(0.05\pi t)$, $y_t = 0.25\sin(0.05\pi t)$ and $z_t = 0.15\sin(0.05\pi t)$ have been applied as the reference inputs. The simulation results are given from Figure 4.9 to Figure 4.13.

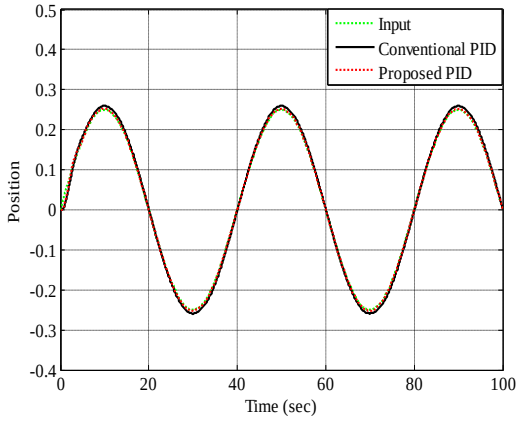

(a) Position x Vs Time

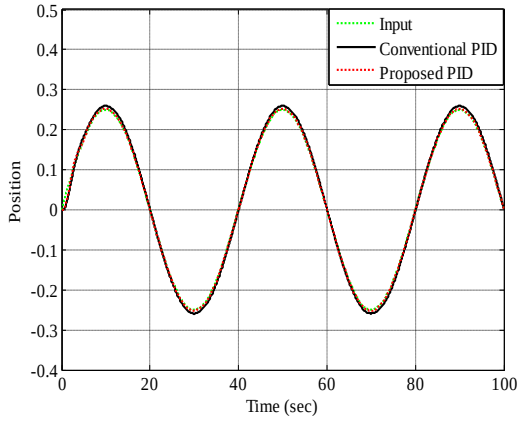

(b) Position y Vs Time

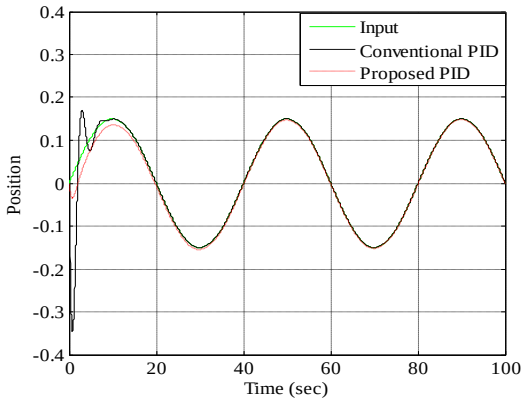

(c) Position z Vs Time

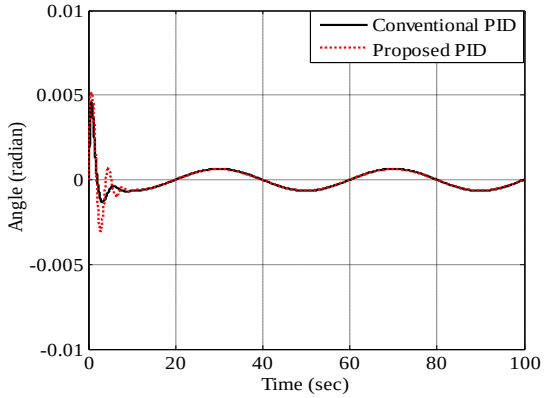

(d) Angle θ Vs Time

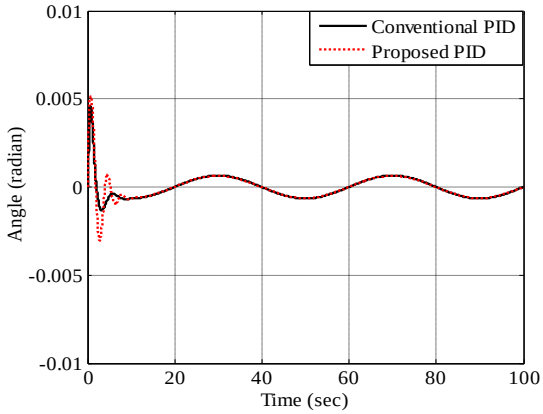

(e) Angle ϕ Vs Time

Figure 4.9 Tracking control of x - y - z Inverted Pendulum using Time AGS PID Controllers without Disturbance

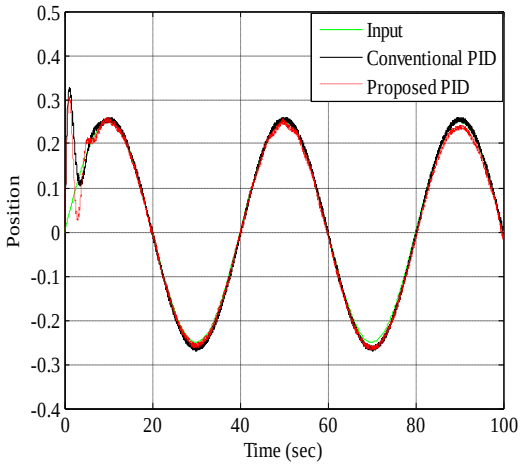

(a) Position x Vs Time

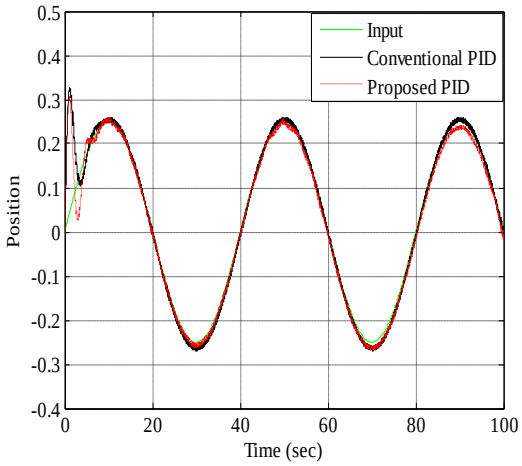

(b) Position y Vs Time

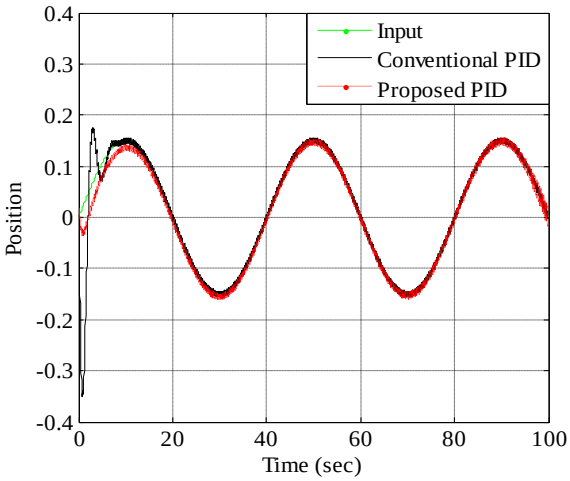

(c) Position z Vs Time

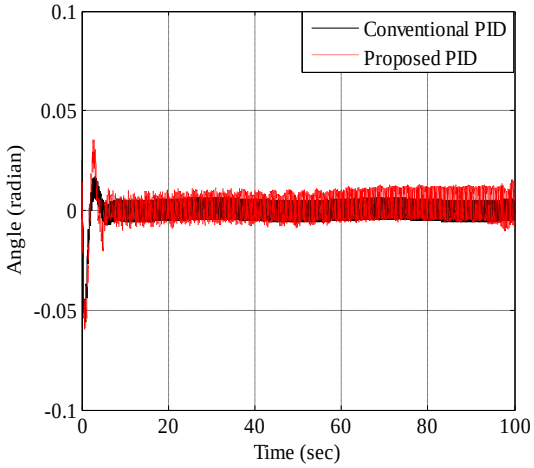

(d) Angle θ Vs Time

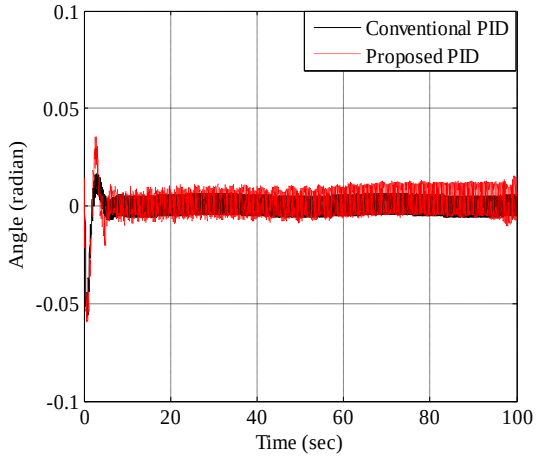

(e) Angle ϕ Vs Time

Figure 4.10 Tracking control of x - y - z Inverted Pendulum using Time AGS PID Controllers with Disturbance

The simulation results in Figure 4.9 and Figure 4.10 show that both conventional and AGS PID controllers have almost same output responses when a sinusoidal tracking signal is applied as the reference input.

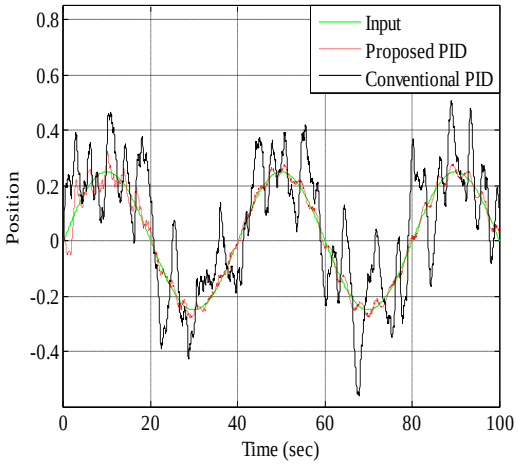

(a) Position x Vs Time

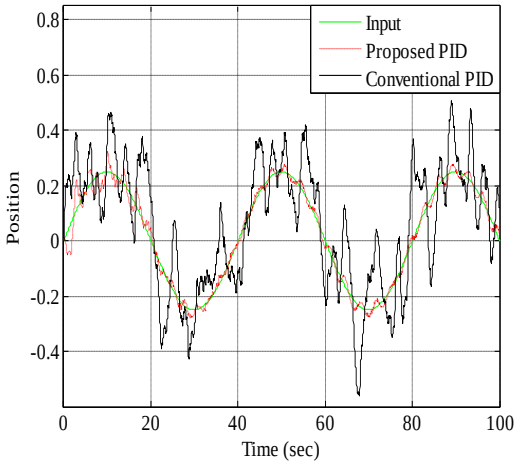

(b) Position y Vs Time

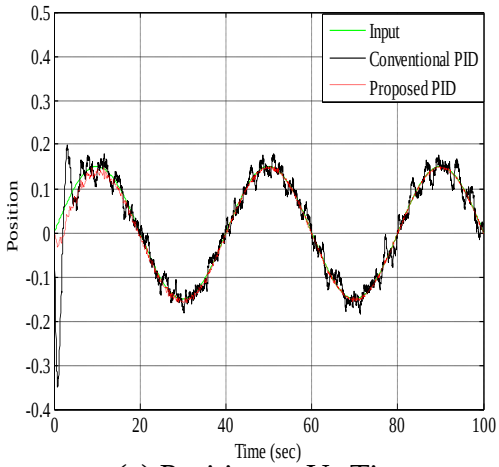

(c) Position z Vs Time

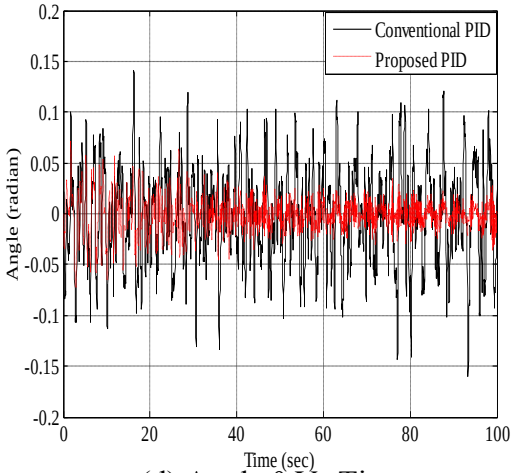

(d) Angle θ Vs Time

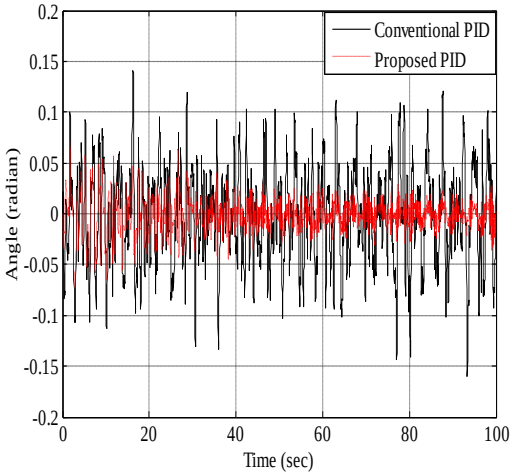

(e) Angle ϕ Vs Time

Figure 4.11 Tracking control of x - y - z Inverted Pendulum using Time AGS PID Controllers with noise in the Controllers

When the effect of noise is considered as shown in Figure 4.11 time AGS PID controllers outperform conventional PID controllers in terms of chattering in the system response.

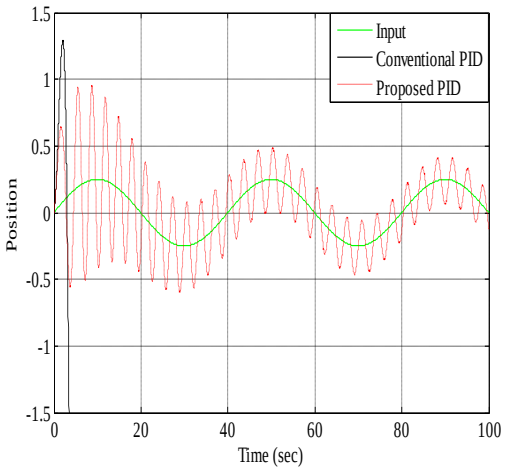

(a) Position x Vs Time

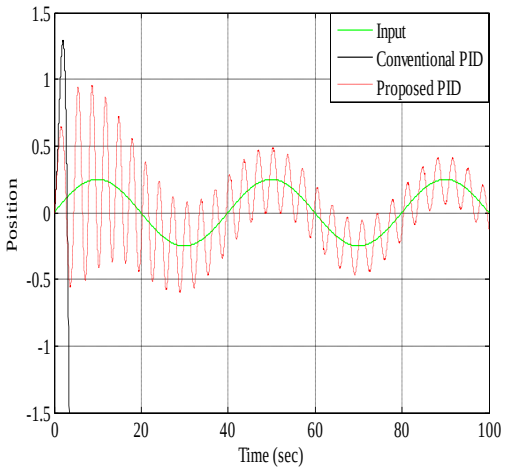

(b) Position y Vs Time

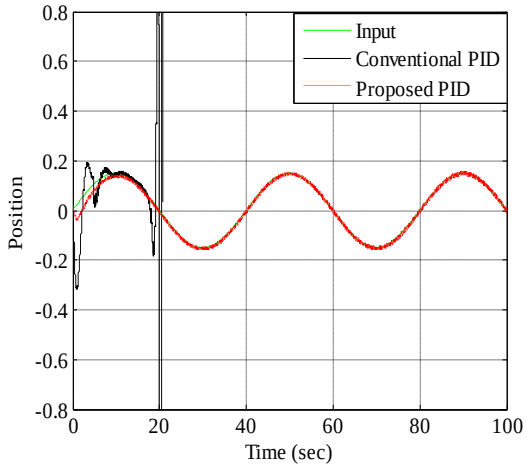

(c) Position z Vs Time

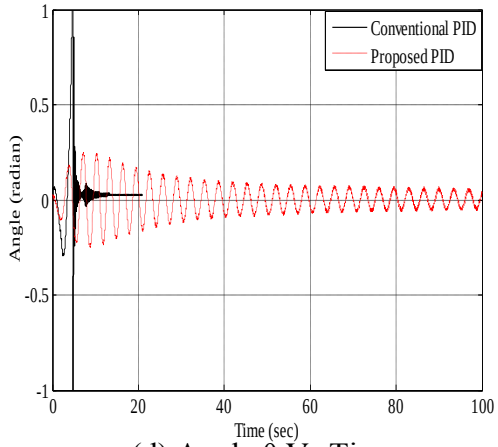

(d) Angle θ Vs Time

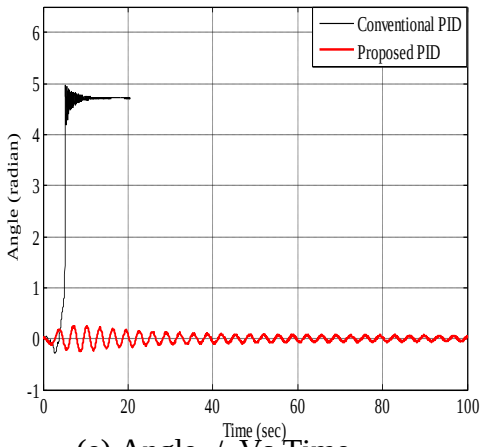

(e) Angle ϕ Vs Time

Figure 4.12 Tracking control of x - y - z Inverted Pendulum using Time AGS PID Controllers with Simple Friction Model

The simulation results in Figure 4.12 shows that when the effect of friction is considered in terms of simple friction model the conventional PID controllers fail to respond while the time adaptive gain scheduling PID controllers give a satisfactory performance.

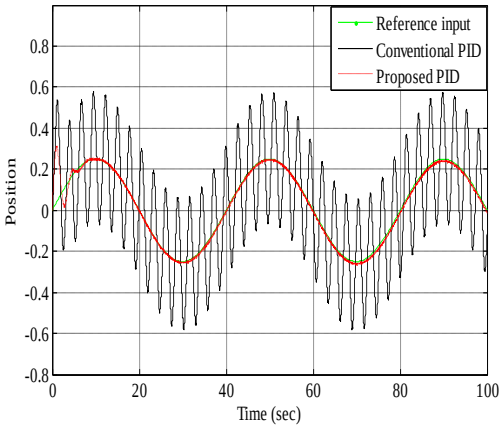

(a) Position x Vs Time

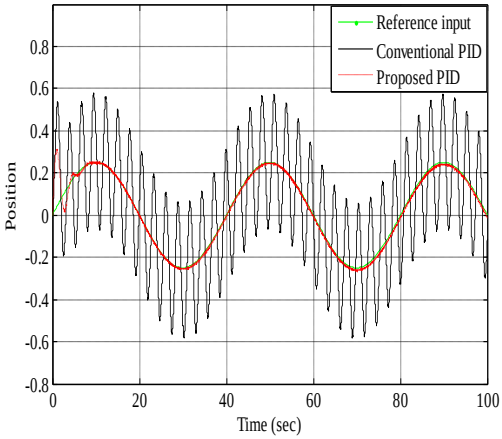

(b) Position y Vs Time

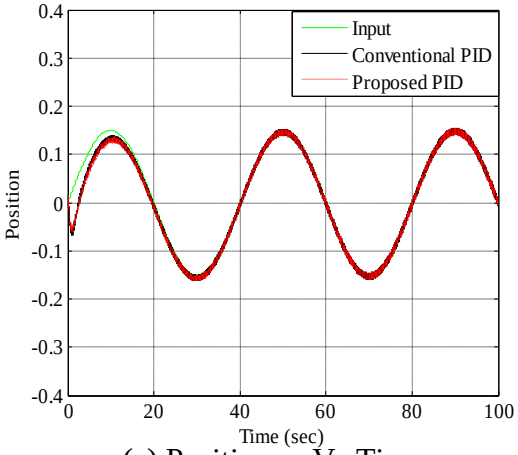

(c) Position z Vs Time

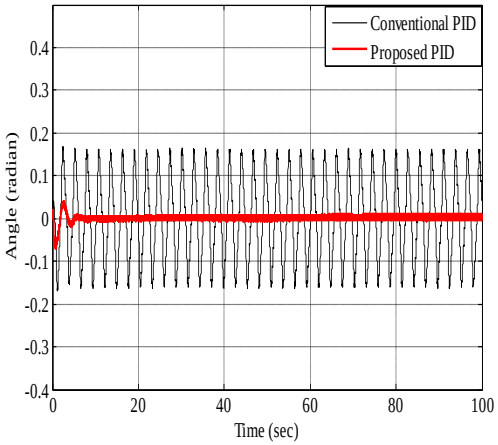

(d) Angle θ Vs Time

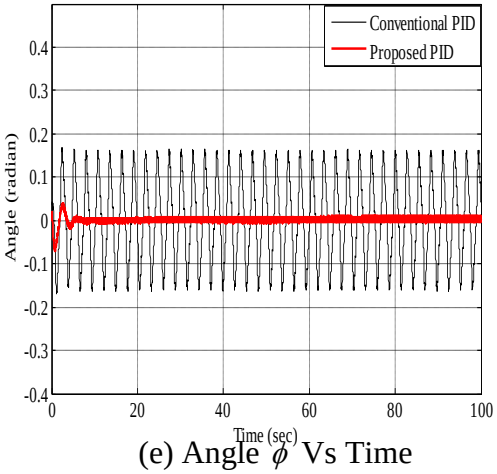

(e) Angle ϕ Vs Time

Figure 4.13 Tracking control of x - y - z Inverted Pendulum using Time AGS PID Controllers with Exponential Friction Model

As shown in Figure 4.13 the time adaptive gain scheduling PID controllers provide almost perfect control while the conventional PID controllers give oscillatory response.

4.5.3 Stabilization with Error AGS PID Controllers

The time AGSPID controllers are replaced by error AGSPID controllers. The simulation results under different conditions are shown below:

4.5.3.1 Stabilization without Uncertainties

The simulation results for the stabilization of x - y - z inverted pendulum without the effect of uncertainties are shown in Figure 4.14 while its quantitative analysis in terms of various performance specifications is given in Table 4.4.

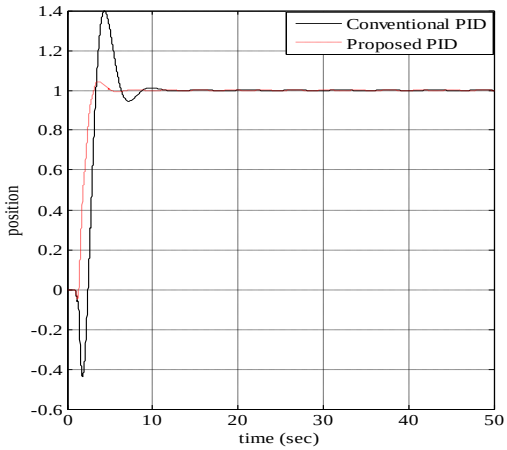

(a) Position x Vs Time

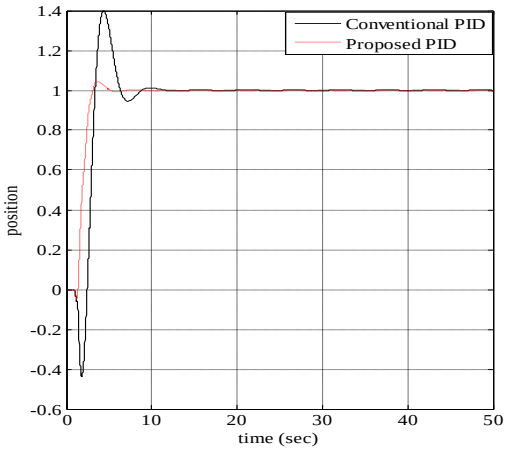

(b) Position y Vs Time

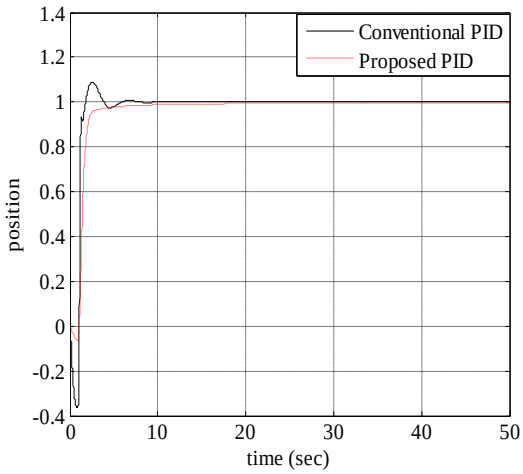

(c) Position z Vs Time

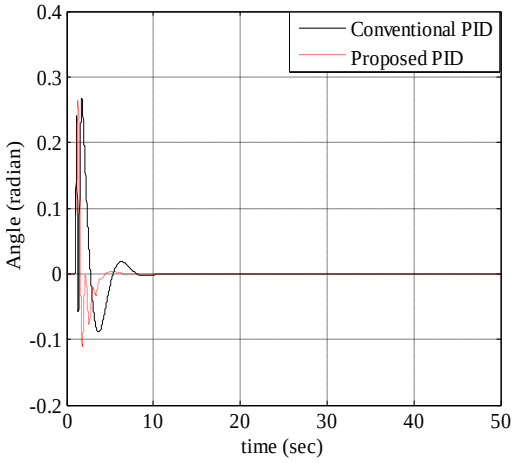

(d) Angle θ Vs Time

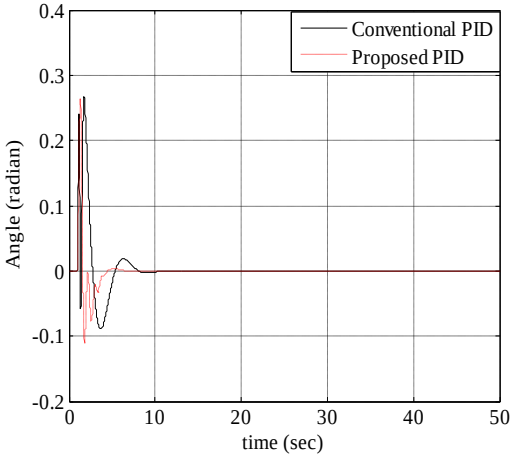

(e) Angle ϕ Vs Time

Figure 4.14 Stabilization of x - y - z Inverted pendulum using Error AGS PID Controllers without Uncertainties

Table 4.4 Quantitative analysis of x - y - z Inverted Pendulum Control using Error AGS PID Controllers without Uncertainties

Parameters	Conventional PID					Adaptive Gain Scheduling PID					% Improvement				
	x	y	z	θ	ϕ	x	y	z	θ	ϕ	x	y	z	θ	ϕ
M_p	0.40	0.40	0.09	0.27	0.27	0.04	0.04	0	0.26	0.26	900	900	__	3.84	3.84
t_r	3.25	3.25	1.25	__	__	2.62	2.62	2.06	__	__	24.04	24.04	39.3	__	__
t_s	8.32	8.32	5.1	4.99	4.99	4.54	4.54	5.58	3.59	3.59	83.25	83.25	8.60	38.99	38.99
e_{ss}	0	0	0	0	0	0	0	0	0	0	0	0	0	0	0

Table 4.4 shows that there is a huge amount of improvement in M_P, t_r and t_s in case of x and y position control while using error AGS PID controllers. Also the inverse response behavior of the system has been improved to a good amount. Similarly for angle control the overshoot has been improved slightly and settles down fast towards the desired value.

4.5.3.2 Stabilization with Uncertainties

Figure 4.15 show simulation results under the effect of fast acting external disturbances.

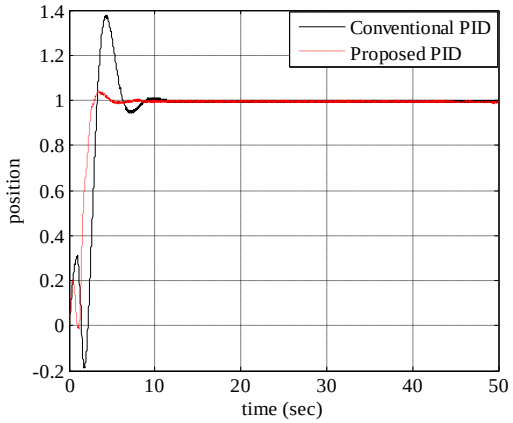

(a) Position x Vs Time

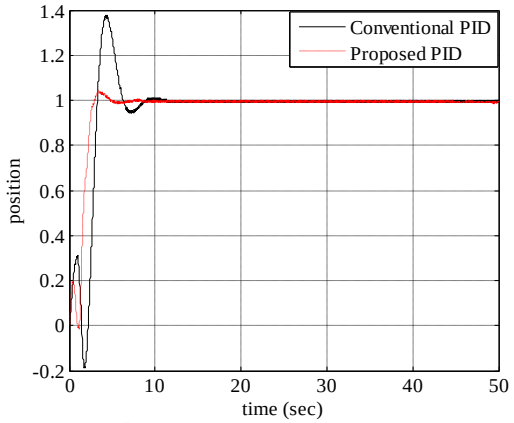

(b) Position x Vs Time

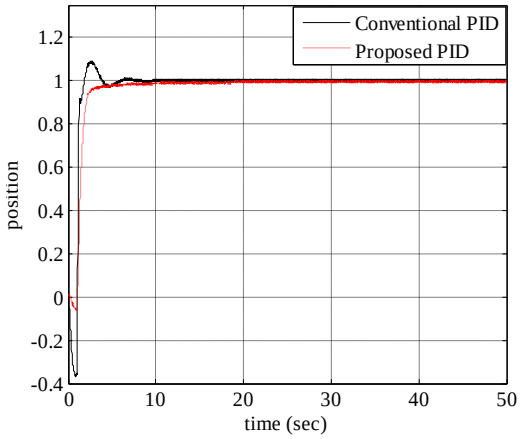

(b) Position z Vs Time

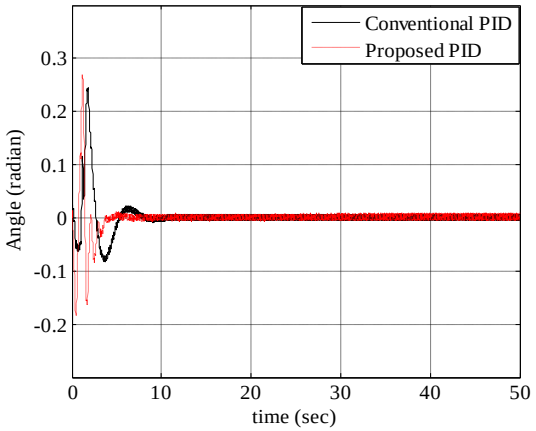

(d) Angle θ Vs Time

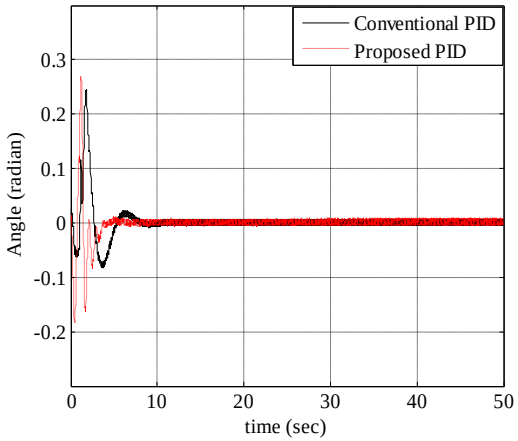

(e) Angle ϕ Vs Time

Figure 4.15 Stabilization of x - y - z Inverted Pendulum using Error AGS PID Controllers with Disturbance

Table 4.5 gives the quantitative analysis in terms of various performance specifications.

Table 4.5 Quantitative analysis without disturbance of x - y - z Inverted Pendulum Control using Error AGS PID Controllers with Disturbance

Parameters	Conventional PID					Error Adaptive Gain Scheduling PID					% Improvement				
	x	y	z	θ	ϕ	x	y	z	θ	ϕ	x	y	z	θ	ϕ
M_p	0.38	0.38	0.09	0.24	0.24	0.04	0.04	0	0.27	0.27	850	850	__	-11	-11
t_r	3.15	3.15	1.26	__	__	2.76	2.76	2.05	__	__	14.13	14.13	38.53	__	__
t_s	8.43	8.43	5.33	6.78	6.78	4.29	4.29	7.62	3.44	3.44	96.50	96.50	-30.0	97.0	97.0
e_{ss}	0	0	0	0	0	0	0	0	0	0	0	0	0	0	0

Table 4.5 shows that there is a huge amount of improvement in M_P, t_r and t_s in case of x and y position control while using error adaptive gain scheduling PID controllers. For z position control the system response has become slightly sluggish with zero overshoot. Also the inverse response behavior of the system has been improved to a good amount. Similarly in case of angle control the overshoot has been improved to a small amount and settles down fast towards the desired value.

A band limited white noise has been introduced into the controllers. The simulation results are shown in Figure 4.16

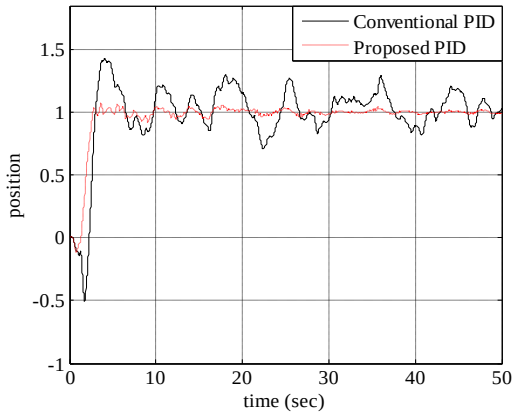

(a) Position x Vs Time

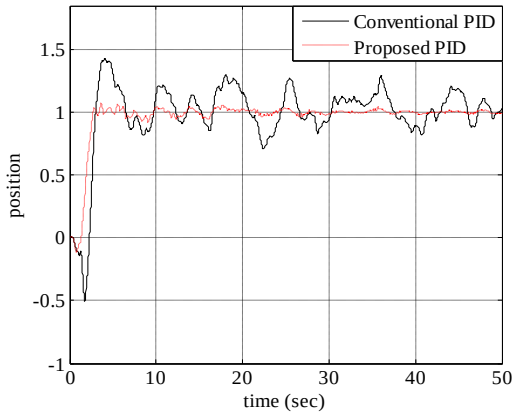

(b) Position y Vs Time

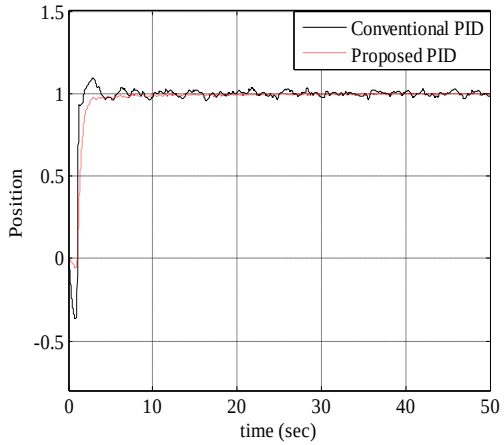

(c) Position z Vs Time

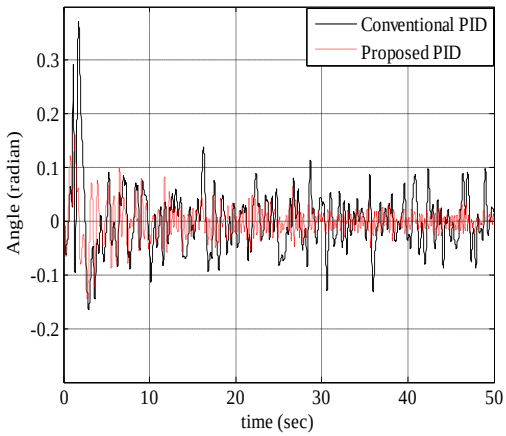

(d) Angle θ Vs Time

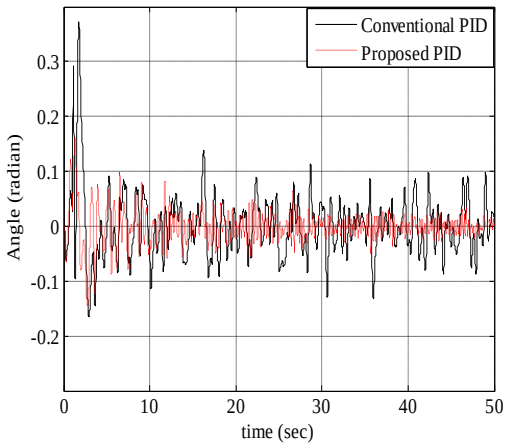

(e) Angle ϕ Vs Time

Figure 4.16 Stabilization of x - y - z Inverted Pendulum using Error AGS PID Controllers with Noise in the Controllers

The simulation results show that while using error AGS PID controllers less chattering has been observed in the output response as compared to the conventional PID scheme.

The simulation results when considering the effect of friction on the inverted pendulum system are given in Figure 4.17 and Figure 4.18 for simple and exponential friction models respectively.

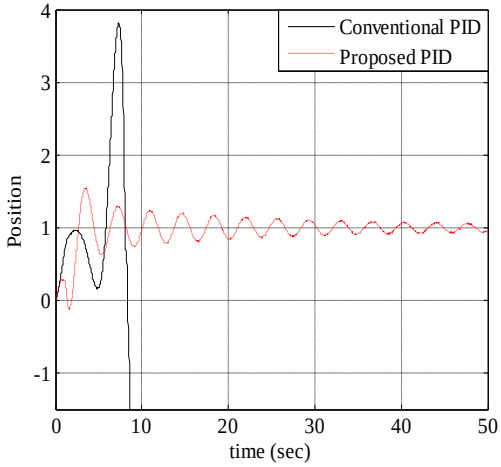

(a) Position x Vs Time

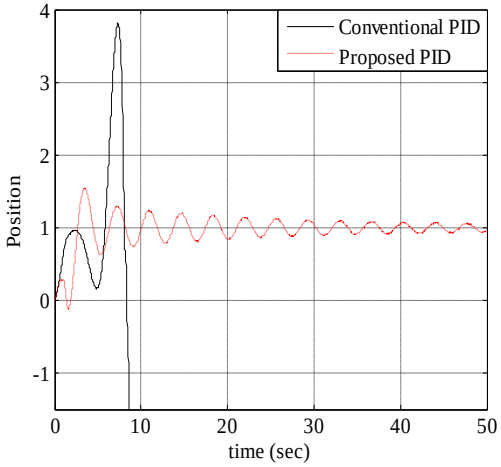

(b) Position y Vs Time

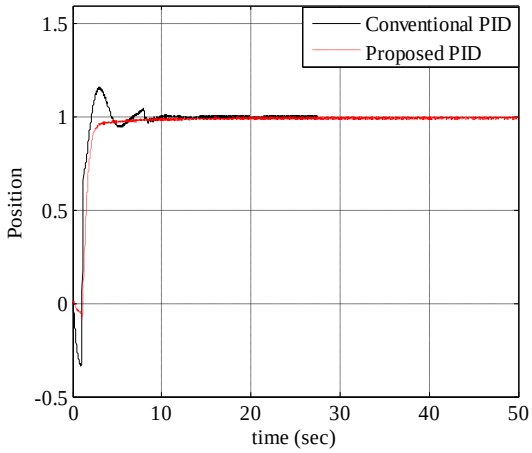

(c) Position z Vs Time

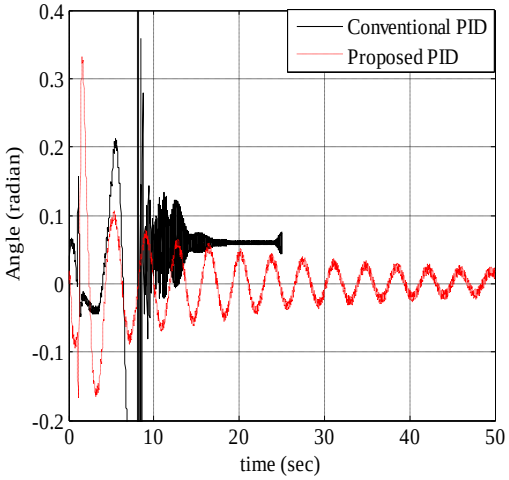

(d) Angle θ Vs Time

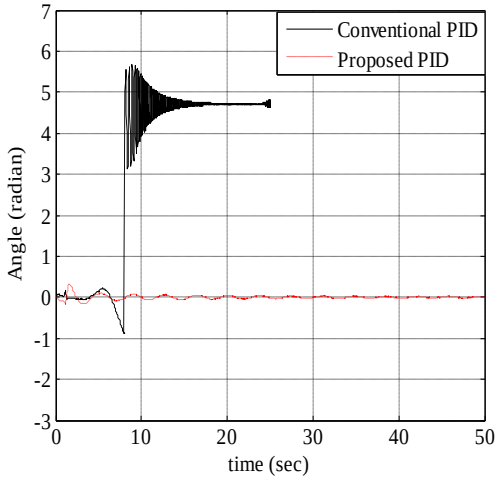

(e) Angle ϕ Vs Time

Figure 4.17 Stabilization of x - y - z Inverted Pendulum using Error AGS PID Controllers with Simple Friction Model

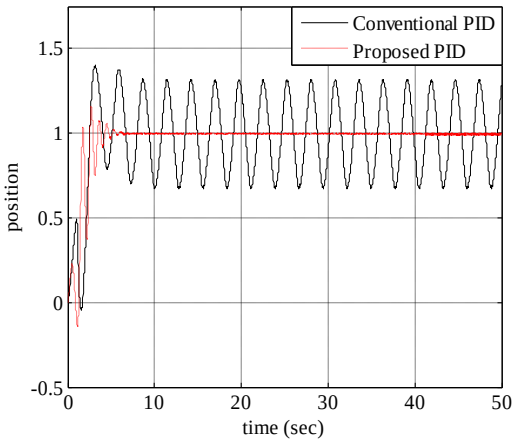

(a) Position x Vs Time

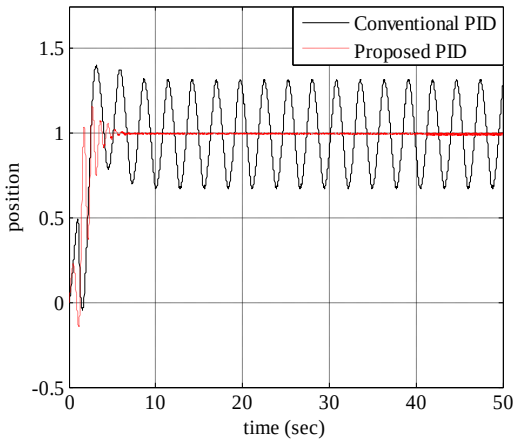

(b) Position y Vs Time

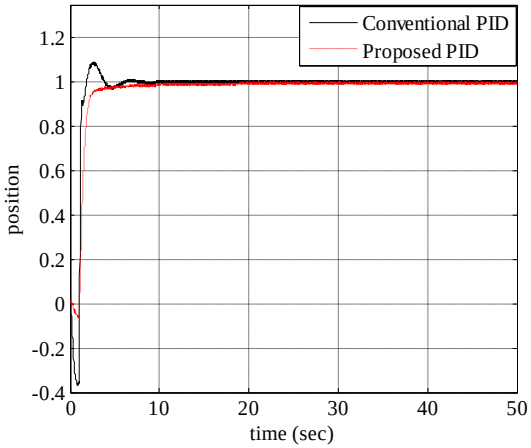

(c) Position z Vs Time

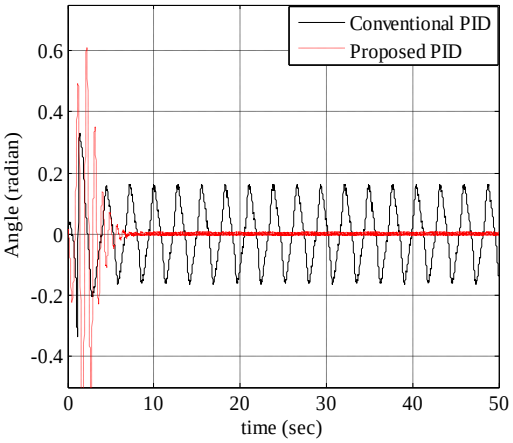

(d) Angle θ Vs Time

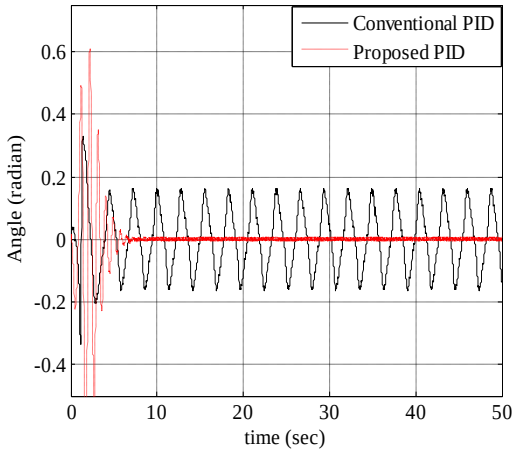

(e) Angle ϕ Vs Time

Figure 4.18 Stabilization of x - y - z Inverted Pendulum using Error AGS PID Controllers with Exponential Friction Model

The simulation results show that the system response becomes unbounded when the effect of friction is considered in terms of simple friction model in case of conventional PID controllers. On the other hand the error AGS PID controllers give satisfactory results. Similarly when the exponential friction model is considered the error AGS PID controllers

provide almost perfect control with zero e_{ss} while the conventional PID controllers give oscillatory response.

4.5.4 Tracking Control with Error AGS PID Controllers

The simulation results for tracking control under different conditions are given from Figure 4.19 to Figure 4.23.

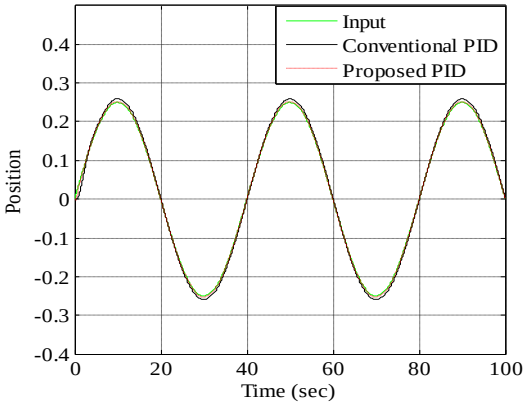

(a) Position x Vs Time

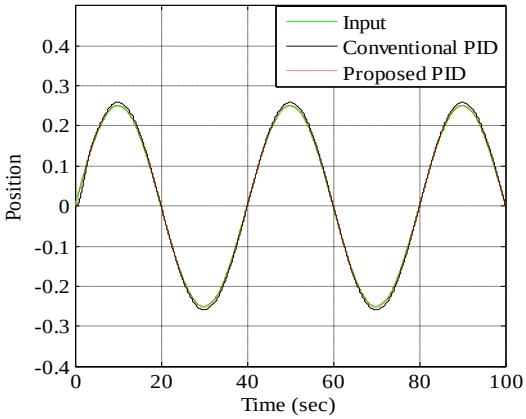

(b) Position y Vs Time

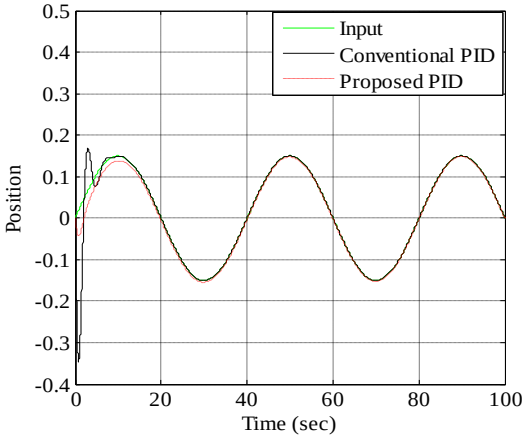

(c) Position z Vs Time

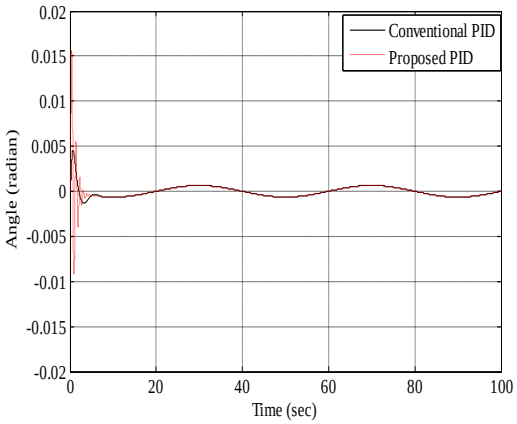

(d) Angle θ Vs Time

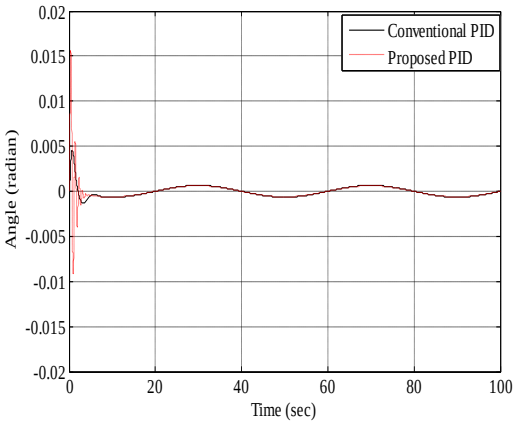

(e) Angle ϕ Vs Time

Figure 4.19 Tracking control of x - y - z Inverted Pendulum using Error AGS PID Controllers without Disturbance

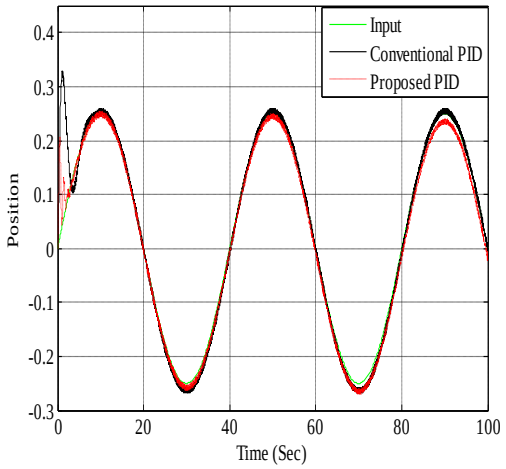

(a) Position x Vs Time

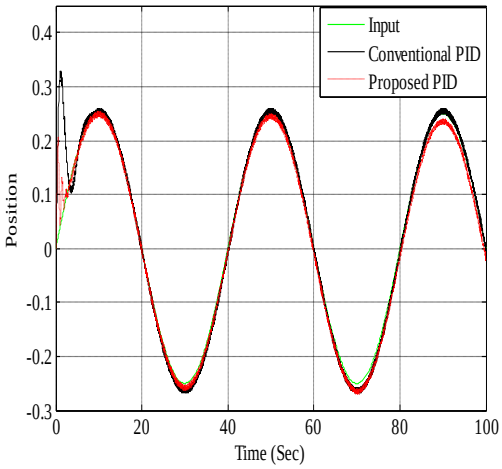

(b) Position y Vs Time

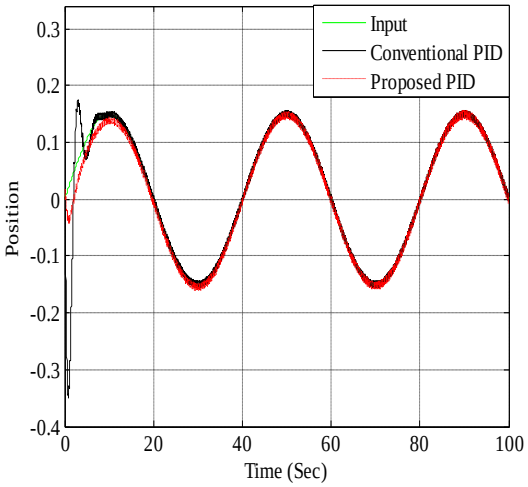

(c) Position z Vs Time

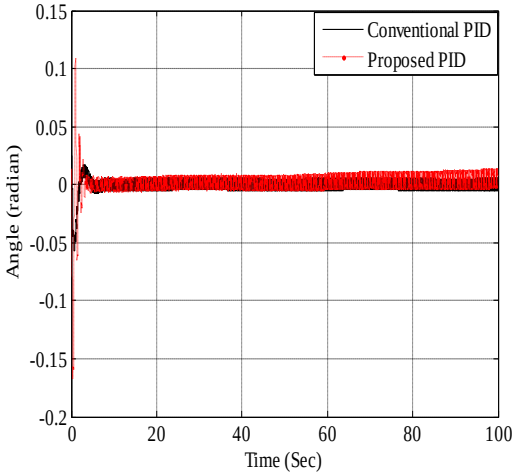

(d) Angle θ Vs Time

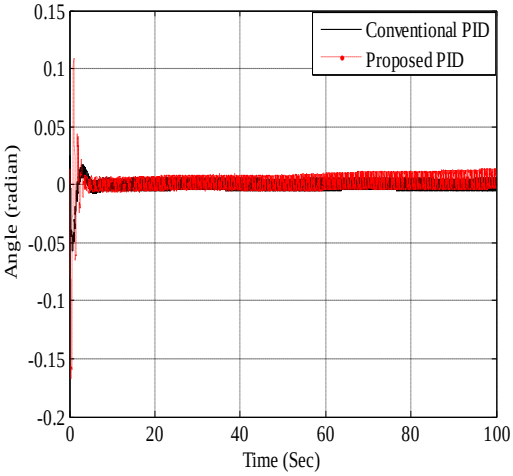

(e) Angle ϕ Vs Time

Figure 4.20 Tracking control of x - y - z Inverted pendulum using Error AGS PID Controllers with Disturbance

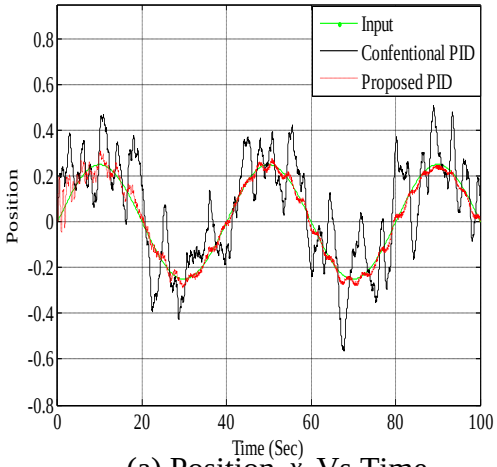

(a) Position x Vs Time

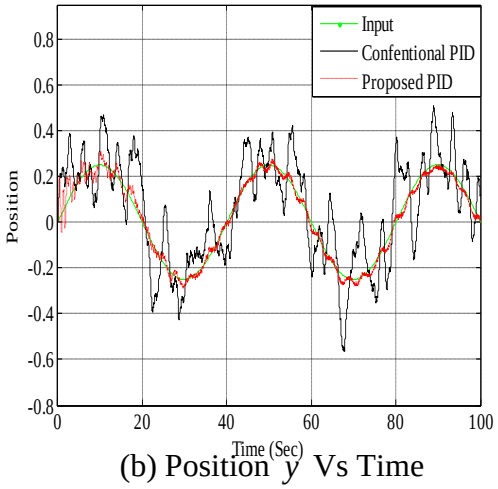

(b) Position y Vs Time

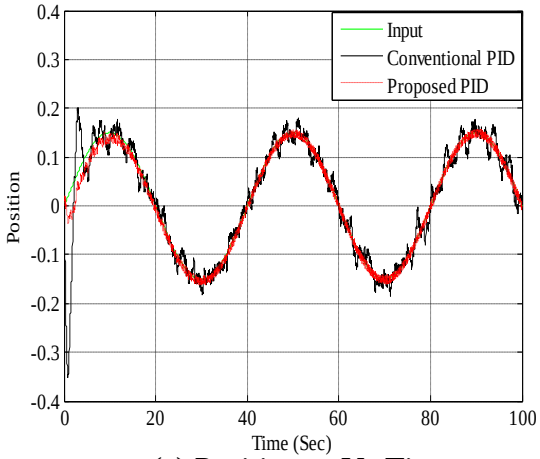

(c) Position z Vs Time

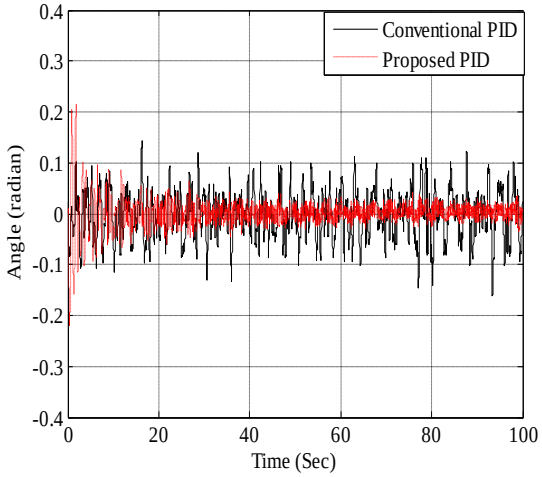

(d) Angle θ Vs Time

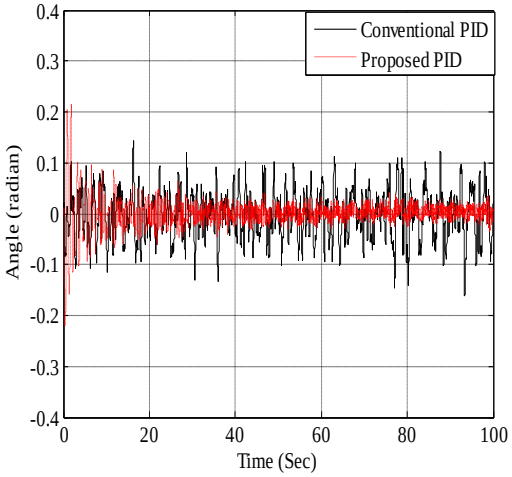

(e) Angle ϕ Vs Time

Figure 4.21 Tracking control of x - y - z Inverted Pendulum using Error AGS PID Controllers with Noise in the Controllers

The simulation results in Figure 4.19 and Figure 4.20 shows that both the conventional and error AGS PID controllers have almost same output responses but when the effect of noise is

considered as shown in Figure 4.21 error AGS PID controllers outperforms conventional PID controllers in terms of chattering in the system response.

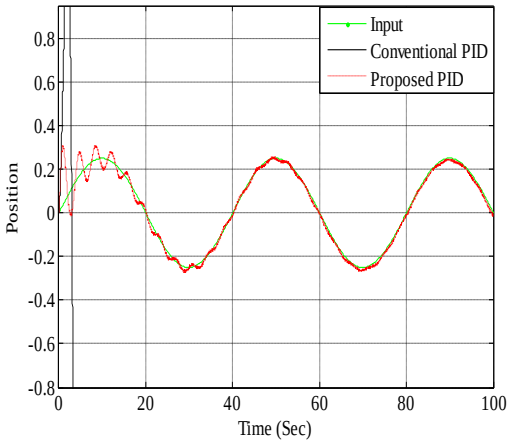

(a) Position x Vs Time

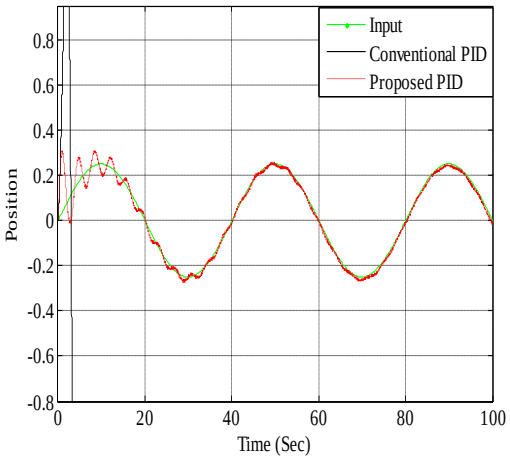

(b) Position y Vs Time

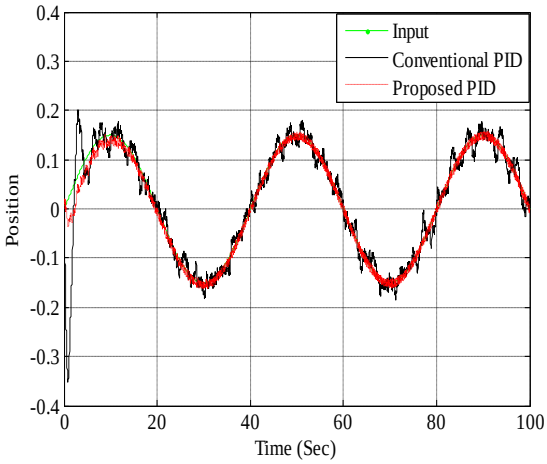

(c) Position z Vs Time

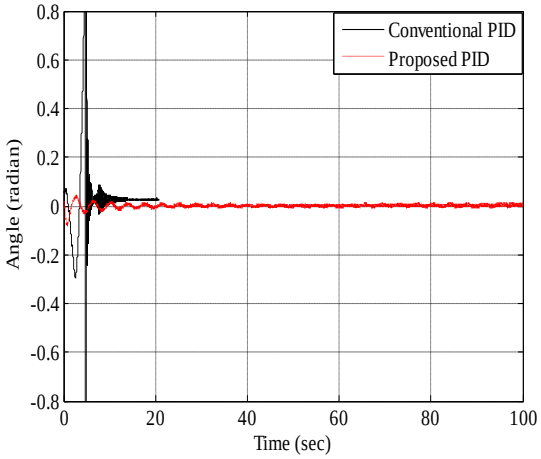

(d) Angle θ Vs Time

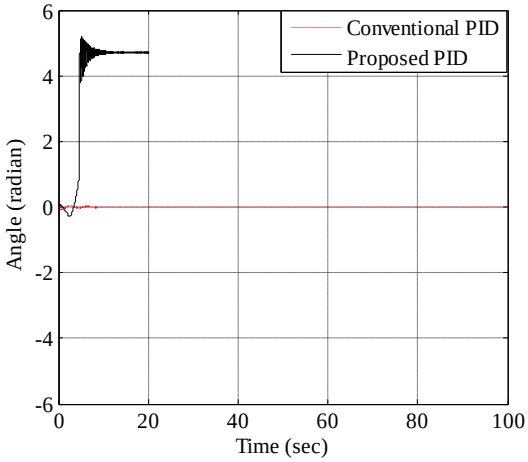

(e) Angle ϕ Vs Time

Figure 4.22 Tracking control of x - y - z Inverted Pendulum using Error AGS PID Controllers with Simple Friction Model

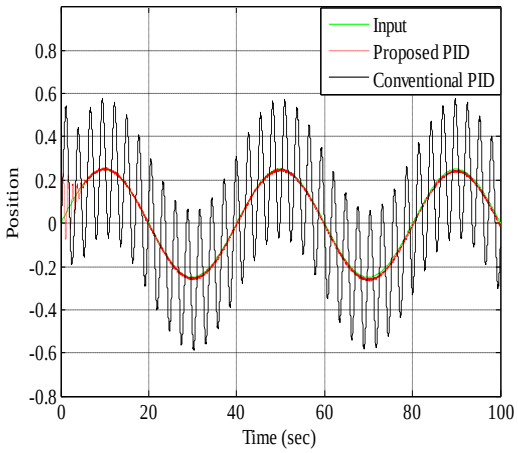

(a) Position x Vs Time

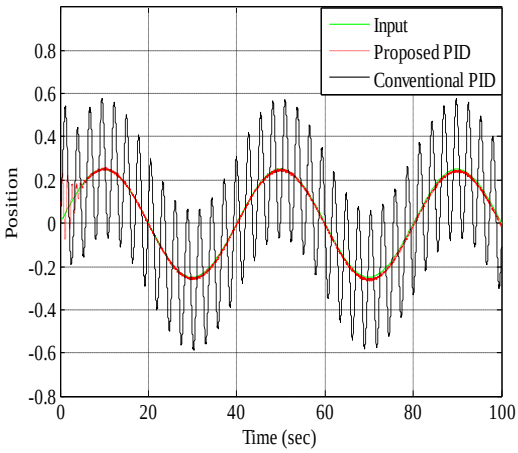

(b) Position y Vs Time

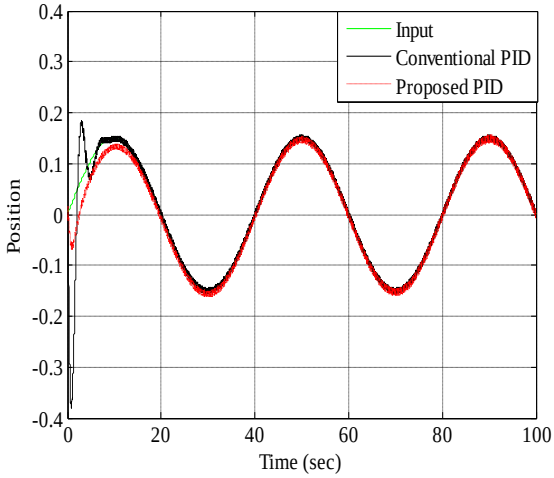

(c) Position z Vs Time

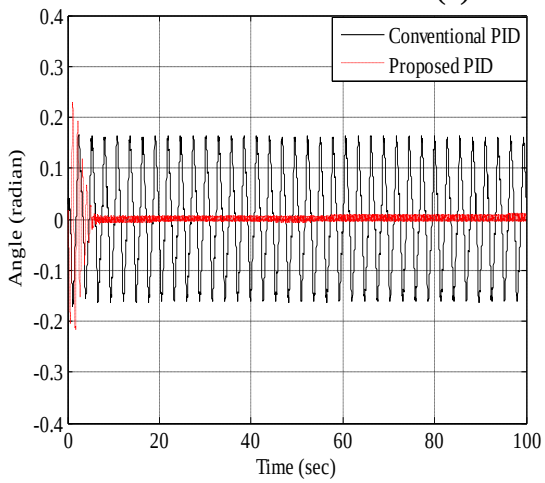

(d) Angle θ Vs Time

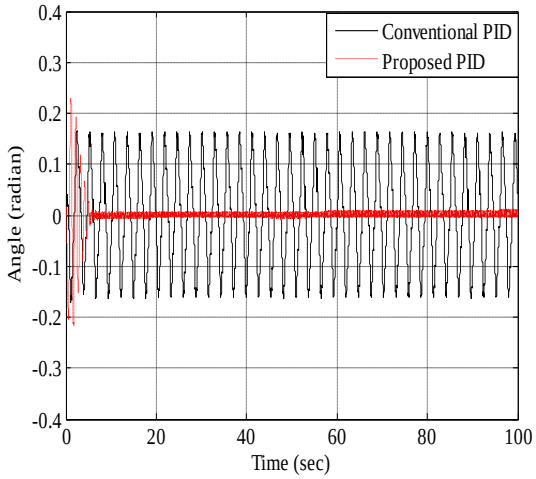

(e) Angle ϕ Vs Time

Figure 4.23 Tracking Control of x - y - z Inverted Pendulum using Error AGS PID Controllers with Exponential Friction Model

The simulation results in Figure 4.22 shows that when the effect of friction is considered in terms of simple friction model the conventional PID controllers fail to respond while the

time adaptive gain scheduling PID controllers give a satisfactory performance. Similarly in case of exponential friction model the tracking control provided by the time adaptive gain scheduling PID controllers is almost perfect which is not in case of conventional PID controllers.

4.6 Conclusion

In this chapter the mathematical model of a new x-y-z inverted pendulum has been developed. The modelling equations obtained in the state space form are used to develop the simulink model of x-y-z inverted pendulum. The proposed AGS PID controllers have been implemented for the stabilization and tracking control of the inverted pendulum. The performance of the proposed controllers has been compared with the conventional PID controllers given in literature. The simulation results show a reduction in maximum overshoot (M_p) of 37.93% in case of x and y position control and 68.75% in case of θ and ϕ control when the time AGS PID controllers are used for stabilization. Also there is an improvement in rise time (t_r) and settling time (t_s) of 32.65% and 13.97% respectively in case of x and y position control with time AGS PID controllers. Similarly when error AGS PID controllers are used a huge amount of improvement in M_p i.e. 900% and a significant amount of improvement in settling time (t_s) of 83.25% for x and y position control has been observed in the system response. A comparative study between time AGS PID controllers and error AGS PID controllers reveal that for x and y position control M_p and t_s are less by 625% and 60.79% in case of error AGS PID controllers while the rise time (t_r) improves by 6.93% with time AGS PID controllers. Similarly for θ and ϕ control M_p in case of time AGS is less by 62.5% while t_s with error AGS PID controllers is less by 60.79%.

Moreover, the proposed controllers are stable and provide good reference tracking even in the presence of uncertainties such as, disturbance in the inverted pendulum, noise in the controller and friction.

The control of a nonlinear system can also be achieved using linear models. In the next chapter the linearized model of a nonlinear system (CSTR) is considered for control.

CHAPTER 5

Hybrid Control of a Continuous Stirred Tank Reactor

5.1 Introduction

Chemical reactors are an important part of a process industry. A continuous stirred tank reactor (CSTR) is a vessel in which the reactions are carried out to produce the desired products. The reactions taking place in a CSTR are either exothermic or endothermic. The exothermic reactions require the removal of heat generated during the course of reaction while, in endothermic reactions, heat is added into the reactor for the reaction to take place. In this chapter, a CSTR with an exothermic reaction has been considered. The heat generated during the reaction has been removed by a coolant flowing around the reactor through a jacket. The control objective is to regulate the concentration of the desired product. This has been achieved using different hybrid controllers such as fuzzy logic (FL) based PID controller, artificial neural network (ANN) based PID controller, adaptive neuro fuzzy inference system (ANFIS) based PID controller and genetic algorithm (GA) based PID controller. The performance of the hybrid controllers has been compared with the conventional PID controller tuned by Ziegler Nichols method.

Furthermore, to improve reference tracking and disturbance rejection H_∞ based preview control scheme has been implemented for controlling a CSTR.

5.2 Model of a Continuous Stirred Tank Reactor

A CSTR with a cooling jacket is shown in Figure 5.1.

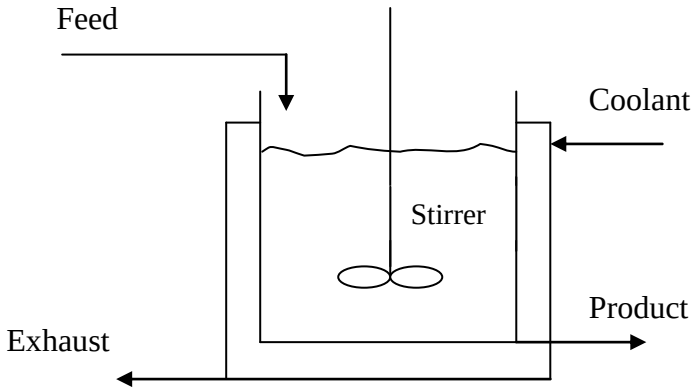

Figure 5.1 CSTR with a Cooling Jacket

The heat generated during reaction has been removed by a coolant flowing through the outer jacket.

The reactions taking place in the reactor are of the following form:

$A \rightarrow B \rightarrow C$

$2A \rightarrow D$

Here component B is the desired product.

The modeling equations of a CSTR have been obtained using the mass balance equations given as (Bequette, 2003):

$$\frac{dC_A}{dt} = \frac{F}{V}(C_{Af} - C_A) - k_1 C_A - k_3 C_A^2 \tag{5.1}$$

$$\frac{dC_B}{dt} = -\frac{F}{V}C_B + k_1 C_A - k_2 C_B \tag{5.2}$$

k_1, k_2 and k_3 are the reaction rate constants. C_{Af}, C_A and C_B represents the feed concentration, concentration of component A and concentration of component B respectively while $\frac{F}{V}$ represents the dilution rate.

Depending upon the steady state operating conditions of $C_{As} = 3$ gmol/liter, $C_{Bs} = 1.117$ gmol/liter, $\frac{F_s}{V} = 0.5714 \text{min}^{-1}$ and the reaction rate constants as $k_1 = 0.83$, $k_2 = 1.66$ and $k_3 = 0.16$

The state space model of the reactor is represented as (Bequette, 2003):

$$\frac{dx_1}{dt} = -2.4048x_1 + 7u \tag{5.3}$$

$$\frac{dx_2}{dt} = 0.8333x_1 - 2.2381x_2 - 1.1170u \tag{5.4}$$

$$y = x_2 \tag{5.5}$$

Here x_1 and x_2 represent the concentration of component A and B while u is the dilution rate.

From Eq. (5.4)

$$x_1 = \frac{1}{0.8333}\left(\frac{dx_2}{dt} + 2.2381x_2 + 1.1170u\right) \tag{5.6}$$

$$\frac{dx_1}{dt} = \frac{1}{0.8333}\left(\frac{d^2x_2}{dt^2} + 2.2381\frac{dx_2}{dt} + 1.1170\frac{du}{dt}\right) \tag{5.7}$$

Put Eq. (5.6) and Eq. (5.7) in Eq. (5.3)

$$\frac{d^2y}{dt^2} + 4.6429\,\frac{dy}{dt} + 5.3821\,y = -1.1170\,\frac{du}{dt} + 3.1472\,u \tag{5.8}$$

Taking Laplace Transform of Eq. (5.8)

$$s^2 y(s) + 4.6429\,sy(s) + 5.3821\,y(s) = -1.1170\,su(s) + 3.1472\,u(s) \tag{5.9}$$

Therefore the input output transfer function for the reactor is :

$$g(s) = \frac{y(s)}{u(s)} = \frac{-1.1170\,s + 3.1472}{s^2 + 4.6429\,s + 5.3821} \tag{5.10}$$

The output $y(s)$ represents the concentration of the desired product while the input $u(s)$ represents the dilution rate. The system is of second order with right half plane (RHP) zero. To control this system, conventional and hybrid controllers have been used and are implemented in the next section.

5.3 Conventional Control of a CSTR

A PID controller tuned by the Ziegler Nichols (ZN) method is the most commonly used controller in many industrial process. The concentration control of a CSTR has been achieved using a PID controller. The PID algorithm is described by (Astrom and Hagglund, 1995):

$$u(t) = k_p\left(e(t) + \frac{1}{T_i}\int e(t)dt + T_d\,\frac{de(t)}{dt}\right) \tag{5.11}$$

Where $u(t)$ is the control signal, $e(t)$ the error signal defined as the difference between the set-point and the output, k_p the proportional gain, T_i the integral time and T_d the derivative time. These are the parameters of the PID controller to be tuned.

5.3.1 Conventional PID Controller

A fixed gain PID controller is called as a conventional PID controller. The parameters of the conventional PID controller are tuned using ZN method. ZN method is based mainly on the step response of the plant and avoids the need for a plant model. In this method only the proportional term is implemented first, and the proportional gain k_p is increased till the ultimate gain k_u, at which the system output starts oscillating with a constant amplitude. The time period of oscillations is represented by T_u. Using Table 5.1 the parameters of PID

controller parameters are determined.

Table 5.1 Ziegler Nichols Method for PID Controller Tuning

Controller Type	k_p	T_i	T_d
P	$0.5\ k_{cu}$	—	—
PI	$0.45\ k_{cu}$	$T_u/1.2$	—
PID	$0.6\ k_{cu}$	$T_u/2$	$T_u/8$

The step response of the system represented by Eq. (5.10) with a conventional PID controller tuned by ZN method is given in Figure 5.2.

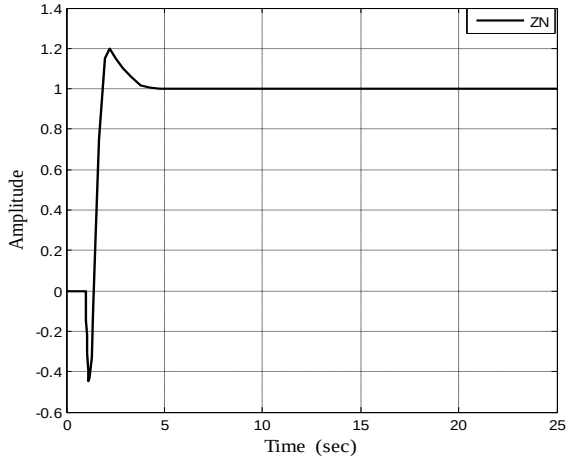

Figure 5.2 Closed loop Response with ZN based PID Controller

The simulation result shows an inverse response behavior in the system response with a magnitude of 44.46% due to RHP zero. The maximum overshoot comes out to be 20.05%. While the rise time and the settling time comes out to be 1.79 seconds and 3.74 seconds respectively with zero steady state error.

5.4 Hybrid Control of a CSTR

The hybrid control of a CSTR has been achieved using a PID controller tuned by various intelligent methods such as fuzzy logic (FL), artificial neural network (ANN), adaptive neuro fuzzy inference system (ANFIS) and genetic algorithm (GA). Also to improve reference tracking and disturbance rejection a hybrid H_∞ based preview control scheme has been implemented for controlling a CSTR.

5.4.1 Fuzzy Logic Based PID Controller

Conventional PID controllers may not give satisfactory performance for processes, which are complex, having time delays, non-linearity and poorly defined dynamics (Tang *et*

al., 2001). The parameters of the conventional PID controller are not often accurately tuned for such type of systems. Hence, there is a need to automatically tune the PID parameters. The automatic tuning of the PID parameters has been done using fuzzy logic. The fuzzy logic controller (FLC) converts a linguistic control strategy based upon expert knowledge into an automatic control strategy (Ross, 2009). A fuzzy PID controller is a self-tuning controller (STC) in which the parameters of the PID controller are tuned using rules formed by analyzing the behavior between inputs and output of the conventional system. The block diagram of a closed-loop system with self-tuning fuzzy PID controller is shown in Figure 5.3 (Sinthipsomboon et al., 2011).

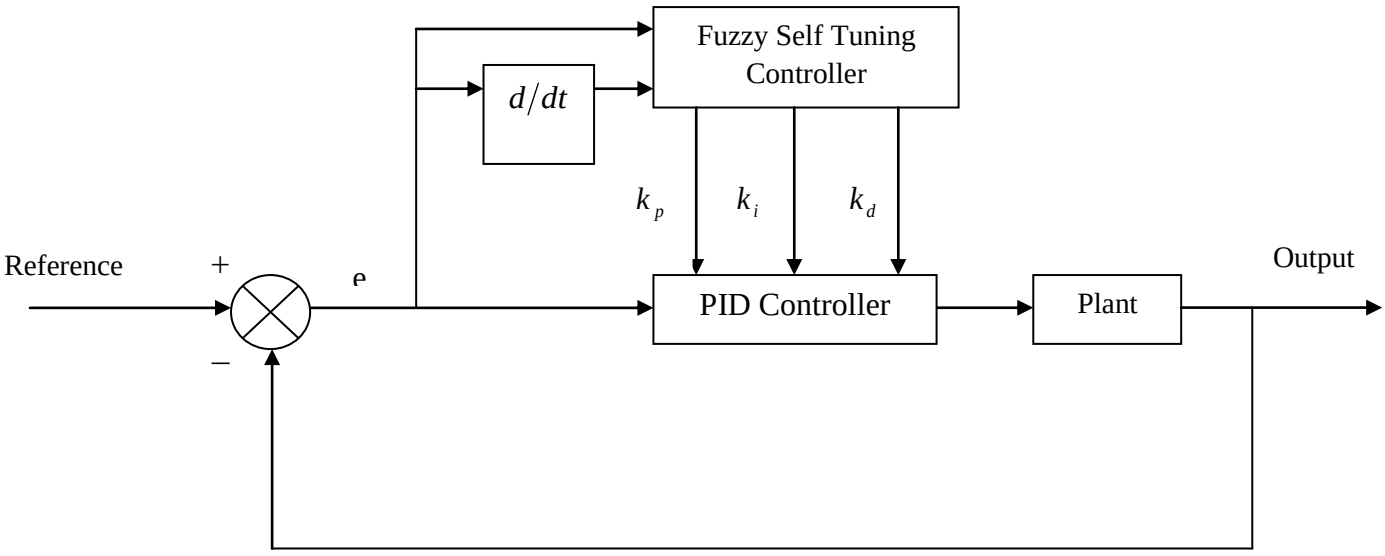

Figure 5.3 Closed-Loop System with Fuzzy-PID Controller

The structure of fuzzy-PID controller is a two input three output structure. The inputs to the controller are the error (e) and the rate of change of error (de/dt) while the outputs are the PID controller gains k_p, k_i and k_d. The inference engine used is of Mamdani type.

The range or the universe of discourse of the input and output membership functions has been obtained from the conventional PID controller tuned by ZN method. The universe of discourse of these input and output fuzzy sets is given in Table 5.2.

Table 5.2 Universe of Discourse for Input and Output Fuzzy Sets

Name	Input/Output	Minimum Value	Maximum Value
e	Input	-1.44	1.56
de/dt	Input	-15.7	4.3
k_{p1}, k_{i1} and k_{d1}	Output	0	1

For the output fuzzy sets the scaling of range has been done (from 0 to 1) corresponding to the formula given as (Zulfatman and Rahmat, 2009):

$$k_{p1} = \frac{k_p - k_{p\min}}{k_{p\max} - k_{p\min}} \tag{5.12}$$

$$k_{i1} = \frac{k_i - k_{i\min}}{k_{i\max} - k_{i\min}} \tag{5.13}$$

$$k_{d1} = \frac{k_d - k_{d\min}}{k_{d\max} - k_{d\min}} \tag{5.14}$$

The minimum and the maximum value of various gains have been obtained from the conventional ZN method.

The linguistic variables used for defining fuzzy sets are given as: negative big (NB), negative small (NS), zero (ZE), positive small (PS) and positive big (PB).

The fuzzy membership functions, for e and de/dt are shown in Figure 5.4 and Figure 5.5 The type of membership functions and their ranges are given in Table 5.3 and Table 5.4.

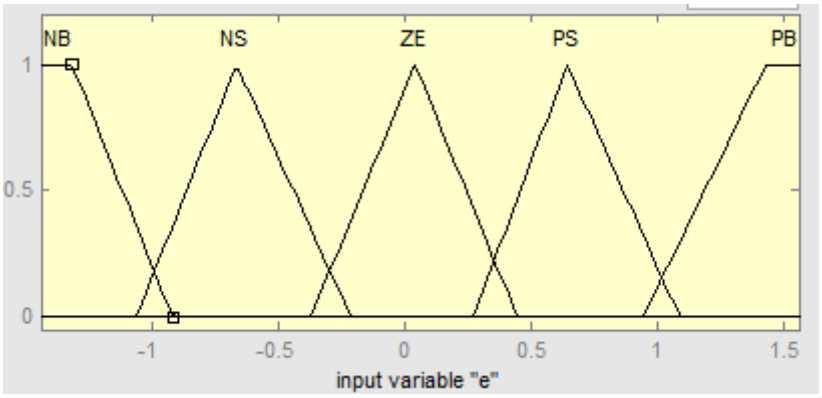

Figure 5.4 Fuzzy Membership functions for e

Table 5.3 Fuzzy Variable Ranges and Membership Functions for e

Crisp Input Range	Fuzzy Variable	Membership Function
(-2.43) – (-0.92)	Negative Big	Trapezoidal
(-1.063) – (-0.214)	Negative Small	Triangular
(-0.3725) – (0.445)	Zero	Triangular
(0.27) – (1.088)	Positive Small	Triangular
(0.9449) – (2.64)	Positive Big	Trapezoidal

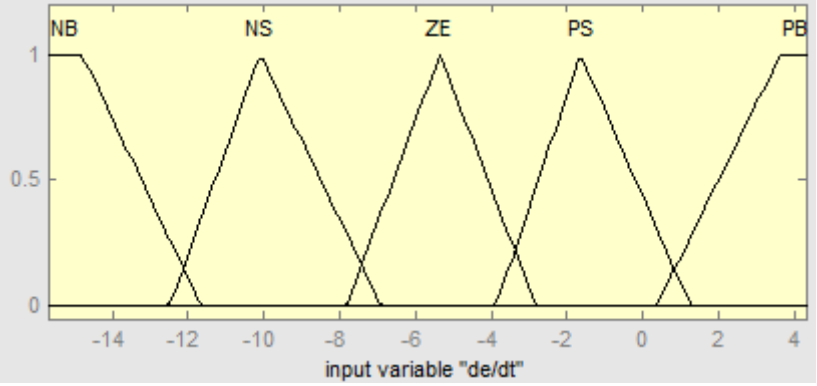

Figure 5.5 Fuzzy Membership functions for de/dt

Table 5.4 Fuzzy Variable Ranges and Membership Functions for de/dt

Crisp Input Range	Fuzzy Variable	Membership Function
(-22.9) – (-11.65)	Negative Big	Trapezoidal
(-12.5) – (-6.89)	Negative Small	Triangular
(-7.835) – (-2.817)	Zero	Triangular
(-3.88) – (1.258)	Positive Small	Triangular
(0.358) – (11.5)	Positive Big	Trapezoidal

The fuzzy membership functions for k_{p1}, k_{i1} and k_{d1} are shown from Figure 5.6 to Figure 5.8. The type of membership functions and ranges are given from Table 5.5 to Table 5.7.

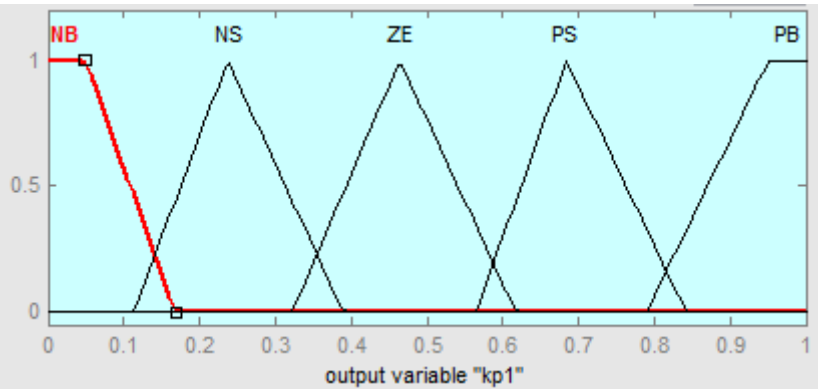

Figure 5.6 Fuzzy Membership functions for k_{p1}

Table 5.5 Fuzzy Variable Ranges and Membership Functions for k_{p1}

Crisp Input Range	Fuzzy Variable	Membership Function
(-0.36) – (0.168)	Negative Big	Trapezoidal
(0.1124) – (0.39)	Negative Small	Triangular
(0.322) – (0.617)	Zero	Triangular
(0.564) – (0.842)	Positive Small	Triangular
(0.7897) – (1.36)	Positive Big	Trapezoidal

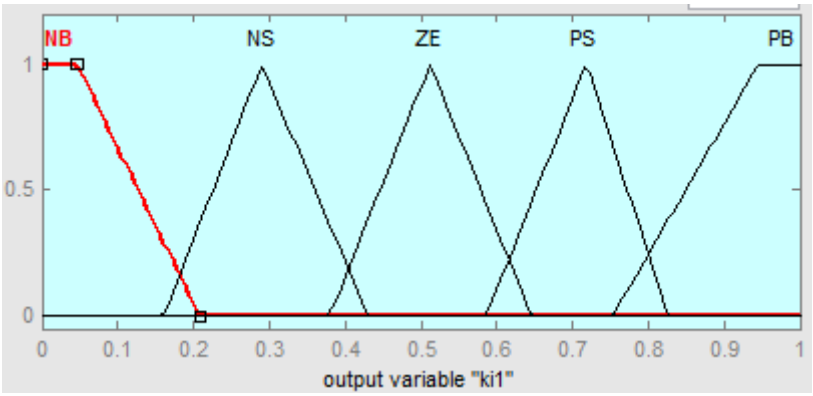

Figure 5.7 Fuzzy Membership functions for k_{i1}

Table 5.6 Fuzzy Variable Ranges and Membership Functions for k_{i1}

Crisp Input Range	Fuzzy Variable	Membership Function
(-0.321) – (0.208)	Negative Big	Trapezoidal
(0.16) – (0.43)	Negative Small	Triangular
(0.379) – (0.646)	Zero	Triangular
(0.586) – (0.827)	Positive Small	Triangular
(0.753) – (1.32)	Positive Big	Trapezoidal

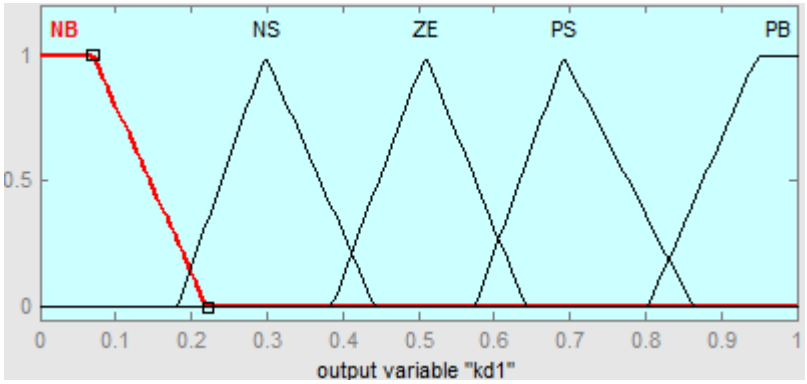

Figure 5.8 Fuzzy Membership functions for k_{d1}

Table 5.7 Fuzzy Variable Ranges and Membership Functions for k_{d1}

Crisp Input Range	Fuzzy Variable	Membership Function
(-0.334) – (0.221)	Negative Big	Trapezoidal
(0.181) – (0.443)	Negative Small	Triangular
(0.3849) – (0.642)	Zero	Triangular
(0.575) – (0.864)	Positive Small	Triangular
(0.8029) – (1.36)	Positive Big	Trapezoidal

The rule base for the fuzzy-PID controller is explained as follows:

1. If e is negative big AND de/dt is negative big then k_{p1}, k_{i1} and k_{d1} are negative big.

2. If e is negative small AND de/dt is negative big then k_{p1}, k_{i1} and k_{d1} are negative big.

3. If e is zero AND de/dt is negative big then k_{p1}, k_{i1} and k_{d1} are negative small.

4. If e is positive small AND de/dt is negative big then k_{p1}, k_{i1} and k_{d1} are negative small.

5. If e is positive big AND de/dt is negative big then k_{p1}, k_{i1} and k_{d1} are zero.

6. If e is negative big AND de/dt is negative small then k_{p1}, k_{i1} and k_{d1} are negative big.

7. If e is negative small AND de/dt is negative small then k_{p1}, k_{i1} and k_{d1} are negative small.

8. If e is zero AND de/dt is negative small then k_{p1}, k_{i1} and k_{d1} are negative small.

9. If e is positive small AND de/dt is negative small then k_{p1}, k_{i1} and k_{d1} are zero.

10. If e is positive big AND de/dt is negative small then k_{p1}, k_{i1} and k_{d1} are positive small.

11. If e is negative big AND de/dt is zero then k_{p1}, k_{i1} and k_{d1} are negative small.

12. If e is negative small AND de/dt is zero then k_{p1}, k_{i1} and k_{d1} are negative small.

13. If e is zero AND de/dt is zero then k_{p1}, k_{i1} and k_{d1} are zero.

14. If e is positive small AND de/dt is zero then k_{p1}, k_{i1} and k_{d1} are positive small.

15. If e is positive big AND de/dt is zero then k_{p1}, k_{i1} and k_{d1} are positive small.

16. If e is negative big AND de/dt is positive small then k_{p1}, k_{i1} and k_{d1} are negative small.

17. If e is negative small AND de/dt is positive small then k_{p1}, k_{i1} and k_{d1} are zero.

18. If e is zero AND de/dt is positive small then k_{p1}, k_{i1} and k_{d1} are positive small.

19. If e is positive small AND de/dt is positive small then k_{p1}, k_{i1} and k_{d1} are positive small.

20. If e is positive big AND de/dt is positive small then k_{p1}, k_{i1} and k_{d1} are positive big.

21. If e is negative big AND de/dt is positive big then k_{p1}, k_{i1} and k_{d1} are zero.

22. If e is negative small AND de/dt is positive big then k_{p1}, k_{i1} and k_{d1} are positive small.

23. If e is zero AND de/dt is positive big then k_{p1}, k_{i1} and k_{d1} are positive small.

24. If e is positive small AND de/dt is positive big then k_{p1}, k_{i1} and k_{d1} are positive big.

25. If e is positive big AND de/dt is positive big then k_{p1}, k_{i1} and k_{d1} are positive big.

The Simulink block-set for the implementation of fuzzy based PID controller is shown in Figure 5.9.

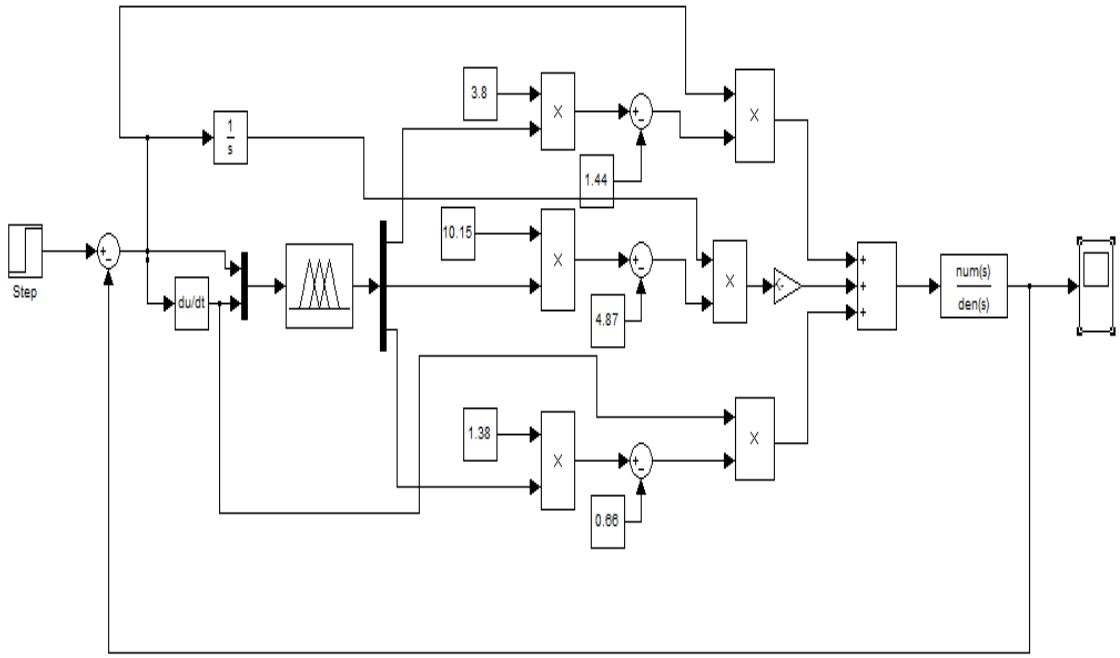

Figure 5.9 Fuzzy PID Controller Implementation in MATLAB Simulink

The closed loop system response subjected to a step input is shown in Figure 5.10.

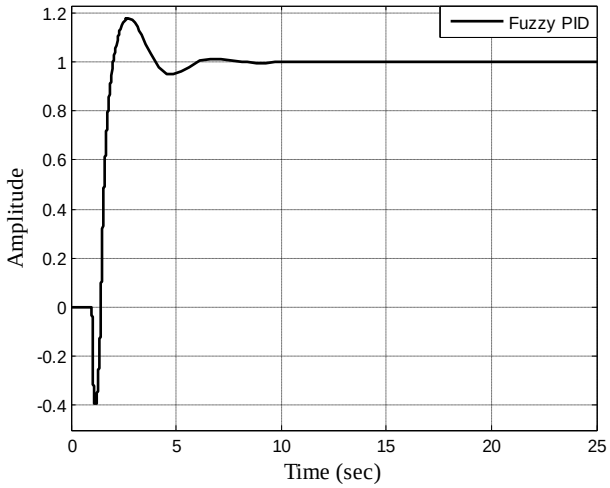

Figure 5.10 Closed Loop Response using Fuzzy PID Controller

From the step response, it has been observed that the magnitude of the inverse response behavior is 39.98% with an overshoot of 17.95%. The rise time and the settling time comes out to be 1.86 seconds and 5.62 seconds with zero steady state error.

5.4.2 Artificial Neural Networks based PID Controller

Artificial neural networks (ANNs) can be defined as a system or mathematical model influenced by biological neural networks. The network consists of an interconnected collection of artificial neurons, and processes information using a connectionist approach to computation (Jang *et al*., 2009). Learning process means updating the ANN weights by some learning algorithms to attain the desired objective. The PID controller has been tuned using single neuron ANN structure as shown in Figure 5.11 (Liu, 2008).

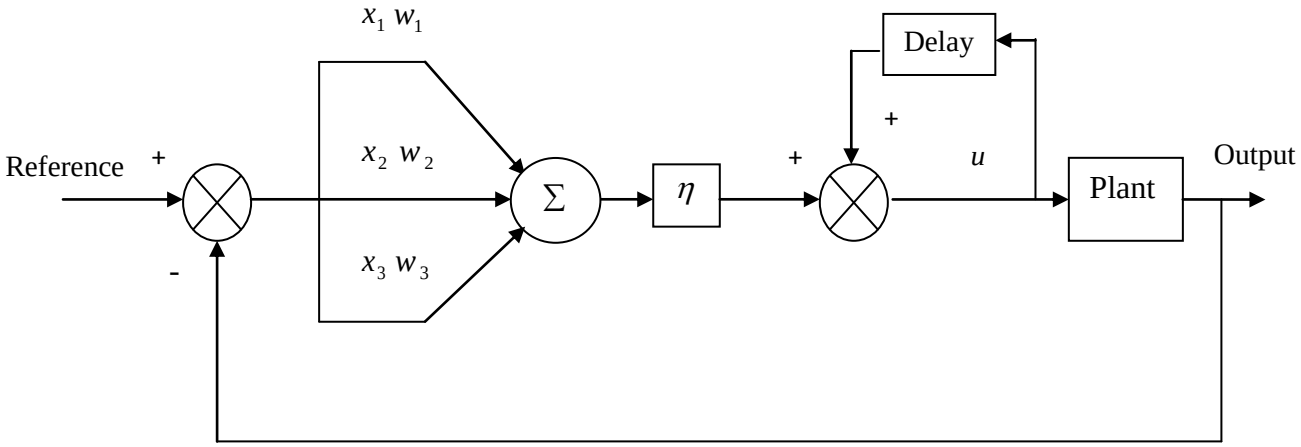

Figure 5.11 Closed Loop System with Single Neuron ANN Structure

The gains k_P, k_i and k_d have been replaced by connection weights of the neuron i.e. w_1, w_2 and w_3 respectively. The input to the single neuron is the proportional error $x_1(k)$, the integral error $x_2(k)$ and the derivative error $x_3(k)$ multiplied with their corresponding weights w_1, w_2 and w_3 where

$$x_1(k) = e(k) - e(k-1) \tag{5.15}$$

$$x_2(k) = e(k) \tag{5.16}$$

$$x_3(k) = e(k) - 2e(k-1) - e(k-2) \tag{5.17}$$

The neuron output is given by:

$$u(k) = u(k-1) + \eta \sum_{i=1}^{3} w_i(k) x_i(k) \tag{5.18}$$

η is called neuron proportion coefficient. Larger the value of η, faster is the closed loop response. But too large a value for η, results in large overshoot.

The various steps in tuning a PID controller using ANN are as follows:

Step 1: Choose the value of the weights randomly.

Step 2: Calculate the error (i.e. the difference between the reference input and the output)

Step3: Decide the gains of the PID controller by supervised delta learning method, using the error signal.

Step 4: Multiply the output of the single neuron with a gain η to obtain a better closed loop response.

The updated weights will act as the proportional, the integral and the derivative gains respectively.

The supervised delta learning algorithm for updating the weights has been given by (Liu, 2008):

$$\begin{aligned} w_1(k) &= w_1(k-1) + \eta_P e(k-1)u(k-1) \\ w_2(k) &= w_2(k-1) + \eta_I e(k-1)u(k-1) \\ w_3(k) &= w_3(k-1) + \eta_D e(k-1)u(k-1) \end{aligned} \tag{5.19}$$

where η_P, η_I and η_D are the proportional, integral and the derivative learning speeds. The closed loop response of the system subjected to a step input is shown in Figure 5.12.

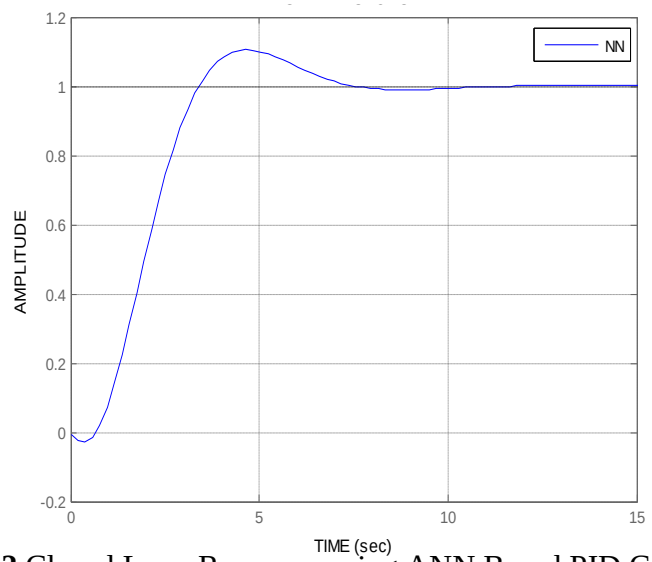

Figure 5.12 Closed Loop Response using ANN Based PID Controller

From the simulation result it has been observed that the inverse response behavior has been reduced to only 2.9% with a maximum overshoot is 10.47%. The rise time and the settling time come out to be 2.98 seconds and 6.85 seconds while the steady state error is zero.

5.4.3 Adaptive Neuro Fuzzy Inference System (ANFIS) based PID Controller

ANFIS is a type of neural network based on Takagi–Sugeno fuzzy inference system. It combines the features of neural networks and fuzzy logic to get the benefits of both in a single structure (Nedjah and Mourelle, 2006). ANFIS combines the features both fuzzy logic (expert knowledge) and ANN (learning capability) into a single structure. ANFIS develops an input-output mapping based on both the human knowledge and the input-output data

pairs (Shing and Jang, 1993). Figure 5.13 shows the ANFIS structure, which is a two input single output feed-forward structure having three hidden layers.

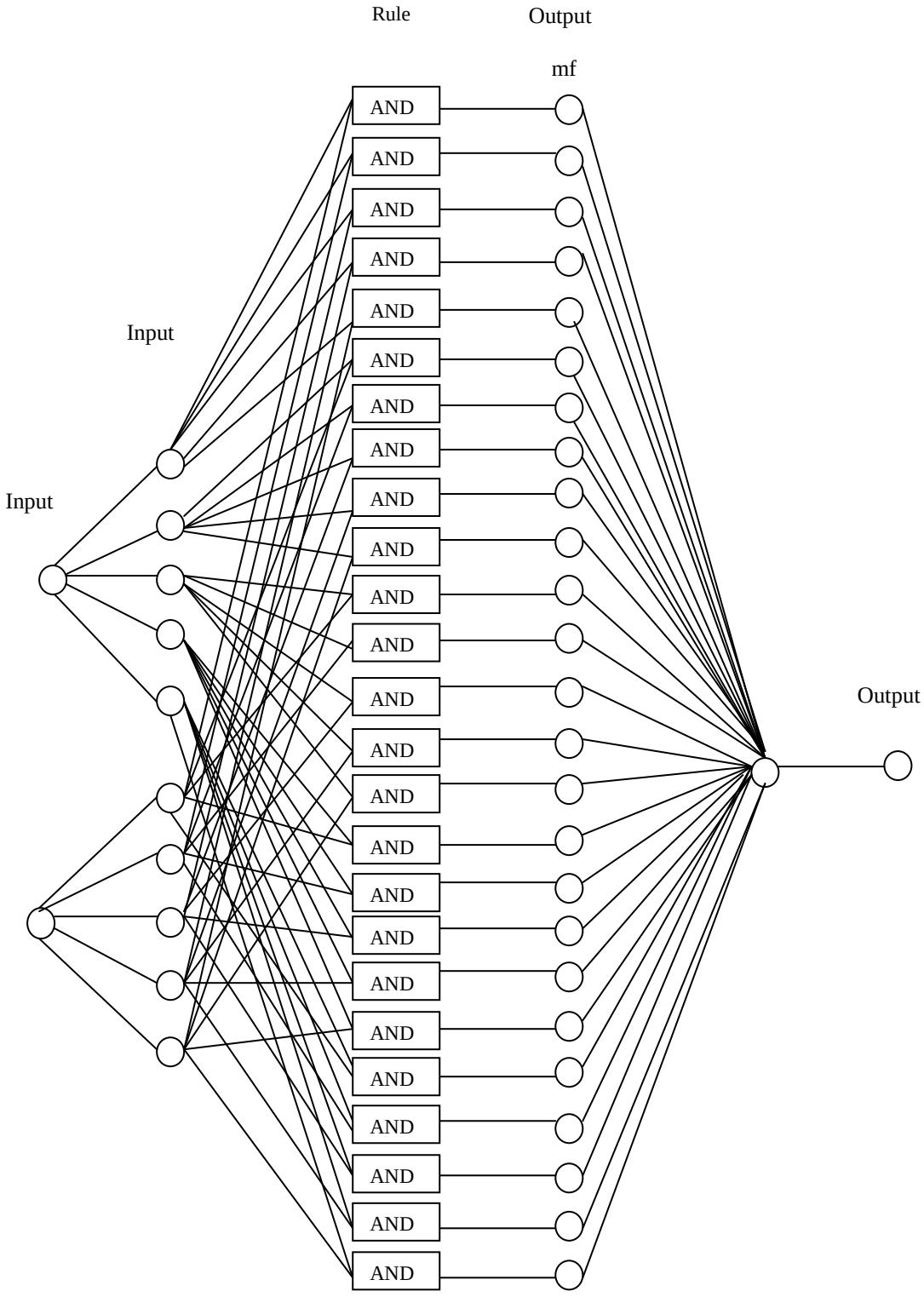

Figure 5.13 ANFIS Structure

The inputs to the proposed adaptive neuro fuzzy controller are the error (e) and the rate of change of error (de/dt) while the outputs are the proportional gain k_P, the integral gain k_i and the derivative gain k_d. The input output data set has been taken from a PID controller tuned using conventional ZN method

The simulink block-set for the implementation of the given method is shown in Figure 5.14.

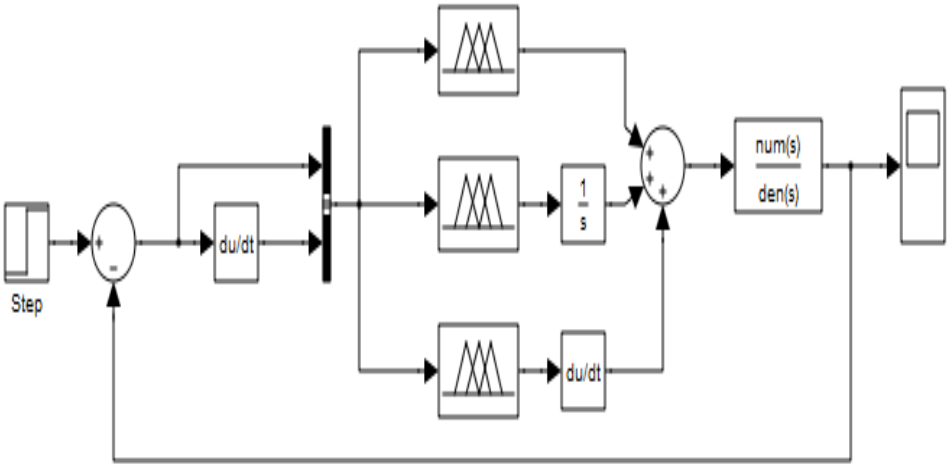

Figure 5.14 Adaptive Neuro Fuzzy Controller Implementation using MATLAB Simulink

As shown in Figure 5.14 the inputs to the adaptive neuro fuzzy controller are e and de/dt while the outputs are k_p, k_i and k_d.

The system behavior subjected to a step input is shown in Figure 5.15.

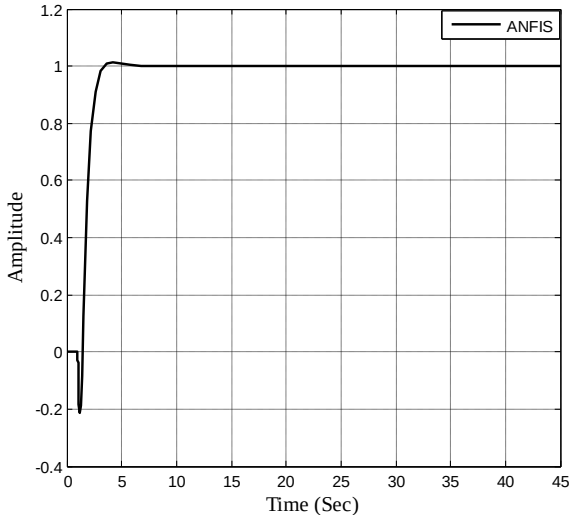

Figure 5.15 Closed Loop Response using ANFIS Based PID Controller

The simulation result shows that the maximum overshoot is reduced to 1.01% while the inverse response behavior magnitude is 21.2%.

5.4.4 Genetic Algorithms based PID Controller

Genetic algorithms are derivative free stochastic optimization methods. They are based upon the principle of natural selection and evolutionary processes (Jang *et al*., 2009). They can be implemented on parallel processing machines due to their parallel search procedures, to speed up their operation (Singla and Arora, 2012). Genetic algorithms are used in control systems for tuning the parameters of a PID controller in an optimized way (Saini *et al.*, 2005).

Figure 5.16 shows the block diagram for tuning of PID parameters using GA (Tang, 2005).

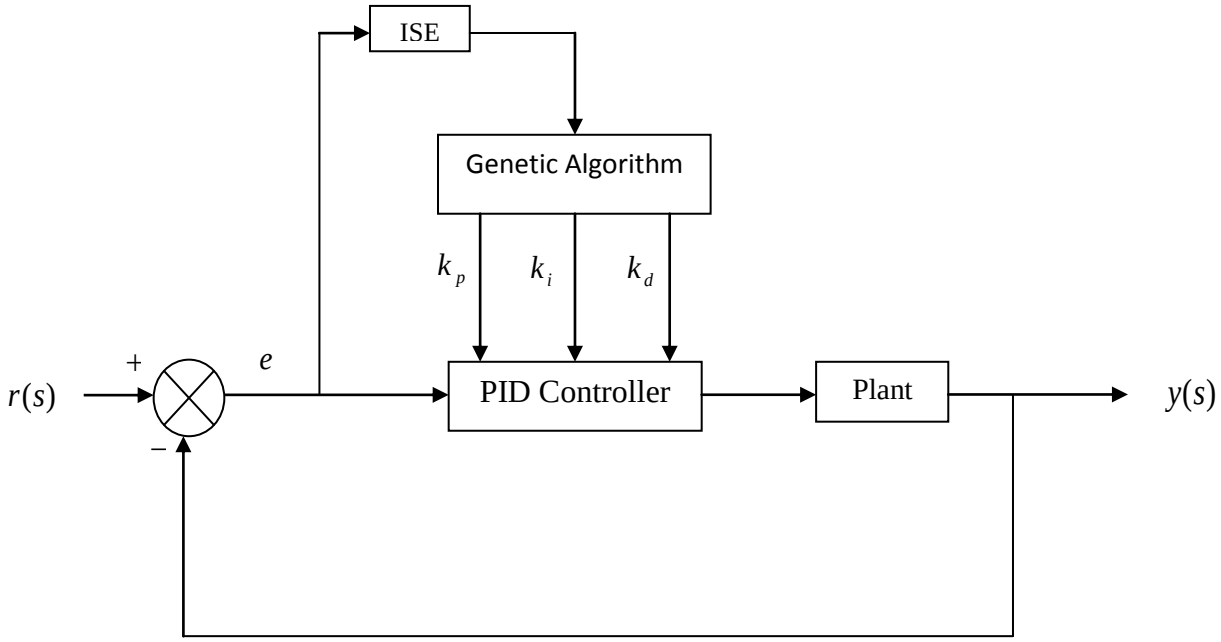

Figure 5.16 Closed Loop System with GA Based PID Controller

Auto-tuning of the PID controller has been done using GA by minimizing the integral of square error (ISE). The ISE criterion is defined as:

$$ISE = \int (r(t) - y(t))^2 dt \tag{5.20}$$

The various steps in finding the parameters of a PID controller are:

Step 1: Define the Plant transfer function.

Step 2: Initialize k_p, k_i and k_d calculate ISE.

Step 3: Obtain pbest and gbest values.

Step 4: Calculate new population using Mutation.

Step 5: Obtain pbest1 and gbest1.

Step 6: Compare pbest and pbest1.

Step 7: Compare gbest and gbest1.

Step 8: Obtain the new values of k_p, k_i and k_d find out the step response for the closed loop system.

The closed loop response of the system subjected to a step input is shown in Figure 5.17.

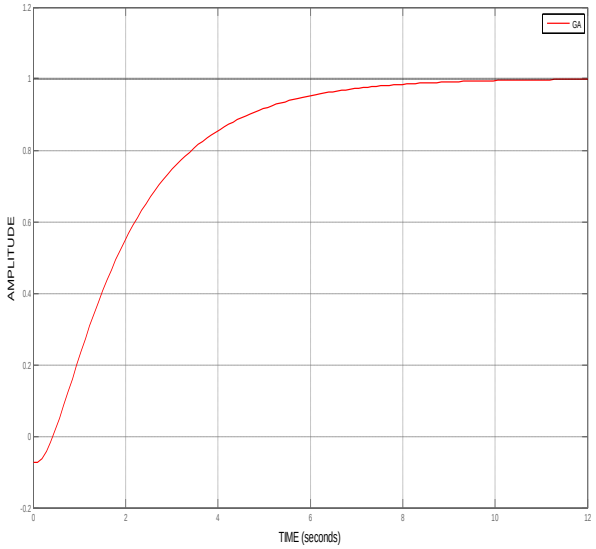

Figure 5.17 Closed Loop Response using GA Based PID Controller

The simulation result shows that the system response has become sluggish as compared to the other PID tuning methods with zero maximum overshoot and an inverse response behavior of 7.29%.

The quantitative analysis in terms of various time domain performance specifications such as rise time (t_r), settling time (t_s) (within 2% of the final steady state value), maximum overshoot (M_p) and steady state error (e_{ss}) has been carried out and is presented in Table 5.8.

Table 5.8 Quantitative Analysis Among Different PID Tuning Methods

Parameters	Tuning Methods				
	ZN	Fuzzy	ANN	ANFIS	GA
t_r (sec)	1.78	1.865	2.98	2.57	4.84
t_s (sec)	3.74	5.624	6.85	3.42	7.12
M_p (%)	20.05	17.95	10.47	1.01	0
e_{ss}	0	0	0	0	0

From Table 5.8, it can be concluded that the various performance specifications have been improved greatly using the hybrid methods except the rise time which is less in case of ZN method. The best performance in terms of settling time and overshoot has been given by

ANFIS. Moreover, the inverse response behaviour in case of ANFIS method is less than the ZN and fuzzy PID methods.

5.5 H_∞ based Preview Control

H_∞ methods are used in control theory for designing robust controllers such that the resulting system satisfies the following conditions (Wang *et al*, 2009):

(i) The closed-loop system is internally stable.

(ii) The transfer function Σ_{zw} from *w* to *z* satisfies $\|\Sigma_{zw}\|_\infty < \gamma$ for a prescribed $\gamma > 0$.

Here w represents the disturbance and z the output.

The use of future information about reference signal or disturbance for designing controllers is termed as preview control. The preview controller makes use of future information about reference and disturbance to obtain better tracking and disturbance rejection in order to minimize the control effort (Katoh, 2004). The preview information appears in the form of delayed exogenous or reference signal. The delayed magnitude is usually referred as the preview length, and it shows the ability of the system to obtain information in advance. Figure 5.18 shows the block diagram representation of the closed-loop preview control scheme (Takaba, 2003).

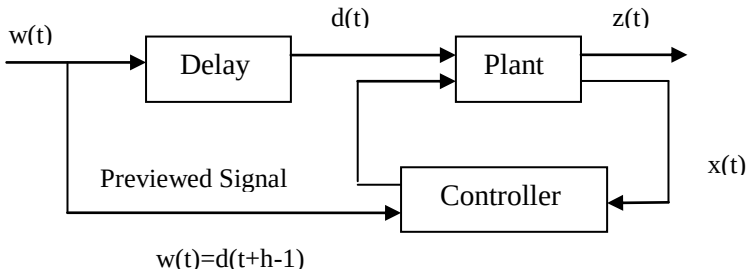

Figure 5.18 Closed Loop Preview Control Scheme

The previewed signal is represented by $w(t) = d(t+h-1)$ where $w(t)$ is exogenous or the reference signal and the values of $d(t), d(t+1) \ldots, d(t+h)$ are available for control, h represents the preview length.

The control effort is the sum of measured plant output and the previewed signal i.e.

$$u(t) = kx(t) + \sum_{i=0}^{h} k_{di} d(t+i) \tag{5.21}$$

So as to minimize the following performance criterion:

$$J = \sum_{t=0}^{\infty} \left\| z(t) \right\|^2 \tag{5.22}$$

The simulation results using H_∞ preview control scheme are shown in Figure 5.19. The results are compared with H_2 preview control.

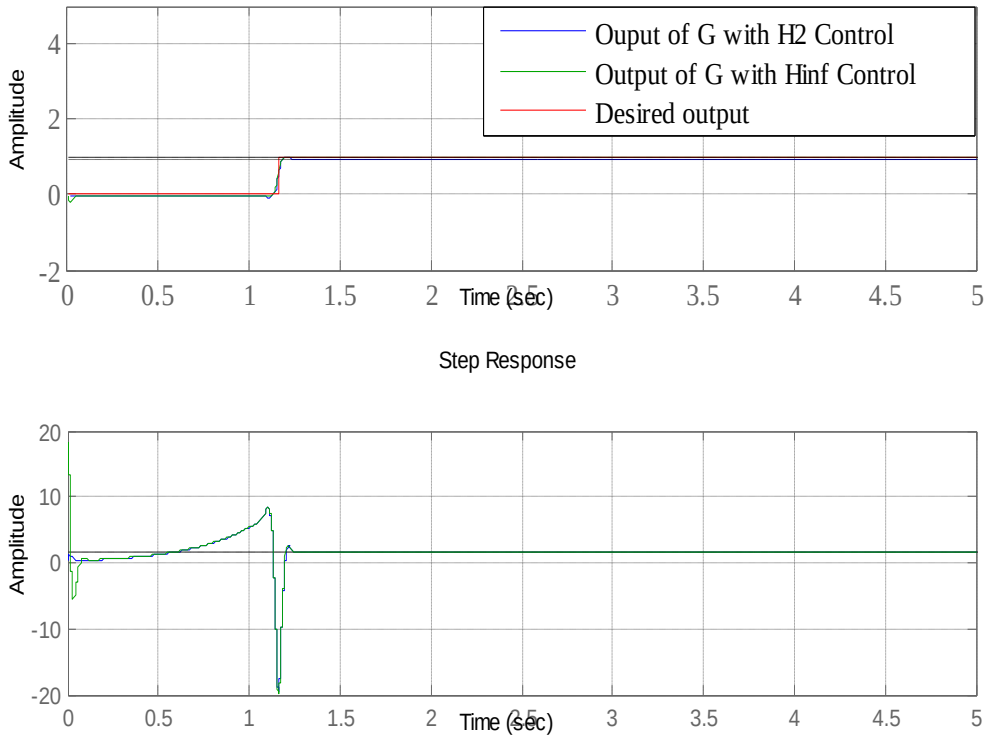

Figure 5.19 Closed Loop H_2 and H_∞ Preview Control of a CSTR

The simulation results show an improvement in the steady state tracking performance of the system with minimum control effort.

5.6 Conclusion

In this chapter different hybrid control schemes based on fuzzy logic, artificial neural network, adaptive neuro fuzzy inference system and genetic algorithms have been implemented for the concentration control of a CSTR.

The simulation results show that the various performance specifications have been improved greatly using the hybrid methods except the rise time which is less in case of ZN tuned PID controller method. The best performance in terms of settling time with a value of 3.42 seconds and maximum overshoot of 1.01% has been given by ANFIS based PID controller. Also, the magnitude of the inverse response behaviour in case of ANFIS based PID controller is 21.2% which is less than the ZN and fuzzy based PID methods.

To improve reference tracking and disturbance rejection H_∞ based preview control has been implemented for controlling a CSTR. The simulation results show an improvement in the steady state tracking performance in the system response with minimum control effort.

CHAPTER 6

Conclusions and Future Scope

In this thesis, control of nonlinear systems using, nonlinear and linear models have been discussed and developed. The systems considered are an inverted pendulum and a continuous stirred tank reactor (CSTR). The inverted pendulum system uses the nonlinear state space model while the CSTR uses the linear transfer function model. The outcome of work has been presented in this chapter along with the future scope in this area.

6.1 Conclusions

The conclusions of the work are being presented in the point wise manner and are given below.

- For a nonlinear system a fixed gain PID controller may not produce satisfactory performance under all operating regions. Therefore adaptive controller is preferred over a conventional controller for such type of systems. An adaptation mechanism using gain scheduling as a function of time and error has been proposed for the tuning of PID controller gains. The proposed time adaptive gain scheduling (AGS) and the error AGS PID controllers have been implemented for the stabilization and tracking control of x, $x-y$ and $x-z$ type of inverted pendulums. The performance of the proposed controllers has been compared with the conventional PID controllers in terms of various time domain performance specifications. Simulation results reveal that the proposed AGS PID controllers provide better stabilization control for all the three types of inverted pendulums (especially a considerable amount of improvement in overshoot for both position and angle control due to which wear and tear on the system will be less) while keeping the tracking control at the same level as of conventional PID controllers.
- The mathematical modelling of a new type of three dimensional inverted pendulum, i.e. $x-y-z$ inverted pendulum has been developed using Euler Lagrange's method. The stabilization and tracking control of the proposed $x-y-z$ inverted pendulum has been obtained using conventional and proposed AGS PID controllers. The simulation results for stabilization show that the AGS PID controllers provide better performance than the conventional PID controllers (in terms of maximum overshoot,

rise time and settling time for x, y, θ and ϕ control) while keeping the tracking control at the same level as of conventional PID controllers. Moreover, the inverse response behaviour of the system has been reduced to a good amount using the proposed controllers.

- The stability conditions for x, x-y, x-z and x-y-z inverted pendulums has been analysed and proved using Lyapunov stability criterion.
- The effect of uncertainties on the performance of different type of inverted pendulums has been analysed using conventional and AGS PID controllers. The uncertainties considered are the fast acting external disturbances, noise in the controllers and frictional forces (incorporated into the state equations in the form of simple friction model and exponential friction model). The simulation results show that while using AGS PID controllers in the presence of noise, lesser chattering has been observed in the system response as compared to the conventional PID scheme. Similarly when the effect of friction is considered in the form of simple friction model, the system response with the proposed AGS PID controllers is quite satisfactory as compared to the conventional PID controllers, whose response becomes unbounded in the presence of friction. When the exponential friction model is considered, a perfect stabilization and tracking control is provided by AGS PID controllers, which are not in case of conventional PID controllers.
- Hybrid control schemes which are, fuzzy logic (FL) based PID controller, artificial neural network (ANN) based PID controller, adaptive neuro fuzzy inference system (ANFIS) based PID controller, have been implemented for the concentration control of a CSTR. The simulation results show that the best performance has been achieved by ANFIS based controller in terms of settling time and overshoot because it combines the features of neural networks and fuzzy logic to get the benefits of both in a single structure while the moderate performance has been given by artificial neural network tuned PID controller as it reduces the overshoot and inverse response magnitude to a great amount in comparison with the other methods.
- A closed-loop H_∞ preview control scheme has been implemented for concentration control of a continuous stirred tank reactor. The implemented scheme provides improvement in reference tracking and disturbance rejection with lesser control effort.

6.2 Scope for Future Work

From the research work presented in this thesis, the following are recommended for further investigation and future work:

- The proposed time as well as error AGS PID controllers may be implemented for the stabilization of other type of systems such as a rotary inverted pendulum system or flexible link robots.
- The work can further be extended by estimating the uncertainties of the inverted pendulum system. A fuzzy system may be employed to approximate the unknown system uncertainties.
- Intelligent control techniques such as fuzzy logic or artificial neural networks may also be implemented for the stabilization and tracking control of x-y-z inverted pendulum system with parameter uncertainties.
- Preview control scheme may be implemented on the different type of inverted pendulum systems.

References

Adhikary, N. and Mahanta, C. (2013). Integral backstepping sliding mode control for underactuated systems: Swing-up and stabilization of the cart-pendulum system. *ISA Transactions,* 58, 870–880.

Anderson, C. (1989). Learning to control an inverted pendulum with neural networks, *IEEE Control Systems Mag*azine, 9, 31–37.

Angeli, D. (2001). Almost global stabilization of the inverted pendulum via continuous state feedback, *Automatica, 37,* 1103–1108.

Aoyama, A., Doyle, F. and Venkatasubramanian, V. (1995). A fuzzy neural-network approach for nonlinear process control, *Engineering Applications of Artificial Intelligence*, 8, 483-498.

Astrom, K.J. and Furuta, K. (1999). Swinging up a pendulum by energy control, *Automatica,* 3, 287-295.

Astrom, K.J. and Hagglund, T. (1995). PID Controllers: Theory, Design and Tuning, *Instrument Society of America, 2*, USA.

Astrom, K.J. and Wittenmark, B. (2009). Adaptive Control, *Pearson Education*.

Balan, R. and Umapathy, M. (2002). Design of variable structure control for CSTR process, *Proceedings of National Conference on Modern Trends in Electrical and Instrumentation Systems*, Coimbatore.

Bardini, M. and Nagar, A. (2014). Interval type-2 fuzzy PID controller for uncertain nonlinear inverted pendulum system, *ISA Transactions*, 53, 732-743.

Bettayeb, M., Boussalem, C., Mansouriand, R. and.Al-Saggaf, U.M. (2014). Stabilization of an inverted pendulum-cart system by fractional PI-state feedback, *ISA Transactions,* 53, 508- 516.

Bequette, B.W. (2003). Process Control: Modeling, Design and Simulation, *PHI* .

Bloch, A.M., Leonard, N.E. and Marsden, J.E. (2000). Controlled lagrangians and the stabilization of mechanical Systems I: the first matching theorem, *IEEE Transactions on Automatic Control* ,45, 2253–2270.

Bloch, A.M., Chang, D.E., Leonard, N.E. and Marsden, J.E (2001). Controlled Lagrangians and the stabilization of mechanical systems II: potential shaping, *IEEE Transactions on Automatic control,* 46, 1556–1571.

Boubaker, O. (2012). The inverted Pendulum: A fundamental Benchmark in Control Theory

and Robotics, *International Conference on Education and e-Learning Innovations*, Sousse, 1-6

Burghart, J.H. (1969). A technique for online steady state optimizing control, *IEEE Transactions on System, science & Cybernatics*, 5, 125-132.

Cao, W. and Xu, J. (2004). Nonlinear integral-type sliding surface for both matched and unmatched uncertain systems. *IEEE Transactions on Automatic Control*, 49, 1355–1360.

Champbell, S.A. (2004). Friction and the Inverted Pendulum Stabilization Problem, *Department of Applied Mathematics*, University of Waterloo, Canada, 1-21.

Chang, L.H. and Lee, A.C. (2007). Design of nonlinear controller for bi-axial inverted pendulum system, *IET Control Theory and Application*, 1, 979–986.

Chatterjee, D., Patraa, A. and Joglekar, H.K. (2002). Swing-up and stabilization of a cart–pendulum system under restricted cart track length, *Systems & Control Letters*, 47, 355 – 364

Chen, B. and Liu, X. (2005). Fuzzy approximate disturbance decoupling of MIMO nonlinear systems by backstepping and application to chemical processes, *IEEE Transactions on Fuzzy Systems*, 13, 832-847.

Chen, C.T. and Peng, S.T. (2005). Design of a sliding mode control system for chemical processes. *Journal of Process Control*, 15, 515–530.

Daly, J.M. and Wang, D.W.L. (2009). Output feedback sliding mode control in the presence of unknown disturbances, *Journal of Systems & Control Letters*, 58, 188-193.

Dasgupta, S., Sadhu, S. and Ghoshal, T.K. (2010). Internal Model Control based controller design for a Stirred Water Tank, *INDICON*, 1-4.

Gallegos, J.A. (1988). Application of nonlinear system transformations to control design for a chemical reactor, *IEE Proceedings*, 135, 90-94.

Galluzo, M. and Cosenza, B. (2011). Control of a non-isothermal continuous stirred tank reactor by a feedback-feedforward structure using type-2 fuzzy logic controllers, *Journal of Information Sciences*, 181, 3535-3550.

Ghosh, A., Krishnan, T.R. and Subudhi, B. (2012). Robust PID compensation of an inverted cart-pendulum system: an experimental study, *IET Control Theory and Applications, 6*, 1145-1152.

Ginoya, D., Shendge, P.D. and Phadke, S.B. (2014). Sliding mode control for mismatched uncertain systems using an extended disturbance observer, *IEEE Transactions on Industrial Electronics*, 61, 1983-1992.

Goodwin, G.C., Graebe, S.F. and Salgado, M.E. (2000). Control system Design, 2nd Edition, *Prentice Hall.*

Henmi, T., Park ,Y., Deng ,M. and Inoue, A. (2010). Stabilization Controller for a Cart-type Inverted Pendulum via a Partial Linearization Method, *International Conference on Modelling, Identification and Control*, Okayama, Japan, 248-253.

Hoanga, H., Couennea, F., Jallut, C. and Gorrecc, Y.L. (2011). The port Hamiltonian approach to modeling and control of Continuous Stirred Tank Reactors. *Journal of Process Control*, 21, 1449-1458.

Hoanga, H., Couenne, F and Gorrec,Y.L. (2012). Lyapunov-based control of non isothermal continuous stirred tank reactors using irreversible thermodynamics, *Journal of Process Control*, 22, 412-422.

Huebsh, J., Sandoval, L.A.R. and Budman, H. (2009). Tuning an adaptive controller using a robust control approach, *International Journal of Control*, 82, 894-909.

Hu, Q. and Rangaiah, G.P. (2000). Anti-windup schemes for uncertain nonlinear systems, *IEE Proceedings on Control Theory Application*, 147, 321-329.

Hu, Q. and Rangaiah, G.P. (2010). Internal model control with feedback compensation for uncertain non-linear systems, *International Journal of Control*, 74, 1456-1466.

Hussain, M.A. (1999). Review of the applications of neural networks in chemical process control simulation and online implementation. *Artificial Intelligence in Engineering*, 13, 55-68.

Ibanez, C.A., Gutierrez, O. and Sossa-Azuela, H. (2006). Lyapunov Approach for the stabilization of the Inverted Spherical Pendulum, *45th IEEE Conference on Decision & Control* , San Diego, 6133-6137.

Ingber, L. (2012). Adaptive Simulated Annealing in Stochastic global optimization and its applications with fuzzy adaptive simulated annealing, *Springer New York*, 33-61.

Jaleel, J.A. and Francis, R.M. (2013). Simulated annealing based control of an inverted pendulum system, *IEEE International Conference on Control, Communication and Computing*, Trivendrum, 204-209.

Jang, J.S.R. ,Chen, C.T and Mizutani, E. (2009). Neuro Fuzzy & Soft computing, 2nd Edition, *PHI.*

Joglekar, H.K., Chatterjee, D. and Patra, A. (2001). Swing-up and stabilization of a cart–pendulum system using energy control, *in: EAIT Conference Proceedings*, Kharagpur, 33–37.

Kar, I. and Behera, L. (2009). Direct adaptive neural control for affine nonlinear systems, *Applied Soft Computing*, 9, 756-764.

Katoh, H. (2004). H_∞ optimal preview controller and its performance limit, *IEEE Transactions on Automatic Control*, 49, 2011-2017.

Khalil, H. K. (2002). Nonlinear Systems, 3rd Edition , *Prentice Hall.*

Kojima, A. (2015). H_∞ controller design for preview and delayed systems, *IEEE Transactions on Automatic Control*, 60, 404-419.

Kumar, A.S. and Ahmad, Z. (2012). Model Predictive control and its current issues in chemical engineering, *Chemical Engineering Communications*, 199, 472-511.

Kumar,V. and Jerome, J. (2013). Robust LQR Controller Design for Stabilizing and Trajectory Tracking of Inverted Pendulum, *Procedia Engineering, 64*, 169-178.

Kuntanaprida, S. and Marusak, P.M. (2012). Nonlinear extended output feedback control for CSTRs with Van de Vusse reaction, *Journal of Computers & Chemical Engineering*, 41, 10-23.

Kuo, B.C. and Golnaraghi, F. (2002). Automatic Control Systems, 8th Edition, *Wiley*.

Lee, C.C (1990). Fuzzy Logic in Control Systems: Fuzzy Logic Controller, Part I1. *IEEE Transactions on Systems, Man and Cybernatics*, 20, 419-435.

Lee, S.M. and Park, J.H. (2014). Approximate output regulation of spherical inverted pendulum by neural network control, *Neurocomputing*, 142, 542-550.

Li, D.J. (2014). Neural network control for a class of continuous stirred tank reactor process with dead-zone input, *Neurocomputing*, 131, 453-459.

Lightbody, G. and Irwin, G.W. (1995). Direct neural model reference adaptive control, *IEE Proceedings on Control Theory Application*, 142, 31-43.

Lin, C.E. and Sheu, Y.R. (1992). A hybrid control approach for pendulum–cart control, *IEEE Transactions on Industrial Electronics,* 39, 208–214.

Lin, C., Wang, Q.G. and Lee, T.H. (2005). Stabilization of uncertain fuzzy time-delay systems via variable structure control approach, *IEEE Transactions on Fuzzy Systems*, 13, 787-798.

Liu, G.Y., Nesic, D. and Mareels, I. (2008). Non-linear stable inversion-based output tracking control for a spherical inverted pendulum, *International Journal of Control, 81,* 116–133.

Liu, X. (2008). Single Neuron Self-tuning PID Control for Welding Molten Pool Depth, *Proceedings of the 7th World Congress on Intelligent Control and Automation*, Chongqing, China, 7922-7925.

Longchamp, R. (1980). Stable feedback control of bilinear systems, *IEEE Transactions on Automatic Control*, 25, 302-306.

Lozano, R. and Fantoni, D.J. (2000). Stabilization of the inverted pendulum around its homoclinic orbit, *Systems Control Letters*, 40, 197–204.

Lu, H.C., Chang, M.H. and Tsai, C.H. (2011). Adaptive self-constructing fuzzy neural network controller for hardware implementation of an inverted pendulum system, *Applied Soft Computing*, 11, 3962-3975.

Maravall, D. (2004). Control and stabilization of the inverted pendulum via vertical forces Robotic welding, intelligence and automation. *Lecture notes in control and information sciences*, Berlin: Springer-Verlag, 299, 190–211.

Mason, P., Broucke, M. and Piccoli, B. (2008). Time optimal swing-up of the planar pendulum, *IEEE Transactions on Automatic Control*, 53, 1876–1886.

Muskinja, N. and Tovornik, B. (2006). Swinging up and stabilization of a real inverted pendulum, *IEEE Transaction on Industrial Electronics*, 53, 631-639.

Nagar, A., Bardini, M. and Rabaie, N. M. (2014). Intelligent control for nonlinear inverted pendulum based on interval type-2 fuzzy PD controller, *Alexandria Engineering Journal*, 53,
23-32.

Nasir, A. (2007). Modeling and controller design for an inverted pendulum system, *Master of Technology Degree, Faculty of Electrical Engineering*, Universiti Teknologi Malaysia.

Nedjah, N. and Mourelle, L. (2004). Studies in Fuzziness and Soft Computing, Germany, Springer Verlag.

Ozkan, G.O., Hapog, L.H. and Alpbaz, M . (2006). Non- linear generalised predictive control of a jacketed well mixed tank as applied to a batch process-A polymerisation reaction, *Applied Thermal Engineering*, 26 , 720-726.

Park, M., and Chwa, D. (2009). Swing-up and stabilization control of inverted pendulum systems via coupled sliding-mode control method. *IEEE Transactions on Industrial Electronics*, 56, 3541–3555.

Pendharkar, I. and Pillai, H.K. (2011). Application of quadratic differential forms to designing linear controllers for nonlinearities, *Asian Journal of Control*, 13, 449-455.

Perez, M. and Albertos, P. (2004). Self-oscillating and chaotic behavior of a PI-controlled CSTR with control valve saturation, *Journal of Process Control*, 14, 51-59.

Ping, Z. (2013). Tracking problems of a spherical linverted pendulum via neural network enhanced design , *Neurocomputing*, 106, 137–147.

Ping.Z and Huang, J. (2012). Approximate output regulation of spherical inverted pendulum by neural network control, *Neurocomputing* ,85, 38–44.

Postelnik. L, Liu, G., Stol, K. and Swain, A. (2011). Approximate output regulation for a spherical inverted pendulum, *in: Proceedings of the 2011 American Control Conference*, San Francisco, California, 2011, 539–544.

Prakash, J. and Srinivasan, K. (2009). Design of nonlinear PID controller and nonlinear model predictive controller for a continuous stirred tank reactor, *ISA Transactions*, 48, 273-282.

Prasad, R. and Kulshrestha, A.K (1997). Application of model reduction methods for controller design, *Proc. of Int. Conf. on Computer Applications in Electrical Engineering, CERA*, Roorkee, 97, 503-508.

Prasad, L.B., Tyagi, B. and Gupta, H.O. (2011). Intelligent Control of Nonlinear Inverted Pendulum Dynamical System with Disturbance Input using Fuzzy Logic Systems, *IEEE International Conference on Recent Advancements in Electrical, Electronics and Control Engineering*, Sivakasi, India, 136-141.

Ramirez, J.A and Femat, R. (1999). Robust PI stabilization of a class of chemical reactors, *Systems & Control Letters*, 38, 219–225.

Ray, G., Das, S. K. and Tyagi, B. (2007). Stabilization of Inverted Pendulum via Fuzzy Control, *IE(I) Journal-EL*, 88, 58-62.

Roopaei, M. , Zolghadri, M. and Meshkar, S. (2009). Enhanced adaptive fuzzy sliding mode control for uncertain nonlinear systems, *Communication in Nonlinear Science & Numerical Simulation*, 14, 3670-3681.

Ross, T. J. (2009). Fuzzy Logic with Engineering Appplications, *Wiley India Edition*.

Saini, J.S., Gopal, M. and Mittal, A.P.,(2005), Genetic algorithm based PID tuner, *Journal of IE(I)*, 85, 216-221.

Shahraz, A. and Boozarjomehry, R. (2009). A fuzzy sliding mode control approach for nonlinear chemical processes, *Journal of Control Engineering Practice*, 17, 541-550.

Shen, X., Liu, S. and Varshney, P. K. (2014). Sensor Selection for Nonlinear Systems in Large Sensor Networks, *IEEE Transactions on Aerospace and Electronic System*, 50, 2664-2678.

Shing, J. and Jang, R. (1993). ANFIS: Adaptive Network Based Fuzzy Inference System, *IEEE Transactions on Systems, Man, and Cybernetics*, 23, 665-684.

Sing, C.H. and Postlethwaite, B. (1997). pH control: handling nonlinearity and deadtime with fuzzy relational model-based control, *IEE Proceedings on Control Theory Application*, 144, 263-268.

Singla, S.K. and Arora, A.K. (2012). Optimizing the rotation and translation of fingerprint images using genetic Algorithm, *Applied Artificial Intelligence*, 26, 541-553.

Sinha, A., Prasoon, P., Bharadwaj, P.K. and Ranasinghe, A.C. (2015). Nonlinear autonomous control of a Two-wheeled inverted pendulum mobile robot based on sliding mode, *International Conference on Computational Intelligence & Networks*, Bhubaneshwar, 52-57.

Sinthipsomboon, K., Pongaen, W. and Pratumsuwan, P. (2011). A Hybrid of Fuzzy and Fuzzy self-tuning PID Controller for Servo Electro-hydraulic System, *6th IEEE Conference on Industrial Electronics and Applications*,Beijing, *220-225.*

Sivanandam, S.N., Sumathi, S. and Deepa, S.N. (2007). Neural Networks using Matlab 6.0, *The McGraw Hill Companies*.

Slotin, J.E. and Li, W. (1999). Applied nonlinear control, *PHI.*

Spong, M. W. and Praly, L. (1996). Control of underactuated mechanical systems using switching and saturation. *In Proceedings of the block island workshop on control using logic based switching, 1256-1270.*

Takaba, K. (2003). A tutorial on preview control, *SICE Annual Conference*, Fukui, Japan 1388-1393.

Tang, K. S., Man, K. F., Chen, G. and Kwong, S. (2001). An Optimal Fuzzy PID Controller, *IEEE Transactions on Industrial Electronics*, 48, 757-765.

Tang, K. S., Chen, G. R., Man, K. F. and Kwong, S. (2005). Fuzzy Logic and Genetic Algorithm Methods in PID Tuning, Springer.

Thornhill, N.F., Patwardhan, S.C. Sachin and Shah, S.L. (2008). A continuous stirred tank heater simulation model with applications, *Journal of Process Control*, 18, 347–360.

Utkin, V.I. (1993). Sliding Mode Control Design Principles and Applications to Electric Drives, *IEEE transactions on Industrial Electronics*, *40*, 23-36.

Viel, F., Jadot, F. and Bastin, G. (1997). Robust Feedback Stabilization of Chemical Reactors, *IEEE Transactions on Automatic Control*, 42, 473-481.

Wang, H., Zhang, H., Xie, X. and Liu, S. (2009). Discrete time H_∞ preview control, *Proceedings of the 7th Asian Control Conference*, Hongkong, 57-62.

Wang, J.J. (2011). Simulation studies of inverted pendulum based on PID controllers, *Simulation Modelling Practice and Theory*, 19, 440-449.

Wang, J.J. (2012). Stabilization and tracking control of X–Z inverted pendulum with sliding-mode control, *ISA Transactions, 51*, 763-770.

Wanli, Z. and Guoxin, L. (2014). Research on the control method of inverted pendulum based on Kalman filter, *IEEE 12th International Conference on Dependable, Autonomic and Secure Computing*, Dalian, China, 520-523.

Woo, P.Y. (1992). Linearization and PID Parameters Design for Nonlinear Systems, *Proceedings of 1992 IEEE International Conference on System Engineering*, Kobe, Japan, 444-447.

Woo, P.Y. (2002). The Design of a Novel Neural-Fuzzy Control System for Robotic Manipulators, *IEEE Control Systems Magazine,* 22, 53-64.

Wu, Y., Shen, L. and Zhang, L. (2011). Study of nonlinear pH control strategy based on external recurrent neural network, *Procedia Engineering*, 15, 866-871.

Xu, J., Guo, Z., and Lee, T. H. (2013). Design and implementation of integral sliding mode control on an under actuated two-wheeled mobile robot. *ISA Transactions*, 58, 870–880.

Yadav, A.K., Gaur, P., Mittal, A.P. and Anzar, M. (2010). Comparative Analysis of Various Control Techniques for Inverted Pendulum, *India International Conference on Simulation of custom power electronic device,*New Delhi, 1-6.

Yang, Y.Y. and Linkens, D.A. (1994). Adaptive neural-network-based approach for the control of continuously stirred tank reactor, *IEE Proceedings on Control Theory Application*, 141, 341-349.

Yu, D.L., Chang, T.K. and Yu, D.W. (2005). Fault tolerant control of multivariable processes using auto-tuning PID controller, *IEEE Transactions On Systems, Man and Cybernetics Part B: Cybernetics*, 35, 32-43.

Yu, D.L., Chang, T.K. and Yu, D.W. (2007). A stable self-learning PID control for multivariable time varying systems, *Journal of Control Engineering Practice*, 15, 1577-1587.

Zhang, T. and Guay, M. (2009). Piecewise Fuzzy Anti-Windup Dynamic Output Control of Nonlinear Processes With Amplitude and Rate Actuator Saturations, *IEEE Transactions on Fuzzy Systems*, 17, 253-264.

Zhao, J., Spong, M.W. (2001). Hybrid control for global stabilization of the cart-pendulum system, *Automatica*, 37, 1941-1951.

Zheng, F., Wang, Q.G. and Lee, T.H. (2004). Adaptive and robust controller design for uncertain nonlinear systems via fuzzy modeling approach, *IEEE Transactions on Systems, Man and Cybernetics—Part B: Cybernetics*, 34, 166-178.

Zhu, Q.M. and Warwick, K. (2000). A neuro PID controller for complex dynamic plants, *IFAC Workshop on Digital Control, Past, present and future of PID Control*, Terrassa, Spain, 59-64.

Zhu, Q.M. and Guo, L.Z. (2002). A pole placement controller for nonlinear dynamic plant, *Journal of Systems and Control Engineering, Proceedings of the Institution of Mechanical Engineers Part I*, 216, 467-476.

Zhu, Q.M. and Guo, L.Z. (2007). Stable adaptive neuro-control for nonlinear discrete-time systems , *IEEE Transactions on Neural Networks*, 15, 653-662.

Appendix A

The frictional forces in x, y and z directions are given as f_{xfric}, f_{yfric} and f_{zfric}. These are defined in a generalized manner by two friction models as given below:

(i) ***The simple friction model*** (Champbell, 2004)

For x direction movement

$$F_{xfric} = (F_{xstatic} \text{ if } \dot{x} = 0)$$

$$F_{xfric} = (F_{xcoloumb} + F_{xviscous} \text{ if } \dot{x} \neq 0)$$

Here $F_{x\,static} = -F_{xapplied}$ if $\left|F_{x\,applied}\right| < \mu_s F_N$

$$F_{xstatic} = -\mu_s F_N \operatorname{sgn}(F_{x\,applied}) \text{ if } \left|F_{x\,applied}\right| \geq \mu_s F_N)$$

The coulomb and the viscous friction are defined as:

$$F_{x\,coloumb} = -\mu_C F_N \operatorname{sgn}(\dot{x})$$

$$F_{x\,viscous} = -\varepsilon\dot{x}$$

For y direction movement

$$F_{yfric} = (F_{ystatic} \text{ if } \dot{y} = 0)$$

$$F_{yfric} = (F_{ycoloumb} + F_{yviscous} \text{ if } \dot{y} \neq 0)$$

Here $F_{y_{static}} = -F_{yapplied}$ if $\left|F_{yapplied}\right| < \mu_s F_N$

$$F_{ystatic} = -\mu_s F_N \operatorname{sgn}(F_{yapplied}) \text{ if } \left|F_{yapplied}\right| \geq \mu_s F_N)$$

The coulomb and the viscous friction are defined as:

$$F_{ycoloumb} = -\mu_C F_N \operatorname{sgn}(\dot{y})$$

$$F_{yviscous} = -\varepsilon\dot{y}$$

For z direction movement

$$F_{zfric} = (F_{zstatic} \text{ if } \dot{z} = 0)$$

$$F_{zfric} = (F_{zcoloumb} + F_{zviscous} \text{ if } \dot{z} \neq 0)$$

Here $F_{zstatic} = -F_{zapplied}$ if $\left|F_{zapplied}\right| < \mu_s F_N$

$$F_{zstatic} = -\mu_s F_N \operatorname{sgn}(F_{zapplied}) \text{ if } \left|F_{zapplied}\right| \geq \mu_s F_N)$$

The coulomb and the viscous friction are defined as:

$$F_{zcoloumb} = -\mu_C F_N \operatorname{sgn}(\dot{z})$$

$$F_{zviscous} = -\varepsilon \dot{z}$$

Here F_N is the magnitude of the normal force and is defined as, $F_N = (m + M)g$

(ii) Exponential friction model (Champbell, 2004)

The exponential friction model is defined as follows:

$$F_{xfric} = (F_{xstatic} \text{ if } \dot{x} = 0)$$

$$F_{xfric} = -[\mu_c + (\mu_s - \mu_c)e^{-(\frac{\dot{x}}{v_s})\gamma}]F_N \operatorname{sgn}(\dot{x}) - \varepsilon \dot{x} \text{ if } \dot{x} \neq 0$$

Similarly $F_{yfric} = (F_{ystatic} \text{ if } \dot{y} = 0)$

$$F_{yfric} = -[\mu_c + (\mu_s - \mu_c)e^{-(\frac{\dot{y}}{v_s})\gamma}]F_N \operatorname{sgn}(\dot{y}) - \varepsilon \dot{y} \text{ if } \dot{y} \neq 0$$

and $F_{zfric} = (F_{zstatic} \text{ if } \dot{z} = 0)$

$$F_{zfric} = -[\mu_c + (\mu_s - \mu_c)e^{-(\frac{\dot{z}}{v_s})\gamma}]F_N \operatorname{sgn}(\dot{z}) - \varepsilon \dot{z} \text{ if } \dot{z} \neq 0$$

Here γ = form factor=2 and v_s = Stribeck velocity=0.105

List of Publications (SCI Listed Journals)

➢ Papers Published

- Preview Control: A Review, PRZEGLĄD ELEKTROTECHNICZNY, ISSN 0033-2097, Vol. 89, No. 2(a), pp. 134-138, 2013.

- Comparative Analysis of Tuning a PID Controller using Intelligent Methods, Acta Polytechnica Hungarica, IEEE Hungary Section, ISSN 1785-8860, Vol. 11, No. 08, pp. 235-249, 2014.

➢ Paper Accepted

- Stabilization of an x-y Inverted Pendulum Using Adaptive Gain Scheduling PID Controllers in the Presence of Uncertainties, *Journal of Engineering Research*, Kuwait, ISSN (print): 2307-1877.

➢ Papers Communicated

- Modelling and Control of a New Type of *XYZ* Inverted Pendulum Using Conventional and Adaptive Gain Scheduling PID Controllers, *Applied Mathematical Modelling, Elsevier,* ISSN: 0307-904X.

- Stabilization and Tracking control of Inverted Pendulum using Adaptive Gain Scheduling PID Controllers in the Presence of Uncertainties, *Bulletin of the polish academy of science and technology.* ISSN:0239-7528.

- Stabilization of an X-Z inverted pendulum using adaptive gain scheduling PID controllers in the presence of uncertainties, *Journal of Applied Research and Technology.* ISSN:1665-6423.

- Stabilization of inverted pendulum using adaptive controllers in the presence of uncertainties, *Journal of Theoretical and Applied Mechanics.* ISSN: 1429-2955.